TFIIH:
at the Crossroads of Cancer and Ageing

TFIIH: op het kruispunt van kanker en veroudering

Proefschrift

ter verkrijging van de graad van doctor
aan de Erasmus Universiteit Rotterdam
op gezag van de
Rector Magnificus
Prof.dr. S.W.J. Lamberts
en volgens besluit van het College voor Promoties

De openbare verdediging zal plaatsvinden op
woensdag 20 oktober 2004 om 13.45 uur

door
Jaan-Olle Andressoo
geboren te Tallinn

Promotiecommissie

Promotor:	Prof.dr. J.H.J. Hoeijmakers
Overige leden:	Prof.dr. L.H.F. Mullenders
	Dr. W. Kleijer
	Prof.dr. I.P. Touw
Copromotor:	Dr. G.T.J. van der Horst

Pühendusega emale, isale, vendadele ja muule perele

Contents

Aim and outline of the thesis

It is widely although not uniformly accepted that ageing is caused by time-dependent accumulation of damage. A side effect of ageing is an increased risk of developing a disease, such as cancer. Yet, the primary molecular target of damage accumulation has remained obscure. A clue has emerged from the notion that human inborn premature ageing syndromes are often associated with mutations in genes involved in DNA metabolism such as nucleotide excision repair (NER). In this thesis, mechanisms of pathological and normal ageing are addressed by genocopying naturally occurring human NER mutants with accelerated ageing and/or cancer phenotype in mouse model systems. Pathological conditions associated with mutations in the *XPD* and *XPB* genes, encoding the helicase components of the multifunctional TFIIH complex, range from a dramatic 1000 times elevated cancer predisposition (Xeroderma pigmentosum) to the severe neurodevelopmental premature ageing disorders trichothiodystrophy (TTD) and XP combined with Cockayne syndrome (XPCS). The aim of this thesis is to understand the mechanisms of accelerated ageing and to uncover variables determining the immense clinical heterogeneity of NER disorders. **Chapter 1** introduces the theory of ageing, summarizes clinical consequences of NER mutations and describes the basic DNA repair mechanims involved. **Chapter 2** presents experiments revealing TTD as a progeroid syndrome and defines the crucial role of DNA damage and repair in the rate of TTD-related ageing. **Chapter 3** reveals interallelic complementation between differentially compromised XPD molecules in mice and suggests a new variable in genotype-phenotype relationships within human recessive disease. **Chapter 4** shows that CS and TTD share a common root cause in defective DNA repair. **Chapter 5** uncovers the widely pleiotropic effects of combining different NER defects with the latent Xpb^{XPCS} mutation, ranging from moderately enhanced ageing to immediate postnatal lethality. **Chapter 6** describes how interallelic complementation can be used for the reconstitution of CS pathology in mice and outlines some potentials for therapy. **Chapter 7** reviews all major features of the NER mouse models generated in this thesis and elsewhere and sets forward a model for NER- associated disease.

CHAPTER 1

Introduction

Mechanisms of ageing

1.1 What is the root cause of ageing?

Ageing is usually defined as the progressive loss of function accompanied by decreasing fertility and increasing risk for pathological changes and mortality with advancing age. One of the most intriguing questions for contemporary science is how ageing evolved in evolution, what the basic mechanisms are and if and how age-related changes can be alleviated or reversed. It is now generally accepted that ageing is caused by time-dependent accumulation of damage (Finch and Schneider 1985; Finkel and Holbrook 2000; Kirkwood and Austad 2000; Hasty et al. 2003). The ongoing debate and research is focused on defining the primary cause(s) of ageing. First, why do we age? In our evolutionary past, most individuals within reproductive age or past the reproductive age but with secondary beneficial effect to progeny died before growing old because of external hazards, such as predators, starvation or infections, leaving no- or very few individuals under selection against senescence. Thus, the older the individual, the higher the chance for age-associated pathology, as evolutionary pressure for improving somatic repair and maintenance declines rapidly with increasing age. Senescent individuals survive only in protected surroundings, such as isolated natural habitats (e.g. islands with no or few external hazards) or protected environments such as contemporary society, and conditions created for laboratory animals (Kirkwood and Austad 2000). As a consequence of achievements in social well fare and medicine in the western society we are facing a new spectrum of human pathologies-those that come with an increasing age. Age-dependent neuronal decline, such as Alzheimer's disease, Parkinson's disease and dementia; cardiovascular diseases and dramatically increased cancer frequency as a function of age serve as well known examples. Left without the benefits of evolutionary heritage on fitness as we grow old, society and science are inevitably facing a new challenge - can we understand and intervene with the process of ageing? Though essentially no one is dreaming of "eternal life" ageing with grace - free of the above diseases should be considered as a human right and thus regarded as one of the important goals for contemporary research and medicine.

What is the root cause of ageing? First clues emerged as long as nearly a century ago, when it was noted that animals with higher metabolic rate have in general shorter life expectancy. These observations led to the "rate of living hypothesis", which states that the metabolic rate of a species ultimately determines its life expectancy (Finkel and Holbrook 2000). In the mid- 50, Denham Harman postulated the "free radical theory" of ageing, speculating that endogenous reactive oxygen species (ROS) were generated in cells and resulted in a pattern of cumulative damage (Harman 1956). ROS, produced in every day life of each cell by normal mitochondrial respiration, damages the integral components of the cell, such as lipids, proteins and DNA. However, although the correlation between life-span, and metabolic rate and endogenous production of ROS in general holds between species (Ku et al. 1993; Herrero

and Barja 1999; Barja and Herrero 2000), exceptions exist, e.g. birds and primates. In the latter animals including humans, despite of high metabolic rate, less ROS is produced (Ku et al. 1993). Yet, the rate of ageing is not only determined by the amount of intracellular ROS but also by the effectiveness of defense mechanisms, such as ROS scavenging, damage removal, and repair. Since most individuals in the wild die because of external hazards, no or very few older individuals within reproductive age or of secondary benefit to the progeny remain under evolutionary selection against senescence. Thereby, evolution has had little chance to select for better integration and function of scavenging- and repair mechanisms in species with high external mortality rate in the wild, such as mice (Mus musculus), but had much better possibilities to do so in species which have acquired adaptations that reduce external mortality (for example wings, protective shells, large brain, big body size; for review see (Kirkwood and Austad 2000)). Reflections of such qualitative differences in scavenging-, repair- and maintenance mechanisms between species can be observed in routine laboratory practice. For example, mouse but not human fibroblast cells undergo quick chromosomal rearrangements, early growth arrest and spontaneous transformation under routine 20% oxygen culturing conditions (Parrinello et al. 2003). We and others have observed a clear distinction between mouse and human cells in surviving oxidative stress induced by paraquat or H_2O_2. Mice kept in captivity do not survive for more than ~ 3 years. As the correlation between stringency of genome maintenance systems and tumor progression is a well-established phenomenon, it is perhaps not surprising that most of the laboratory mice do not enjoy long lives but experience an array of quickly progressing cancers.

Are ROS always detrimental? Since most life forms evolved in the presence of oxygen and consequently ROS, this cannot merely be as simple. Indeed, cells have evolved a complex system of sensing mechanisms and ROS are involved as secondary messengers in several cellular signaling pathways. For example, cytokines, UV, chemotherapeutic agents, hyperthermia and growth factors can generate high levels of ROS which perturbs the normal redox balance and shifts cells into a state of oxidative stress (Finkel and Holbrook 2000). Depending on the cell type and the severity of the stress, cells either e.g. receive a stimulus for growth or production of hormones or, if the stress is severe and repair mechanisms cannot replace the damaged molecules, cease to exist via apoptosis or necrosis - processes, which also involve ROS as essential mechanistic components. Thus, although detrimental when deregulated or overproduced, ROS can be considered as an integral and essential component for cellular physiology.

In parallel with ageing, involvement of ROS in the onset of major age-related degenerative diseases is quite well established. Those include artherosclerosis (Lusis 2000), diabetes (Brownlee 2001), Pakinson disease (Betarbet et al. 2002), and, more controversially, Alzheimer's disease (Butterfield et al. 2001) and cancer (Feig et al. 1994).

The above complexity of ROS biology raises the question how we can reduce the detrimental effects of ROS while keeping oxidative metabolism and the role of ROS as intracellular signaling molecule intact. Attempts to interfere with ROS toxicity in model organisms have provided a plethora of intriguing results. These include increasing the lifespan of the worm (C. elegans) and the fly (D. melanogaster) by at least 30-50% via external or genetic increase of ROS scavenging capacity and/ or stress tolerance mechanisms (Larsen 1993; Vanfleteren 1993; Orr and Sohal 1994; Parkes et al. 1998). Moreover, mutations in certain mitochondrial proteins in the worm which are able to reduce the level of ROS production lead to enhanced longevity (Hekimi and Guarente 2003).

Keeping in mind the correlation between life-expectancy and ROS production as a function of the metabolic rate, it is not surprising that caloric restriction (CR) or, with other words, reduction of "fuel" combustion extends life-span in all model organisms tested sofar. Mutations which down-regulate glucose and insulin/IGF-I like signaling resulting in life-span extension in worm, fly and mice are believed, at least in part, to do so by simulating the starvation conditions (Longo and Finch 2003). Although the exact mechanism of signaling from CR and/or a reduced IGF-I pathway to lifespan extension mechanisms is still unclear, both reduce the levels of intracellular ROS while increasing stress tolerance mechanisms. The latter include elevation of antioxidant enzyme levels, such as superoxide dismutase and catalase; as well as enhancement of protein turnover pathways which allows quick replacement of damaged proteins. Furthermore, in mammals, CR has stimulating effects on the immune-system, it attenuates inflammatory responses and provokes production of neurotrophic factors in the brain consequently leading to reduced tumorigenesis and neurodegeneration in ageing rodents (Longo and Finch 2003).

The adverse effects of metabolic rate and CR on longevity make it tempting to compare a living cell with a simple combustion engine. Virtually every car owner realizes that the engine will last longer, if rpm (rounds per minute) are kept within the limit indicated as optimal by the manufacturer. Rpm and metabolic rate can both be raised by burning more fuel (food) in the engine (cell) within the same period of time. The inevitable outcome of raising the turnover is faster oxidation. While the duration of the engine depends on the quality of the repair-man in your garage, quality of life, health and lifespan of the cell (organ, and organism) depends on its internal repair capacity. ROS damage basic components of the cell, including lipids, proteins and DNA. Based on the information coded by DNA, lipids and proteins are continuously turned over, folded, remodeled and positioned in each cell. DNA itself is irreplaceable, therefore damage on DNA, if not repaired, should have the strongest biological consequence. Indeed, DNA repair capacity has been shown to correlate with mammalian life span in a number of comparative studies (Kirkwood 1989), as has the level of poly(ADP-ribose) polymerase (Grube and Burkle 1992), an enzyme that is important in the maintenance of genomic integrity. Inborn defects in proteins that

sense or repair DNA damage give rise to symptoms of partial (segmental) accelerated ageing (Hasty et al. 2003). Although ROS are considered to be the major offender of the genome, DNA homeostasis is under continuous insult by various other endogenous and exogenous chemicals and electromagnetic radiation such as UV- and gamma rays. Therefore evolution has equipped all organisms with a sophisticated and often highly specialized and interwoven network of complementary DNA repair systems.
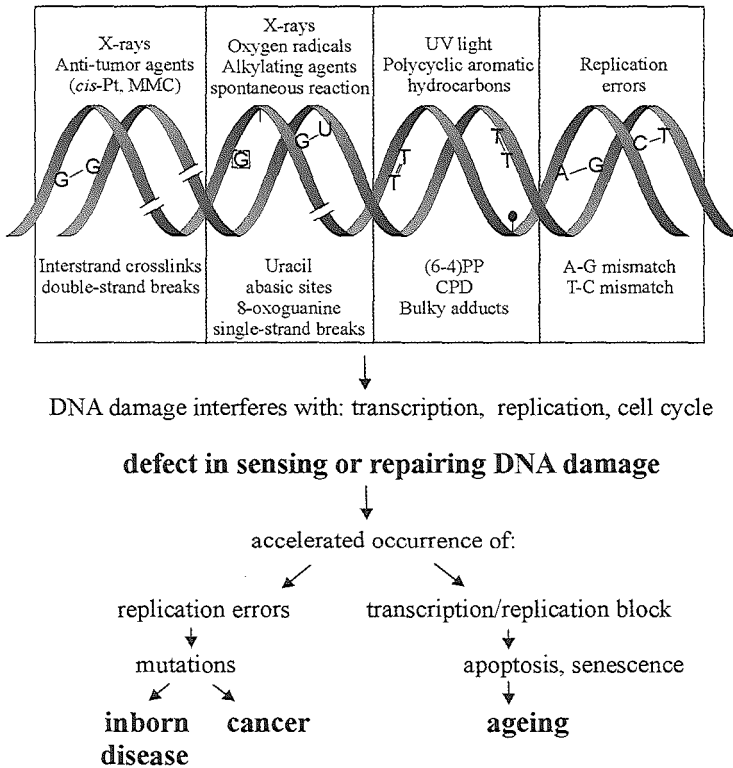
Why are accelerated ageing features observed in several DNA repair mutants only in part mimicking normal ageing? Different DNA lesions result in specific phenotypic effects (e.g. ROS are believed to result in at least 100 different types of DNA lesions (Hoeijmakers 2001)). Provided the high specificity of various DNA repair systems in parallel with the different nature of DNA repair inactivating mutations which range from full, to partial inactivation, it is expected, rather than surprising, that defects in various DNA repair proteins occasionally result in segmental, not full reconstitution of ageing.

1.2 DNA integrity and human pathology

Due to oxidative metabolism and concomitant production of ROS and reactive metabolic intermediates DNA in every cell of our body is continuously damaged. Furthermore, exogenous physical or chemical toxic agents, such as UV or ionizing radiation and cigarette smoke, damage DNA. Lesions in DNA hamper crucial cellular processes, such as transcription and replication. Underscoring the vital importance of genome integrity, basic DNA repair mechanisms are conserved in evolution from unicellular bacteria and simple eukaryotes such as bakers yeast to higher eukaryotes, such as primates (Hoeijmakers 2001). Serious defects in DNA repair are either embryonic lethal or result in pathological conditions later in life. The effects on the cellular level range from accumulation of mutations to premature cellular senescence or cell death, which can lead to cancer and/or ageing respectively (Figure 1.) (Friedberg et al. 1995; Hoeijmakers 2001; Hasty et al. 2003).

Figure 1. The major sources of DNA damage and its consequences

X-rays Anti-tumor agents (cis-Pt, MMC)	X-rays Oxygen radicals Alkylating agents spontaneous reaction	UV light Polycyclic aromatic hydrocarbons	Replication errors
Interstrand crosslinks double-strand breaks	Uracil abasic sites 8-oxoguanine single-strand breaks	(6-4)PP CPD Bulky adducts	A-G mismatch T-C mismatch

DNA damage interferes with: transcription, replication, cell cycle

defect in sensing or repairing DNA damage

accelerated occurrence of:

replication errors   transcription/replication block

mutations   apoptosis, senescence

inborn   cancer   ageing
disease

Among the human population, the biological significance of functional DNA damage repair is apparent from the severe clinical features seen in individuals with DNA repair related disorders. These patients display a common phenotype of segmental premature ageing (progeria), cancer predisposition, or both at the same time. Li-Fraumeni syndrome, ataxia telangiectasia (AT), Fanconi Anemia (FA), Nijmegen Breakage syndrome (NBS), Bloom syndrome (BL), Werner syndrome (WR), heredi-tary nonpolyposis colon cancer (HNPPC), cerebro-oculo-facio-skeletal syndrome (COFS), xeroderma pigmentosum (XP), XP with DeSanctis-Cacchione Syndrome (XP-DSC), Cockayne Syndrome (CS), trichothiodystrophy (TTD), are just examples in the far from complete list of such disorders. The mechanistic cause of the above human diseases is malfunctioning in sensing and/or repairing DNA damage (Rotman and Shiloh 1998; Graham et al. 2001; Bootsma et al. 2002; Duker 2002; Thompson and Schild 2002; Varley 2003). The latter five syndromes - COFS, XP, XP-DSC, CS and TTD can be caused by mutations in proteins involved in nucleotide excision repair (NER) (Hoeijmakers 2001). Notably, all five disorders (and combinations XP/TTD and XPCS) can be triggered by mutations in one NER gene-*XPD* (Cleaver et al. 1999; Broughton et al. 2001; Graham et al. 2001; Hoeijmakers 2001).

1.3 Nucleotide excision repair (NER) associated disorders

Mutations in the highly conserved NER pathway can lead to autosomal recessive XP, XP-DSC, CS, TTD, COFS and combinations like XP/TTD and XPCS (Cleaver et al. 1999; Broughton et al. 2001; Graham et al. 2001; Hoeijmakers 2001). Although NER involves at least 30 proteins in a multi-step repair reaction, mutations in 11 NER proteins have sofar been found to be associated with human pathology. XP can be caused by the mutations in *XP-A, C, D, E, F, G* genes, CS syndrome can be caused by mutations in *CSB*, and *-A* genes, *TTD* can be caused by mutations in *XPD, XPB* and *TTD-A* genes, COFS can be triggered by mutations in *XPD, XPG, ERCC1* and *CSB* genes, XP combined with TTD (XP/TTD) has sofar been found to be associated exclusively with *XPD*, and XPCS is triggered by mutations in either *XPD, XPB, XPG* and/or *XPF* genes (Cleaver et al. 1999; Broughton et al. 2001; Graham et al. 2001; Hoeijmakers 2001; Giglia-Mari et al. 2004) (N. Jaspers per. comm). NER-associated diseases and causative genes are listed in Table 1.

XP	XP-DSC	CS	TTD	XPCS	XP/ TTD	COFS
XPA[2]	*XPA[2]*	*CSA[1]*	*XPB[2]*	*XPB[2]*		*CSB[2]*
XPC[2]	*XPC[2]?*	*CSB[2]*	*TTD-A[1]*	*XPF[2]?*		*XPG[3]*
XPD[6]	*XPD[6]*		*XPD[6]*	*XPD[6]*	*XPD[6]*	*XPD6*
XPE[1]				*XPG[3]*		*ERCC1[1]?*
XPF[2]						
XPG[3]						

Table 1. *NER associated human diseases and causative genes. Number in upper case behind each gene indicates the number of different syndromes in which the given gene has been implicated as causative. Question mark behind gene name indicates rare, (in case of XPC associated XP-DSC only one patient have been found) or recent cases where pathology and/or causative gene is not yet confirmed (N. Jaspers, per.comm.).*

Note that distinct mutations in the *XPD* gene are causative for 6 clinically different conditions. It can be postulated that defects in *XPD* and other genes listed below each disorder, must affect the common biological process in a similar manner, thereby leading to a specific clinical condition.

While CS and TTD share neuro-developmental features, XP is mostly associated with sun induced skin cancer proneness not observed in either TTD or CS. In about 20% of XP cases, neuronal degeneration occurs (XP with DeSanctis-Cacchione syndrome, XP-DSC), resulting in e.g. dementia, memory loss or intellectual impairment (Kraemer et al. 1987). The nature of neuropathy in XP-DSC, although reminiscent of premature brain ageing, is quite distinct from what is observed in CS and TTD. CNS anomalies in CS and TTD are mostly associated with demyelination (white matter

degeneration), while neuronal loss (grey matter degeneration) is the primary cause of XP with DeSanctis-Cacchione syndrome (Brooks 2002). Yet, similar to CS and TTD patients, XP patients with neuronal manifestations often display developmental delay, gait disturbance and deafness, underlying a link between neuronal failure and the above developmental features. Unlike in CS and TTD patients, defects in neuronal migration and innervation in COFS (CNS anomalies include both white and grey matter) is believed to start already during development in utero (Graham et al. 2001)(Roger Brumback per. comm.). Rapid postnatal degeneration of both the glial and neuronal compartment in COFS and severe failure to thrive leads to death during the first few years of life (Del Bigio et al. 1997; Graham et al. 2001). Notably, the severe form of CS (CS type II), COFS and infantile XPCS complex are one of the most severe dwarfing illnesses known (Rapin et al. 2000).

To understand the mechanisms of NER-related disease, one has to be aware of disease etiology associated with each disorder. In the following sections, NER-associated pathology is discussed in a greater detail.

Cockayne syndrome (CS) and COFS
CS is a rare autosomal recessive disorder, resulting in progressive postnatal growth failure (cachexia), neurological dysfunction and symptoms reminiscent of segmental accelerated ageing (progeria) resulting in early death on average ~12.5 years of age (Nance and Berry 1992; Nakura et al. 2000). In general, older CS patients have a very characteristic appearance, including overall "aged" look, big ears and nose, sunken eyes, unsteady, wide based gait and thin appearance due to progressive loss of subcutaneous fat tissue (Nance and Berry 1992). Normal in utero development of a CS patient is followed by profound growth failure, which generally begins within the first year of life. Soon after birth, the brain of CS patients fails to grow and remains extraordinarily small throughout their lives, but remarkably, is not grossly malformed. CS patients cognition and social behavior are less impaired than one would predict from diminutive brain size. The above findings and the almost exclusive postnatal timing of growth impairment in CNS make it unlikely that the cause of extreme microcephaly (small head and brain) of CS results from pre-natal premature curtailment of neurogenesis, disordered neuronal migration, or grossly aberrant connectivity. Postnatal interference with the proliferation, branching, and deployment of neuronal processes seems more plausible (Rapin et al. 2000). The postnatal increase in oxidative DNA damage load (Randerath et al. 1997a; Randerath et al. 1997b; Randerath et al. 2001) may help to explain the almost exclusive postnatal onset of CS. The earliest common neurological symptom in CS is delayed psychomotor development. The progressive gait disorder is a manifestation of the combination of spasticity of the legs, (mainly cerebellar) ataxia, tremors, contractors of the hips, knees and ankles often accompanied by kyphosis of the vertebral column (Nance and Berry 1992). All CS patients are mentally retarded, yet, this feature varies from mild to severe

retardation. Despite progressive cognitive, sensory, and communicative difficulties, CS patients are described as happy, social, interactive or friendly (Nance and Berry 1992). It is important to note that the early onset of cataracts, neurological dysfunctioning and microcephaly is associated with poor prognosis and survival. To date, among ~200 CS cases (Rapin et al. 2000) no patients have been reported   with normal neuronal functioning but severe other CS symptoms, arguing, that progressive neuronal failure may be among the primary causes of the systemic pathological outcome. This notion is supported by post-mortem pathological findings, which in general reveal the lack of overall chronic tissue degeneration or cell-death (necrosis or apoptosis) in any organ system except for the central nervous system (CNS) and peripheral nervous system (PNS)(Nance and Berry 1992)(Roger Brumback per. comm.). Due to progressive neuronal decline and cachexia, patients gradually lose ability to move and make contact with the outside world, become passive and fail to feed actively. Tube feeding can in some cases provide temporary alleviation (J.O.A. per. comm. with CS patient parent). Progressive failure to thrive is often followed by increased susceptibility to infectious diseases such as pneumonia/respiratory infections, which are often reported as an ultimate cause of death. Perhaps secondary to cachexia, renal or hepatic failure has also been noted as a cause of death in several cases (Nance and Berry 1992).

Laboratory tests of hematologic and immunologic parameters as well as thyroid, adrenal, and hepatic function do not show abnormalities in CS. Glucose tolerance tests, basal or stimulated growth hormone levels, and responses to insulin, arginine, and glucagon have not revealed the causes of the dramatic dwarfing and cachexia (Rapin et al. 2000), nor did growth hormone therapy result in significant progress in growth (Nance and Berry 1992).

Most frequent radiological findings include intracranial calcifications, sclerotic epiphyses most prominent in the fingers and pelvic and vertebral anomalies including kyphosis. Osteoporosis was noted in a few patients pointing to premature ageing of the skeleton. Nevertheless, bone age in CS has been reported to be variable: in 10 patients, the bone age was advanced, in 6 delayed and in 5 normal. It should be noted that data in the clinical reports are often from different stages of the disease. Thus, in many case reports, absence of certain CS features such as accelerated bone ageing may well result from examinations of younger CS patients. Visual or auditory evoked potentials in CS were always found abnormal. This is reminiscent of profound cataracts, retinal degeneration and deafness observed in CS. Nerve conduction velocity analysis (EMG/NCV) is impaired in most patients. Muscle biopsies have shown variable changes, none thought to be primary.

Analysis of CNS by MRI or CT scans has revealed increased ventricular size and/or cerebellar and cerebral atrophy and/or calcifications in basal ganglia and elsewhere (Nance and Berry 1992). Calcifications as well as appearance of neurofibrillary tangles reported in some cases of CS (Takada and Becker 1986), are features of normal

ageing, but appear early in CS. Most of the brain anomalies in CS are associated with white matter, or so-called glial compartment. The glial cells, more specifically oligodendrocytes are the cells, which isolate axons of the neurons (grey matter) by wrapping them into a myelin sheet. Proper myelinization is required for high velocity conduction as well as neuronal survival. It has been proposed, that demyelinization is the primary neuronal defect in CS (Brooks 2002). Nevertheless, recent post-mortem examinations of CS patients have revealed neuronal loss within several neuronal populations, such as those in the Meynert nucleus, putamen/caudate, thalamus, globus pallidus, dentate nucleus, spinal motor neurons, granule cells and Purkinje cells (Itoh et al. 1999). These changes are likely to be primary since demyelinization was not reported in those areas. Many CS patients display hypogonadism, such as undescended testis. It is tempting to speculate that underdeveloped gonadal axis may contribute to neuronal loss as gonadal steroid hormones are implicated in survival of several neuronal populations, such as hippocampal neurons, also implicated in CS (Hayashi 1999; Azcoitia et al. 2003). Astrocytes, the second of the three glial populations in the CNS, are also affected in CS. They are found pleomorphic, a few are multinucleated, and many are bizarre and irregularly shaped with swollen, lobulated, hyperchromatic nuclei (Rapin et al. 2000). Interestingly, similar bizarre astrocytes and Purkinje cell loss is found in ataxia-telangiectasia (AT) patients (Lindenbaum et al. 2001). AT-mutated (ATM) protein is a key regulator of signaling downstream of DNA damage. Thus, the cellular signaling as a response to defective DNA repair in CS, or defective signaling on its own in AT can lead to similar pathology.

COFS can be also regarded as a severe form of CS. To date only 11 patients have been described (Graham et al. 2001) (N. Jaspers per. comm.). Symptoms include reduced birth weight, early microcephaly with subsequent brain atrophy, reduced white matter, patchy grey matter, hypotonia, deep-set eyes and cataracts. Movement is markedly decreased, joint contractures common. Like in case of CS patients (and XP patients with DeSanctis-Cacchione syndrome, see below) a frequent cause of death is pneumonia/respiratory infections.

About 50% of CS patients are sun-sensitive and patient derived fibroblast cells display a defect in nucleotide excision repair (NER) of UV-induced DNA lesions in the transcribed strand of active genes (Venema et al. 1990; Nance and Berry 1992). A similar notion has been made for COFS cells (Graham et al. 2001).

Trichothiodystrophy (TTD)

The clinical manifestation of TTD patients, including developmental delay, cachexia, neurodyemyelination, cerebellar ataxia, mental retardation, microcephaly, sensorineural deafness and cause of death is largely overlapping with that of CS (Itin et al. 2001). Distinguishing hallmark of TTD from CS is scaling skin, and brittle hair and nails. The latter is thought to be caused by greatly reduced content of cysteine-rich matrix proteins in the hair-shafts, leaving the hair fragile and vulnerable to physical

breakdown (Lehmann 2001). Pathological changes in the epidermis include hyperke-ratosis (thickened keratin layer responsible for the scaling skin) and acanthosis (thic-kening of epidermal layer). Both absence or hypertrophy of the granular layer in the skin has been reported in some cases (Itin et al. 2001). Similar to CS and COFS, cells from about 50% of TTD patients are UV sensitive and display a defect in nucleotide excision repair (NER) of UV-induced DNA lesions.

Xeroderma Pigmentosum (XP) and XP with DeSanctis-Cacchione syndrome (XP-DSC)

Unlike CS, TTD and COFS, XP is always associated with clinical and cellular sensi-tivity to ultraviolet radiation and defective repair of UV-induced DNA lesions. To date ~ 1000 XP patients have been described in the clinical literature. First symptoms of sun sensitivity in XP become evident at average age of 2 years, when intense freckling and/or sun-burn is first noted. XP patients display a more than 1000 fold elevated risk to develop sun-induced malignant skin neoplasms such as squamous cell carcinomas (SCC) and basal cell carcinomas (BCC). Yet, the frequency of metastasis appears to be quite low (5 out of 112 XP patients with SSC). Interestingly, only 5% of XP patients are reported to develop melanomas. While 97% of SCC and BCC appear on sun-exposed areas such as face, head or neck, only 65% of melanomas were associated with this area, indicating that induction of a melanoma involves more complex and probably systemic factors. Among ocular tissues, the eyelids, conjuncti-va and cornea receive substantial amounts of UV radiation and subsequently are strongly affected in XP patients. Anomalies of the eyelid include sunburn, atrophy of the skin, loss of lashes or even the whole eyelid (Kraemer et al. 1987).
Corneal abnormalities include corneal clouding and/or vascularization. Neoplasms of the eye are exclusively associated with conjuctiva, eyelid and/or cornea whereas SCC is the most frequently occurring neoplasm.
Neurological abnormalities are reported in about 20% of XP patients (XP with DeSanctis-Cacchione syndrome (XP-DSC)). Although extraneurologic features such as number and agressiveness of skin tumors between XP and XP-DSC patients appe-ar similar, the average onset of sun sensitivity for XP-DSC is 6 months versus 2 years for classical XP (Kraemer et al. 1987), indicating that neurological dysfunctioning may be involved in the onset of UV-induced dermal and ocular pathology. 80% of XP-DSC patients are mentally retarded, whereas less than a quarter of the patients display concomitant microcephaly, growth retardation, gait anomalies such as spasti-city and ataxia; and sensorineural deafness, all of which have a progressive character (Kraemer et al. 1987; Itoh et al. 1999; Brooks 2002). As in case of CS, COFS and TTD, the earlier the onset of neuronal features in XP-DSC, the more pronounced retardation of growth and sexual development is noted (Kraemer et al. 1987; Itoh et al. 1999; Rapin et al. 2000) again strongly suggesting a link between DNA repair, neuronal deployment and survival, and somatic development and maintenance. The

above notion is supported by studies in model organisms, such as the fruit fly
(Drosophila melanogaster). When oxidative damage load in motorneurons is lowered
by over-expressing ROS scavenger enzyme superoxide dismutase 1 (SOD1), the flies
live 140% longer than wt (Parkes et al. 1998).
What is the difference between CS and XP-DSC? CS is associated with more severe
symptoms, including microcephaly and cachexia. The predominant difference seems
to lie in the cell-type affected in the CNS. Except for the neuronal loss in the cerebel-
lum, CS specific demyelination in other areas of CNS leaves the neurons relatively
intact. In XP-DSC myelin is not affected, yet besides neuronal death in the cerebel-
lum (resulting in CS like ataxia) several other neuronal populations die in the other
areas of the CNS, such as in the cortex and substantia nigra, resulting in progressive
intellectual deterioration, dementia and gait anomalies (Itoh et al. 1999; Rapin et al.
2000; Brooks 2002). Why the CS defect primarily affects the myelinating cells (oli-
godendrocytes) and XP-DSC defect the neuronal cells, and how this results in often
overlapping phenotype remains to be elucidated. Since neuronal conductivity is a
function of proper myelination (Brooks 2002) and neurons and not oligodendrocytes
establish the cellular connections both within CNS and with the soma, it is tempting
to speculate that at least a subset of overlapping features of CS and severe XP-DSC
are caused by a defect in neuronal functioning.

XP combined to CS (XPCS)
In rare cases (n= 9), (plus several unpublished cases (A.R. Lehmann per. comm.,
W. Kleijer per. comm.)) a combined XPCS pathology has been reported (Lindenbaum
et al. 2001). There is a remarkable degree of clinical variation in XPCS. The three
patients with XPCS carrying a defect in the *XPB* gene (see Table 1) had a much less
severe CS phenotype with survival between the forth and the fifth decade of life
compared to those in groups *XPD* and *XPG*. Two patients in *XPD* group and the
remaining four in *XPG* group all displayed very severe disease (Lindenbaum et al.
2001). The patient XPCS2 (XPD-G602D) phenotype at 9 years of age included clas-
sical features of both XP and CS. He had CS characteristic facies associated with
acquired microcephaly, severe mental retardation and progressive dementia, gait
abnormalities and cachectic dwarfism, retinal degeneration, demyelinating neuropa-
thy, spasticity, reduced nerve conduction of the leg, cryptorchidism (a form of under-
developed testis) and hyperactive reflexes in the lower extremities. He died at the age
of 13. XP pigmentary changes were evident as early as at 2 weeks of age, the first
skin tumor was noted at 2.5 years of age (Dupuy et al. 1974; Moshell et al. 1983;
Lindenbaum et al. 2001). The other XPD-XPCS patient and all XPG-XPCS patients
displayed even more severe pathology and died at age of 7 months, 1.7, 2, 6.2 and
6.5 years respectively (Lindenbaum et al. 2001). Unfortunately, an overall
chronological pathology record for the most of the above patients is absent.
Pathology of patient XP20BE (XPG-XPCS, see Figure 2) has been documented the

Age:
4 months   1.5 years   6 years   6 years   6 years
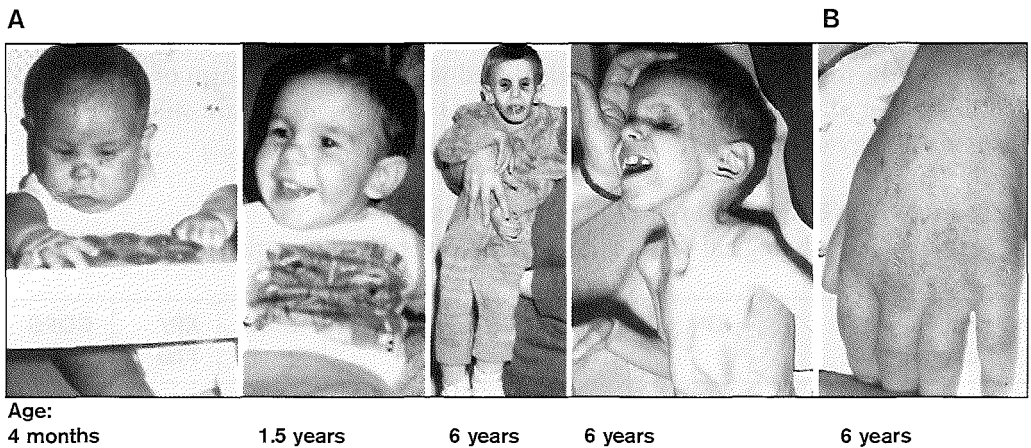
Figure 2. *XPCS patient XP20BE (XPG-XPCS). A. Progressive pathology of Cockayne syndrome. Note the nor-*
mal fullness of the face at 4 months and 1.5 years of age and the typical CS appearance with deep-
set eyes, prominent ears and profound cachexia at the age of 6 years. B. Age 6 years. XP pigmentary
changes and CS specific wrinkling of the skin of the hand showing signs of premature ageing.
Adapted from (Lindenbaum et al. 2001).

best and will be herein described briefly.
Electromyogram (EMG) analysis suggested primary neuropathic but notably also pri-
mary myopathic features, suggesting that muscle cell degeneration can also occur
independently of axonal loss in PNS of XPCS. Patient XP20BE died at the age of 6.2
years because of profound cachexia and pneumonia. His brain weight was 350g,
while the expected brain weight of a child at that age is 1200g. Most of the pathologi-
cal findings in the brain were typical for CS. In the midbrain the substantia nigra had
focal neuronal loss-a feature characteristic for XP-DSC. Neuronal loss was noted also
in hippocampus and certain brainstem nuclei. The cerebellum displayed typical CS
features, including neuronal loss in Purkinje and internal granular layers. Taken toge-
ther, loss of myelinated fibers and neurons was profound with resultant dementia,
ataxia and notably-dysmetria (a polar neuropathological condition, where one body
side is affected more than the other) (Lindenbaum et al. 2001). Is neuronal cell death
primary or secondary to de-myelination? Most of the demyelinating lesions are found
outside of the cerebellum. Purkinje cells are innervated mostly by granular cells
within the cerebellum and not by neurons from other brain areas. Thus, the loss of
Purkinje cells (and granular cells) is likely the primary neuronal defect and not
secondary to oligodendrocyte defect. Taken together, the extreme CNS pathology
seen in XPCS and CS likely results from the primary DNA repair defect in oligoden-
drocytes, some neuronal populations and to some extent, a combination of these cell
types.

XP combined with TTD (XP/TTD)

Very recently, four patients have been identified with a combined form of XP/TTD (Broughton et al. 2001) (K. Kraemer per. comm.). All the patients are still alive and disease etiology of this condition is still largely unexplored.

Summary of NER associated clinical features

A summary of pathological features of NER disorders is summarized in Table 2.

Clinical symptoms	XP	XP-DSC	CS	TTD	XPCS	XP/TTD	COFS
UV sensitivity	++	++	++(*)	++(*)	++	++	?
Increased freckling	++	++	-	-	++	++	?
Skin cancer	++	++	-	-	++	+	?
Cachectic dwarfism	-	+	++	++	++	+	+++
Microcephaly	-	+	++	++	++	?	+++
Progressive cognitive impairment	-	+	++	++	++	++	+++
Sensorineural deafness	-	+	++	++	++	-	+++
Eye abnormalities	-	+	++	++	++	?	+++
Skeletal abnormalities	-	-	+	+	+	?	++
Spasticity	-	+	++	++	++	?	+++
Ataxia	-	+	++	++	++	-	+++
Axonal neuropathy	-	++	+/-	?	+	?	?
Demyelinating neuropathy	-	-	++	++	++	?	?
Myopathy	-	-	-	-	+/-	-	?
Brain calcification	-	-	++	++	++	?	+++
Hypogonadism	-	+	++	++	++	?	?
Brittle hair and nails	-	-	-	++	-	+	?
Hyperkeratosis	-	-	-	++	-	+	?
Progeria	-	+/-	++	++	++	?	?

Table 2. Clinical symptoms of NER disorders
(*) ~50% of patients display this feature
Assembled from recent literature reports (Rapin et al. 2000; Broughton et al. 2001; Itin et al. 2001).

1.4 What defines the specifity of NER-associated disease?

Although NER is an ubiquitous repair mechanism likely auditing the genome in each cell of our body, associated disorders display substantially different pathologies, ranging from mild UV sensitivity to >1000 times elevated cancer risk (XP) to accelerated ageing (CS) and combinations of these. From this pathological diversity it is clear that not all the tissues and cell-types are affected in a similar manner. For example,

the enhanced skin-cancer in XP is attributable to UV-induced enhanced mutation rates in the basal layer of the skin. The most prominent feature of XP-DSC is the loss of neurons, while likely primary oligodendrocyte dysfunctioning constitutes a dominant pathology in CS. Thus, different mutations in different NER genes can lead to cell-type specific pathologies.

Why do mutations in NER proteins specifically affect cells of neuronal origin? Several lines of evidence suggest neuronal type of cells to utilize NER in a highly specific manner. First, neurons and especially differentiated neurons are dramatically more UV sensitive than e.g. Hela cells (James et al. 1982). It has been shown, that GG-NER activity declines dramatically during neuronal differentiation in vitro (Nouspikel and Hanawalt 2000) and thus e.g. cannot support DNA repair when TCR activity is hampered by a CS type of mutation. From clinical studies it is known, that demyelination (white matter loss) is a late response to CNS gamma irradiation (van der Maazen et al. 1993). Pathological findings in the brains of chemotherapeutically treated or gamma irradiated patients (and laboratory animals) reveal neuronal and glial degeneration (Brooks 2002)(D. Dickson per. comm.) and post-mortem comparison of brains from the above patients with those from CS patients and normal ageing individuals revealed a remarkable degree of pathological similarity (D. Dickson per. comm.). Taken together these observations suggest that neurons and glia are hypersensitive to DNA damage of both exogenous (e.g. gamma rays) and endogenous (reactive metabolites, e.g. ROS) origin. Time-dependent preferential vulnerability of neuronal tissue to endogenous damage is also supported by studies suggesting the involvement of ROS in the onset of Parkinson's disease, dementia and Alzheimer's disease (reviewed in (Butterfield et al. 2001; Betarbet et al. 2002)) as well as by studies with non-homologous end-joining (NHEJ) defective (XRCC4 knock-out) mice, which display embryonic lethality likely due to massive neuronal apoptosis (Gao et al. 2000).

Both, neurons and glia are transcriptionally highly active (Brooks 2002) and thus likely hypersensitive to TCR defects. Why neurons in XP-DSC and oligodendrocytes (and to a lesser extent astrocytes and specific neuronal populations) in CS are primarily affected and what defines this specificity is currently unknown. Recently, it was found, that in differentiated neurons TCR has a different mode, so-called differentiation associated repair or DAR. DAR preferentially repairs both, transcribed and non-transcribed strands of genes (Nouspikel and Hanawalt 2000). The importance of DAR in XP-DSC or CS neuropathy is unknown.

Why CS, COFS and TTD patients gradually loose subcutaneous fat tissue is currently unknown, but the absence of any detectable endocrine symptoms suggests that the defect might lie in the adipocyte stem-cell compartment in the bone marrow.

Recently, we found that embryonic stem cells are more vulnerable to genotoxic stress than fibroblasts or keratinocytes (de Waard et al. 2003), suggesting, that stem cells, in order to avoid damage accumulation and subsequent tissue malfunctioning and/or

carcinogenesis have a lower apoptosis threshold than other cell types. In concordance with that notion, various CS mouse models presented in this thesis display time-dependent loss of tubular germinal epithelium in the testis. Although hypogonadism is a prominent feature in CS, COFS and TTD, to our knowledge, histological examinations have not been performed and thus human-mouse comparisons of that tissue type can not be made.
Dramatic neuropathy is the most severe disease feature of XP-DSC, CS, COFS and TTD. Our pathological knowledge is sofar mainly based on post-mortem findings. The main obstacle in defining the progressive disease etiology and intervention strategy lies in the fact that mouse-models for those disorders have thus far failed to phenocopy the human neuropathy.

1.5 DNA metabolism and other progeroid syndromes

Werner syndrome, Bloom syndrome and Rothmund-Thomson syndrome
All the above conditions are triggered by mutations in 3 different Rec-Q like DNA helicases respectively. Rec-Q like helicases are involved in DNA metabolism such as repair and replication and thereby safeguard genomic stability. Mutations in the above genes lead to accelerated ageing features including early alopecia (loss of hair), osteoporosis, malignancies, artherosclerosis, diabetes, cataracts, telangiectasia, skin atrophy and greying of hair.

Ataxia telangiectasia
Ataxia telangiectasia mutated (ATM) protein is a DNA damage sensing signalling protein kinase. AT symptoms include skin atrophy/sclerosis, telangiectasia, immuno-deficiencies, malignancies (mainly lymphomas), greying of hair, poikiloderma, neurodegeneration (cerebellar ataxia resulting from loss of Purkinje cells) (see (Hasty et al. 2003) and references therein).

Hutchinson-Gilford progeria syndrome (HGPS) and atypical Werner syndrome
Mutations in LMNA gene (encodes for the type A nuclear lamins) are responsible for HGPS and atypical Werner syndrome. HGPS is known as progeria of childhood, with features including atrophy of subcutaneous fat, alopecia, short stature, premature artherosclerosis and panel a of muscuskeletal abnormalities. LMNA is a structural component of the nuclear envelope involved in regulating mitotic signalling pathways. Mutations in LMNA cause reduced mitotic instability, shortened telomere length and diminished DNA repair (Martin and Oshima 2000; Mounkes and Stewart 2004).

1.6 Other human premature ageing syndromes

While in several model organisms caloric restriction and inhibition of the insulin pathway leads to lifespan extension, defects in energy metabolism pathways such as lipid and carbohydrate metabolism in humans can lead to segmental accelerated ageing symptoms, such as observed in type 2 diabetes mellitus or in congenital generalized lipodystrophy (Seip-Berardinelli syndrome). The latter syndrome is associated with profound generalized atrophy and agenesis or dystrophy of metabolically active adipose tissue which leads to hyperinsulinaemia, hypertriglyceridaemia, retinopathy, cardiomyopathy, angina pectoris, myocardial infarction, osteosclerosis, proteinuria and renal failure (Seip and Trygstad 1996). Another remarkable progeroid phenotype in humans is called "anabolic syndrome". These young patients have voracious appetites and exhibit rapid pre-pubertal growth, advanced bone age and muscular hypertrophy which is followed by an array of accelerated degenerative pathologies including diabetes and its sequelae (Martin and Oshima 2000). What is the primary cause of progeria in the above metabolic diseases? Although the exact mechanism remains unknown, several clues are starting to emerge. Recently, it was found that caloric restriction directly reduces mitochondrial H_2O_2 production (and thus intracellular oxidative damage load) with no change in mitochondrial respiration rate. The effect could be reversed by increase in insulin levels, a finding which may bridge the insulin and ROS theory of ageing (Lambert and Merry 2004). Currently, the major bottleneck in relating the ROS theory of ageing to DNA repair lies in our inability to quantitatively evaluate endogenous DNA damage level (which likely includes hundreds of different lesion types per cell per day) and the repair rate. If and how genome maintenance is involved in the onset of accelerated ageing features in metabolic disorders such as diabetes, remains to be addressed.

1.7 DNA repair pathways

Basic DNA repair mechanisms are conserved in evolution from unicellular bacteria and simple eukaryotes such as bakers yeast to higher eukaryotes, such as primates. In mammals, multiple partially overlapping DNA repair mechanisms exist, each with their own damage specificity. These repair mechanisms use different modes of damage recognition, which in most cases depends on the effect the damage poses on the DNA in terms of helix distortion, obstruction of DNA probing, or blockage of DNA replication or transcription (Hoeijmakers 2001). Base excision repair (BER), mismatch repair (MMR), double strand break repair, replication-associated lesion bypass synthesis and nucleotide excision repair (NER) are the main DNA repair pathways. Below, the basic mechanism and clinical relevance of each pathway is briefly summarized followed by more extensive introduction into the mechanism of NER.

Base excision repair (BER)

Oxidative damage, which most often delivers small, non-helix distorting changes to the DNA, is considered to be the main damage to the genome. BER removes bases with small chemical alterations, like oxidative and alkylating damages and thus serves in a frontline battle in eliminating the deleterious consequences of ROS produced by normal oxidative metabolism. There are likely more than 100 different types of oxidative lesions alone in the mammalian DNA, illustrating the diversity of lesions BER is coping with. Furthermore, spontaneous formation of abasic sites – another lesion type BER is dealing with, is estimated to be ~10.000 per cell per day. Other examples of frequently induced and often highly mutagenic BER lesions are 8-oxoguanine, O6-methylguanine, deaminated methylated cytosine (uracil) and thymine glycol (Beckman and Ames 1997; Krokan et al. 1997; Wilson and Thompson 1997). The first step in BER reaction is damage recognition and release of damaged base, an event carried out by enzymes called DNA glycosylases. This step is followed by the "core" BER reaction, which involves APE/HAP1, XRCC1, LIG1, Polβ proteins. "Core" BER removes the abasic site followed by either one-nucleotide gap filling (short patch repair) or removal and renewal of a short stretch of DNA next to the damage (long patch repair). Disruption of "core" BER components in the mouse causes embryonic lethality (Wilson and Thompson 1997), explaining the apparent absence of BER-deficient human syndromes. Disruption of specific glycosylases, such as Ogg1, Agg or mNTH in mice results in a wt phenotype. In vitro studies suggest, that glycosylases have an overlapping, redundant activity, and thus likely elimination of one is compensated by the others. Notably, repair of 8-oxoguanine in the transcribed strand of active genes is defective in human Cockayne syndrome patients (Le Page et al. 2000), highlighting the interwoven character of transcription- coupled NER and BER. Nevertheless, concomitant inactivation of either Ogg1, Aag or mNTH in CS or TTD mouse models did not result in an overt enhanced disease phenotype (I. van der Pluijm et al., manuscript in prep., J.O.A. et al., manuscript in prep.) likely due to the redundant character of glycosylases.

Mismatch repair (MMR)

DNA mismatch repair can recognize and repair all 8 possible mismatches as well as small 1-5 bp insertion/deletion mispairs that are left behind by the DNA polymerases (Modrich 1997). The error rate of mammalian polymerases depends on their proofreading capacity and varies between 10^5 and 10^6 (Umar and Kunkel 1996), thus leaving behind thousands of mismatches per replication cycle per cell. After recognition of damage the MMR pathway distinguishes between the correct and "wrong" strand, which at least in E. coli occurs according to the strand-specific methylation fingerprint. Subsequently, MMR exonucleases degrade the "wrong" strand, which can include hundreds of bases followed by gap filling and ligation. The best known clinical consequence of mutated MMR genes (such as MLH1, MSH2 or PMS2) is the

human hereditary nonpolyposis colon cancer (HNPCC)(de Wind et al. 1995; Modrich and Lahue 1996).

Double strand break, and interstrand crosslink repair

Endogenously produced oxidative radicals (ROS) and ionizing radiation can both induce double strand breaks (DSB-s) which together with interstrand DNA crosslinks are considered the most toxic type of DNA damage. DSB-s are repaired by homologous recombination (HR) - an essentially error-free pathway mainly dominating in germ- and stem-cells and proliferative cells in S and G2 phases of the cell cycle and non-homologous end-joining (NHEJ), a more error-prone pathway mainly associated with differentiated cells.

HR includes nucleolytic processing of the DNA ends and a search for the homologous sequences, present on the sister chromatid during or after S phase DNA replication. Next, a joint molecule between the homologous damaged and undamaged duplex is formed, followed by DNA synthesis, ligation and resolution of recombination intermediates. Molecules involved in mammalian HR include the Rad50 complex, (consisting of Rad50, Mre11 and NBS1), Rad51, Rad52 and Rad54 (van Gent et al. 2001). Besides repair, the Rad50 complex is also involved in cell cycle checkpoints via NBS1 phosphorylation by ATM (Falck et al. 2002). A common feature of AT (ataxia telangiectasia) and NBS (Nijmegen breakage syndrome) is chromosomal instability and increased frequency of lymphomas (Duker 2002). Mutations in Mre11 result in AT-like disorder (ATLD)(Stewart et al. 1999). Defects in NHEJ can lead to hypersensitivity to ionizing radiation, genomic instability, severe immunodeficiency due to defective V(D)J recombination and segmental premature ageing (Vogel et al. 1999; Hasty et al. 2003). This pathway uses very limited or no sequence homology. In yeast, the initial step in NHEJ requires Rad50, Mre11 and the yeast homologue of NBS1 Xrs2. The Ku heterodimer, consisting of subunits Ku80 and Ku70 binds to DNA ends and recruits the DNA-dependent protein kinase catalytic subunit DNA-PKCS, forming a complex which is referred to as DNA-PK. Further steps in NHEJ include XRCC4 and DNA ligase IV (Jeggo 1997; van Gent et al. 2001). Ku80 (Ku86) -deficient mice exhibit several characteristics of segmental premature ageing (Vogel et al. 1999). Interstrand cross-links are extremely toxic DNA lesions. One cross-link per cell is lethal in cross-link repair- deficient mutant of bakers yeast (S. cerevisiae) (Magana-Schwencke et al. 1982) and mammalian (Chinese hamster) mutant cells can be up to 100 times more sensitive to cross-linking agents than wild-type cells. The repair process involves homologous recombination proteins but notably also depends on some NER proteins, such as the XPF/ERCC1 complex. ERCC1-deficient mice display symptoms of segmental accelerated ageing (Weeda et al. 1997; Mitchell et al. 2003).

Nucleotide excision repair

One of the most versatile DNA repair mechanisms is nucleotide excision repair (NER) that can remove a wide variety of DNA helix-distorting injuries of both exogenous and endogenous origin. NER is responsible for the removal of cis-syn-cyclobutane dimers (CPDs) and pyrimidine (6-4) pyrimidone photoproducts (6-4PPs), induced by the UV component of the sunlight. The clinical relevance of the above types of lesions is evident from the sun-sensitivity and cancer predisposition of xeroderma pigmentosum patients. NER also removes bulky chemical adducts, intrastrand cross-links and several forms of oxidative damage such as cyclopurines induced by reactive chemicals, e.g. ROS or cigarette smoke (Smith and Pereira-Smith 1996; Hoeijmakers 2001). In concordance with the latter notion, XP patients display ~ 10 to 20 fold elevated risk for developing internal tumors (Kraemer et al. 1984). NER is a multistep process that requires the concerted action of at least 30 proteins. Two major pathways can be distinguished: global genome NER (GG-NER) and transcription-coupled NER (TC-NER). These pathways utilize different modes of damage recognition. In GG-NER, the hHR23B/XPC complex recognizes the lesion, followed by the recruitment of the rest of the NER machinery. For some lesions the UV-DDB (XPE) complex is an important auxiliary factor. In TC-NER, blockage of the elongating RNA-PolII is believed to initiate the repair, a process which requires the CSB and CSA proteins (de Laat et al. 1999). The lesion recognition step is followed by the recruitment of TFIIH complex and XPA. The XPD and XPB helicase components of the ten subunit TFIIH complex melt ~30bp of DNA around the lesion, whereas XPA is essential for the damage demarcation and NER complex stability. Studies with cells derived from XPA-deficient patients and rodents demonstrate the lack of both GG-NER and TC-NER activity as well as the absence of core NER complex formation (Volker et al. 2001). Next, the structure-specific endonuclease XPG performs incision 3' from the lesion, followed by 5'cleavage by the XPF/ERCC1 complex. NER is completed by gap-filling of the excised patch by DNA polymerases (such as DNA-Polε or-σ) and the resulting nick is ligated, likely by DNA ligase I. Notably, reversible phosphorylation of NER factors is important for dual incision in vitro (Ariza et al. 1996), hinting to tight probing and regulation of the reaction. Moreover, strong functional interactions between TFIIH and XPC and XPG have been noted, suggesting the formation of a highly complex structure (Araujo et al. 2001). In vivo, the NER complex is assembled at the site of damage in a relatively short time, (few seconds). Then the complex stays stable for about 4 minutes during which the repair reaction is believed to take place, which is then followed by simultaneous release of all of its components (Hoogstraten et al. 2002). The scheme of GG-NER and TC-NER reaction is depicted in Figure 3. The NER mechanism and implications for the phenotype are revisited in Chapter 8 where findings in this thesis and recent results by other researchers are discussed.
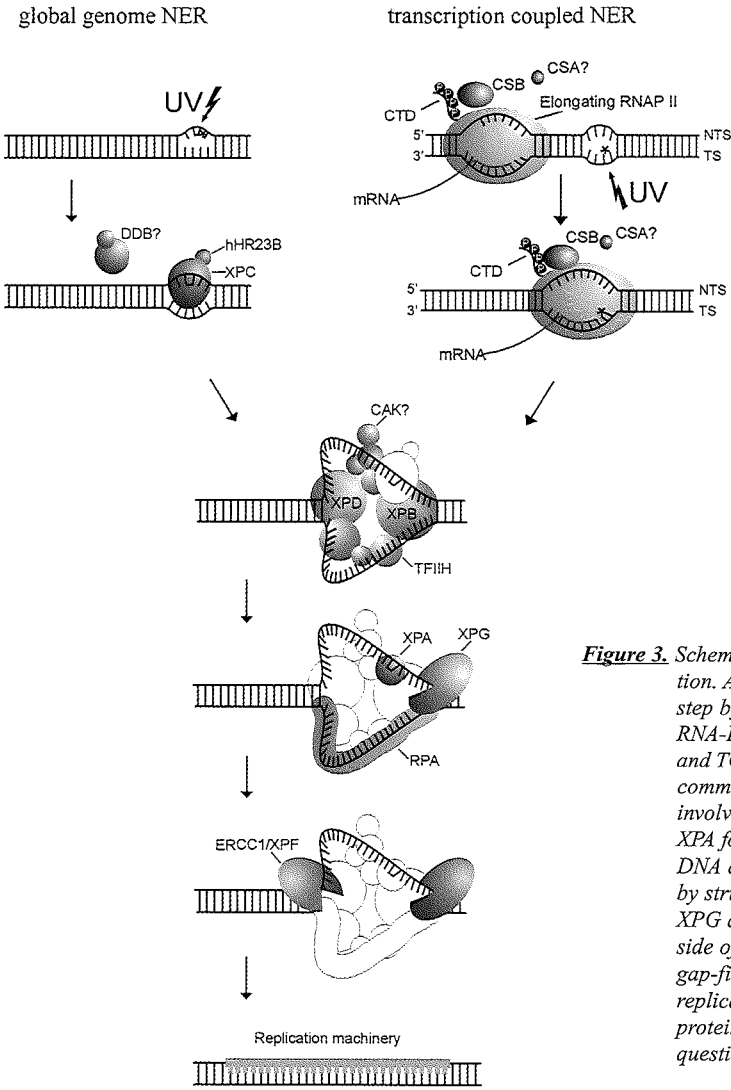
Figure 3. Schematic outline of the NER reaction. After the damage recognition step by hHR23B/XPC or elongating RNA-PolII respectively, GG-NER and TC-NER pathways utilize the common core NER reaction, which involves recruitment of TFIIH and XPA followed by melting of the DNA around the lesion and excision by structure specific endonucleases XPG at 3' and XPF/ERCC1 at 5' side of the lesion respectively; and gap-filling and ligation by the replication machinery. The role of proteins in NER indicated with a question mark is uncertain.

1.8 The enigmatic differences between clinical phenotypes of NER disorders

The large differences in disease etiology of XPA (completely defective in both GG-NER and TC-NER) and e.g. CSB and CSA (defective only in TC-NER) patients led researchers to hypothesize, that mutations in NER proteins resulting in symptoms different from XP such as those observed in CS, TTD, XPCS, XP/TTD and COFS might be due to the fact that the encoded proteins perform functions outside the context of the classical NER pathway.

Two parallel mutually non-exclusive hypotheses have been considered. First, the "transcription syndrome" hypothesis, based on TFIIH dual functionality in NER and transcription. Mutations in these proteins may, besides NER, also affect the basal and/or activated transcription (Bootsma and Hoeijmakers 1993; Vermeulen et al. 1994b; Bergmann and Egly 2001; Keriel et al. 2002). Due to the exclusive association of mutations in TFIIH subunits with TTD, this condition has been suggested to result at least in part from defects in basal transcription (Vermeulen et al. 1994b; de Boer et al. 1998a; Bergmann and Egly 2001). The latter hypothesis was supported by early findings that mRNA levels of proteins responsible for the lower level of cros-slinking of keratin filaments in the skin of TTD mice are reduced (de Boer et al., 1998). In addition, recent biochemical studies demonstrate that TTD, but not XPCS type of mutations in TFIIH result in defective basal transcription initiation in vitro (Dubaele et al. 2003). Secondly, the transcription coupled repair (TCR) hypothesis, based on the notion that CS, and XPCS cells are sensitive to oxidative agents. Since oxidative lesions are normally repaired by BER and not by NER, the existence of a general TCR pathway was suggested, in which proteins involved in CS are required to repair not only transcription-stalling NER lesions but also BER, and perhaps other transcription-blocking injuries (Cooper et al. 1997; Citterio et al. 2000b).

To what extent the above hypothesis reflects the molecular cause of CS, TTD or other NER-associated severe neurodevelopmental conditions still remains obscure. The largely overlapping disease etiology of TTD and CS is best rationalized via a common molecular mechanism: defective general transcription-coupled repair causing the premature ageing features shared between TTD and CS. However, evidence for defective repair of ROS-induced lesions in TTD patient cell-lines is lacking whereas mouse TTD cells appear not significantly sensitive to oxidative agents (this thesis) making it difficult to interpret TTD as a consequence of a common defect in TCR. Which mechanisms discriminate CS from TTD? Which factors underlie the severity of these diseases? In order to gain insight into the above questions several knock-in mouse models systems were generated and analyzed in this thesis.

1.9 The multifunctional protein complex TFIIH

TFIIH consists of 10 subunits of which six (XPB, p62, p52, p44 and p34) form a tight "core" complex. The XPD helicase is less tightly associated via interaction with the p44 subunit and serves as a bridge between the core and the ternary cyclin-activating kinase (CAK) complex, consisting of CDK7, MAT1 and cyclinH (Egly 2001; Giglia-Mari et al. 2004). Besides a plethora of protein-protein interactions, TFIIH complex embodies three enzymatic activities: XPB and XPD subunits are DNA helicases with opposite polarity, while the CDK7 component of the CAK complex is a kinase. TFIIH is involved in multiple cellular processes such as (i) RNA-PolII driven

basal transcription initiation, (ii) RNA-PolI transcription initiation, (iii) both GG-NER and TC-NER and perhaps general TCR as well (iv) some forms of activated transcription and may have implications in cell-cycle regulation (Harper and Elledge 1998; Le Page et al. 2000; Hoeijmakers 2001; Keriel et al. 2002; Chen et al. 2003).

TFIIH in transcription
TFIIH is essential for RNA-PolII transcription (Schaeffer et al. 1993). Complete Xpd inactivation in mice leads to embryonic lethality at around the 2-cell-stage of embryonal development (de Boer et al. 1998b). For in vitro transcription, XPB helicase activity is absolutely essential, while helicase-dead point-mutated XPD was found to be functional in transcription but not NER (Tirode et al. 1999; Winkler et al. 2000). The CDK7 subunit of TFIIH can phosphorylate the carboxy terminal domain (CTD) of RNA-PolII in vitro, a step essential for the transition of transcription from initiation to elongation in vivo (Dahmus 1995). While the in vivo relevance of CDK7 in this process is still unclear, several transcription factors, such as the nuclear receptors for retinoic acid (RAR), estrogen (ER) and androgen (AR) have been shown to depend on CDK7 phosphorylation for transcriptional activation (Bastien et al. 2000; Keriel et al. 2002). Another type of specific regulation by TFIIH involves transcription of c-myc genes (Liu et al. 2001).
Recent cell-based and biochemical experiments strongly suggest a role for TFIIH in RNA-PolI transcription (Iben et al. 2002). In vivo, an individual TFIIH complex is involved in RNA-PolI and RNA-PolII transcription for about 25 and 6 seconds respectively (Hoogstraten et al. 2002).

TFIIH in cell cycle regulation
Cyclin-dependent kinases (cdk) are key-regulators of the cell cycle. CDK7, the kinase component of the CAK complex, is capable of phosphorylating several components of the cell-cycle regulation machinery, such as CDK1-cyclinB, CDK4-cyclinD and CDK2-cyclinA at least in vitro (Harper and Elledge 1998). The role of TFIIH bound CAK (about 20-30% of the total cellular pool of CAK) in cell cycle progression is unknown. However, it has been shown, that the transcriptional activity of TFIIH is regulated by the factors that control progression through the cell cycle. For example, the phosphorylation of CDK7 renders TFIIH inactive in transcription (Akoulitchev and Reinberg 1998).

1.10 *XPD*-clinically the most diverse NER gene

XPD, one of the two helicase subunits of TFIIH, is pathologically the most diverse NER gene, resulting in 6 different human conditions- XP, XP-DSC, XP/TTD, TTD, XPCS and COFS. Which mechanisms underlie this clinical potential of XPD has

remained obscure. XPD disorders are considered monoallelic diseases, in which the mutant protein product originating from one *XPD* allele (called the 'causative' allele) is thought to determine the clinical outcome as it usually is found linked with one clinical outcome in several patients. The protein originating from the other allele which in many but not all cases carries a molecularly more severe mutation (such as a deletion) is considered a functional null. Representative mutations in the XPD protein are presented in Figure 4. (for review see (Cleaver et al. 1999).
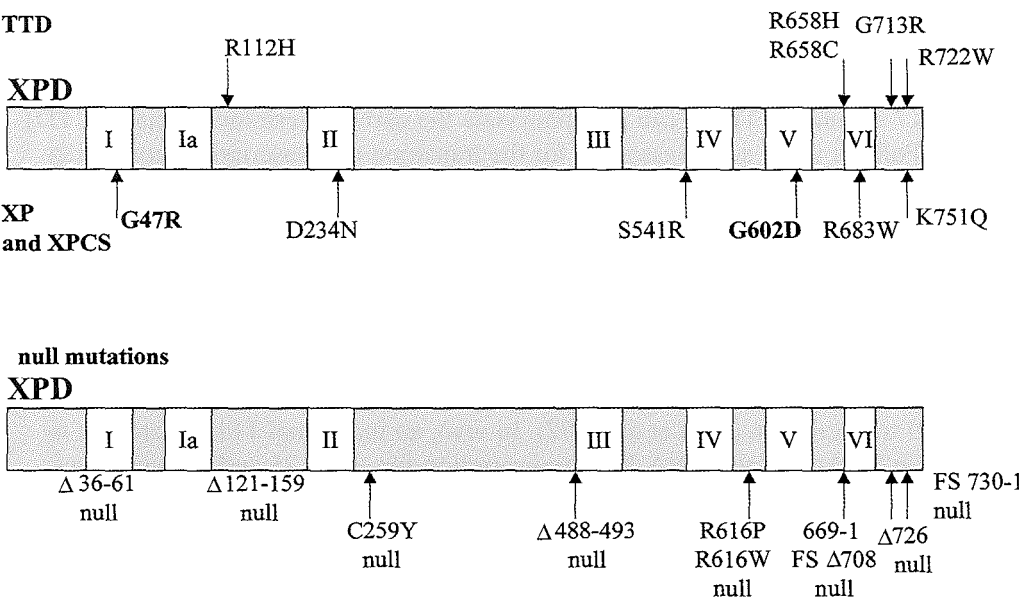
Figure 4. *Predicted proteins from representative disease causing and null alleles in the XPD gene. XPCS causative mutations are indicated in bold.*

Our understanding of the genotype-phenotype relationship of the *XPD* locus is based on the notion that some null alleles can be associated with different XPD diseases and thus are considered unlikely to contribute to the phenotype. Moreover, genocopying of some of the common null alleles in a haploid S. pombe mutant of the *XPD* homologue Rad 15 resulted in a lethal phenotype, arguing, that those *XPD* alleles may be inactive in the diploid mammalian system as well. Nevertheless, the single allele based genotype-phenotype model fails to explain both the exclusive clinical diversity of XPD as well as the heterogeneity in phenotype seen within each XPD disorder. Most of the XPD patients are in fact compound heterozygotes, carrying different *XPD* alleles. The genotype-phenotype relationship of XPD disorders is addressed in greater detail in chapter 3.

1.11 Mouse models for NER disorders prior this thesis

Currently, no biochemical or cell-based assay is able to correlate the NER genotype with the clinical outcome. The classic cellular UV-sensitivity assay does not correlate with accelerated ageing features of CS, TTD or COFS, and about half of those patients are not sensitive to UV light. Although XP cells are always UV sensitive, the likelihood of developing DeSanctis-Cacchione features is unpredictable by this assay. Thus, cell culture systems are limited in studying and predicting the systemic pathological outcomes. Therefore genetically uniform mouse models should be utilized in studying the mechanism and intervention of complex NER associated disease. In chapter 7 at the end of this thesis, the summary of all NER-related mouse models, including the ones generated within this thesis are reviewed and discussed. Below, the general features of mouse models existing prior this thesis are listed.

XPA mice
Mice harbouring an inactive *Xpa* gene carry a complete defect in GG-NER and TC-NER pathways. Although about 20% of human patients carrying an XPA defect display XP-DSC, XPA mice appear to be free of those features (de Vries et al. 1995). Nevertheless, unpublished behavioural studies with XPA mice performed in the Lund University Neuroscience Center, revealed a learning defect using the Morrison water-maze test (Tomasevic et al. 2004). Thus, cognitive defects may be present, but apparently do not take a clear histo-pathological manifestation. In terms of UV sensitivity and cancer predisposition, XPA mice faithfully phenocopy the human situation (de Vries et al. 1995) (Nakane et al. 1995). Moreover, XPA mice display a small, but significant reduction in life-span with no clear pathological manifestation. This notion strongly supports the relevance of NER type of lesions in normal ageing (I. van der Pluijm manuscript in prep.)

CSB and CSA mice
Mice with inactive *Csa* or *Csb* genes carry a defect in TCR but are GG-NER proficient. Both mouse models display a mild CS phenotype, including placid growth delay, mild cognitive and/or neuromotoral deficiency in open field- and rotarod tests, mild cachexia and retinal degeneration. No white matter or neuronal loss has been detected (van der Horst et al. 1997; van der Horst et al. 2002).

XPC mice
Mice lacking *Xpc* are completely deficient in the GG-NER pathway. Similar to all except for one XPC patient, XPC mice are free of XP-DSC neurological features and like their human counterparts, display mildly enhanced photosensitivity and are strongly predisposed to UV induced skin-cancer (Sands et al. 1995; Friedberg et al. 2000)

TTD (XPD-R722W)

TTD mice carry a partial GG-NER and TC-NER defect. How transcription and/or TCR are affected in those mice is addressed later in this thesis. TTD mice display a relatively mild form of the disease compared to human patients with the identical (R722W) XPD mutation. They show mild developmental delay, moderate to severe progressive lipodystrophy, kyphosis, osteoporosis, cachexia, sclerosis of the scull, anemia, sebacious gland hyperplasia and TTD hallmark features - brittle hair and scaling skin (de Boer et al. 1998a)(this thesis). Although occasional tremors were noted, myelin at the sciatic nerve at few months of age was not detectably affected in those mice. General brain pathology at 1.5 years of age also appeared normal (J.O.A. et al., unpublished).

ERCC1

Mice carrying mutations in the *Ercc1* gene and thus defective in the 5' endonuclease step of the NER reaction, live only 2-3 weeks and display severe cachexia and liver and kidney abnormalities. Since totally NER defective XPA mice are devoid of these features, the additional involvement of ERCC1 in interstrand cross-link repair was put forward as causative for the phenotype (Weeda et al. 1997). As a matter of fact the rapidly progressing cachexia and ataxia in ERCC1 mice resembles the human CS condition. The genotype-phenotype relationship of the ERCC1 mouse model is discussed in greater detail in chapter 7.

.

CHAPTER 2

Premature aging in mice deficient in DNA repair and transcription

Jan de Boer,[1][*] Jaan Olle Andressoo,[1] Jan de Wit,[1] Jan Huijmans,[2]
Rudolph B. Beems,[5] Harry van Steeg,[5] Geert Weeda,[1]
Gijsbertus T. J. van der Horst,[1] Wibeke van Leeuwen,[3]
Axel P. N. Themmen,[4] Morteza Meradji,[6] Jan H. J. Hoeijmakers[1][†]

1 Medical Genetics Center, Department of Cell Biology and Genetics,
  Center for Biomedical Genetics
2 MGC Department of Clinical Genetics, CBG
3 Department of Experimental Radiology
4 Department of Endocrinology and Reproduction, Post Office Box 1738,
  Erasmus University, 3000 DR Rotterdam, Netherlands
5 National Institute of Public Health and the Environment, Post Office Box 1,
  3720 BA Bilthoven, Netherlands
6 Department of Radiology, Sophia Kinderziekenhuis, Rotterdam, Netherlands
* Present address:
  Isotis N.V., Prof. Bronkhorstlaan 10 D, 3723 MB Bilthoven, Netherlands.
† To whom correspondence should be addressed. Email: jhoeijmakers@erasmusmc.nl

Summary

One of the factors postulated to drive the aging process is the accumulation of DNA damage. Here, we provide strong support for this hypothesis by describing studies of mice with a mutation in *XPD*, a gene encoding a DNA helicase that functions in both repair and transcription and that is mutated in the human disorder trichothiodystrophy (TTD). TTD mice were found to exhibit many symptoms of premature aging, including osteoporosis and kyphosis, osteosclerosis, early greying, cachexia, infertility, and reduced life-span. TTD mice carrying an additional mutation in *XPA*, which enhances the DNA repair defect, showed a greatly accelerated aging phenotype, which correlated with an increased cellular sensitivity to oxidative DNA damage. We hypothesize that aging in TTD mice is caused by unrepaired DNA damage that compromises transcription, leading to functional inactivation of critical genes and enhanced apoptosis.

Introduction

DNA damage, particularly oxidative lesions derived from normal metabolism, is thought to contribute to aging, but the mechanisms involved remain obscure (Martin et al. 1996; Dolle et al. 1997; Johnson et al. 1999; Kirkwood and Austad 2000). To counteract the effects of DNA damage, an intricate network of DNA repair pathways has evolved (Lindahl and Wood 1999; Hoeijmakers 2001). One important pathway is nucleotide excision repair (NER), which removes helix distorting damage including major ultraviolet (UV)-induced lesions, bulky chemical adducts, and some forms of oxidative damage (de Laat et al. 1999). Xeroderma pigmentosum (XP) patients show the consequences of inherited defects in NER: sun (UV) hypersensitivity, cancer predisposition, accelerated aging of the skin, and, frequently, neurodegeneration (Bootsma et al. 2002). Of the seven XP genes (*XPA–G*), *XPB* and *XPD* are exceptional because different mutations in these genes also cause Cockayne syndrome (CS) and a photosensitive form of the brittle hair disorder trichothiodystrophy (TTD) (Bootsma et al. 2002). TTD and CS are characterized by postnatal growth failure, progressive neurological dysfunction, impaired sexual development, skeletal abnormalities, and a strongly reduced life expectancy, but not cancer predisposition (Itin et al. 2001; Bootsma et al. 2002). A clue to the intriguing clinical heterogeneity linked with *XPB* and *XPD* mutations came with the discovery that these genes encode DNA helicase subunits of the transcription factor IIH (TFIIH) complex (Schaeffer et al. 1993; Schaeffer et al. 1994), which have dual functions: local opening of the DNA around a lesion during NER (Evans et al. 1997) and opening of the promoter DNA during transcription initiation (Holstege et al. 1996). Thus, *XPB* and *XPD* mutations may not only compromise NER, causing photosensitivity, but may also affect tran-

scription (Vermeulen et al. 1994b). To obtain insight into the complex pathophysiology of TTD, we generated mice carrying an *XPD* point mutation [Arg722Trp (R722W)] found in TTD patients. TTD mice displayed many features of the human disease and partial defects in transcription and repair (de Boer et al. 1998a; de Boer and Hoeijmakers 1999). Here, we report that TTD mice develop premature aging features caused by DNA damage.

Premature aging phenotype.

Through regular observation of a large group of TTD and wild-type (wt) littermates, we noticed that TTD mice acquired an "aged" appearance beginning at ~3 months of age (Figure 1). This, together with a shortened life-span (average < 12 months, compared with >2 years for wt littermates, P < 0.0001), early cessation of development (see(de Boer et al. 1998a)), and cachectic dwarfism, prompted us to conduct a more systematic analysis of parameters indicative of premature aging. TTD mice have brittle hair, the hallmark of TTD (de Boer et al. 1998a), that is normally pigmented (Figure 1B).
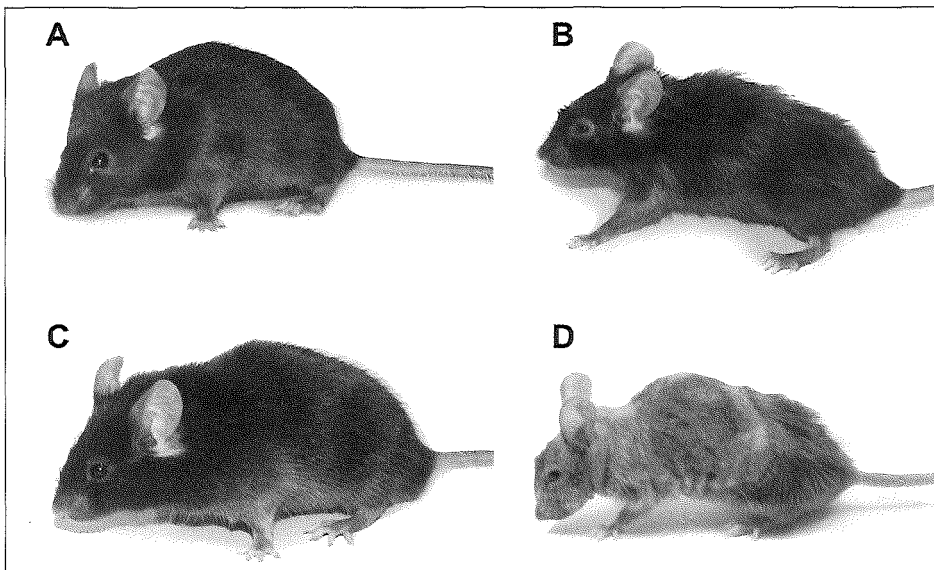
Figure. 1. TTD mice develop normally, then show a premature aging phenotype.
    Shown are wt (A and C) and TTD (B and D) mice at age ~3 months (A) and (B) and 15 to 16 months (C) and (D). Progeroid symptoms (cachexia and kyphosis) start to develop in TTD mice at age 3 to 4 months onward and become increasingly severe.

A
B
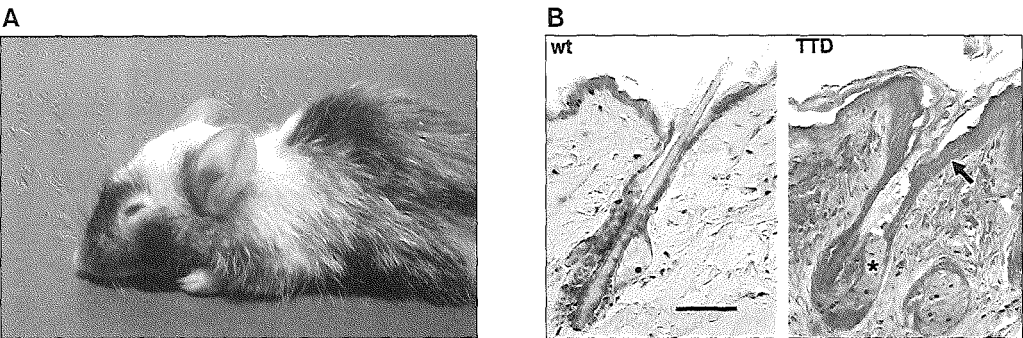
Figure. 2. *Cutaneous symptoms of aging in TTD mice. (A) Typical example of early depigmentation in the fur of a 13-month-old black TTD mouse. No depigmentation was observed in age-matched wt mice (see table 1). (B) Follicular dilation and sebaceous gland hyperplasia (asterisk) in TTD compared to wt skin. Note the hyperkeratotic TTD epidermis (indicated by an arrow). The bar is ;100 μm.*

However, they showed patchy depigmentation (Figure 2A) earlier and more frequently than did wt littermates (Table 1). Melanocytes were absent from grey skin patches, with foci of melanin granules in macrophages as found in normal greying (J. de Boer, et al., unpublished). Young TTD mice also developed greasy hair and showed (benign) hyperplasia of the sebaceous gland (Figure 2B), as observed in human aging (Kumar et al. 1988). The sexual behavior of most young female TTD mice appeared unimpaired (indicative of a normal hormonal status) and occasionally led to full-term pregnancy. TTD males were also fertile until at least 7 months of age (Table 1); thus, initial sexual development per se is unimpaired.

Table 1. *Summary of Aging Phenotype TTD mice.*

|	**Wildtype**	**TTD**
Life span: 50% mortality mark	>2 year	~ 7 months, for survival curve see (1)[1]
Body weight	Normal, obesity in mid life, later loss of weight	Mild growth retardation, later in life more severe with fatty tissue hypoplasia and cachexia
Osteoporosis	Normal at age 14 months	Reduced to 54% of wt, kyphosis of spinal column[2]
Artherosclerosis	Normal [2]	Normal
Red blood cell count	Normal	84% of wild-type, reduced Hb values
Organs	Normal	Normal, except enlarged spleen (anemia?)
Blood chemistry	Normal	Reduced values of branched-chain amino acids
Fertility Male	Normal	Normal (at least to 7 months)
Female	Normal	Initially fertile (reduced), early atrophy of ovary
Hair greying[3,4]	Sporadic	Frequent[1], melanocyte depletion
Skin[3]	Normal	Sebaceous gland hyperplasia
Neurology	Normal	Increased frequency of mild tremors, no overt myelination defect
Sarcopenia	Normal	Increased levels of 1-methyl histidine

1) Influenced by the genetic background; in pure C57/Bl6 life span is significantly longer;
2) Mice in general rarely show artherosclerosis;
3) No correlation apparent with degree of cachexia;
4) At the age of ~14 months 5/5 TTD mice (with sufficient hair) showed pronounced greying, in contrast to 0/22 age-matched wt mice (p < 0,001), at >2 years a significant fraction of wt Bl6 mice shows occasional grey hair.

However, TTD females appeared to lose fertility over time, and to lose it early, because they never produced more than one litter and never after 6 months of age. TTD females (n = 8, age ~16 months) displayed ovarian dysfunction ranging from complete anovulation to sporadic, seemingly normal, ovulation (Figure. 3).
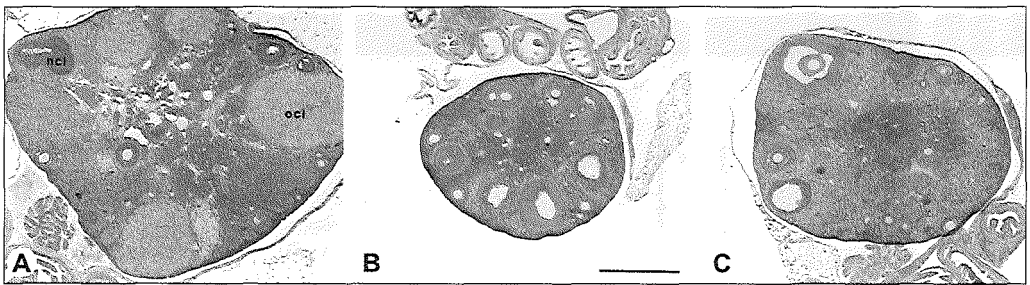
Figure. 3. *Heterogeneous ovarian dysfunction in TTD females. (A) Ovary from a wt control animal at oestrus. Note the presence of old and new corpora lutea. (B and C) Ovaries from TTD females. Two groups of TTD animals could be discerned on the basis of ovarian histology. In the first group (three animals), no signs of an active oestrus cycle were found (B). Ovaries were very small and contained immature preantral and small antral follicles, but no preovulatory follicles. In addition, little interstitium and absent corpora lutea implied complete anovulation. In these animals, a copulatory plug was never observed, probably resulting from the absence of an oestrus cycle. (C) In the other group (five TTD females), a broad range of ovarian dysfunction ranging from complete anovulation to sporadic normal ovulation was found (note the presence of antral follicles with new corpora lutea, but absence of corpora lutea from previous cycles, indicating infrequent ovulation). Ncl, newly formed corpus luteum; ocl, old corpus luteum. The bar is 500 μm.*

There was no correlation between the severity of cachexia and the degree of anovulation, which suggests that the fertility defects were not due to nutritional problems. Rather, they resembled the fertility defects seen in aging rodents (Gosden et al. 1983) and in menopausal women. Although 2- to 4-month-old TTD mice showed no detectable skeletal abnormalities, radiographs of 14-month-old TTD mice revealed prominent kyphosis (curvature of the spinal column) (Figure. 4, A to D) and a generalized reduction in radiodensity of the skeleton, except for the skull. The mineral density of TTD vertebrae was 56% that of wt mice (P < 0.01), and the density of the TTD skull was 119% that of wt (P < 0.05, Figure 4E). Osteosclerosis of the cranium and characteristic birdlike facies have been reported in TTD patients (McCuaig et al. 1993). The osteoporosis and concomitant kyphosis exhibited by TTD mice are hallmarks of aging in humans.
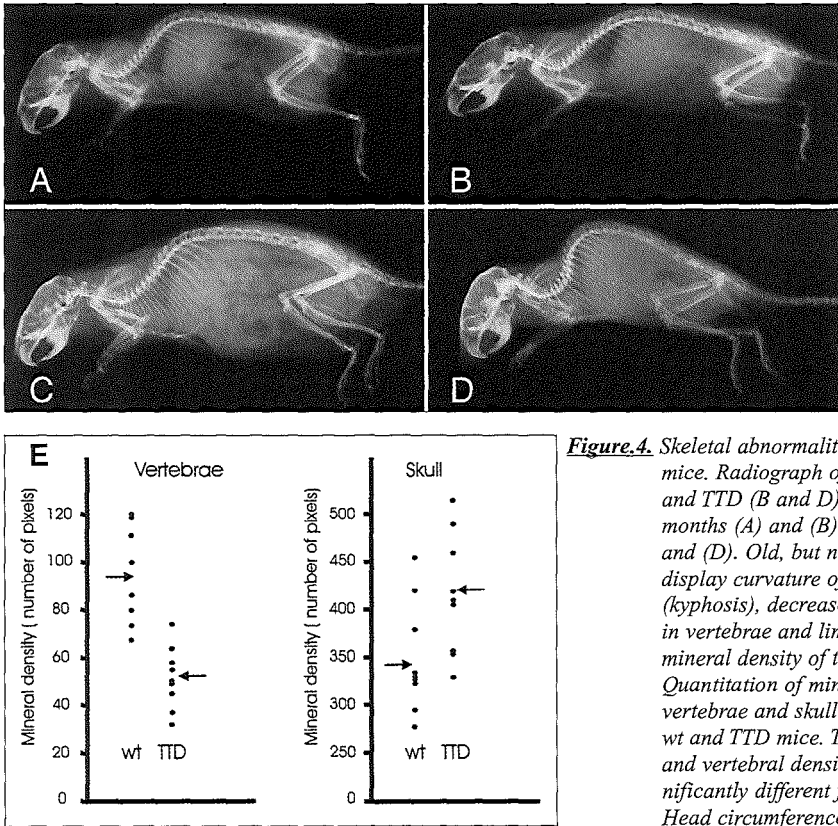
Figure.4. Skeletal abnormalities in aging TTD mice. Radiograph of a wt (A and C) and TTD (B and D) mouse at age 2 months (A) and (B) and 14 months (C) and (D). Old, but not young, TTD mice display curvature of the spinal column (kyphosis), decreased mineral density in vertebrae and limbs, and increased mineral density of the skull. (E) Quantitation of mineral density of the vertebrae and skull in 14- month-old wt and TTD mice. The average for skull and vertebral density (arrows) was significantly different from wt (P<0.01). Head circumference and length of the tibia were not significantly different (J.de Boer et al., unpublished).

The most life-threatening symptom of TTD patients is failure to thrive, which leads to cachexia and, in turn, to a susceptibility to infections, which is a frequent cause of death (Itin et al. 2001). Cachexia in TTD mice was progressive, heterogeneous in onset and severity, and followed by premature death. At 6 months of age, TTD mice showed mild normochrome anemia (Table 2) and significantly decreased serum levels of the branched-chain amino acids (valine, leucine, and isoleucine) (Table 3), which is indicative of starvation (Bremer et al. 1981). Anatomical, histological, and biochemical analysis indicated that starvation was not due to aberrant food uptake or malabsorbtion (J. de Boer et al., unpublished). The TTD mice did not show histological abnormalities in other vital organs such as the liver, kidney, or heart, except for an enlarged spleen, which might be related to the mild anemia.

Table 2. Blood analysis of TTD mice.

	Wt	TTD	p-value[1]
red blood cell count (10^{12}/L)	10.3	8.7	< 0.01
hemoglobin (mmol)	9.4	8.1[2]	< 0.01
hematocrit (L/L)	0.56	0.47	< 0.01
mean cell volume (fL)	54.5	54.3	ns

Table 3. Analysis of serum of TTD mice.

component [μ Mol]	wt mice	TTD	p-value
Valine	222	169	< 0.05
Isoleucine	103	69	< 0.01
Leucine	164	118	< 0.05
1-me-histidine	15.7	21.2	0.05
Phenylalanine	78	60	< 0.05
Proline	166	139	ns
Arginine	130	120	ns
Asparagine	25	27	ns
albumine	0.40	0.48	ns
glucose	1.34	1.04	ns
creatinine	63.4	54.6	ns
urea	11.4	14.7	ns

ns: not significant
1) No significant difference between wt and TTD mice was seen at the age of 3-4 weeks
2) Reduced levels of haemoglobin were recently also observed in TTD patients (2)

ns: not significant, this includes all other amino acid concentrations, as well LDH levels (3)

A complete NER defect dramatically enhances the severity of the TTD phenotype.

In view of the dual function of XPD, the accelerated aging features could be a result of impaired transcription, impaired NER, or a combination of the two. A DNA repair defect alone seemed unlikely because TTD patients and mice have considerable residual NER activity (de Boer et al. 1999), whereas XP-A patients and mice, who have a complete NER defect, do not display premature aging (de Vries et al. 1995; Nakane et al. 1995; Bootsma et al. 2002). To examine whether TTD aging was due to a defect in transcription, independent of NER status, we crossed TTD mice with mice carrying an *Xpa* null allele (de Vries et al. 1995). Combined homozygosity for XPA and TTD was found to be compatible with normal embryogenesis but was associated with increased neonatal lethality (Table 4) ,which suggests that the combined mutations reduced the tolerance of mice to stress.

Table 4. Recovery of XPA/TTD double mutant embryos and mice.

	Found	Expected	# analysed[1]
XPA/TTD E13.5	13	9.5	56
XPA/TTD E18.5	10	15.5	69
XPA/TTD newborn (7-10 days)	12	32	223

1) Total number of offspring analysed (including mutants, heterozygotes and wt)

The surviving doublemutant mice exhibited a retarded but steady growth in the first 1.5 weeks, but failed to gain further weight after 2 to 3 weeks, and developed dramatically runted growth and extreme cachexia resulting in a severely shortened life-span of only 22 days (n = 10) (Figure 5). The life-span could not be extended by providing newly lactating mothers to the pups. Most double mutants showed a disturbed gait, suggesting that neurodysfunction was more pronounced than in the TTD mice, and all double mutants developed spinal kyphosis indicative of osteoporosis. Two XPA/TTD double mutants escaped juvenile death and lived to 4 and 12 months of age. Pathological analysis did not reveal defects in any organ, except for complete absence of body fat, including subcutaneous fat (Figure 5C). The cachexia in the XPA/TTD mice resembled the progressive pathology of the TTD mutants in manifestation and as a cause of death, but it developed at a vastly accelerated rate. Surprisingly, other typical TTD characteristics were also much more pronounced in XPA/TTD mutants: excessive epidermal hyperkeratosis and severe dilation of hair follicles (Figure 5C). This suggests that the complete absence of NER enhances the transcriptional insufficiency thought to be responsible for the cutaneous abnormalities (de Boer et al. 1998a).

A

B

C

wild-type
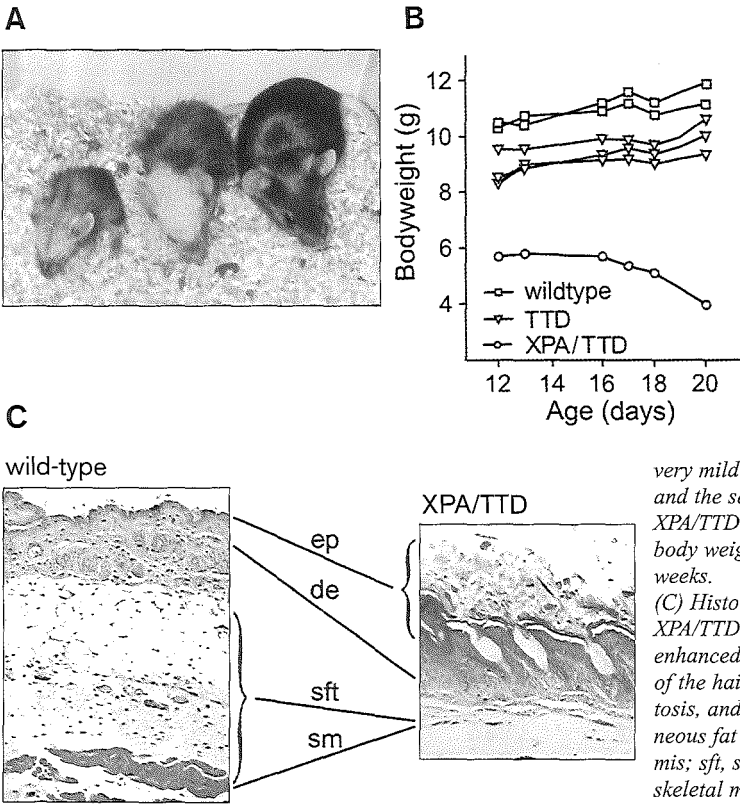
XPA/TTD

Figure 5.
Phenotype of XPA/TTD double-mutant mice.
(A) Photograph of a 3-week-old XPA/TTD double-mutant (left), TTD (middle), and XPA (right) mouse. After normal embryogenesis, double mutants develop severe growth retardation, neurologic abnormalities, kyphosis (indicative of osteoporosis), and extreme cachectic appearance.
(B) Body weight of wt, TTD, and XPA/TTD double-mutant littermates. Note the very mild growth delay of TTD mice and the severe growth retardation of the XPA/TTD mouse, with typical loss of body weight preceding death within; 3 weeks.
(C) Histology of wt and XPA/TTD skin. XPA/TTD skin exhibits a dramatically enhanced phenotype of severe dilation of the hair follicles, massive hyperkeratosis, and complete absence of subcutaneous fat tissue. ep, epidermis; de, dermis; sft, subcutaneous fat tissue; sm, skeletal muscle. The bar is ;200 μm.

TTD/XPA double-mutant cells are hypersensitive to oxidative stress

TTD symptoms in double-mutant mice. Although oxidative DNA damage is primarily –(but not exclusively) repaired by the base-excision repair pathway rather than by NER (Lindahl and Wood 1999), we focused on this type of endogenous damage, because it has already been implicated in aging. As expected, experiments measuring survival, DNA repair synthesis, and the recovery of RNA synthesis after UV exposure all showed that the partial repair deficiency of TTD was converted to the total NER defect of XPA (Figure 6, A to C). Sensitivity to oxidative injury was determined by exposure of cells to a continuous low dose of paraquat for 3 days (Murakami et al. 1995; Day and Crapo 1996). Although XPA and TTD single-mutant cells showed a survival curve similar to that of wt cells, XPA/TTD double mutants were clearly more sensitive (Figure 6D), showing a survival curve similar to that of Cockayne Syndrome group B (CSB)– deficient fibroblasts, which are completely deficient in repair of transcription-blocking lesions (de Laat et al. 1999).
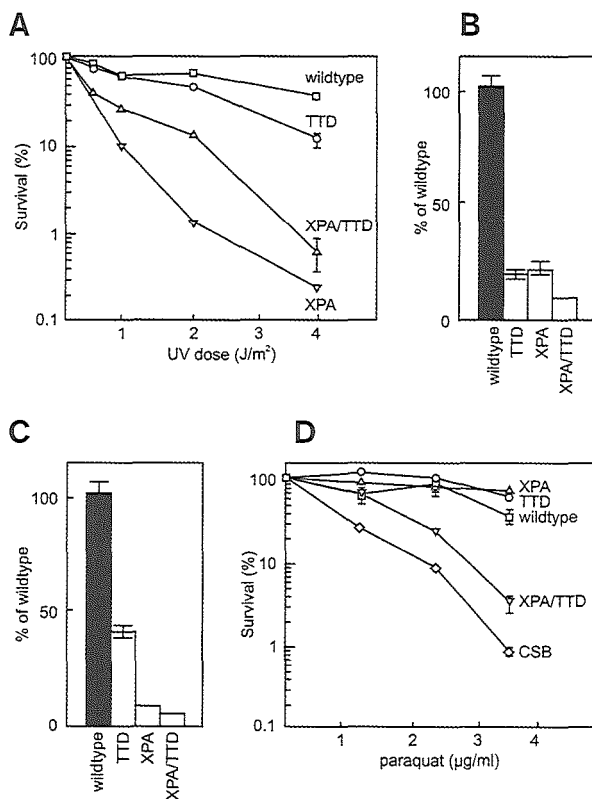
Figure 6. DNA repair functions of MEFs from TTD, XPA, and XPA/TTD double-mutant embryos.
(A) UV sensitivity of MEFs of the indicated genotypes.
(B) UV-induced DNA repair synthesis and
(C) recovery of RNA synthesis after UV-irradiation of MEFs of the indicated genotype (expressed as % of wt activity).
(D) Hypersensitivity of XPA/TTD cells to oxidative damage. MEFs of the indicated genotype were exposed to increasing concentrations of paraquat for 3 days. Three wt and two XPA/TTD double-mutant MEF cell lines have been tested in >4 experiments with identical results.

The TTD/XPA and CSB cells were also hypersensitive to a fractionated dose of x-irradiation (J. de Boer et al., unpublished). The synergistic effect of the XPA/TTD double mutant both at the organismal level and in terms of sensitivity to oxidative damage provides evidence for a causal link between DNA damage and the dramatically enhanced aging features.
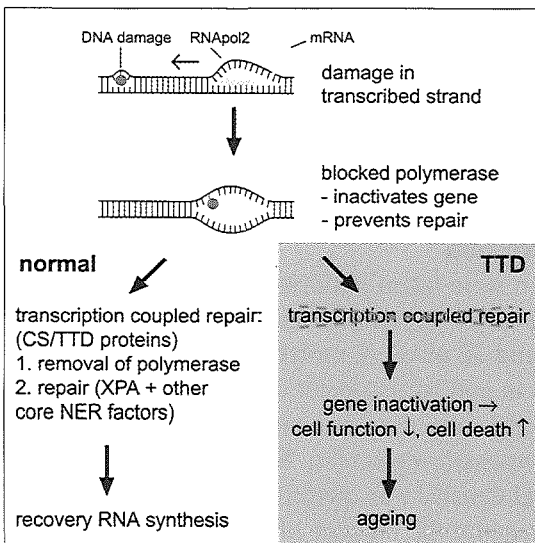
Discussion

The fact that TTD mice develop normally until adulthood indicates that the phenotype we describe here is not the result of aberrant development but rather reflects bona fide aging. Because TTD is associated with several features of normal aging, it can be considered a segmental progeroid disorder (Martin and Oshima 2000). In comparison to other progeroid disorders, such as Werner, Cockayne, and Bloom syndromes (Nehlin et al. 2000; Oshima 2000), TTD is associated with much faster aging. Patients with the XPD R722W mutation mimicked in the mouse did not live longer than 5 years (Botta et al. 1998). This interpretation is reinforced by the recent description of two TTD sisters who were less than 5 years old but were described as looking prematurely aged (Toelle et al. 2001). Moreover, many TTD symptoms overlap with those seen in CS, a well-characterized progeroid condition (Vermeulen et al. 1994b; Nakura et al. 2000; Bootsma et al. 2002). Several observations suggest that DNA is a critical target in relation to premature aging. For example, telomere shortening has been implicated in the aging phenotype of highly proliferative tissues (Rudolph et al. 1999; Campisi 2000; Goyns and Lavery 2000). Cells from patients with Werner, Cockayne, and Bloom syndromes display genome instability that is caused by defects in DNA helicases (Troelstra et al. 1992; Ellis et al. 1995; Yu et al. 1996) similar to the XPB and XPD helicases affected in TTD. Our work on TTD mice, and particularly on XPA/TTD double-mutant mice, highlights the role of DNA damage, repair, and transcription in the onset of premature aging. Interestingly, CSB and Cockayne Syndrome group A mice, which have a defect in the repair of transcription-blocking lesions (transcription - coupled repair) but normal global genome NER, exhibit the same dramatic TTD/XPA double-mutant phenotype when crossed with XPA mutants (van der Horst et al. 1997)((I. van der Pluijm et al., unpublished). However, when the NER defect is incomplete—as in the cases of TTD/CSB and TTD/XPC double mutants (which have some residual repair)— the enhancement of the TTD features is less pronounced (J. de Boer et al., unpublished). These results suggest that the residual repair activity in TTD and in the latter double mutants can still cope with the low level of endogenous damage and thus prevent most of the deleterious effects. Thus, the level of residual repair appears to modulate the severity and rate of CS/TTD aging symptoms. In the complete absence of any NER and transcription-coupled repair, death can occur within 3 weeks. The candidate lesions that trigger the onset of aging in TTD are most likely those that arise from endogenous insults, block transcription, and serve as substrates for NER. Although some alkylating and cross-link lesions fall into this category, we favor 5',8- purine cyclodeoxynucleotides (Brooks et al. 2000; Kuraoka et al. 2000) and other oxidative damage (Le Page et al. 2000). First, a causal relation between oxidative stress and aging has long been suspected. For example, caloric restriction experiments have implicated the generation of reactive oxygen species and oxidative damage derived from cellular

metabolism in the pathogenesis of aging (Martin et al. 1996). Second, defective tran-scription-coupled repair of oxidative DNA injury is thought to trigger the onset of CS symptoms (Leadon and Cooper 1993; Cooper et al. 1997; Le Page et al. 2000). Third, we find that the TTD/XPA doublemutant mouse embryo fibroblasts (MEFs) are hypersensitive to x-rays and paraquat. However, other types of DNA lesions may also be important. TTD cells are not sensitive to paraquat or x-rays, suggesting a role for other lesions in TTD aging. Endogenously generated DNA cross-links are thought to be involved in the cellular and hepatic senescence phenotype of mice deficient in the repair gene ERCC1 (Weeda et al. 1997), and a previously undescribed premature aging syndrome in man has been traced to mutations in the ERCC1/XPF complex (N. Jaspers et al., unpublished). Finally, mice defective in the double- strand break-repair protein Ku86 exhibit features of segmental premature aging (Vogel et al. 1999). Together, these observations suggest that DNA damage–induced genome dysfunction may underlie the aging process. What is the molecular mechanism underlying the premature aging in TTD mice? Because telomere length in lymphoblasts isolated from up to 1.5-year-old TTD mice appeared normal, this pathway of accelerated ageing can be considered unlikely (J.O.A. et al., unpublished). We propose that DNA damage persists longer and accumulates in TTD mice because the XPD mutation impairs not only global genome NER but also transcription-coupled repair of any lesions that stall elongating RNA polymerase II. Because XPD is also thought to function in removal of the blocked polymerase (de Laat et al. 1999; Lindahl and Wood 1999; Le Page et al. 2000; Hoeijmakers 2001), the stalled RNA polymerase II complex may persist longer in TTD, in turn preventing repair (Citterio et al. 2000b; Hanawalt 2000; Le Page et al. 2000).

Conceivably, this would cause gene inactivation and trigger apoptosis (Yamaizumi and Sugano 1994; Ljungman and Zhang 1996; Conforti et al. 2000), leading to functional decline and depletion of cell renewal capacity. Both cell death and impaired cell functioning may underlie the aging phenotype in TTD (Figure 7).

In support of this model is recent work showing that mice expressing a hyperactive p53 mutant also exhibit accelerated aging (Tyner et al. 2002) that is likely to be due to increased apoptosis. Obviously, any events cau-sing gene inactivation or cell death

Figure 7. Model for ageing in TTD

such as telomere attrition, chromosomal instability, and increased levels of oxidative damage might accelerate aging. In conclusion, our data strongly support the DNA damage theory of aging and suggest a significant role of transcription decay and subsequent cell death in its pathophysiology. The TTD mice may also prove to be a useful experimental model for further dissecting the molecular basis of aging.

Experimental procedures

Establishment and culturing of cells
Mouse embryo's of the required genotypes (13.5 days after gestation) were used for derivation of primary mouse embryo fibroblasts (MEFs) (de Boer et al. 1998a). We used established lines from primary MEFs that survived after crisis.
Determination of DNA repair parameters
Cellular survival after exposure to the indicated UV-C dose (J/m2) was assayed using the 3H-Thymidine incorporation method (de Boer et al. 1999). For experiments with paraquat (1,1'-Dimethyl-4,4'-bipyridinium dichloride, Sigma) cells were seeded at 20-40% confluency and split on each of the three subsequent days. Then, equal numbers of cells were seeded on gelatin-coated plates (1,6 x 104 cells per well of a 6-well plate) and cultured in the presence or absence of paraquat. Medium was refreshed every 24 hours. Cell survival was measured after 68 hours using the 3H-thymidine incorporation method (de Boer et al. 1999).

Determination of blood parameters
Blood cell values were analysed using a Sysmen F800 apparatus (Toa Medical Electronics) and general blood content values via spectrophotometry on an Elan Autoanalyzer (Eppendorf Merck). Amino acids in plasma were measured by ion exchange chromatography on a Pharmacia Biochrome 20 amino acid analyser with ninhydrin detection. Organic acids in urine were extracted with ethylacetate, dried and converted into methylesters by diazomethane. Measurements were performed by gaschromatography-mass spectrometry (Fisons MD-800).

Radiological analysis of bone mineralization
Radiographs with a two-fold magnification were taken in dorso-frontal and lateral direction. A special X-ray system, developed for human mammography (CGR Senograph 500T) was operated at 30 kV and 32 mAS. A molybdeen focus (0.1 mm) was utilised, with focus-film distance 65 cm and focus-object distance 32.5 cm. Kodak X-ray films (MIN-R MA 18 x 24 cm) were used in combination with a Dupont Cronex low-dose mammography-intensifying screen. Mice were sedated during the radiographic procedure. Mineral density was quantified by scanning the radiographs (DuoScan Agfa). Using Imagequant the number of pixels in a defined

area of the skull or of the complete sixth tail vertebra was determined. For histological examination, dissected tissues fixed in 10% formal saline were processed and embedded in paraffin and stained with hematoxylin and eosin, or formalan (melanin staining) using routine procedures.

Acknowledgements

CHAPTER 3

Life-saving potential of lethal recessive alleles in mammals

Jaan-Olle Andressoo[1], James R. Mitchell[1],[*], Judith Jans[2],[*], Jan de Wit[1],
Deborah Hoogstraten[1], Jan Huijmans[3], Bin Thio[4], Wibeke van Leeuwen[5],
Jan de Boer[6], Jan H.Hoeijmakers[1] and Gijsbertus T.J.van der Horst[1]

1 Medical Genetics Center, Department of Cell Biology and Genetics,
  Center of Biomedical Genetics,
3 MGC-Department of Clinical Genetics, CBG,
4 Department of Dermatology,
5 Department of Experimental Radiology, PO Box 1738, Erasmus MC,
  3000DR Rotterdam, NL
2 Present address: Department of Molecular and Cell Biology, University of
  California at Berkeley, 125 Koshland Hall, Berkeley, California
6 Present address: Isotis N.V., Prof. Bronkhorstlaan 10, D, 3723MB, Bilthoven, NL
* these authors contributed equally to this work

Summary

Elucidation of straightforward genotype-phenotype relationships in the ~3000 auto-somal recessive diseases known in man is complicated by mutational diversity and clinical heterogeneity. Although compound heterozygosity is common, the potential of interactions between two different mutant alleles to influence disease outcome is rarely considered. Here, we used mouse models to address recessive disease etiology at the *Xpd* locus, an essential gene encoding a helicase involved in DNA repair and basal transcription with associated pathologies ranging from elevated cancer predis-position (xeroderma pigmentosum) to accelerated segmental ageing (trichothiodystro-phy, TTD). We report partial to full interallelic complementation between defective (*Xpd^{TTD}*) and homozygous lethal *Xpd* alleles for UV sensitivity, hampered develop-ment and accelerated ageing. Our data predict recessive biallelic effects as important determinants of normal and pathological phenotype.

Introduction

Accurate prediction of phenotype based on genotype is essential to understand gene-tic disease. Differences in environment and genetic background (modifying genes) are known to confound this relationship. Both can lead to enormous differences in disease symptoms even between individuals homozygous for the same recessive alle-le. A third variable - interactions between two different recessive alleles- is rarely considered as a cause of pleiotropic disease symptoms. This is not due to a lack of affected individuals carrying two different mutant alleles, known as compound heterozygotes, as allelic variation in recessive disorders can be enormous (e.g. ~1200 mutations in the CFTR gene affected in the common autosomal recessive disease cystic fibrosis alone can give rise to ~700,000 unique combinations of different alle-les). Rather, it reflects our inability to dissect interallelic effects from those of envi-ronment and genetic background. Here, we used combinations of recessive *Xpd* alle-les in a mammalian model system with uniformity in genetic background and envi-ronment to demonstrate the enormous potential of compound heterozygosity to impact the phenotypic outcome of autosomal recessive disease associated with defects in the DNA repair/basal transcription factor TFIIH.

The human *XPD* gene is an example of an autosomal recessive disease-associated locus for which the potential of two different recessive alleles to produce disease plei-otropy clearly exists. Alterations in this essential DNA repair/basal transcription fac-tor are associated with at least six rare UV-sensitive, multisystem disorders with remarkable clinical variation: xeroderma pigmentosum (XP), XP combined with DeSanctis-Cacchione syndrome (XP-DSC), XP combined with Cockayne syndrome (XPCS), trichothiodystrophy (TTD), XP combined with TTD (XP/TTD) and the

recently identified Cerebro-oculo-facio-skeletal syndrome (COFS) (Cleaver et al. 1999; Broughton et al. 2001; Graham et al. 2001; Bootsma et al. 2002). XP is marked by sun-induced pigmentation anomalies and a 1000-fold or greater elevation in skin cancer risk. CS and TTD are segmental progeroid disorders characterized by progressive postnatal growth failure and severe neurological abnormalities, but without clear cancer predisposition (Nakura et al. 2000). TTD patients additionally display hallmark sulphur-deficient brittle hair and nails and scaling skin (Itin and Pittelkow 1990). The identification of different "causative" point mutations associated exclusively with TTD (e.g. R722W) or XP (e.g. R683W) (Taylor et al. 1997; Cleaver et al. 1999) gave rise to the current monoallelic paradigm of *XPD*-related disorders. Further support was added by the discovery of presumed null alleles, identified on the basis of their failure to support viability in a yeast complementation assay and/or their occurrence in patients with phenotypically distinct disorders and thus the unlikelihood that they contribute to either (Taylor et al. 1997). Still, this paradigm does not allow accurate prediction of the variant phenotype corresponding to a particular *XPD* genotype, particularly in compound heterozygotes that make up the majority of cases (www.xpdmutations.org). These include patients with causative TTD mutations who also display XP features (Broughton et al. 2001); and XP and XPCS patients with the same "causative" allele but with completely different disease outcomes (Ueda et al. 2004)(A.R. Lehmann unpublished).

Previously, we generated a TTD mouse model by mimicking a known human TTD-associated point mutation (R722W) in the mouse *Xpd* locus. This mouse exhibits a striking phenotypic resemblance to the human syndrome (de Boer et al., 1998 and 2002). Here we generated two different *Xpd* knock-in alleles associated with human XP (R683W) or XPCS (G602D) (Figure 1). Unexpectedly, homozygous mutant animals were not observed, neither amongst live births nor E13.5 or E3.5 embryos (Table 1) and thus the corresponding alleles were designated as lethal (†XP and †XPCS). Early lethality was likely due to a ~ 5 fold reduction in mRNA originating from the targeted *Xpd* alleles (Fig. 1e and data not shown) and the inability of the corresponding level of Xpd protein to support its essential function in basal transcription initiation.
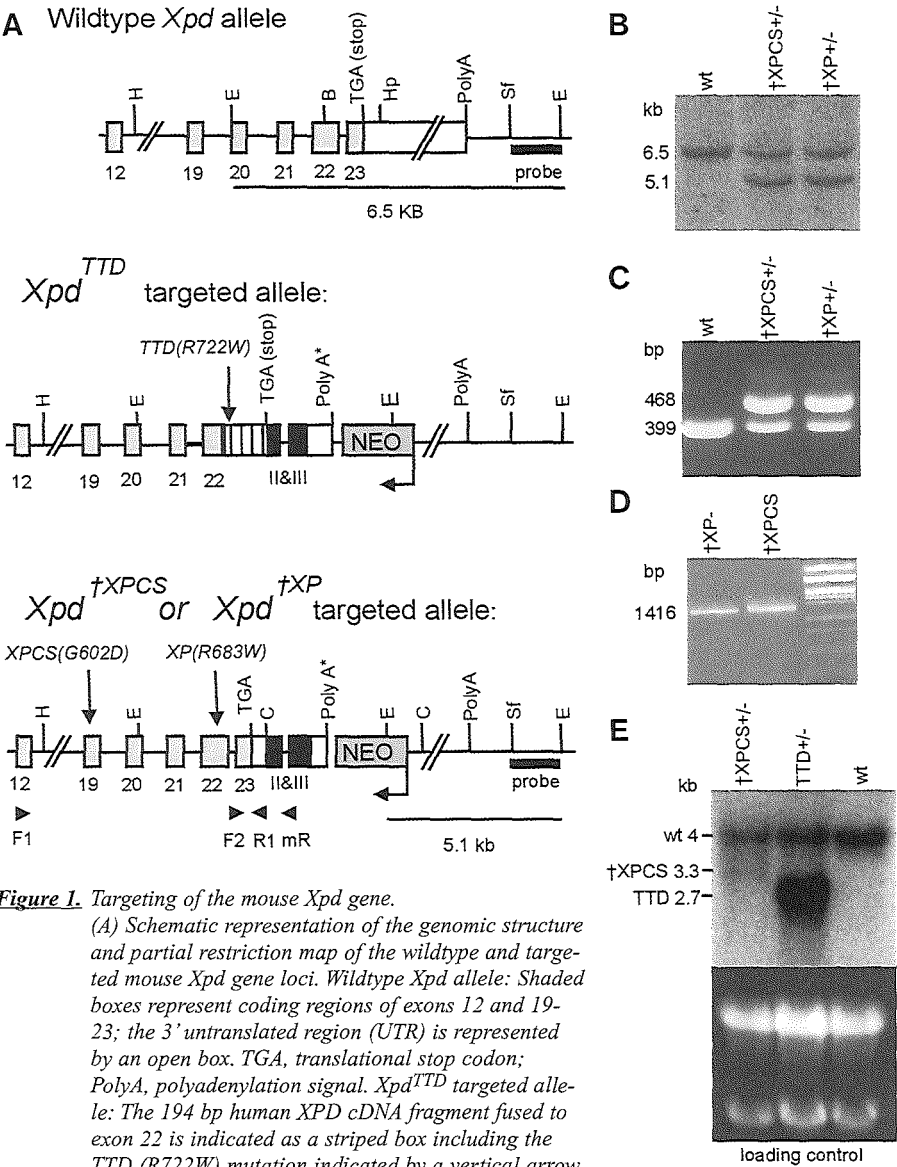
Figure 1. *Targeting of the mouse Xpd gene.*

(A) Schematic representation of the genomic structure and partial restriction map of the wildtype and targeted mouse Xpd gene loci. Wildtype Xpd allele: Shaded boxes represent coding regions of exons 12 and 19-23; the 3' untranslated region (UTR) is represented by an open box. TGA, translational stop codon; PolyA, polyadenylation signal. Xpd^{TTD} targeted allele: The 194 bp human XPD cDNA fragment fused to exon 22 is indicated as a striped box including the TTD (R722W) mutation indicated by a vertical arrow. Chicken β-globin exons 2 and 3 including the 3' UTR are indicated as black boxes with corresponding Roman numerals followed by the β-globin polyadenylation signal (PolyA*). $Xpd^{†XP}$ and $Xpd^{†XPCS}$ targeted alleles: Vertical arrows indicate XPCS (G602D) and XP (R683W) mutations in exons 19 and 22, respectively. The unique 3' probe located outside the targeting construct is marked by a thick black line. Restriction sites: (H), HindIII; (E), EcoRI; (B), BamHI; (Hp), HpaI; (Sf), SfiI; (C) ClaI.

(B) Southern blot analysis of EcoRI-digested genomic DNA from wt, †XPCS and †XP recombinant ES cell clones hybridized with the 3' probe depicted in (A). The wt allele yields a 6.5 kb fragment whereas both targeted †XP and †XPCS alleles yield a 5.1 kb fragment.

(C) Genotyping of wt and targeted alleles by PCR using primers F2, R1 and mR as indicated in (A) yields fragments of 399 bp and 468 bp, respectively.
(D) RT-PCR detection of mRNA expression originating from the targeted †XPCS and †XP alleles in ES clones using primers F1 and mR as indicated in (A) results in a 1416bp fragment.
(E) Northern blot analysis of total RNA isolated from testis of wt, †XPCS heterozygous (Xpd†XPCS/wt) and TTD heterozygous (XpdTTD/wt) mice. Hybridization with a 1.4 kb mouse Xpd cDNA probe detects mRNAs of 4, 3.3 and 2.7 kb from wt, †XPCS and TTD alleles, respectively. Ethidium bromide-stained gel showing equal loading of total RNA is shown below.

Table 1. *Genotype analysis of †XP, †XPCS and compound heterozygous †XP/†XPCS offspring and embryos*

	Analyzed	Expected* (if Mendelian)	Found
†XPCS			
E3.5	26	6.5	0
E13.5	26	6.5	0
Newborn	129	32	0
†XP			
E3.5	29	7	0
Newborn	144	36	0
†XP/†XPCS			
Newborn	33	8	0

*   *Derived from †XP+/-, †XPCS+/- and †XP+/- to †XPCS+/- intercrosses*

In order to test the potential of these homozygous lethal "null" alleles to still contribute to organismal phenotype, we genetically mimicked compound heterozygosity by combining $Xpd^{†XPCS}$ or $Xpd^{†XP}$ alleles with a viable Xpd^{TTD} allele by crossing the corresponding heterozygous animals. Similar to hemizygous TTD mice carrying one true Xpd knockout allele (Xpd^{KO})(de Boer et al. 1998), compound heterozygous $Xpd^{TTD/†XPCS}$ and $Xpd^{TTD/†XP}$ mice were born at Mendelian frequencies. Much to our surprise, multiple disease symptoms were partially to even fully rescued in all compound heterozygous animals. These included the hallmark brittle hair and cutaneous features that are normally fully penetrant in homo- and hemizygous TTD mice. Fragile hair observed both in TTD patients and mice is associated with reduction of cysteine-rich matrix proteins that normally strengthen the hair by cysteine-cysteine protein bridges (Lehmann et al. 1988; de Boer et al. 1998a). In marked contrast to $Xpd^{TTD/TTD}$ mice which display complete hair loss in the first hair cycle and partial hair loss in subsequent cycles throughout their lives (de Boer et al. 1998a), compound heterozygous $Xpd^{TTD/†XPCS}$ and $Xpd^{TTD/†XP}$ mice displayed visible hair loss only during the first hair cycle and only locally at the back (Figure 2A). Scanning electron microscope (SEM) analysis of $Xpd^{TTD/†XPCS}$ hair revealed an almost normal appearance, with TTD-like features such as broken hairs found only at very low

frequency (Figure 2B and data not shown). Amino acid analysis further revealed that cysteine levels in the hair of the $Xpd^{TTD/\dagger XPCS}$ and $Xpd^{TTD/\dagger XP}$ compound heterozygote mice were remarkably higher compared to that of the Xpd^{TTD} animals, but remained below the wt level (Figure 1D). It is important to note that TTD hemizygotes carrying one true null allele ($Xpd^{TTD/KO}$) do not display significant differences in cutaneous features and longevity when compared to homozygous $Xpd^{TTD/TTD}$ mice (de Boer et al. 1998a). Other prominent TTD features in the epidermis, including acanthosis (thickening of the layer of the nucleated cells), hyperkeratosis (prominent thickening of the cornified layer), pronounced granular layer and sebacious gland hyperplasia (causing greasy appearance of the hair), were absent in the skin of the compound heterozygote mice, as established by "blind" microscopic examination of skin sections (Figure 1C and data not shown). Anemia, another symptom reported for TTD patients (Viprakasit et al. 2001) as well as the $Xpd^{TTD/TTD}$ mouse model (de Boer et al. 2002), was similarly rescued in $Xpd^{TTD/\dagger XPCS}$ compound heterozygote mice (Figure 1E). Thus, in compound heterozygous mice, two independent alleles that on their own were unable to support viability (and thus interpretable as null alleles) were nonetheless able to contribute enormously to phenotypic outcome by ameliorating TTD hallmark symptoms.
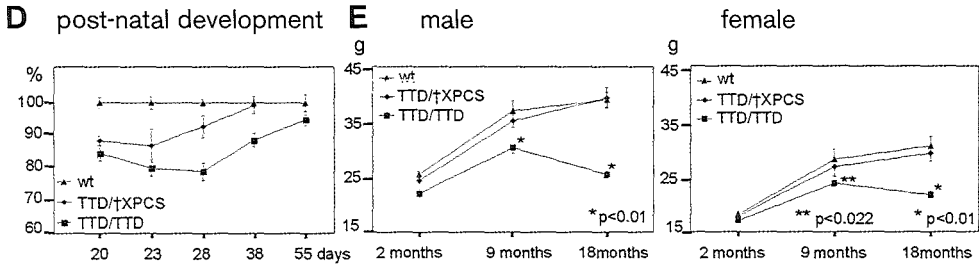
Figure 2. *Partial rescue of TTD cutaneous and blood phenotypes in compound heterozygous TTD/†XPCS mice*

(A) Photographs of 4-week-old homozygous TTD, compound heterozygous TTD/†XPCS and wt mice showing differences in the extent of hair loss.
(B) Scanning electron micrograph of TTD, TTD/†XPCS and wt mouse skin and hair. Note the frequent appearance of broken hairs (indicated by asterisks) and lesions (indicated by arrows) specific to the TTD mouse. Magnification 450X.
(C) Histological analysis of the skin of TTD, TTD/†XPCS and wt mice. Note that TTD-associated acanthosis (thicker

D

Cysteine content of hair

E

Haematocrite

epidermis), pronounced granular layer (indicated by arrows), prominent cornified layer (indicated by vertical bar) and sebacious gland hyperplasia (indicated by vertical dotted line) are absent in the epidermis of TTD/†XPCS and wt mice. Magnification 400X.

(D) Cysteine content of hair from wt, TTD, TTD/†XPCS and TTD/†XP mice. P value indicates highly significant differences between mutants and wt as well as between TTD and TTD/†XPCS or TTD/†XP mice.

(E) Hematocrite values from blood of TTD and TTD/†XPCS mice. P values indicate the significance of the difference between mutants and wt.

We next addressed the developmental and segmental progeroid features in $Xpd^{TTD/†XPCS}$ and $Xpd^{TTD/†XP}$ mice. This aspect was of particular interest as the symptomatically overlapping accelerated ageing observed in TTD and CS (but not XP) patients and mice has been proposed to result from a subtle but viable defect in basal transcription of damaged DNA templates (Vermeulen et al. 1994b). $Xpd^{TTD/TTD}$ animals show a prominent reduction in bone mineral density as an indication of early onset osteoporosis at 14 months of age . Surprisingly, tail vertebra from compound heterozygote $Xpd^{TTD/†XPCS}$ mice did not show these features even at 20 months of age (Figure 3B, C).

A 20 months **B** 20 months **C**

D post-natal development **E** male   female
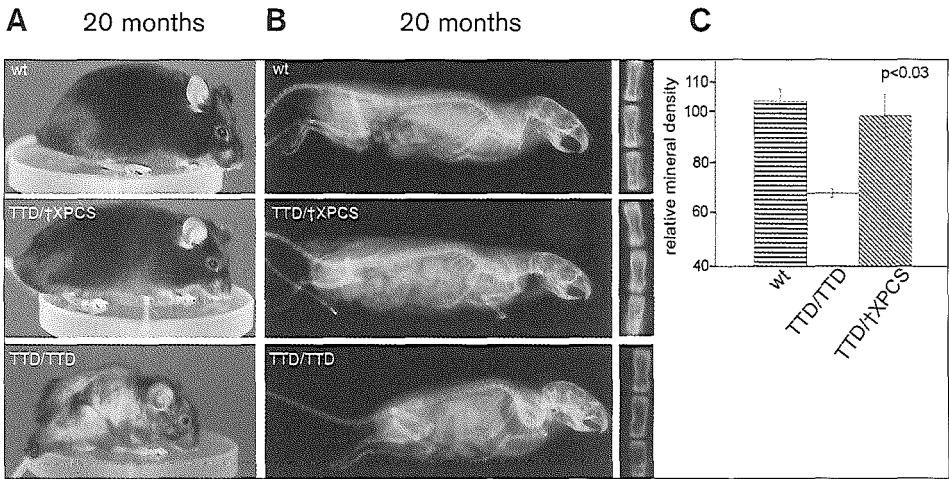

Figure 3. *Rescue of TTD premature segmental ageing features in compound heterozygous TTD/†XPCS mice.*
(A) Photographs of 20-month-old wt compound heterozygous TTD/†XPCS and homozygous TTD mice. Note the extreme cachexia (lack of subcutaneous fat) in the TTD mouse and the lack of this phenotype in wt and TTD/†XPCS mice.
(B) Radiographs of 20-month-old male wt, TTD/†XPCS and TTD mice. Aging TTD mice develop kyphosis (curvature of the spinal column) and reduction of bone mineral density as shown in the 6-8 segment of the tail vertebra counted from the pelvis (see close-up at right). Note the absence of these features in the TTD/†XPCS mouse. (C) Quantification of relative bone mineral density of tail verte-bra from the 20 month old male wt, TTD/†XPCS and TTD mice. P value indicates the significance of the difference between TTD and TTD/†XPCS.
(D) Bodyweights of developing wt, TTD and TTD/†XPCS animals plotted as a percentage of the weight of control littermates (set at 100%).
(E) Bodyweight curve as a function of time. Note the rescue of age-dependent cachexia observed in TTD in both male and female TTD/†XPCS mice. Significant differences between wt and TTD but not TTD/†XPCS mice were observed at 9 and 18 months of age as indicated.

Furthermore, while $Xpd^{TTD/TTD}$ mice developed severe kyphosis dramatically earlier than wt animals (onset ~3 months vs. 12-20 months), compound heterozygote $Xpd^{TTD/†XPCS}$ and $Xpd^{TTD/†XP}$ mice did not (Figure 2B). Age-related premature cachexia observed in $Xpd^{TTD/TTD}$ mice was also rescued by both alleles to the same extent (Figure 3e and data not shown). Similarly, the developmental delay observed in $Xpd^{TTD/TTD}$ mice, as manifested by a delay in reaching the weight of littermate con-trols during maturation, was partially rescued in compound heterozygote $Xpd^{TTD/†XPCS}$ mice (Figure 3d). Finally, the lifespan of compound heterozygotes was extended relative to $Xpd^{TTD/TTD}$ mice. In conclusion, the lethal $Xpd^{†XPCS}$ and $Xpd^{†XP}$ alleles largely rescued Xpd^{TTD}-associated segmental progeroid features. Taken toge-ther, these data demonstrate interallelic complementation, or the ability of DNA repair/basal transcription associated TFIIH complexes carrying two differentially alte-red XPD proteins to achieve what neither can accomplish individually.
We next assayed the ability of individual and combinations of mutant Xpd alleles to complement repair of UV-induced DNA lesions in primary fibroblasts prepared from day 13.5 embryos. Unscheduled DNA Synthesis (UDS) and Recovery of RNA Synthesis (RRS) assays reflect global genome repair (GG-NER) and transcription coupled repair (TC-NER) capacities of UV-irradiated cells, respectively. We observed reduced GG-NER and cellular survival of $Xpd^{TTD/KO}$ hemizygote cells after exposure to increasing doses of UV-C (Figure 4). In $Xpd^{TTD/†XPCS}$ compound heterozygous

cells, UV survival was significantly improved relative to $Xpd^{TTD/KO}$ hemizygous cells (Figure 4C). Because of early embryonic and cellular lethality, we were unable to test UV survival associated exclusively with the $Xpd^{\dagger XPCS}$ allele. However, hemizygous XPD^{XPCS} (G602D) patient cells are known to be highly sensitive to UV (Vermeulen et al. 1991; Broughton et al. 1995), as are cells from a recently engineered viable homozygous $Xpd^{XPCS/XPCS}$ (G602D) mouse model with wildtype levels of associated mRNA expression (J.O. Andressoo et al., manuscript in prep.(J.O. Andressoo et al., manuscript in prep.); Figure 4, dotted line). Thus, the survival of $Xpd^{TTD/\dagger XPCS}$ cells represents a level of UV resistance that neither mutant allele can likely impart on its own. Interestingly, complementation of UV survival was not clearly evident in $Xpd^{TTD/\dagger XP}$ compound heterozygous cells (Figure 4) despite partial rescue of numerous TTD symptoms in vivo, indeed indicating, that different allelic combinations can affect various endpoints.
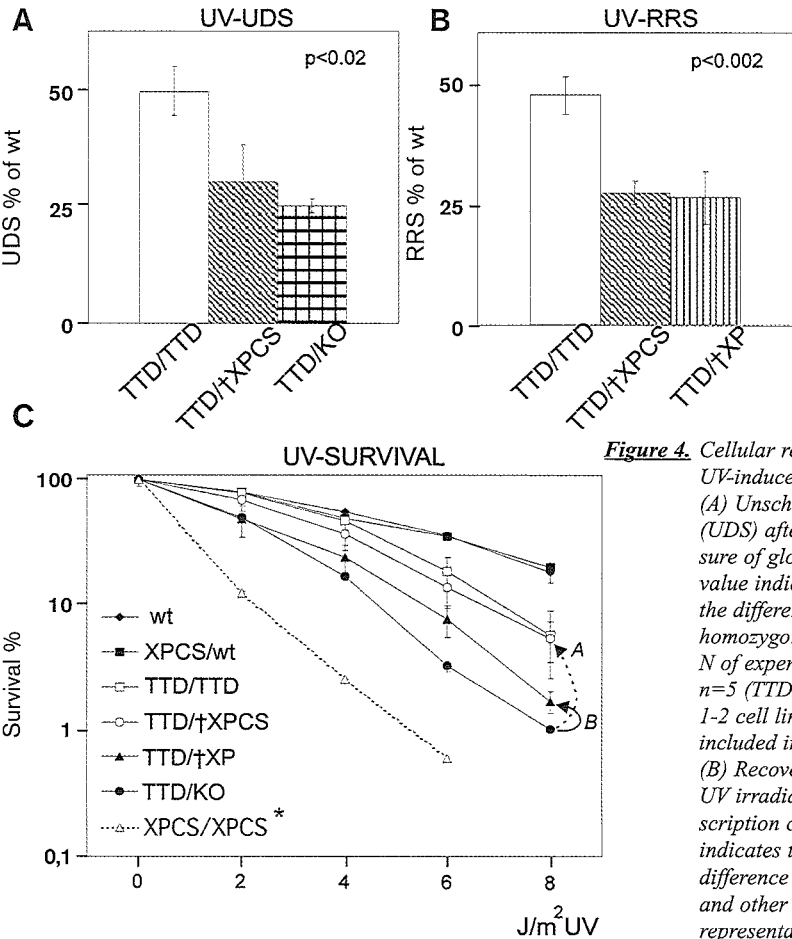

Figure 4. *Cellular response to acute UV-induced damage*
(A) Unscheduled DNA synthesis (UDS) after UV irradiation, a measure of global genome repair. (P value indicates the significance of the difference in between TTD homozygotes and other genotypes. N of experiments: n=14 (TTD/TTD); n=5 (TTD/KO); n=2 (TTD/†XPCS). 1-2 cell lines per genotype were included in each experiment.
(B) Recovery of RNA synthesis after UV irradiation, a measure of transcription coupled repair. (P value indicates the significance of the difference between TTD homozygotes and other genotypes within the representative experiment).

(C) Cellular survival after UV irradiation. Rescue of hemizygous TTD/KO survival by †XPCS and †XP alleles are represented by A and B arrows, respectively. UV survival of homozygous †XPCS cells (asterisk) from a newly constructed viable allele is depicted by a dotted line. Survival curves represent an average of 4 independent experiments. 1-2 cell lines per genotype were included in each experiment. Error bars indicate SEM between experiments.

Reduced levels of TFIIH caused by specific alterations in the XPD helicase have been proposed to cause TTD-specific disease symptoms. (Vermeulen et al. 2001; Botta et al. 2002; Giglia-Mari et al. 2004). We thus asked if the $Xpd^{†XPCS}$ and $Xpd^{†XP}$ alleles, despite decreased mRNA expression, ameliorated TTD symptoms by increasing overall TFIIH levels in compound heterozygous $Xpd^{TTD/†XPCS}$ and $Xpd^{TTD/†XP}$ cells. Previously, using comparative immunohistochemistry we and others have shown an up to 70% reduction of TFIIH levels in primary fibroblasts from TTD patients compared to wt controls (Vermeulen et al. 2000; Botta et al. 2002; Giglia-Mari et al. 2004). Despite overexpression of mRNA from the Xpd^{TTD} allele relative to the wt allele (Figure 1E), TFIIH protein levels were reduced by 50% in primary mouse $Xpd^{TTD/TTD}$ fibroblasts (Figure 5A, B), thereby mimicking the situation in the human TTD patients. In accordance with the gene dosage, a further reduction of up to 70% of the wt level was observed in hemizygous $Xpd^{TTD/KO}$ cells.

Consistent with low mRNA expression levels, neither the $Xpd^{†XPCS}$ nor the $Xpd^{†XP}$ allele was able to restore TFIIH abundance to wildtype levels in Xpd^{TTD} compound heterozygote cells (Figure 5).

Figure 5. *Xpd dose-dependent reduction of TFIIH in homozygous TTD, hemizygous TTD/KO and compound heterozygous TTD/†XPCS and TTD/†XP cells*

A anti-p62

phase-contrast
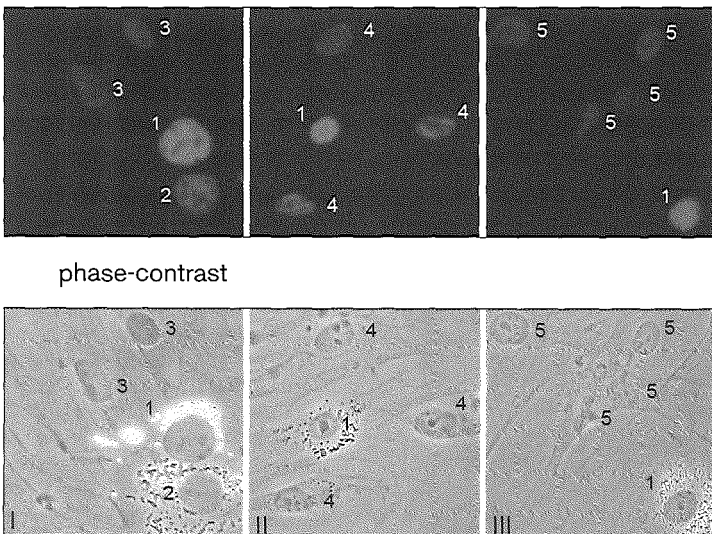
(A) Comparative immunofluorescence of the p62 subunit of TFIIH. Roman numerals represent different microscopic slides and Arabic numerals different cell lines labelled as follows:
I - wt cells (1) were labelled with 2μm beads, TTD cells (2) with 0.79μm beads and TTD/KO cells (3) with no beads.
II - wt cells (1) were labelled with 0.79μm beads, TTD/†XPCS cells (4) with no beads.
III - wt cells (1) labelled with 0.79μm beads, TTD/†XP cells (5) with no beads.

B TFIIH level
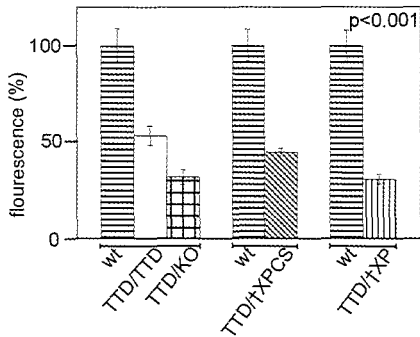
(B) Quantification of immunofluorescent signal from at least 50 nuclei per cell line and 2-6 experiments per genotype. Bars representing cells analyzed on the same microscopic slide are depicted side by side. P value indicates minimum significant difference between cell lines analysed on the same microscopic slide within one experiment.

Thus, the improved UV survival observed in $Xpd^{TTD/\dagger XPCS}$ compound heterozygote cells (Figure 4C) was not due to normalization of TFIIH levels, suggestive of a qualitative rather than a quantitative effect. Similarly, the pronounced UV sensitivity of $Xpd^{XPCS/XPCS}$ cells cannot merely be attributed to a reduced TFIIH level, as this measure is comparable between $Xpd^{TTD/TTD}$ and $Xpd^{XPCS/XPCS}$ cells (J.O.A. et al., manuscript in prep.)

Taken together, these data suggest, somewhat surprisingly, that particular combinations of *Xpd* alleles can be detrimental or neutral to NER activity and cell survival in response to acute UV irradiation and at the same time beneficial with respect to organismal symptoms of segmental premature aging. The explanation behind this apparent paradox most likely lies in the enormous inherent differences in lesion spectrum and damage load between acute UV-induced DNA lesions and the oxidative DNA lesions that are thought to accumulate with age as a result of endogenously-produced reactive oxygen species.

Here we demonstrated interallelic complementation of basal transcription and DNA repair defects between recessive *Xpd* alleles in vivo. To the best of our knowledge, this is the first demonstration of this phenomenon in a mammalian model system between clinically relevant alleles. What light does the occurrence of interallelic complementation shed on the mechanism of XPD and TFIIH action? Although interallelic complementation has been reported for monomeric proteins (Ohya and Botstein 1994) it was first characterized and is most often observed in proteins that homo- or hetero-multimerize (Ullmann et al. 1967). In vivo, NER is a dynamic multistep process involving more than 30 proteins in a ~ 4 minute reaction. Since recruitment of the XPD-containing TFIIH complex is an early event (Volker et al. 2001; Hoogstraten et al. 2002) we envisage different mutant XPD molecules harbouring differential capacities to perform discrete tasks (e.g. DNA unwinding, protein interactions, conformational changes) along the spatio-temporal axis of the repair reaction. Thus, either (i) XPD multimerization within TFIIH; (ii) sequential action of TFIIH complexes carrying different XPD molecules during a single repair event; or (iii)

exchange of XPD molecules within one TFIIH complex during a single NER reaction may underlie the observed complementation. Although the TFIIH complex is not known to multimerize and contains only one XPB helicase subunit (Winkler et al. 1998), biochemical studies suggest XPD to be relatively loosely bound to the XPB-containing "core" subcomplex of TFIIH and to serve as a molecular bridge between the cyclin-activating kinase (CAK) and core TFIIH subcomplexes (Schaeffer et al. 1994). Unfortunately, of the several measurable parameters of TFIIH action in vitro, including basal transcription initiation and helicase activity, the assay most likely to shed light on the molecular basis of interallelic complementation, namely in vitro reconstitution of the transcription coupled repair reaction, is currently unavailable. Recessive alleles typically encode truncated or mutant proteins that are unable to carry out wildtype function and do not significantly interfere with the wildtype protein, but may still be able to exert some partial activity. However, in the absence of a wildtype allele, two different "recessive" alleles may assume a spectrum of relationships to one another, ranging from dominance or co-dominance to complementation or antagonism, depending on the particular combination of mutant alleles, expression levels and the specific function(s) affected by each individual mutation. Interallelic complementation resulting in amelioration of disease symptoms, as observed here, is only one possible outcome, albeit the least likely to be identified within the human population. Whatever the phenotypic outcome, the probability of such interallelic effects increases with mutational diversity. While XPD is associated with "only" ~ 50 different mutations, two of the most common autosomal recessive human diseases, cystic fibrosis (CF) and phenylketonuria (PKU), are marked by enormous allelic variation. There are more than 1200 mutations and polymorphisms identified in the CFTR gene associated with CF and >400 in the PAH gene associated with PKU and a less severe variant, hyperphenylalaninemia. Both genes encode proteins that function in multimeric forms in vivo, and both disorders display enigmatic clinical heterogeneity. In support of the potential of biallelic interactions to affect the course of recessive disease, several asymptomatic compound heterozygotes carrying two different CF alleles normally associated with disease pathology have recently been identified (Chmiel et al. 1999; White et al. 2001).

Our data strongly suggest that a subset of compound heterozygote phenotypes, from pathological to normal, previously assigned to differences in genetic background and/or environmental variation, can in fact result from biallelic interactions. Importantly, previously designated null alleles with little or no detectable expression may still have the ability to contribute enormously to phenotype. Such biallelic effects can be accurately elucidated best in a controlled mammalian model system with clinical endpoints often unreachable by conventional cell-culture systems, or by epidemiological studies attempting to relate genotype to phenotype in compound heterozygotes patients with autosomal recessive disease. Where cellular assays with predictive value are available, (e.g. assays to measure PAH activity) combinations of

alleles should be tested in addition to single alleles. Given that the potential number of combinations of recessive alleles for a single autosomal recessive disease such as CF is on the order of 700,000, and that the combinations of different allelic SNPs is currently incalculable, we suggest biallelic effects as an important new variable in considering genotype-phenotype relationships from autosomal recessive disease to normal phenotypic diversity in man.

Experimental procedures

Derivation of Mutant Mice and Mouse Embryonic Fibroblast Lines

Xpd^{TTD} (Xpd^{R722W}) and $Xpd^{TTD/KO}$ mice were generated as described previously (de Boer et al. 1998a). Targeting constructs for $Xpd^{†XPCS}$ and $Xpd^{†XP}$ alleles carrying G602D and R683W mutations, respectively, were generated similarly. Briefly, a ClaI linker inserted into the HpaI site 311 bp downstream of the translational stop codon in exon 23 was used for the introduction of a human β-globin cassette containing partial β-globin exon 2, intron 2, exon 3 and poly(A) signal followed by the pMC-1 neo cassette. The HSV-tk gene for counter selection was inserted into the SfiI site at the 3'end of the homologous arm as described previously (de Boer et al. 1998a). Xpd^{G602D} (G1805A) and Xpd^{R683W} (C2047T) point mutations were generated via site-directed mutagenesis. Silent mutations (G1803A and A1809G) were included in the $Xpd^{†XPCS}$ construct to facilitate screening by restriction digest. Electroporation, culturing and screening of 129/Ola-derived ES cells were performed as described previously (de Boer et al. 1998a). Blastocyst injections and derivation of chimeric mice were performed according to standard methods. Chimeras were mated with C57Bl6 mice and the resultant heterozygous animals were intercrossed. Mice used in this study were in 129Ola/C57bl6 mixed background unless otherwise noted.

Histological and Electron Microscopic Studies

For histological examination, dissected mouse skin samples fixed in 4% paraformaldehyde were embedded in paraffin and stained with hematoxylin and eosin using routine procedures. Microscopic slides were numbered and subjected to "blind" examination by our expert (Figure 2C). For scanning electron microscopy, mouse skin was fixed in a mixture of glutaraldehyde and paraformaldehyde, post-fixed in OsO4, dehydrated in ethanol, and critically point dried. After mounting on stubs and coating with gold, the dried skin was examined in a Jeol JSM-25 electron microscope (Figure 2B).

Amino Acid Analysis of Hair Samples

Amino acid analysis was conducted by standard procedures. Briefly, hair of age-matched mice was hydrolyzed in 12M HCl at 1100C for 24h. The separation was

performed on a Biotronik 7000 amino acid analyzer by ion change chromatography using lithium citrate buffers and ninhydrin detection with a dual wavelength detector at 570 and 440 nm. The amount of cysteine was expressed as the molar percentage of the total amino acids (Figure 2D) averaged from multiple measurements from multiple animals and the P value indicated reflects minimum significant difference in cysteine content of the hair between $Xpd^{TTD/TTD}$ and compound heterozygote as well as between all mutant and the wt mice.

Measurement of Blood Parameters
Blood values were analyzed using Animal Blood Counter Vet (ABX Diagnostix, France). Results published previously from our lab (de Boer et al. 2002) were obtained using different equipment (Sysmen F800 apparatus, Toa Medical Electronics); therefore the absolute values from the two different experiments were not directly comparable. Due to that reason we indicate the hemotocrite levels for the mutants as a percentage of the wt hemotocrite level within the experiment (Figure 2E). P values indicate the difference between the average of the mutant and the wt animals.

Radiology
Radiographs with two-fold magnification were taken in lateral direction. A special X-ray system, developed for human mammography (CGR Senograph 500T) was used at 30 kV and 32 mAS. Kodak X-ray films (MIN-R MA 18X24 cm) were used in combination with Dupont Cronex low-dose mammography-intensifying screen. Relative mineral density was quantified by scanning the radiographs (DuoScan Agfa). Using Adobe Photoshop 4.0 the total relative intensity of the sixth, seventh and eighth tail vertebra counted from the pelvis was determined (Figure 3C). P value indicates the significant difference between TTD and wt. Data concerning 20 month old TTD vertebrae were mostly obtained from pure C57bl6 background TTD mice. In C57bl6 background TTD premature ageing phenotype is less severe compared to 129Ola|C57bl6 mixed background and TTD mice sometimes live up to 20 months of age or more. In the 129Ola|C57bl6 mixed background used in this study only 3 TTD control mice out of 6 survived to the age of 20 months. Nevertheless no significant difference between the bone mineral density of TTD mice in C57bl6 and mixed background was detected.

UV-survival
The UV survival curve represents an average of 4 independent experiments containing 1-2 cell lines per mutant genotype per experiment. Data is represented as an average survival curve per genotype; error bars indicate SEM between experiments.

Comparative immunofluorescence
Latex bead labeling and comparative immunofluorescence analysis of the p62 subunit

of the TFIIH was performed as described earlier (Vermeulen et al. 2000; Botta et al. 2002). Briefly, primary MEFs at passage 2-5 were grown to confluence in 50:50 DMEM/Ham's F10 medium supplemented with 10% FCS and antibiotics (penicillin and streptomycin) with either 0.79μm or 2μm latex beads (Polybead Carboxylate Microspheres, Polysciences) or without beads. Following the 2-day bead labeling, cells were plated onto coverslips at a 1:1 ratio. Two days later cells were fixed with 2% paraformaldehyde for 10 minutes at RT, permeablized with 0.1% TritonX-100, and blocked in PBS+ (PBS + 0.15% glycine and 0.5% BSA). Primary anti-p62 (3C9) and secondary Cy3-conjugated goat-anti-mouse (The Jackson Laboratory) antibodies were used at dilutions of 1:2000 and 1:800, respectively, in PBS+ at RT and mounted in Vectashield (Vector Laboratories) containing 1.5μg/ml DAPI. Epifluorescent and phase-contrast images were produced on a Leitz-Aristoplan microscope equipped with a 3-CCD camera (DXC-950P Sony) and digitally processed using Adobe Photoshop 4.0. 25-50 microscopic fields in each experiment were photographed in a "blind" fashion. To avoid the effect of possible differences in background fluorescence in different parts of the coverslip as well as within a microscopic field to the measurements, background levels measured beside each individual nucleus were subtracted. A standard Student T-test using two-tailed two-sample equal variance setting was used to verify statistical significance within each experiment. Three representative experiments are depicted. Standard karyotyping was performed to verify that the observed differences in signal intensity between cells with different genotypes was not due to altered karyotype of the primary MEF cells. In all the cell lines used in this study, ~80% of the nuclei were diploid and ~20% tetrapolid. Two or more cell lines per genotype (except for the $Xpd^{TTD/†XP}$ cells in which case one cell-line was used in repeated experiments) were used, and experiments were repeated 2-6 times per genotype.

Acknowledgements

CHAPTER 4

Cockayne syndrome and trichothiodystrophy share a common mechanism in defective DNA repair

Jaan-Olle Andressoo[1], James R. Mitchell[1],, Jan de Wit[1], Deborah Hoogstraten[1], Rudolph B. Beems[2], Harry van Steeg[2], Judith Jans[3], Chris I. de Zeeuw[4], Jan H. Hoeijmakers[1] and Gijsbertus T.J.van der Horst[1]

1 Medical Genetics Center, Department of Cell Biology and Genetics,
Center of Biomedical Genetics,
4 Department of Neuroscience, PO Box 1738, Erasmus MC, 3000DR Rotterdam,
The Netherlands,
2 National Institute of Public Health and the Environment, Post Office Box 1,
3720 BA Bilthoven, Netherlands,
3 Present address: Department of Molecular and Cell Biology,
University of   California at Berkeley, 125 Koshland Hall, Berkeley, California, USA

Summary

Among the ~35,000 known genes in humans, inherited mutations affecting a single gene that results in both cancer predisposition and accelerated ageing are rare. Among these few genes is *XPD*, mutations in which are implicated in a variety of clinically diverse disorders including the cancer predisposition syndrome xeroderma pigmentosum (XP); XP combined with the segmental progeroid disorder Cockayne syndrome (XPCS); and in the scaling skin/fragile hair and accelerated aging syndrome trichothiodystrophy (TTD). XPD is a helicase component of the 10 subunit protein complex TFIIH, which is involved in multiple cellular processes including several forms of transcription, nucleotide excison repair (NER); it also has implications in apoptosis and cell-cycle regulation. This functional diversity of XPD has made it difficult to relate clinical diversity to defects in a specific function. Here, we report the generation and analysis of a knock-in mouse model for XPD-XPCS. Xpd^{XPCS} mice displayed dramatic cancer predisposition and mildly accelerated segmental ageing features. Xpd^{XPCS} mice carrying an additional mutation in *Xpa*, which enhances the DNA repair defect, showed vastly accelerated aging features including ataxia, spasticity, loss of Purkinje neurons, cachexia, kyphosis and lifespan of 2-3 weeks; thus largely overlapping with the phenotype of *Xpa*-deficient Xpd^{TTD} mice. Furthermore, in both double mutant genotypes we detected a common molecular defect in the spatio-temporal architecture of the NER reaction. Taken together, our data indicate that TTD and CS share a common root cause in defective DNA repair, and that cancer predisposition and premature ageing in XPCS are parallel but mechanistically distinct processes.

Introduction

Numerous genotoxins of both endogenous and exogenous origin are capable of inducing a wide range of lesions in DNA. Unrepaired DNA damage can give rise to mutations and thereby contribute to cancer, but may also block transcription or replication which can lead to cell-death and/or senescence and thereby contribute to ageing (Hoeijmakers 2001; Hasty et al. 2003; Mitchell et al. 2003). To prevent these deleterious effects, all organisms are equipped with a network of complementary DNA repair systems. The highly conserved Nucleotide Excision Repair (NER) pathway removes a wide diversity of helix-distorting DNA lesions, including UV-induced photoproducts, bulky chemical adducts, intrastrand crosslinks and several forms of oxidative lesions (de Laat et al. 1999; Brooks et al. 2000; Hoeijmakers 2001). NER is divided in two subpathways: global genome NER (GG-NER) and transcription coupled NER (TC-NER). In GG-NER, the hHR23B/XPC complex is a damage sensor and initiator of the NER reaction. In TC-NER, blockage of transcribing RNA-PolII is believed to

trigger NER (van den Boom et al. 2002). NER involves sequential binding of ~ 30 proteins in a ~ 4 minute reaction followed by release of NER factors from the repaired site (Hoogstraten et al. 2002).

The consequences of inborn defects in NER proteins are highlighted by autosomal recessive syndromes Xeroderma Pigmentosum (XP), Cockayne Syndrome (CS) trichothiodystrophy (TTD) and the rare combined XPCS and XP/TTD syndromes (Broughton et al. 2001; Bootsma et al. 2002). XP patients display prominent sun-sensitivity and have a dramatically elevated (>1000 fold) risk of developing sun-induced skin cancer. Sun sensitivity in CS and TTD can be as pronounced as in XP, but does not result in enhanced cancer risk. Instead, CS and TTD are characterized as severe neuro-developmental diseases with a component of segmental accelerated ageing leading to death usually before puberty (Nance and Berry 1992; Nakura et al. 2000; Itin et al. 2001). In addition, TTD patients display hallmark cutaneous features, such as sulphur-deficient brittle hair and nails and scaling skin (ichtyosis).

Accelerated ageing in CS and TTD patients has been hypothesized to result from elevated apoptosis which, as a trade-off, may protect against cancer predisposition (Hoeijmakers 2001; de Boer et al. 2002; Mitchell et al. 2003). From the 9 human XPCS patient phenotypes described so far, firm conclusions about disease etiology are hard to draw due to variation in disease progression among patients probably resulting from normal differences in their environments (exposure to sun light, early hospitalisation) and genetic backgrounds. Nevertheless, in addition to a clear cancer predisposition, the CS pathology does not appear to differ grosso modo from that of typical CS (Rapin et al. 2000; Lindenbaum et al. 2001). This suggests that cancer predisposition and segmental accelerated ageing are not mutually exclusive processes but can evolve independently.

The molecular defect underlying the greatly elevated skin cancer incidence in XP has been related to defective NER of UV-induced lesions in DNA (Hoeijmakers 2001). Since patients lacking XPA protein are completely defective in both GG-NER and TC-NER but do not display CS or TTD features, proteins implicated in CS and TTD are thought to be involved in other processes in addition to NER. Indeed, TTD and XPCS causative mutations are associated with XPD and XPB helicase components of the multifunctional TFIIH complex. Besides its role in NER, this multisubunit complex is vital for RNA PolII transcription initiation (Schaeffer et al. 1993), has implications in RNA PolI transcription (Bradsher et al. 2002; Hoogstraten et al. 2002), and controls some forms of activated transcription (Keriel et al. 2002). TFIIH can also impact p53-dependent apoptosis (Wang et al. 1996) and may participate in regulation of the cell cycle (Harper and Elledge 1998). In addition, it participates in DNA repair reactions of non-helix-distorting lesions outside the classical NER lesion spectrum and independent of the NER reaction itself (Le Page et al. 2000).

Clinically, CS and TTD share a remarkable degree of similarity. Both syndromes are associated with a nearly exclusive postnatal onset of developmental delay, microcep-

haly, skeletal abnormalities, progressive mental degeneration, sensorineural deafness, ataxia, spasticity and gait anomalies, demyelination, brain calcifications, hypogonadism and overall aged appearance (Nance and Berry 1992; Nakura et al. 2000; Rapin et al. 2000; Itin et al. 2001). Which of the many functions of TFIIH underlies TTD and CS, and whether these disorders share a common or distinct mechanism, has largely remained enigmatic. This is not due to an absence of experimental research; on the contrary, extensive biochemical and cellular studies during the past years has yielded a plethora of results suggesting both overlapping and distinct mechanisms for CS and TTD. A basal transcription initiation defect of RNA-PolII genes has been suggested to explain at least part of the TTD phenotype, a notion which has recently gained some in vivo and in vitro evidence (de Boer et al. 1998a; Dubaele et al. 2003). Defects in RNA PolI-related transcription (Bradsher et al. 2002) and defective transcription-coupled repair of endogenous oxidative DNA lesions (Le Page et al. 2000) have been proposed to contribute to CS, whereas a defect in the activated transcription function of TFIIH has been put forth as a mechanism contributing to neurodegeneration in TTD (Keriel et al. 2002). Nevertheless, to what extent the above mechanisms contribute to disease etiology in vivo is still largely unknown, mostly due to limitations of existing biochemical and cellular assays to predict systemic and/or time-dependent pathology.

The aim of this study was to shed light on the basic mechanism(s) of TFIIH-associated developmental delay and accelerated ageing observed in TTD and XPCS, as well as the XPCS-specific cancer predisposition. Due to limitations of existing biochemical and cell-based systems to report on complex organismal phenotypes, we generated and compared several knock-in and knock-out single and double mutant mouse models. Previously, we mimicked a known human TTD-causing point mutation (XPD^{R722W}) in the mouse Xpd locus. Homozygous Xpd^{TTD} mice display a wide range of TTD-like features including the hallmark cutaneous symptoms as well as segmental premature ageing features (de Boer et al. 1998a). Further reduction of DNA repair capacity by inactivation of the Xpa gene results in dramatically accelerated TTD features and death within 3 weeks after birth (de Boer et al. 2002). Here, we report the generation and characterization of an Xpd^{XPCS} mouse model engineered by genocopying the XPD^{G602D} allele found in the patient XP/CS2. We found that this mutation results in XPCS-like pathology in mice, including cancer predisposition and segmental accelerated aging, thereby further validating the mouse system as relevant for modeling XPD-associated human pathology. Inactivation of Xpa in Xpd^{XPCS} mice resulted in a greatly accelerated segmental ageing pathology overlapping that of Xpa-deficient Xpd^{TTD} mice, strongly suggesting that the progeroid symptoms observed in TTD and XPCS share a common mechanism rooted in defective DNA repair. Further, we provide evidence that in XPCS cancer predisposition and premature ageing are parallel but mechanistically distinct processes.

Results

Derivation of Xpd^{XPCS} (XPD^{G602D}) mice

A dominant selectable Neo-marker was flanked with LoxP sequences (pMC-1 neo-LoxP) and cloned into a unique HpaI site in the 3'UTR of the *Xpd* gene (Figures 1 A and B). The XP/CS2 patient-derived point mutation (XPD^{G602D}) causing XP combined with CS (hereafter referred to as Xpd^{XPCS} or simply XPCS) was introduced by site-directed mutagenesis. The resulting XPCS-neo-LoxP construct was used for gene-targeting by standard procedures as described previously (de Boer et al. 1998a). Southern blotting revealed that homologous integration had occurred in 9% of ES cell clones (Figure 1 D). To determine the expression levels of the mutant allele in ES cells, the dominant selectable marker was removed from the targeted *Xpd* allele in heterozygote ES cells by transient Cre recombinase expression (Figures 1B, C and data not shown). Subsequent RT-PCR analysis showed that the mRNA level originating from the Cre- recombined Xpd^{XPCS} allele is comparable to that from the Xpd^{wt} mRNA level (data not shown; see also Materials and Methods).

Two independent targeted ES cell clones with a normal karyotype were injected into blastocysts for generation of chimeric mice. $Xpd^{XPCS-neo-LoxP}$ heterozygous mutant offspring were obtained at expected Mendelian ratios and further crossed to transgenic CAG-*Cre* mice in which Cre recombination occurs already in the oocyte (Sakai and Miyazaki 1997). The excision of neo-LoxP from the genomic DNA in F1 offspring was monitored by PCR using primers F2 and R. After Cre recombination, the Xpd^{XPCS} allele yields a PCR product 129bp longer than Xpd^{wt} allele (Figure 1 A, C and E). RT-PCR analysis on mRNA isolated from the testis of $Xpd^{XPCS/wt}$ heterozygous mice using primers F1 and R showed comparable amounts of RT-PCR products originating from Xpd^{XPCS} and Xpd^{wt} alleles (Figure 1C and F). The presence of the G602D mutation and the absence of any other undesired mutations originating from cloning or gene-targeting was verified by sequencing. $XpdX^{PCS/XPCS}$ homozygous mutant offspring from matings between heterozygous animals were obtained at the expected Mendelian frequency. Standard genotyping was performed using primers F2 and R (Figure 1E). Because $Xpd^{wt/wt}$ and heterozygous

__Figure 1.__ XPCS (XPD^{G602D}) targeting of the mouse Xpd gene
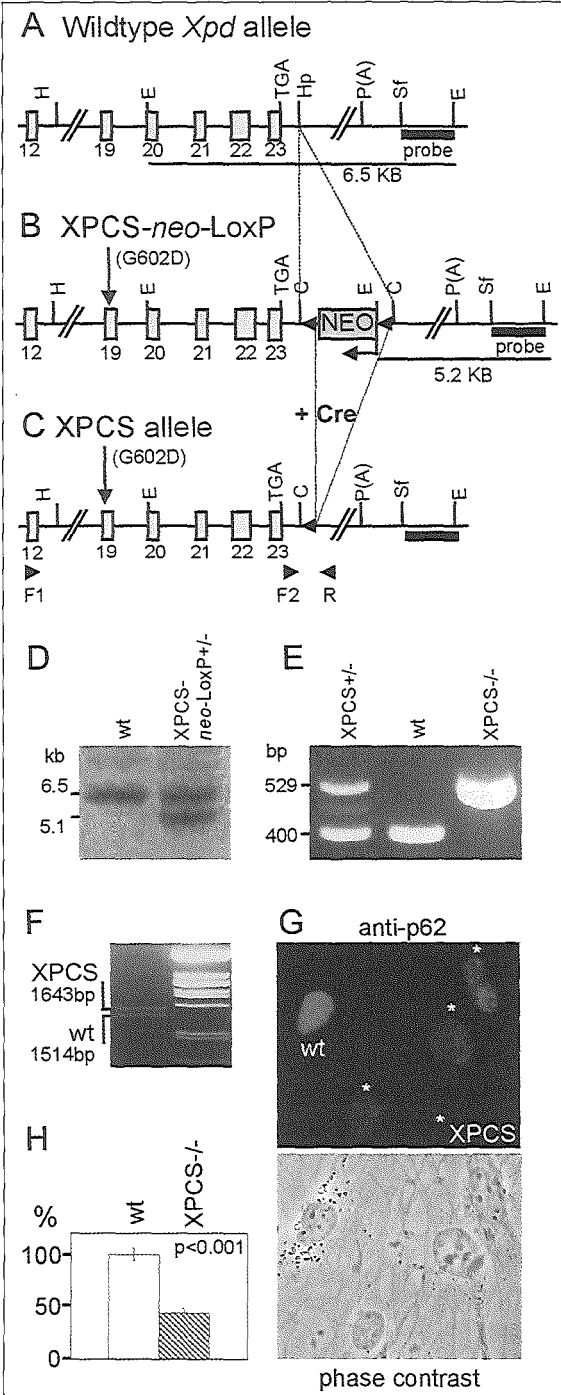
(A) Schematic representation of the genomic structure and partial restriction map of a portion of the wt mouse Xpd gene. The coding parts of exons 12 and 19-23 are indicated as grey boxes. TGA-translational stop codon, P(A)-polyadenylation signal. The unique 3' probe located outside the targeting construct is marked as a thick black line.

(B) XPCS-neo-LoxP targeted allele, containing the XPCS causative mutation (XPD^{G602D}) indicated by a vertical arrow. LoxP sequences are indicated by filled triangles. Direction of transcription from the selectable neo marker is indicated with an arrow.

(C) Targeted allele for XPCS (XPD^{G602D}) mutation in the mouse Xpd allele after excision of the LoxP flanked selectable neo marker by Cre recombination. Primers F1, F2 and R are indicated by triangle.

(D) Southern blot analysis of EcoRI-digested genomic DNA from wt and XPCS-neo-LoxP recombinant clones hybridized with 3' probe. The wt allele yields a 6.5 kb fragment whereas the XPCS-neo-LoxP allele yields a 5.1 kb fragment.

(E) Verification of the Cre excision step of the neo gene (resulting in the XPCS allele) and genotyping of progeny with a genomic PCR assay using primers F2 and R as indicated in (C). The XPCS and wt alleles yield products of 529 and 400 bp respectively.

(F) RT-PCR amplification of mRNA originating from the XPCS+/- testis using primers R and F1. Note the comparable amounts of 1514bp wt and 1643bp XPCS RT-PCR products.

(G) Upper panel: flourescent immunostaining of the p62 subunit of TFIIH in wt and XPCS cells (indicated by asterisks). Note the reduction of cellular TFIIH in XPCS (XPD^{G602}) cells. Lower panel: phase contrast image of the same microscopic field, wt cell is labeled with silicon beads.

(H) Quantification of immunoflourescence from the p62 subunit of the TFIIH complex in wt and XPCS cells. p value indicates the significance of the difference between wt and XPCS cells analyzed on the same microscopic slide.
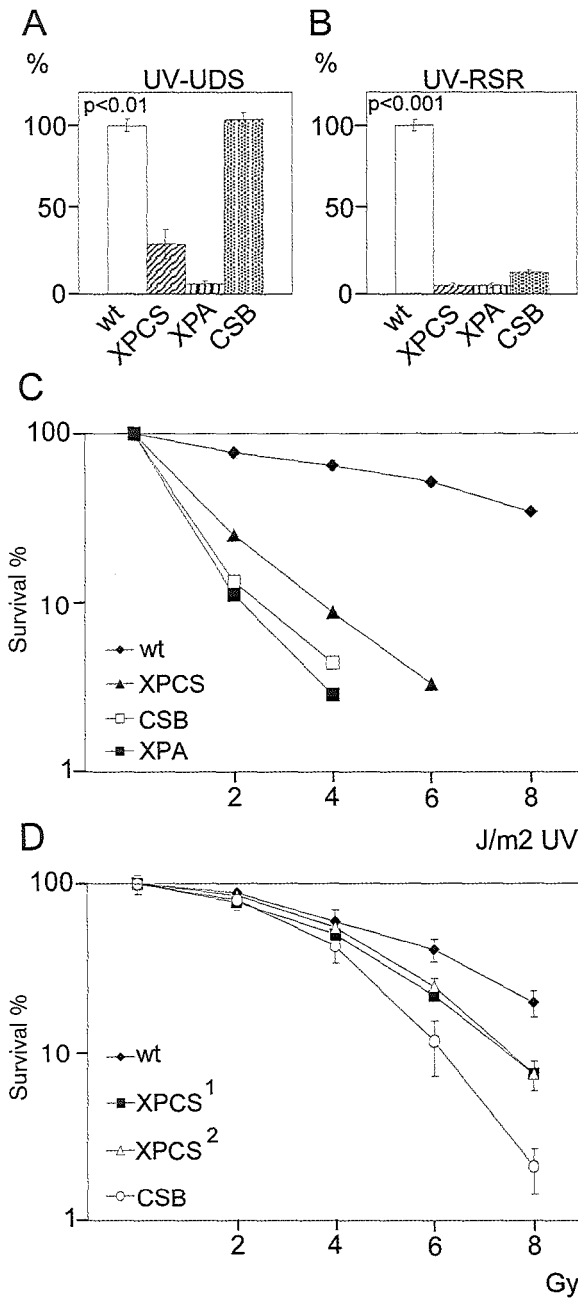
$Xpd^{XPCS/wt}$ mice were indistinguishable in all aspects investigated, we concluded that the mutant allele has no dominant effect over the Xpd^{wt} allele, consistent with the recessive nature of the disease. For simplicity, $Xpd^{wt/wt}$ and $Xpd^{XPCS/wt}$ mice will hereafter be referred to as "wt" and homozygous mutants as "XPCS". Unless noted differently, all the mice used in this study were in a 129Ola|C57BL6|FVB mixed background.

In XP/CS2 (XPD^{G602D}) patient cells, we and others have found a 25% reduction in the cellular TFIIH content (Botta et al. 2002). Using the same strategy of comparative immunohistochemistry based on the detection of the p62 subunit of TFIIH complex, we found TFIIH levels reduced by ~50% in primary XPCS MEF cells (Figure 1G and H). A similar 50% reduction of TFIIH was observed in MEFs prepared from TTD (XPD^{R722W}) mice (data not shown). Since TTD cutaneous features (acanthosis, scaling skin, reduced cysteine content in hair) and anemia have been attributed to the reduced level of TFIIH (Vermeulen et al. 2001; Viprakasit et al. 2001), we studied these parameters in XPCS mice. Biochemical analysis of the amino acid content of the hair, measurements of blood parameters and microscopical examination of the skin revealed XPCS mice to be indistinguishable from the wt in each of those parameters (Figure 4 and data not shown). Thus, reduced TFIIH levels in MEF cells as measured by this method may not be solely responsible for the characteristic TTD cutaneous phenotype.

DNA repair characteristics of XPCS (XPD^{G602D}) cells

Classical NER and TCR defects are well represented by *Xpa-/-* and *Csb-/-* (for simplicity heretofore designated XPA and CSB) defective MEF cells, respectively (de Vries et al. 1995; van der Horst et al. 1997). XPA cells totally lack GG-NER as well as TC-NER. TC-NER defective CSB cells display an additional defect in the more general TCR pathway and thus lack the ability to repair transcription-blocking lesions outside the spectrum of helix-distorting NER substrates, such as thymine glycols (de Vries et al. 1995; van der Horst et al. 1997; Le Page et al. 2000; de Waard et al. 2003). We compared various DNA repair parameters of MEFs isolated from XPCS mice to XPA and CSB MEFs. GG-NER capacity was measured using the UV induced Unscheduled DNA Synthesis (UDS) assay. As shown in Figure 2A, XPCS cells retained ~ 30% GG-NER capacity, pointing to a partial GG-NER defect.

Figure 2. _DNA repair characteristics of XPCS (XPD^{G602}) cells_

A
% UV-UDS
p<0.01
100
50
0
wt XPCS XPA CSB

B
% UV-RSR
p<0.001
100
50
0
wt XPCS XPA CSB

C
Survival %
100
10
1
2 4 6 8
J/m2 UV

- wt
- XPCS
- CSB
- XPA

D
Survival %
100
10
1
2 4 6 8
Gy

- wt
- XPCS 1
- XPCS 2
- CSB

(A) UV induced DNA repair synthesis capacity (UV-UDS). Cells were UV irradiated (16 J/m^2) and incubated for 2 h in 10µCi [methyl-3H]-thymidine containing culture medium. Results were visualized by autoradiography. UV-UDS reflects competence of GG-NER in XPCS primary MEF cells compared to wt, CSB and XPA cells. p value indicates the minimum significance of the difference between each pairwise comparison.

(B) RNA Synthesis Recovery (UV-RSR). Cells were UV irradiated (10J/m^2), cultured for 16 h to recover and incubated for 1h in 10µCi [5,6-3H]-uridine containing culture medium. Results were visualized by autoradiography. UV-RSR reflects TC-NER capacity of XPCS primary MEF cells compared to wt, CSB and XPA cells. Note that the p value indicates the difference between all of the mutants and the wt, mutant cell lines do not significantly differ from each other and the differences seen are within the normal variation of the assay.

(C) UV survival curve of primary XPCS MEF cells compared to wt, XPA and CSB cells. Graph is averaged from several independent experiments containing multiple cell lines per genotype. Error bars lie within symbol size and indicate SEM between different experiments.

(D) Representative gamma ray survival curve of two independent XPCS spontaneously transformed MEF lines (indicated by the numbers). Error bars indicate SEM within the experiment.

Analysis of TC-NER competence after UV irradiation with the RNA Synthesis Recovery (RSR) assay revealed that XPCS cells are completely devoid of TC-NER activity, similar to XPA and CSB cells (Figure 2B). Consistent with this finding, XPCS cells were found to be hypersensitive killing by UV (Figure 2C). An equally severe NER defect has been reported for the XP/CS2 (XPD^{G602D}) patient cells (Broughton et al. 1995).

The TCR defect in repair of oxidative DNA lesions found in CS and XPCS cells can be tested by measuring the sensitivity of these cells to oxidative stress including gamma irradiation (Le Page et al. 2000; de Boer et al. 2002; de Waard et al. 2003). Historically these measurements are done in spontaneously or SV40 transformed mouse or human cells. Comparison of CSB and XPCS spontaneously transformed MEFs in cellular survival experiments in response to increasing gamma ray dose revealed intermediate hypersensitivy for XPCS cells (Figure 2D). Thus in XPCS (XPD^{G602D}) MEFs CS- type of repair deficit is present and G602D mutation causes comparable DNA repair phenotype in cells from mouse and man.

Next, we monitored the kinetics of accumulation of NER factors on locally UV-irradiated areas of the nucleus. We used immunostaining to visualize accumulation of XPC, the initial damage sensor in GG-NER, as well as the p62 subunit of TFIIH at both 15 minutes and 3 hours after application of local UV damage (Mone et al. 2001; Volker et al. 2001).

The accumulation and retention of NER factors at locally UV damaged areas within the nucleus mainly reflects GG-NER of UV-induced 6-4 photoproducts, a process which is finished in ~ 1-2 hours in wt cells (D. Hoogstraten et al., unpublished). In XPA and XPCS cells (and TTD cells, data not shown) we consistently observed both XPC and TFIIH accumulation at sites of local DNA damage within 15 minutes after UV exposure at concentrations similar to or even higher than in wt cells. Three hours later, when NER factors no longer remained in abundance at local damage in wt cells (data not shown), XPA, XPCS and to a lesser extent TTD cells displayed enduring accumulation of XPC and TFIIH at local damage sites, likely reflecting a persistent attempt to repair DNA with an inefficient mutant TFIIH (Figure 3 and data not shown). In cells doubly mutant for XPA and XPCS, both XPC and TFIIH binding at local damage sites was either weak or absent entirely (Figure 3, lower panel). Similar results were obtained in XPA/TTD cells (data not shown). These results indicate that combined homozygosity of XPA with either XPCS (XPD^{G602D}) or TTD (XPD^{R722W}) results in similarily deregulated spatio-temporal organization of the GG-NER reaction, the subpathway of NER mainly visualized by this method.

Since accelerated segmental ageing likely involves chronic accumulation of oxidative damage from low-level endogenous sources rather than acute oxidative damage such as delivered by gamma rays, we next analysed the capacity of XPCS primary MEFs to proliferate under different oxygen tensions. Parallel cultures were maintained under conditions of 3% oxygen tension, which approximates a physiologically

Figure 3 *Accumulation of NER factors at locally UV irradiated areas of the nucleus.*
Note prolonged retention of XPC and TFIIH (immunostained for the p62 subunit) in XPA and XPCS
single mutant cells (but not in wt cells, data not shown) 3h after local UV damage (upper 3 panels).
Lower panel: note that XPA removal in XPCS cells results in severely hampered accumulation of
TFIIH. At both time points TFIIH staining was either absent (in ~ 50% of locally damaged cells) or
weak.
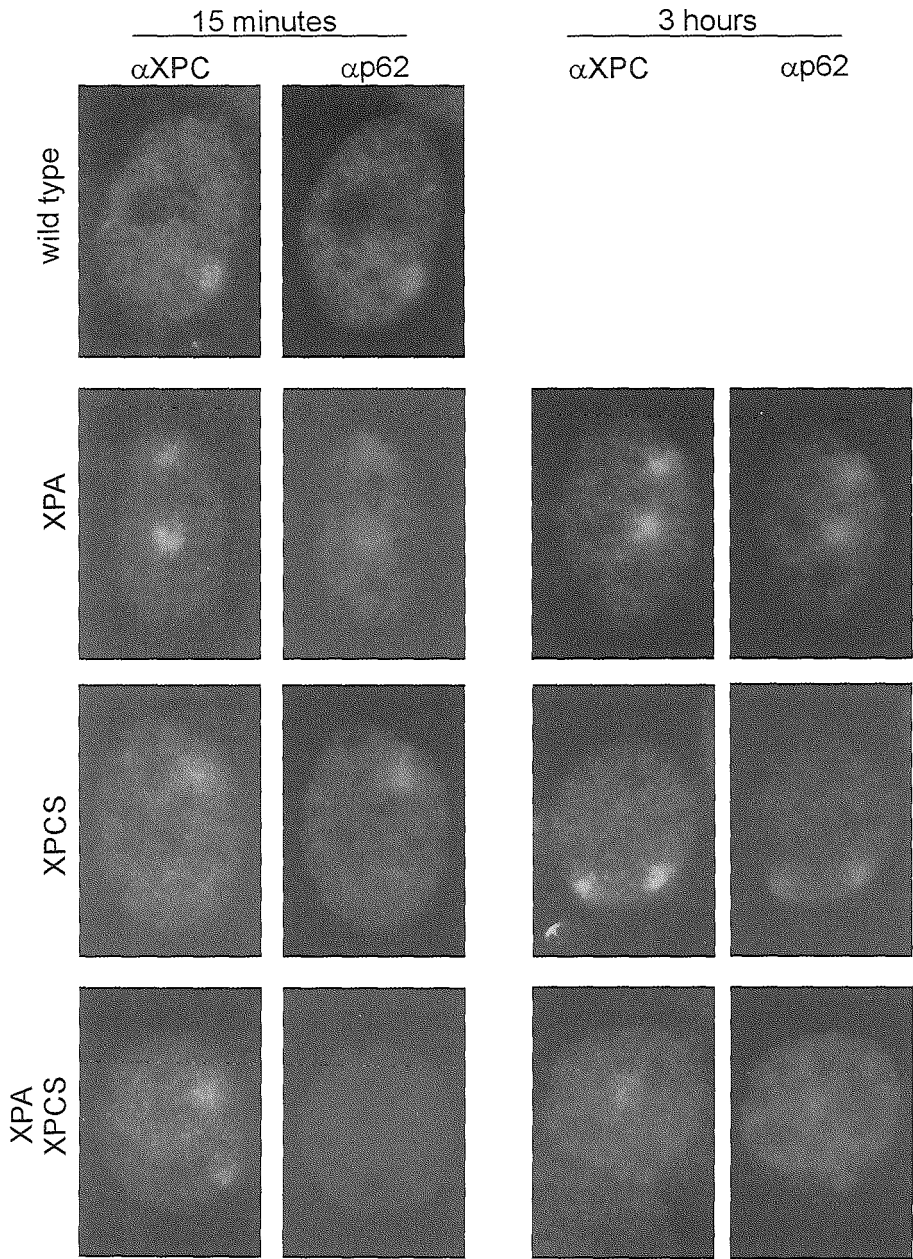
relevant level found in the human body, and atmospheric oxygen (~20%), which is toxic to cells (Parrinello et al. 2003). Under these conditions, growth characteristics of several independent lines of primary XPCS and TTD MEFs did not differ from that of littermate derived controls (data not shown). Similar results were obtained with XPA/XPCS double-mutant MEF cells. We conclude that primary XPCS, XPA/XPCS and TTD MEFs are not hypersensitive to chronic low dose exposure to ROS.

XPCS mice are hypersensitive to UV irradiation and extremely cancer prone

To verify whether the partial NER defect observed in cultured XPCS MEFs is also present in vivo, photosensitivity of XPCS mice was tested by exposing shaven dorsal skin to UV-B light at the environmentally relevant dose of $200J/m^2/day$ for 4 days. XPCS mice but not wt control mice developed erythema within 5 days (data not shown). Histological analysis of skin sections of XPCS mice sacrificed 1 week after the start of UV-B treatment revealed pronounced epidermal hyperplasia, consisting of increased number of viable cell layers (acanthosis) and hyperemia (dilated capillaries, filled with blood) (Figure 4). The latter is consistent with the erythema observed in the skin. Neither erythema nor hyperplasia was observed either in the UV-exposed skin of heterozygous mice or in the unexposed skin of XPCS mice (Figure 4). Direct comparison of results with those previously published for CSB (van der Horst et al. 1997) and XPA (de Vries et al. 1995; Nakane et al. 1995) mice were not possible due
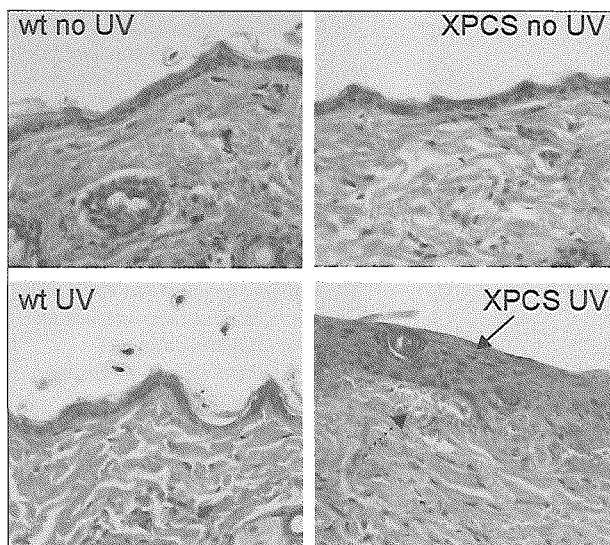

Figure 4 Acute effects of UV-B in the skin of XPCS mice.
Shaven XPCS mice were exposed to $200J/m^2$ UV-B daily for 4 consecutive days and sacrificed 1 week after the start of the treatment. Note the pronounced epidermal hyperplasia, consisting of increased number of viable cell layers, (acanthosis; arrow above) and hyperemia (dilated capillaries, filled with blood; arrow below) and the absence of keratinized layer reflecting "scaling of the skin" at the macroscopic level. 400X

to differences in UVB dose, wavelength and genetic background of the mice. However, our observations suggest that XPCS mice have an equal if not greater sensitivity to UV-B relative to XPA and CSB mice. In conclusion, XPCS (XPD^{G602D}) mutation induces severe photosensitivity in mice, very similar to that of patient XP/CS2.

In addition to the severe photosensitivity, the XP/CS2 patient suffered an early onset of skin cancer (first skin tumor noted at the age of 2,5 years) (Lafforet and Dupuy 1978; Lindenbaum et al. 2001). In order to investigate this important aspect of XPCS, animals were exposed daily to a low, environmentally relevant UV-B dose. Completely NER defective and highly cancer-prone XPA mice in a C57bl6 genetic background were included as a positive control. As an indication of a pronounced UV-B sensitivity, 9 weeks after the start of the UV-B treatment, 4 out of 10 XPCS mice developed corneal opacity; after 11 weeks, all 10 XPCS mice carried this lesion. Interestingly, within the same time span only 3 out of 5 XPA mice, previously shown to be extremely UV-sensitive (de Vries et al. 1995) developed identical lesions. UVB induced cutaneous effects (i.e. erythema) were exclusively observed in UV-treated XPCS mice and appeared already at 7 weeks after the start of the treatment (in 3 out of 10 mice). Within 17 weeks, all XPCS mice developed skin and/or eye tumors on UVB exposed areas (Figure 5, Table 1) whereas none of the XPA mice carried tumors at this time point. The first XPA mouse developed a skin tumor only after 23 weeks; and within 31 weeks all 5 XPA mice carried tumors; within 40 weeks
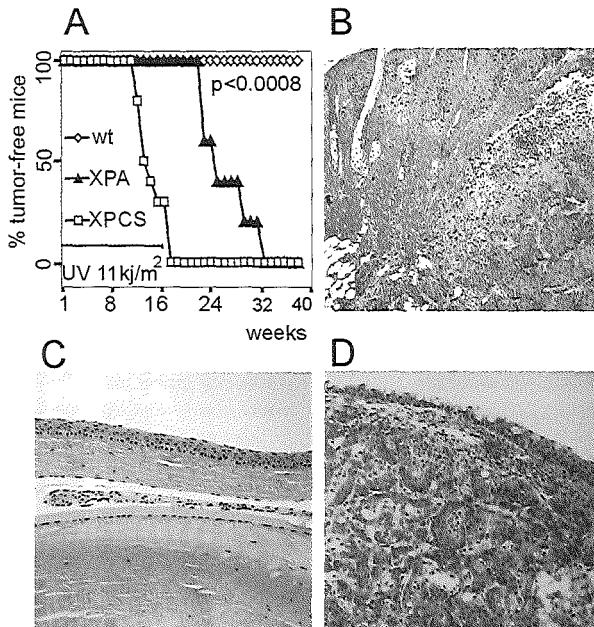
Figure 5 XPCS mice are extremely prone to UV-B induced malignancies. (A) Time course of tumor formation in XPCS and XPA mice during chronic exposure to UV-B. Y-axis indicates % of tumor free animals. Note that all XPCS animals carry tumors at 17 weeks whereas the first tumor among XPA mice appears at 23 weeks after the start of the treatment. (B) Histological examination of UV-B induced skin tumors in XPCS mice. Shown is a typical example of squamous cell carcinoma invading subcutaneous tissues. Magnification 50X (C) Normal cornea of the eye. Magnification 100X (D) Example of UVB induced invading squamous cell carcinoma in the eye of an XPCS mouse. Magnification 100X

none of the wt or heterozygous controls had developed tumors or other skin lesions. A complete overview of the observed tumor response is given in Table1.

Table 1   Abbreviations: hz, XPCS heterozygous; SCC, squamous cell carcinoma; SCP, squamous cell papilloma.
*   average tumor latency time for XPCS mice is 13 weeks; for XPA mice, 25 weeks (p<0.0008)

	Tumor incidence			
Genotype:	wt or hz	XPCS	XPA	Tumor types found (x incidence)
Untreated	0/3	-	-	Not applicable
Untreated	-	0/3	-	Not applicable
UV-treated	0/7	-	-	Not applicable
UV-treated	-	10/10*	-	SCC of an eye, 4x (cases)
				8x SCC + 2 SCP of the skin
				Hemangioma of an eye, 2x
UV-treated	-	-	5/5*	SCC of an eye, 1x
				6x SCC + 1x SCP of the skin

A summary of published UVB carcinogenesis experiments in NER mouse models is presented in Table 2.

*Table 2*   UVB-induced tumorigenesis in XPD-XPCS, XPA, CSB and XPD-TTD mice

	XPCS[a]	XPA[a]	XPA[b]	CSB[c]	TTD[d]
Genetic background	FVB/ C57BL6/ 129Ola	C57BL6	C57BL6/ Ola129	FVB/ 129Ola	C57BL6/ 129Ola
Cumulative UVB dose (kJ/m2)	11	11	22	50	103
Tumor bearing animals (%)	100	100	75	65	100
Onset of tumors (weeks)	12-17	23-31	15-23	23-36	18-29

[a]This study; [b]de Vries et al. (1995); [c]van der Horst et al.(1997); [d]de Boer et al.(1999)

The uniform and quick progression of tumors in 10 XPCS mice and the absence of profound strain-associated changes in cancer predisposition in XPA (Table 2) and TTD (XPD[R722W]) mice (J. Jans et al., unpublished) suggests that the XPD[G602D] mutation, not the genetic background, is causative for the observed cancer predisposition. In conclusion, the above data suggest that among NER deficient mice, XPCS mice are the most prone to UV-induced skin cancer.

XPCS (XPD^G602D) mice display mild Cockayne Syndrome-like symptoms

Developmental delay in CS-affected humans has an almost exclusive postnatal onset (Nance and Berry 1992). Although born at the expected Mendelian frequencies and with normal birth weights, XPCS mice displayed developmental delay starting from about 5 days after birth (Figure 6A). Until about 16 days after birth, both male and female XPCS pups showed a small but significant developmental delay. While female XPCS mice caught up with littermate controls between ~ 2 and 4 weeks of age, developmental delay in male XPCS mice lasted until about 2 months of age (Figure 6B) during which tail-suspension tests revealed spastic and abnormal coordination of hind-limbs (Figure 5D). No correlation between developmental delay and neurological features was observed. After 2 months, the neurological features became less pronounced and gradually disappeared among most, but not all, of the 20 male XPCS animals examined.

A

B male 0,9 months

C

D wt   XPCS
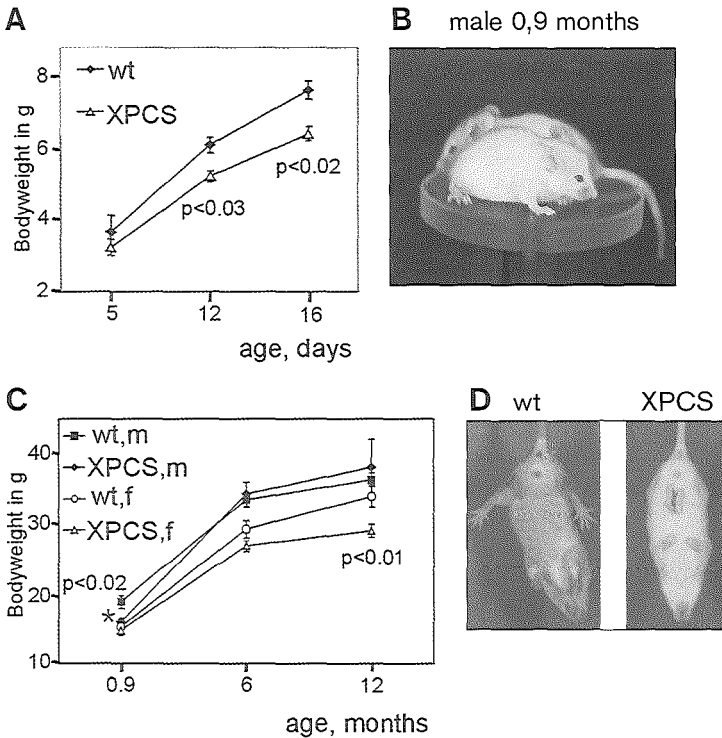
Figure 6
Phenotype of XPCS mice.
(A) Developmental delay in XPCS mice. Bodyweight of 3 independent groups of XPCS mice were measured at the ages of 5,12, and 16 days.
(B) Developmental delay in 27-day-old male XPCS mice. Note the smaller size of the XPCS mouse (in front) compared to the littermate control.
(C) Developmental delay in male XPCS mice at 0.9 months (asterisk, p<0.02) and premature cachexia in female XPCS mice at 12 months (p<0.01). Bodyweight of the same group of female mice was followed in time.
(D) Tail suspension test of 6-week-old male mice. Wt behavior includes spreading of hind limbs and active movements with fore limbs. XPCS mice display heterogeneous

E

male 19 months   male 20 months

F   5 months   12 months   20 months

wt
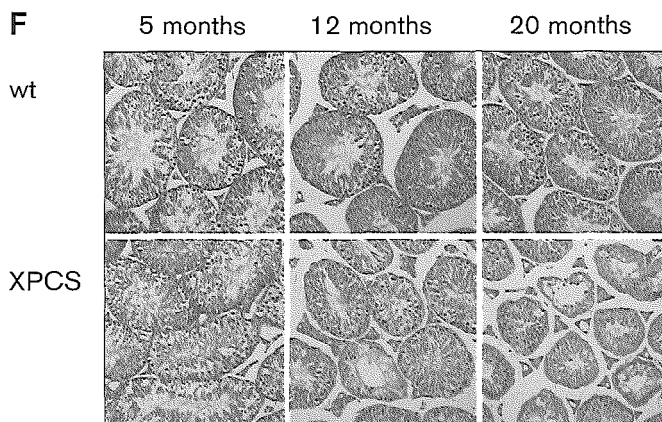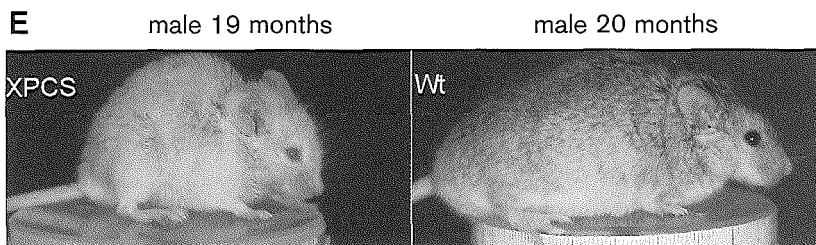
XPCS

phenotypes, ranging from nearly normal to severe cramp-like seizures of both hind and fore limbs and complete inactivity upon tail suspension (depicted in photo). (E) Premature ageing appearance of male XPCS mice at 19 month of age. Note the reduction of subcutaneous fat tissue (cachexia) and kyphosis in the XPCS mouse compared to the normal wt mouse. (F) Progressive loss of germinal epithelium in the testis of male XPCS mice.

Gross behavior, cognitive ability and neuro-motor function of XPCS mice were analyzed by behavioral tests. Although male XPCS mice showed normal behavior, they were significantly less active within the first minute of an open-field exploratory test (p<0.03), indicating that XPCS mice require longer adaption time in a new environment. No age specific differences were found up to 7 months of age, suggesting that within the studied age-range this feature has no progressive character. Next, neuro-motor coordination and learning capacity were examined with the accelerating Rotarod test. XPCS mice (n=22) appeared normal. Footprint pattern analysis did not reveal any gait abnormalities (data not shown). Both male and female XPCS mice were fertile until at least 6 months of age. Litter sizes were normal (data not shown). In conclusion, developmental delay, behavior in an open field test and minor neurological dysfunction displayed by XPCS mice was comparable to that of mice homozygous for a mutation in the *Csb* gene leading to severe truncation of the encoded protein (van der Horst et al. 1997). Thus, in contrast to the human CS condition, XPCS and CSB mice develop only mild CS-like symptoms.

Next, we addressed the ageing effects of the XPCS mutation. Early cachexia (loss of subcutaneous fat tissue) is a common accelerated ageing feature both in CS patients (Nance and Berry 1992) and in a mild form in CSB mice (I. van der Pluijm et al., manuscript in prep.). Our cohort of ageing mice (n=132) included 31 male and 39 female XPCS (XPD[G602D]) mice. At 6 months of age, no difference in bodyweight between genotypes was noted. As an indication of an accelerated age-dependent

cachexia, female XPCS mice (n=14) displayed reduced bodyweight 6 months later (n=13 for control mice, p<0.01) (Figure 6C). The low number of male animals in that age group (n=5) did not allow for firm conclusions. The oldest male XPCS mice (n=2) reached the age of 19 months and displayed cachexia and kyphosis (Figure 6E). Anatomical and histological analysis revealed progressive loss of germinal epithelium in the testis (Figure 6F). Cerebellum, where loss of Purkinje neurons is believed to contribute to ataxia in CS patients, appeared unaffected in XPCS mice up to 19 months of age as concluded from immunohistochemical staining of Purkinje neurons using calbindin antibody (data not shown). To date, no increased spontaneous tumor incidence has been observed among ageing XPCS mice.

Exacerbation of repair deficiency accelerates segmental aging in both XPCS and TTD mice

Previously, we found that further reduction of DNA repair capacity in TTD (Xpd^{R722W}) mice by concomitant inactivation of *Xpa* severely enhances TTD features. XPA/TTD double-mutant mice are born normally, but display enhanced TTD cutaneous features, progressive postnatal growth failure, kyphosis, ataxia, spasticity, balance problems, gait anomalies, severe cachexia and death around 2-3 weeks of age (de Boer et al. 2002). XPA/XPCS mice were born normally (Figure 7B) and displayed a similar set of symptoms as XPA/TTD mice (Figure 7A and C and data not shown). Growth failure in XPA/XPCS mice was not caused by impaired nursing, as double-mutant mice were lactated normally by the mother based on the presence of milk in the stomach of the pups analyzed at 8-12h, 5, 12 and 20 days after birth (data not shown). Similar to XPA/TTD mice, lifespan could not be extended by providing newly lactating mothers at the age of ~20 days. Because TTD cutaneous features in XPA/TTD mice were enhanced, we asked whether aggravated DNA repair in XPCS mice could trigger TTD like features. Skin of XPA/XPCS mice appeared normal under routine histological examination (data not shown).
Observational and footprint analyses of XPA/XPCS mice revealed progressive disturbed balance, ataxia, gait abnormalities, tremors and spasticity during ongoing movements, suggesting that neurodysfunction in XPA/XPCS and XPA/TTD double mutant mice is similarily and dramatically more pronounced than in either of the single mutant TTD (Xpd^{R722W}) or XPCS (Xpd^{G602D}) animals.

A

B 20 h

C 20 days

D XPA−/− / XPCS−/−   XPA+/− / XPCS+/−
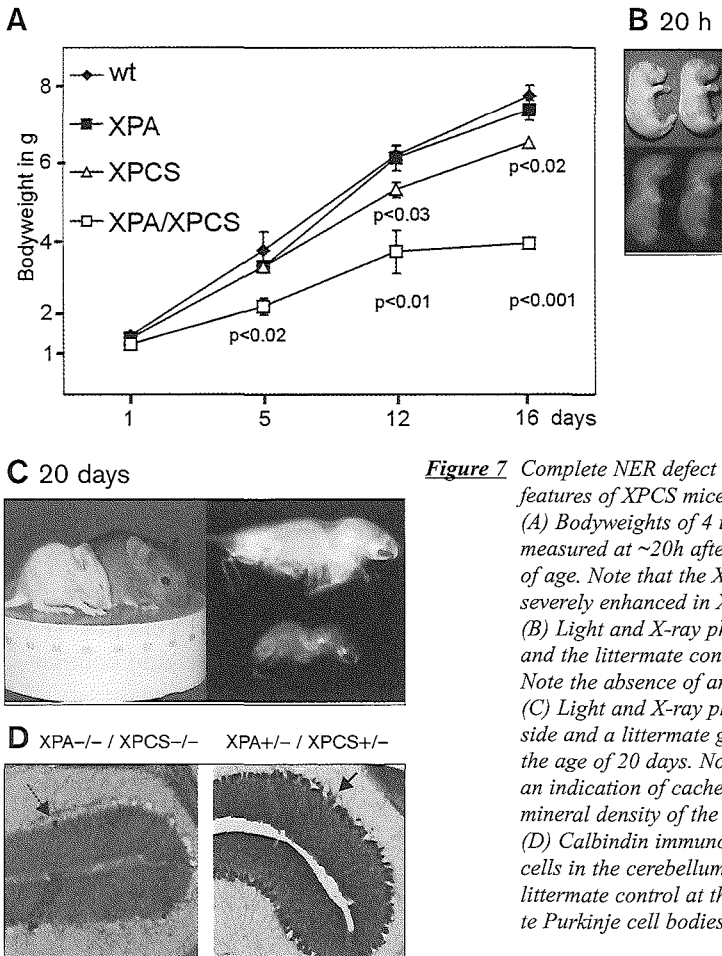
Figure 7 Complete NER defect dramatically enhances the CS features of XPCS mice.
(A) Bodyweights of 4 independent cohorts of mice measured at ~20h after birth and at 5,12, and 16 days of age. Note that the XPCS specific mild cachexia is severely enhanced in XPA/XPCS mice.
(B) Light and X-ray photographs of XPA/XPCS (right) and the littermate control (left) mice ~20h after birth. Note the absence of any overt phenotype.
(C) Light and X-ray photographs of XPA/XPCS along-side and a littermate gender matched control mice at the age of 20 days. Note the ~50% size differential as an indication of cachexia (left) and reduced bone mineral density of the double mutant mouse (right).
(D) Calbindin immunostaining shows loss of Purkinje cells in the cerebellum of XPA/XPCS mouse but not in littermate control at the age of 20 days. Arrows indicate Purkinje cell bodies. Magnification 400X.

Next, we performed neuropathological analyisis of XPA/XPCS mice using a variety of stainings including acetylcholine esterase staining, silver staining, Nissle staining and immunocytochemical labeling with antisera against calbindin, dopamine and tyroxine hydroxylase. XPA/XPCS mice showed a remarkable degeneration of their Purkinje cells (Figure 7D). This degeneration included not only their proximal and distal dendrites but also their cell bodies. The morphology of the remaining Purkinje cells looked relatively normal with a characteristic two- dimensional dendritic tree reaching the top of the molecular layer. In the sections stained for calbindin, the number of Purkinje cells was reduced to 69% ($\pm$ 18%) in the vermis, while that in the hemispheres was reduced to an average of 31% ($\pm$ 14%). The silver stained sections of XPA/XPCS mice at 20 days of age did not reveal any prominent evidence for secondary degeneration in the granule cell layer or inferior olive. This suggests that the maximal age period of 3 weeks is insufficient to allow such a process to progress

at a significant level. In addition, we did not observe any degeneration in higher brain regions such as the striatum, hippocampus, cerebral cortex or thalamus as reported for several cases of CS in humans (Itoh et al. 1999; Lindenbaum et al. 2001).

We and others have previously hypothesized that the segmental ageing observed in mouse models with DNA repair defects (such as in XPA/TTD double mutant, Ku80 or ERCC1-deficient mice) may result from enhanced apoptosis which may lead to an increase in cellular turnover as a consequence of compensatory proliferation (Weeda et al. 1997; Vogel et al. 1999; de Boer et al. 2002). However, except for loss of cellularity in the cerebellum of XPA/XPCS mice (Fig. 6D) and generally reduced size, pathological analysis of the double mutant mice did not reveal obvious defects in any other major organ system investigated. In order to confirm this, we further examined organs of the XPA/XPCS mice for evidence of enhanced apoptosis or proliferation. BrdU incorporation in 5 and 12 day old XPA/XPCS mice, as analyzed by immunostaining of paraffinized tissue sections, did not reveal consistent differences from littermate controls in the number of replicating cells in the intestine, liver, kidney, heart and lung. Similar results were obtained using the proliferative markers PCNA and Ki67. Analysis of DNA fragmentation indicative of apoptosis in the same organs by ligation-mediated PCR also failed to reveal differences between different genotypes (see Materials and Methods for details). We conclude that apoptosis and cellular turnover were within the normal range of interanimal variation at these ages.

Discussion

Recapitulation of the XPCS phenotype in mice
The molecular defects underlying TFIIH-associated pathologies in CS and TTD has largely remained obscure. Cellular and biochemical systems are limited in predicting systemic and time dependent phenotypes, such as accelerated cancer and ageing. To overcome this limitation we generated knock-in mice carrying the XPD-XPCS patient derived XPD^{G602D} causative point mutation in the *Xpd* gene. Characterization of DNA repair parameters in MEFs derived from homozygous XPCS mice demonstrated impaired NER of UV-induced DNA lesions and sensitivity to gamma rays, a known hallmark repair deficiency of CS cells (Le Page et al. 2000). Since gamma rays induce a variety of oxidative lesions, a damage type generally believed to contribute to normal ageing, the CS-specific inability to repair such lesions is currently widely accepted as the cause of developmental delay and accelerated ageing in this syndrome (Le Page et al. 2000; de Boer et al. 2002). In concordance with this and similar to other mouse models for Cockayne syndrome such as CSB and CSA deficient mice, XPCS mice displayed developmental delay and mild segmental ageing features including cachexia and testicular atrophy. Besides the above CS features, XPCS mice exhibited a dramatic predisposition to UV induced skin- and eye cancers.

Thus very similar to humans, the Xpd^{G602D} mutation recapitulated both the xeroderma pigmentosum and Cockayne syndrome components of the combined syndrome in mice.

DNA repair deficiency underlies common mechanism of segmental ageing in CS and TTD

Extensive cellular and biochemical research has resulted in several hypotheses to explain CS and TTD. Deficits in basal transcription initiation and/or certain forms of activated transcription have been proposed as causative or contributing to TTD (Keriel et al. 2002; Dubaele et al. 2003). Hampered transcription coupled repair (TCR) of endogenously rising oxidative lesions and/or deficits in RNA-PolI transcription has been set forward to explain CS (Le Page et al. 2000; Bradsher et al. 2002). Previously, we found that further reduction of DNA repair capacity in TTD (XPD^{R722W}) mice by additional XPA inactivation results in vastly accelerated TTD features and dramatically reduced lifespan of 2-3 weeks, thereby highlighting DNA repair as a key determinant of TTD disease severity and progression (de Boer et al. 2002). We anticipated that if the basic mechanism of disease in CS and TTD was different, for example, if a TCR or RNA-PolI deficit explains CS, and RNA-PolII basal transcription- or gene-specific activation insufficiency causes TTD, one would expect the removal of the exclusively NER-associated *Xpa* gene in XPCS mice to result in a different phenotype than in TTD mice. On the contrary, we found that XPA/XPCS mice display similar phenotype and lifespan to XPA/TTD mice and conclude that DNA repair capacity is determining the rate of disease both in TTD and XPCS in a similar manner. Since XPA/CSB, XPA/CSA and XPC/CSB double mutant mice show analogous phenotype and 2-3 week lifespan (Murai et al. 2001) we suggest that the same conclusion holds for CS only as well. Similar phenotype, lifespan and loss of Purkinje neurons in mice lacking the XPCS associated *Xpg* gene (Sun et al. 2001), XPA/CSB (Murai et al. 2001) and XPA/XPCS mice (this study) further supports this conclusion.

Furthermore, we found that XPA/XPCS and XPA/TTD cells share a common deficit in the spatio-temporal organization of the NER reaction, which may result in similar alterations in down-stream signaling and cellular responses. In the double mutant cells, XPC binding to DNA damage persists, while the XPD- and XPB- containing TFIIH complex occupancy at the site of damage is reduced (Figure 3). How the NER reaction is sensed and downstream signals transmitted is currently not well understood. Candidates for mediating signals from a hampered NER complex to cell-cycle and apoptosis machinery are XPC, XPD and XPB (Wang et al. 1996; Adimoolam and Ford 2003; Chen et al. 2003; Wang et al. 2004). Because TCR capacity of endogenously rising oxidative lesions is believed to contribute to pathological and normal ageing, assays measuring this repair trail would be of great interest. Unfortunately such assays are currently unavailable. Nevertheless, since molecular events downstre-

am of damage recognition in GG-NER (visualized in this study) and TCR (which is difficult to visualize due to the dearth of such a repair relative to GG-NER) share many if not all components, our findings likely reflect the extent of mechanistic changes in both.

Further evidence for a common cause of CS and TTD comes from the recent identification of two patients carrying exactly the same mutations in XPD but displaying CS and TTD, respectively (M. Stefanini per. comm.). Apparently, at least for some XPD mutations genetic background can influence the disease outcome. Finally, it should be noted that without cell or gene based analyses or microscopic examination of hair under polarized light to reveal the tiger-tail appearance specific to TTD hair, TTD and CS patients are sometimes difficult to distinguish phenotypically even by physicians who treat them regularly.

To which extent accelerated ageing in DNA repair defective mice reflects normal ageing? Some hallmark features of normal ageing in mice, including loss of germinal epithelium, cachexia and occasional kyphosis, appeared earlier in XPCS mice. Early germinal epithelium degeneration and cachexia have also been noted in other DNA repair related accelerated ageing models, including mice with a mitochondrial DNA polymerase defect (Trifunovic et al. 2004), mice lacking both Werner helicase and telomerase (Chang et al. 2004) and DNA repair defective XPA/XPB-XPCS double mutant mice (J.O.A. et al., manuscript in prep). TTD and Ku80 deficient mice display progressive cachexia and kyphosis (Vogel et al. 1999; de Boer et al. 2002) and CSB deficient animals display mild cachexia while they age (I. van der Pluijm et al., manuscript in prep.). Taken together, these data points to the uniform causative effect of DNA damage both in pathological and normal ageing.

DNA repair, TFIIH and cancer predisposition

In XPCS MEF cells, defective resumption of transcription after UV exposure reflected a TC-NER deficiency comparable to XPA and CSB, which lack this pathway entirely. The 70% reduction in UV-induced unscheduled DNA repair synthesis revealed a partial defect in GG-NER as well. As a consequence, XPCS MEF cells were hypersensitive to UV-induced cell killing. These features reflect the classical NER deficit suggested as causative of the XP phenotype (Bootsma et al. 2002; Mitchell et al. 2003).

In vivo, XPCS mice were extremely UV sensitive, similar to the XP/CS2 patient. Moreover, when exposed daily to the low, environmentally relevant UVB dose of 100 J/m2, XPCS mice were found to be even more cancer prone than completely NER defective XPA mice, showing that UVB induced carcinogenesis is not merely a function of residual NER activity as previously believed.

In contrast to XPCS mice, TTD mice are only mildly cancer prone upon chronic, daily exposure to a high dose of UVB (Table 2 and refs therein) and not cancer predisposed when exposed daily to a similarly low UVB dose of 80 J/m2 (J. Jans et al.,

unpublished). How XPCS (XPD^{G602D}) and TTD (XPD^{R722W}) mutations result in an enormous difference in cancer predisposition is currently unknown. The recent discovery that XPD-XPCS cells induce genome-wide breaks in the DNA when transfected with UV-damaged plasmid hints for trans-acting deregulation of genome care-taking in XPCS (Berneburg et al. 2000). Further studies are required to uncover the cancer mechanism in XPD-XPCS.

Since TTD (including XPD^{R722W}) patients are cancer free and the XP/CS2 (XPD^{G602D}) patient developed the first tumours already at ~2,5 years of age, we conclude that cancer predispositions in both in mice and man are XPD-mutation specific.

Cancer predisposition vs. accelerated ageing

It is well known that cancer risk increases with age. However, the accelerated aging syndromes CS and TTD are relatively cancer free in comparison to most other DNA repair deficient syndromes including XP. Currently, accelerated ageing in CS and TTD is explained by the hypothetical increase in apoptosis and/or cellular senescence, which as a trade off, protects against cancer; whereas increased mutagenesis in XP is believed to explain the cancer predisposition (Hoeijmakers 2001; Mitchell et al. 2003). Results in this study suggest that accelerated ageing and cancer can in fact be governed by mutually independent pathways. XPCS (XPD^{G602D}) mice are extremely prone to cancer, TTD (XPD^{R722W}) mice are essentially cancer free and CSB mice display intermediate cancer predisposition, indicating lack of correlation between accelerated cancer and ageing phenotypes. The overlapping phenotype and life-span of XPA/CSB, XPA/XPCS and XPA/TTD double-mutant mice shows that in the absence of XPA cancer potential of XPCS or CSB is not modifying the acceleration of CS or TTD like ageing features. Moreover, accelerated ageing in *Xpd* compound heterozygogous mice can be alleviated parallel to enhancement of cellular UV sensitivity (J.O.A. et al., manuscript in prep.). These results strongly suggest that in NER mutant mice, DNA repair relevant in ageing and UV induced cancer predisposition are parallel but mechanistically distinct processes.

These findings are in concordance with observations in human XPCS patients, where XP and CS pathologies have been reported to co-occur (Lindenbaum et al. 2001). Furthermore, the gene defect in nearly half of the CS- and TTD-like patients has remained unknown as cells derived from those individuals lack the classical diagnostic feature-UV sensitivity (N. Jaspers, per. comm.), further arguing that mechanism promoting accelerated ageing is quite distinct from that of involved in the repair of UV induced lesions.

Taken together, our data indicates that cancer predisposition and accelerated ageing in NER defective mice and man result from deficits in mutually independent processes.

Lack of TTD cutaneous features in XPCS mice despite reduced TFIIH levels
Mutations in XPD are also known to cause reduction in the protein level of the TFIIH complex (Botta et al. 2002). In particular, alterations in XPD resulting in the TTD phenotype are known to reduce TFIIH levels dramatically and this reduction has been suggested to contribute to the onset of TTD-specific cutaneous features (Vermeulen et al. 2000; Botta et al. 2002; Giglia-Mari et al. 2004). It has been proposed that in enucleating keratinocytes the lack of continuous de novo synthesis of TFIIH may lead to exhaustion of TFIIH before completion of the differentiation program. As a consequence, the last genes in the transcriptional program, such as cysteine-rich crosslinking gene products in keratinocytes, will not be sufficiently transcribed, and so hair, nails and skin will be delivered in an unfinished state. Endogenous DNA damage can likely further hinder the transcription of those genes as cutaneous features were elevated in XPA/TTD animals (de Boer et al. 2002). By comparing XPCS (XPD^{G602D}) and TTD (XPD^{R722W}) primary MEFs we found that in mice both mutations led to a similar ~50% reduction of the TFIIH levels, yet skin and hair of both XPCS and XPA/XPCS mice appeared normal. Moreover, co-expression of even minute amounts of XP- or XPCS-XPD protein in TTD hemizygous mice results in no detectable alleviation of TFIIH levels, yet TTD skin features are largely rescued (J.O.A. et al., manuscript in prep.). These data indicate that reduction of TFIIH level on its own or in parallel with declined DNA repair capacity is insufficient to trigger TTD-like scaling skin and brittle hair features, suggesting that not only the quantity but also the quality of TFIIH can be implicated in the given disease feature.

Materials and Methods

Derivation of mutant mice and mouse embryonic fibroblast lines
Derivation of XPA and CSB knock-out mice and cells have been described earlier (de Vries et al. 1995; van der Horst et al. 1997). Mouse genomic HindIII-SfiI *Xpd* fragment used to generate *Xpd^{XPCS}* (Xpd^{G602D}) targeting construct carrying XP/CS2 type of mutation has been described (de Boer et al. 1998a). HpaI site 311 bp downstream translational stop-codon in exon 23 was converted into ClaI site and used for inserting the pMC-1 neo cassette flanked by LoxP sequences (pMC-1 neo-LoxP) (Figure 1 A and B). HSV-tk gene was inserted into the SfiI site at the 3'end of the homologous arm as described before (de Boer et al. 1998a). Xpd^{G602D} (G1805A) causative point-mutation was generated via site-directed mutagenesis. In order to facilitate multiple screening steps two silent mutations (G1803A) and (A1809G) were generated nearby the aminoacid changing G1805A mutation in the *Xpd^{XPCS}* (Xpd^{G602D}) construct. Electroporation, culturing and routine screening of 129/Ola-derived ES cells was performed as described before (de Boer et al. 1998a). Heterozygote *Xpd$^{XPCS-neoLoxP}$* ES cells were transiently transfected with plasmid carrying puromycin resistance

marker and Cre recomibanse cDNA (Puro-Cre vector) (courtesy of
L.J. Niedernhofer). Clones resistant to puromycin were analyzed for the excision of
LoxP flanked pMC-1 neo cassette by Southern blotting (data not shown). Equal
mRNA expression from Xpd^{XPCS} versus Xpd^{wt} allele was veryfied by RT-PCR (data
not shown). Details concerning the Puro-Cre vector, Southern blotting and RT-PCR
will be furnished upon request. Blastocyst injections and derivation of chimeric mice
were done by standard methods. Chimeras were mated with C57Bl6 mice and obtai-
ned heterozygous animals were intercrossed with fvb transgenic CAG-cre mice carry-
ing Cre recombinase. CAG-cre mice retain Cre recombinase activity in mature oocy-
tes irrespective of the Cre transgene transmission and thereby LoxP flanked pMC-1
neo cassette is excised before the two cell-stage of embryonal development (Sakai
and Miyazaki 1997) yielding in heterozygote Xpd^{XPCS} mice without the pMC-1 neo-
LoxP cassette. In mice the excision of the pMC-1 neo-LoxP cassette was controlled
by PCR using primers F2 and R and RT-PCR using primers F1 and R (see also
below). The construct for generating CAG-cre mice was kindly provided by prof. P.
Vassalli. Mice used in this study were in 129Ola/C57bl6/fvb mixed background
unless noted differently.
Standard genotyping for Xpd^{XPCS} mice was perfomed using primers F2 (5'-GGGAG-
CAGCTGCAGTCA-3') and R (5'-GCAGGGCATGAAGTGGCTCC-3') yielding in
400bp product from the wt allele and 529 bp product from the targeted allele contai-
ning 1 LoxP site left after Cre recombinase reaction, Cla-linker and the short sequen-
ce inbetween (Figure 1C and E). Primary mouse embryonic fibroblasts were isolated
from E13.5 embryos and cultured as described before (van der Horst et al. 1997).

RT-PCR analysis and DNA sequencing
Total RNA was isolated from the testis of the wt and heterozygote Xpd^{XPCS} mice
using Trizol Reagent (Gibco, USA). To verify the presence of G602D mutation and
the absence of any other undesired mutations originating from cloning or gene-targe-
ting we performed RT-PCR by using primers F1(5'-TCAGCACTTACGCCAAG-3')
hybridizing to the sequence outside of the targeting construct and R as indicated in
Figure 1 C. Due to the presence of sequence orginating from cloning and one LoxP
site left after Cre recombinase reaction, Xpd^{XPCS} allele is 129 bp longer than Xpd^{wt}
allele (Figure 1F). The compareable amount of RT-PCR products originating from
Xpd^{XPCS} and Xpd^{wt} alleles suggested that both transcripts are equally stable. 1643bp
RT-PCR product originating from the Xpd^{XPCS} allele was isolated from the gel and
sequenced in BaseClear Group, The Netherlands.

DNA-damage sensitivity assays
UV-induced UDS, RSR as well as UV and gamma ray survival assays were perfor-
med as described previously (Vermeulen et al. 1994a; de Waard et al. 2003). On
Figure 2 representative experiments are piled and presented on one graph as % of the

wt. Please note that the p value indicated on Figure 2A represents the statistical difference between all the presented cell lines. The p value indicated on Figure 2B indicates the statistical difference between each mutant and the wt cells only. The higher value for the CSB cells on Figure 2B is within the range of the varience of the assay and does not represent statistically significant difference from XPA and/or XPCS cells. For the UV survival tests 2 to 4 experiments using at least 2 independent p2-p5 primary MEF cell lines per genotype were performed. The UV survival curve (Figure 2C) was assembled from 2-4 independent experiments. Data was processed in Excel and represented as an average survival curve per genotype. Error-bars indicate variation between different experiments.

Immuno-histopatholoy of the brain
The animals were anaesthetized (Nembutal; 50 mg/kg) and perfused with 4% paraformaldehyde in 0.1M phosphate buffer. The brains were removed, cryoprotected in sucrose, embedded in gelatin, and one half was cut on a cryotome in sagittal sections while the other half was cut in coronal sections (40 mm). Nissle staining, acetylcholine esterase staining and silver stainings were done according to standard procedures in our laboratory (for details see De Zeeuw et al., 1994 J. Comp. Neurol. and Jaarsma et al., 1992 Hippocampus). Immunocytochemistry was performed by rinsing the sections with 10% normal goat serum in 0.1 M Tris-buffered saline (TBS), incubating them with rabbit anti-antibodies against calbindin (Sigma), dopamine (Mark) or tyroxine hydroxylase (Novus) diluted 1:1000 in 0.1 M TBS for 72 hours, rinsing them with Goat anti-rabbit-biotine for 90 minutes, and ultimately reacting them with avidine-biotine-peroxidase and diaminobenzidine for visualization of the antigen. Subsequently, all sections were mounted, coverslipped, and investigated under the light microscope. Quantitative analyses of the Purkinje cells were done with Neurolucida, NeuroExplorer and analySIS software.

Comparative immunoflourescence analysis of p62 subunit of TFIIH
Latex bead labelling and comparative immunoflourescence analysis of the p62 subunit of the TFIIH was performed as described earlier in the similar studies (Vermeulen et al. 2000; Vermeulen et al. 2001; Botta et al. 2002). For local UV damage, cells were rinsed with PBS and covered with an isopore polycarbonate filter (Millipore) containing 5 micrometer pores before UV irradiation with a Philips TUV lamp (254 nm) at a dose rate of ~0.9 $J.m^2/s$. In total 48 $J.m^2/s$ were given and cells were put back into medium for 15 minutes or 3 hours. We fixed cells with 2% paraformaldehyde for 10 minutes RT, permeabilized 2 times for 10 minutes with 0.1% TritonX-100, followed by wash with PBS+ (PBS + 0.15% glycine and 0.5% BSA). Anti-p62 (3C9) antibodies were diluted 1:2000 and anti-XPC antibodies 1:500 in PBS+ and incubated RT for 1h in the moist-chamber. After incubation, we washed coverslips 5 times 5 minutes with PBS+0.1% TritonX-100 followed by incubation

with Cy3 conjugated goat-anti-mouse (The Jackson Laboratory) diluted in PBS+ 1:800. After 45 minutes incubation and the same wash procedure, we mounted cover-slips in Vectashield mounting medium (Vector Laboratories) containing 1.5 µg/ml DAPI and stored at +40 C in the dark. We produced epifluorescent and phase-contrast images on a Leitz-Aristoplan microscope, equipped with a 3-CCD camera (DXC-950P Sony) and digitally processed using Adobe Photoshop 4.0. For TFIIH level quantification, 25-50 microscopic fields in each experiment was photographed in a "blind" fashion. Background levels were measured beside each individual nuclei. The obtained values were processed further by subtracting the background red fluorescence from the nuclear red fluorescence, the obtained numbers were processed with Excel. Standard Student T-test using 2 tailed two-sample equal variance setting was used to verify the statistical significance of the data. Standard karyotyping was performed to verify that the observed differences in signal intensity are not due to altered karyotype of the primary MEF cells. In all the cell-lines used in this study ~80% of the nucleai were found to be diploid while ~20% had a tetrapolid karyotype. 2 or more cell lines per genotype were used in this study. Experiments were repeated 2 times per genotype and a representative as well as statistical outcome is depicted at Fig1 G and H respectively.

CHAPTER 5

Pace of ageing in mice carrying a latent mutation in *Xpb* helicase is determined by DNA repair efficiency

Jaan-Olle Andressoo[1], Jan de Wit[1], Deborah Hoogstraten[1], James R. Mitchell[1], Rudi Hendriks[2], Harm de Waard[1], Geert Weeda[1], Jan H. Hoeijmakers[1] and Gijsbertus T.J.van der Horst[1]

1 Dept. of Cell Biology and Genetics
2 Dept. of Hematology, Erasmus MC, Erasmus University, Rotterdam
P.O. Box 1738, 3000 DR, The Netherlands

Summary

Multiple human premature ageing syndromes such as Ataxia Telangiectasia, Werner syndrome, trichothiodystrophy (TTD), Cockayne syndrome (CS) and xeroderma pigmentosum combined with CS (XPCS) are caused by defects in proteins sensing or repairing DNA damage. Moreover, when the DNA repair capacity in the XPD helicase defective TTD or XPCS mouse models is further reduced by the removal of the *Xpa* gene, mice live only 1-3 weeks, providing in vivo evidence for the mechanistic link between DNA repair and ageing. Nevertheless, in order to make a strong argument for the causal role of DNA damage in ageing, one should correlate DNA repair efficiency with the rate of ageing and generate phenotypes ranging from mild to severe in a DNA repair dependent but causative gene independent manner. Here, we have approached this goal by generating mice carrying a latent XPCS mutation engineered to mimic the splice-acceptor mutation of an XPB^{XPCS} patient (XP11BE). Despite a DNA repair deficit, and unlike its human counterpart or Xpd^{XPCS} and Xpd^{TTD} mouse models, Xpb^{XPCS} mice display normal development and ageing. Xpa/Xpb^{XPCS} double mutant mice, in which the DNA repair capacity is further reduced by Xpa inactivation, develop pathology similar to Xpd^{XPCS} and Xpd^{TTD} mice. Xpb^{XPCS}/Xpd^{TTD} double mutant mice display normal in utero development but die within 1-2 days after birth. We find a correlation between the severity of the organismal phenotype and the cellular sensitivity to ROS-induced DNA damage. Furthermore, we characterize the effects of single and/or double mutations on the spatio-temporal axis of the NER reaction in cells and speculate on the impact of faulty DNA damage repair sensing on organismal phenotype.

Introduction

Our genome is continuously challenged by various endogenous and exogenous sources. The main culprit is considered to be reactive oxygen species (ROS). ROS result from normal oxidative metabolism and have a potential to deliver more than 100 different types of oxidative lesions in DNA (Hoeijmakers 2001). Unrepaired DNA damage can give rise to mutations and thereby contribute to cancer, but may also block transcription or replication which can lead to cell-death and/or senescence and thereby contribute to ageing (Hoeijmakers 2001; Hasty et al. 2003; Mitchell et al. 2003). The highly conserved Nucleotide Excision Repair (NER) is responsible for removing of a wide variety of helix distorting DNA lesions, including UV-induced photoproducts, bulky chemical adducts, intrastrand crosslinks and several forms of oxidative lesions (Friedberg et al. 1995; de Laat et al. 1999; Hoeijmakers 2001; Brooks 2002). NER consists of two subpathways- global genome (GG-NER) for genome-wide recognition and removal of adducts (hereafter defined as "classical"

NER lesions) and transcription-coupled NER (TC-NER) for removal of transcription blocking adducts from the transcribed strand of active genes (Bootsma et al. 2002). In GG-NER, the hHR23B/XPC complex is a damage sensor and NER initiator. In TC-NER, blockage of transcribing RNA-PolII is believed to trigger NER (Hoeijmakers 2001). The NER reaction involves sequential binding of ~ 30 proteins over the period of ~ 4 minutes (Hoogstraten et al. 2002). The consequences of inborn defects in NER proteins are highlighted by the autosomal recessive syndromes Xeroderma Pigmentosum (XP), Cockayne Syndrome (CS), trichothiodystrophy (TTD), the rare combined XPCS and XP/TTD (Broughton et al. 2001; Bootsma et al. 2002) and cerebro-oculo-facial syndrome (COFS) (Graham et al. 2001). The enormous clinical diversity within NER associated disorders is paralleled by extensive genetic diversity, with causative mutations found in at least 10 genes: 7 in XP (*XPA-XPG*), 2 in CS (*CSA* and *CSB*) and 3 in TTD (*TTD-A, XPB* and *XPD*). *XPD* and *XPB* genes encode the helicase components of TFIIH, an essential multiprotein complex involved in DNA repair and basal transcription initiation by RNA Pol II and I, as well as some forms of ligand-dependent activated transcription (Schaeffer et al. 1993; Iben et al. 2002; Keriel et al. 2002). It has been proposed that multifunctionality of the TFIIH complex contributes to the clinical diversity associated with *XPD* and *XPB* mutations resulting in XPCS and TTD. In addition, *XPD* mutations can also trigger XP/TTD and XP (Vermeulen et al. 1994b; Bootsma et al. 2002; Dubaele et al. 2003). XP patients display prominent sun sensitivity and have a dramatically elevated (>1000 fold) risk of developing UV induced skin cancer. CS and TTD are characterized as severe neuro-developmental diseases with a dominant component of accelerated ageing leading to death usually before puberty (Nance and Berry 1992; Nakura et al. 2000). CS and TTD features include developmental delay, microcephaly, skeletal abnormalities like frequently occurring kyphosis, progressive mental degeneration, sensorineural deafness, ataxia, spasticity, excessive demyelination, brain calcifications, hypogonadism, and overall aged appearance (Nance and Berry 1992; Itin et al. 2001). In addition, TTD patients display hallmark cutaneous features, such as sulphur-deficient brittle hair and nails and scaling skin (ichtyosis). It should be noted that in combined XPCS patients, XP- and CS- related pathologies appear as they do in independent XP and CS cases (Rapin et al. 2000; Lindenbaum et al. 2001).
The molecular defect underlying the greatly elevated skin cancer incidence in XP has been related to defective NER of UV-induced lesions on the DNA (Hoeijmakers 2001). Since patients lacking XPA protein are completely defective in both GG-NER and TC-NER but do not display CS or TTD features, proteins implicated in CS and TTD are thought to be involved in other processes besides classical NER reaction. Recent results from this and other labs suggest that defects in NER proteins such as CSB, XPD, XPB and XPG leading to accelerated ageing conditions Cockayne syndrome (CS) and trichothiodystrphy (TTD) are involved in a broader form of transcription coupled repair (TCR) which besides classical NER lesions also removes

small ROS-induced oxidative base adducts normally repaired by base excision repair (BER), a distinct and essential repair pathway (Le Page et al. 2000; de Boer et al. 2002; de Waard et al. 2003). Since ROS induced DNA damage is considered the main culprit to the genome, accelerated ageing seen in TTD and CS can be rationalized as a consequence of the inability to remove oxidative lesions from transcribed strands of active genes (Citterio et al. 2000b; van den Boom et al. 2002; Mitchell et al. 2003)(J.O.A. et al., manuscript in prep.). Besides a TCR deficit, alternative explanations to rationalize CS and/or TTD phenotypes have been proposed. These are based on the involvement of TFIIH in several forms of basal and activated transcription and the potential of the CSB protein to act as a chromatin remodeling and transcriptional elongation factor in vivo. It has been suggested that defect in one or more of those functions may explain CS and/or TTD phenotype (Vermeulen et al. 1994b; Citterio et al. 2000a; Bradsher et al. 2002; Keriel et al. 2002; Dubaele et al. 2003). Previously, we have generated Xpd^{TTD} and Xpd^{XPCS} mouse models. Although the genocopied mutations in these mice are causative for severe TTD and XPCS condition in humans, XPCS and TTD pathologies reconstitutes in a relatively mild form in mice (de Boer et al. 1998a)(J.O.A. et al., manuscript in prep.). Inactivation of classical NER capacity in those mice by Xpa inactivation led to comparable developmental delay and death within 1-3 weeks (de Boer et al. 2002) (J.O.A. et al., manuscript in prep.), arguing for the causative role of defective DNA repair in both disorders. Nevertheless, early death of the double mutant mice made it difficult to dissect effects of defective DNA repair on juvenile development and ageing. In order to better understand the role of DNA repair in the above processes, we aimed to genocopy a "mild" XPCS mutation in mice. Towards that end, we mimicked the XPB^{XPCS} mutation as found in patient XP11BE, because this patient displayed relatively mild CS features (Lindenbaum et al. 2001).

Results

Xpb is essential for mouse development

The first described XPB^{XPCS} patient (XP11BE) was shown to contain an XPB allele with splice mutation and a silent allele. C to A transversion in the last intron-exon border of the only expressed XPB allele generated an optimal splice-acceptor sequence 4-bp upstream from the normal 3' splice site causing a frameshift starting at codon 741 and replacement of the last 41 amino acid by 40 nonsense codons (Figure 1A). No wt XPB mRNA is detected in XP11BE patient cells, suggesting that the other allele is transcriptionally silent, and that the disease causing 5' proximal splice acceptor site is the one used in most (if not all) XPB mRNAs (Weeda et al. 1990).
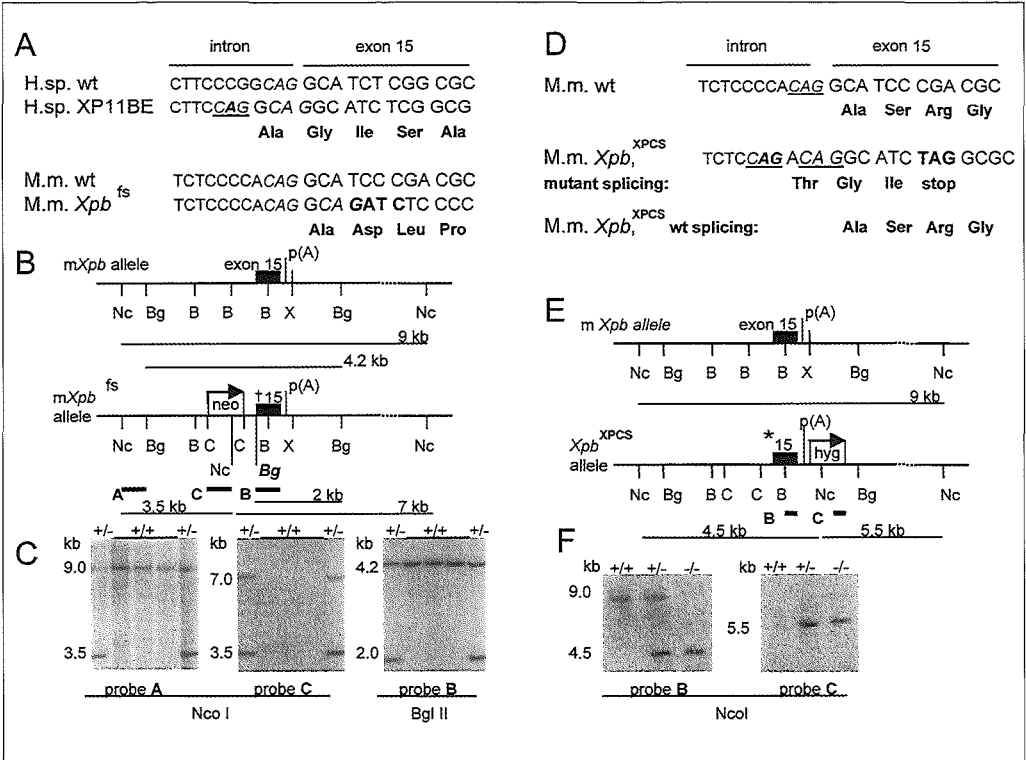
__Figure 1__. Targeting of the mouse Xpb gene.

(A) Sequence of the last intron-exon border of the human XPB and XP11BE and the corresponding mouse Xpb alleles. C to A transversion (bold) creates a new splice acceptor site (CAG, underlined italics), resulting in frameshifted transcript and 40 nonsense amino acids in C-terminus (first 5 nonsense amino acids are indicated). A mouse 4bp insertion in mouse Xpb creates a similar frameshift (Xpb^fs ,bold) resulting in C terminal nonsense amino acid tail.

(B) Schematic representation of the genomic structure and partial restriction map of the wildtype and targeted mouse Xpb loci: black box represent exon 15; P(A), polyadenylation signal. (†)-Xpb^fs 4bp insertion. The probes (A, B, C) are indicated with thick black lines. Restriction sites: (Nc), NcoI; (Bg), BglII; (B), BamHI; (X), XbaI; (C), ClaI. The diagnostic introduced BglII site is indicated in bold italics (Bg).

(C) Southern blot analysis of NcoI and BglII digested genomic DNA from wt, and Xpb^fs recombinant clones hybridized with probes A,C and B respectively.

(D) Sequence of the last intron-exon boarder of mouse wt and Xpb^XPCS mutated alleles. The wt splice acceptor site is underlined. Changed nucleotides in the mutated allele (bold) create an additional additional 5' splice acceptor site (underlined) and stop-codon (TAG)in the altered reading frame only. Amino acides encoded by both wt and Xpb^XPCS reading frames are indicated.

(E) Genomic structure of the Xpb wt and Xpb^XPCS alleles. Southern blot analysis of NcoI digested genomic DNA from wt ES cells(+/+), Xpb^XPCS recombinant ES clones (+/-)and homozygous Xpb^XPCS/XPCS mutant mice (-/-) hybridized with probes B and C.

In our first attempt to generate a mouse model mimicking XPB related XPCS, we inserted 4 bp at the last intron/exon border of the mouse *Xpb* gene, thereby phenocopying the frameshift (*Xpb^fs^*) observed in patient XP11BE (Figure 1A). This mutation results in a transcript coding only the C-terminal frameshift in *Xpb*. Due to differences in the nucleotide sequence between mouse and man, this results in a situation where the last 41 amino acids of murine *Xpb* are substituted by 85 nonsense amino acids (in contrast to the 40 nonsense amino acids in man). The targeting construct containing the frameshift mutation (Figure 1B) was electroporated into E14 129Ola embryonic stem (ES) cells and G418-resistant clones were screened by Southern blot analysis using three probes (Figure 1B and C, probes A-C) and a diagnostic BglII restriction site (Figure 1C). RT-PCR amplification of *Xpb* exons 14 and 15 from mRNA isolated from the recombinant ES cells and subsequent dot-blot analysis of the PCR products using labelled wild-type and mutant primers spanning the mutation indicated that both alleles are expressed (data not shown). Subcloning of RT-PCR products from heterozygous ES clones and subsequent DNA sequencing analysis revealed that only 2 out of 24 independent clones contained the desired mutation (data not shown), which points to a ~90% reduction in the expression level of the targeted allele. We failed to detect any XPB^fs^ protein by Western blot analysis (data not shown).

Chimeric mice were generated by injection of two independent targeted ES clones into C57bl6 blastocysts, and for each ES line we obtained a germline transmitting mouse line respectively. Consistent with the recessive nature of human XPB mutations, heterozygous offspring appeared phenotypically normal and healthy. Intercrosses of heterozygous *Xpb^fs^* mice yielded 43 wild-type and 103 heterozygous pups indicating that homozygosity for the *Xpb^fs^* mutation is not compatible with life. Analysis of embryos showed that homozygous mutants were missing as early as E8.5. The absence of extra-embryonic tissue suggested that embryonic lethality occurred during the preimplantation stage. Since TFIIH is essential for basal transcription initiation by RNA-PolII, then similar to previous results obtained with targeted inactivation or underexpression of mutated Xpd (de Boer et al. 1998b; J.O. Andressoo et al.,manuscript in prep.), homozygous lethality of *Xpb^fs^* mutation likely reflects deficiency in basal transcription.

Generation of a viable *Xpb^XPCS^* mouse model

Although neither wt XPB mRNA nor protein was detected in human XP11BE lymphoblastoid cells, it is still possible that minute amounts of wt XPB mRNA produced via splicing of original 3' splice-acceptor site can give rise to wt protein undetectable by conventional methods used in this study (Weeda et al. 1990). Moreover, some other cells or tissues can use different splicing modes, which may also change during ontogenesis. As such, the presence of the wt 3' acceptor-site may be required for viability and/or accurate reconstitution of the disease in mice. With this in mind, we next

generated a targeting construct in which the human splice mutation was exactly mimicked in the murine genomic *Xpb* DNA (see Figure 1D). To circumvent possible negative effects of the C-terminal stretch of nonsense amino acids we inserted a stop-codon in the altered reading frame while leaving the wt frame unaltered. Thus, usage of the new splice acceptor site would result into a truncated protein lacking the last C-terminal 43 amino acids, whereas usage of wt splice site would lead to unaltered XPB protein (Figure 1D). To avoid any effect of the dominant selectable marker on Xpb expression, the PGKhyg cassette was positioned 0.3 kb downstream of the Xpb polyadenylation signal (see Figure 1E). We obtained 155 hyg resistant ES clones, of which 13 contained a correctly targeted *Xpb* allele (Figure1 F and data not shown). RT-PCR amplification, subsequent cloning and dot-blot analysis of Xpb mRNA deri-ved from heterozygous ES clones revealed that ~50% of the amplified cDNA contai-ned the desired mutation (data not shown). DNA sequencing of independent RT-PCR clones revealed that ~ 90% of the mRNA derived from the targeted allele indeed was obtained by utilizing the proximal splice site encoding the truncated XPB protein, while the remaining ~ 10% splicing had occurred via the wt splice-acceptor site, encoding wt protein. Thus, at least in ES cells, the introduced proximal splice site was used preferentially but not exclusively.

Following blastocyst injections with 2 independent recombinant Xpb^{XPCS} ES clones and subsequent breeding of chimeric offspring, heterozygous $Xpb^{XPCS/wt}$ mice were obtained. Intercrosses between heterozygous animals yielded $Xpb^{XPCS/XPCS}$ homozy-gous offspring at Mendelian frequency. Standard genotyping was performed either by Southern blot analysis (see Figure1 F) or PCR analysis (data not shown). To obtain an isogenic genetic background, heterozygous $Xpb^{XPCS/wt}$ mice were back-crossed to wt C57bl6 mice for more than 8 generations. Consistent with the recessive nature of XPB mutations in human population, $Xpb^{XPCS/wt}$ mice were indistinguishable from wt animals in all aspects studied. For reasons of simplicity $Xpb^{XPCS/wt}$ and $Xpb^{wt/wt}$ mice will hereafter be refered as "wt" and $Xpb^{XPCS/XPCS}$ homozygous mice as Xpb^{XPCS} or XPB-XPCS on figures and figure legends.

Analysis of XPB expression in Xpb^{XPCS} mice.

To determine how Xpb is spliced in Xpb^{XPCS} mice, total RNA was isolated from the liver, amplified by RT-PCR and sub-cloned. Sequencing of independent cDNA clones revealed that 26/28 clones contained the expected 4-bp intron-derived insertion enco-ding the C-terminally truncated XPB protein, the remaining 2 clones were a product of the normal splicing. Thus in ~5-10% of the splicing events wt splice acceptor was used. Analysis of mRNA derived from primary mouse embryonic fibroblasts (MEFs) testis, kidney, spleen and brain of Xpb^{XPCS} mice rendered similar ratios (data not shown). Apparently, the original 3' splice acceptor was used at low 5-10% frequency in XPB-XPCS mice, leading to the presence of wild-type XPB transcripts.

We next analyzed the consequence of these aberrant splicing events for the expres-

sion of XPB protein. To this end we performed western blot analysis using antbodies recognizing the N- (1B3Mab) or C-terminus (2G12Mab) of the XPB protein. The recognition epitope of the latter antibody is absent in the truncated XPB protein. Despite the presence of 5-10% wt Xpb mRNA, expression of wt protein (if any) fell below the level of detection (Figure 2A). Since mutations in the XPB or XPD helicase components of TFIIH frequently lead to a reduction in the content of the whole complex both in human (Vermeulen et al. 2000; Vermeulen et al. 2001; Botta et al. 2002) and mouse fibroblasts (J.O.A. et al., manuscript in prep.), we studied the effect of the Xpb^{XPCS} mutation on the cellular levels of TFIIH. Towards that end we made use of comparative immunohistochemistry-based quantification strategy used in multiple similar studies to detect the p62 subunit of the TFIIH complex (Vermeulen et al. 2000; Vermeulen et al. 2001; Botta et al. 2002; Giglia-Mari et al. 2004)(J.O.A. et al., manuscript in prep.). We found that TFIIH levels were significantly reduced by ~40% in primary Xpb^{XPCS} fibroblasts (see Figure 2B,C).

DNA repair parameters of Xpb^{XPCS} cells and mice

XP11BE patient fibroblasts display severe defects in TC-NER and GG-NER and as a consequence, are hypersensitive to UV induced cell killing (Weeda et al. 1990). XP specific sun-induced freckling and cancer predisposition is believed to result from deficits in TC-NER and GG-NER (classical NER) (Bootsma et al. 2002). Next, we determined the effect of the Xpb^{XPCS} mutation on the classical NER capacity in UV exposed primary cells. GG-NER competence was measured by using the UV induced Unscheduled DNA Synthesis (UDS) assay. As shown in Figure 2D Xpb^{XPCS} cells retained ~30% UDS capacity, pointing to a 70% reduction of GG-NER. TC-NER capacity as measured by Recovery of RNA Synthesis (RRS after UV irradiation) in Xpb^{XPCS} cells was reduced to about 15% of the wt (see Figure 2E). To investigate whether repair defect in Xpb^{XPCS} cells results in cellular hypersensitivity to UV induced cells killing, we performed a UV-survival experiment. In comparison to fully NER deficient Xpa cells, Xpb^{XPCS} cells displayed intermediate hypersensitivy (Figure 2F).

Figure 2. *Expression of the XPB protein and consequences on TFIIH levels and DNA repair*
(A) Western blot analysis of whole cell extracts from Hela cells, two independent homozygous mutant XPB-XPCS MEFs (-/-) , and wt MEFs (+/+). Note that the αXPB monoclonal antibodies 1B3 and 2G12 recognize the conserved epitopes within the N and C terminus respectively and that the C-terminal epitope is absent in the truncated protein. p62 subunit of TFIIH (stained with Mab 3C9, lower panel) served as qualitative control for loading.
(B) Reduction of TFIIH protein levels in homozygous XPB-XPCS primary MEFs visualized by comparative immunoflourescence assay. Wt cells were labelled with 0.79 μm latex beads, XPB-XPCS cells were unlabelled (asterisk). Left panel: phase contrast image; right panel: corresponding immunofluorescent image of the p62 subunit of TFIIH. Note the reduced signal in the XPB-XPCS cells.
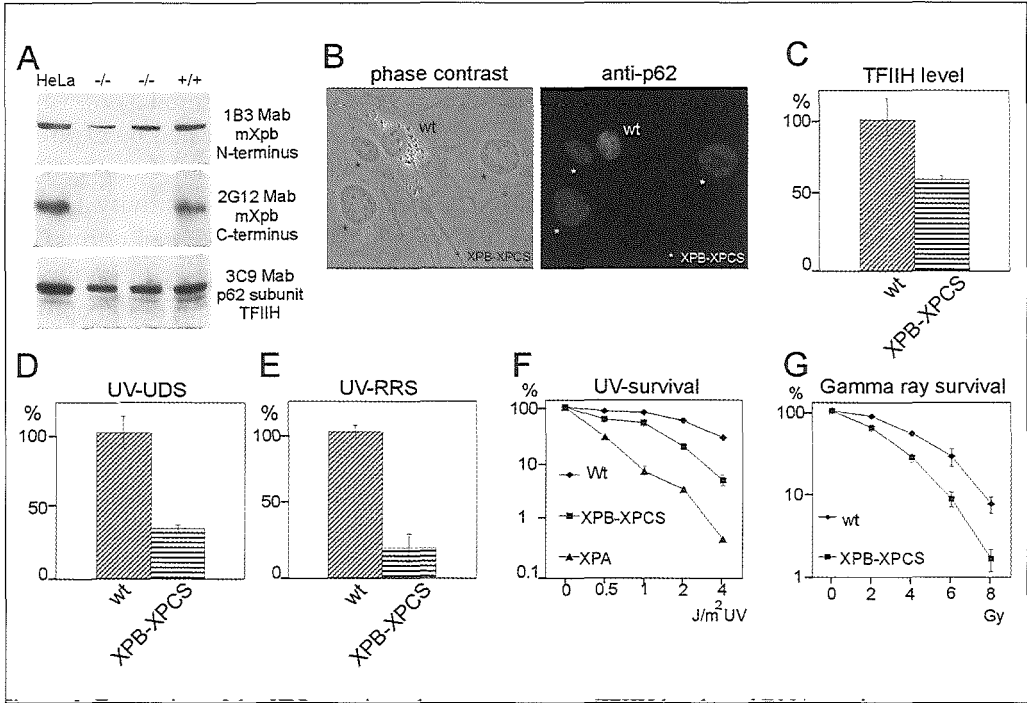
(C) Quantification of the TFIIH level in XPB-XPCS MEFs. The immunofluorescence signal from XPB-XPCS cells was determined (at least 50 nuclei per genotype, 2 separate experiments with 2 independent XPB-XPCS and wt cell lines) and expressed as the average percentage of the level in wt cells analyzed on the same microscopic slide. Error bars indicate SEM between experiments.
(D) UV-induced unscheduled DNA repair synthesis capacity (UDS) of primary homozygous XPB-XPCS MEFs. A representative experiment is depicted.
(E) RNA synthesis recovery after UV irradiation (RSR). A representative experiment is depicted.
(F) UV survival curves averaged from 4 independent experiments. At least 2 cell lines per genotype were included. Error bars indicate SEM between experiments.
(G) Gamma ray survival curves averaged from 5 independent experiments with 2 cell lines per genotype. Error bars indicate SEM between experiments.

The CS related interwoven NER-BER transcription coupled repair (from here onwards designated as TCR) defect can be tested by measuring the sensitivity of cells to oxidizing agents, including gamma irradiation (Cooper et al. 1997; Le Page et al. 2000; de Boer et al. 2002; de Waard et al. 2003). As shown in Figure 2G, Xpb^{XPCS} cells were found to be hypersensitive to exposure to increasing doses gamma rays. From these data we conclude that both XP-and CS-type repair defects are present in Xpb^{XPCS} cells, and that the DNA repair defect elicited by the XPCS mutation is comparable in mouse and human XPB-XPCS cells. Apparently, in Xpb^{XPCS} cells wt XPB

protein, if present, is not significantly contributing to DNA repair, at least within the detection limit of the above assays.

To verify whether the partial "classical" NER defect exhibited by cultured Xpb^{XPCS} cells is also reflected in vivo, photosensitivity of Xpb^{XPCS} mice was tested by exposing the shaven dorsal skin to UV-B light at the dose of 500J/m2/day for 4 consecutive days; XPA mice were included as a positive control for UV hypersensitivity. One week after the start of the treatment, wt and heterozygote animals appeared normal, whereas Xpa-/- mice exhibited pronounced redness of the skin, indicative of erythema and edema (generally known as sunburn) and acanthosis (thickening of the epidermis) accompanied with recurrent loss of the whole epidermis (Figure 3) . Consistent with the partial NER defect as uncovered by cellular studies, Xpb^{XPCS} mice displayed an intermediate phenotype, mirrored by moderately pronounced acanthosis (Figure 3) and thus, reconstitute the hallmark XP feature, - sensitivity to UV light.
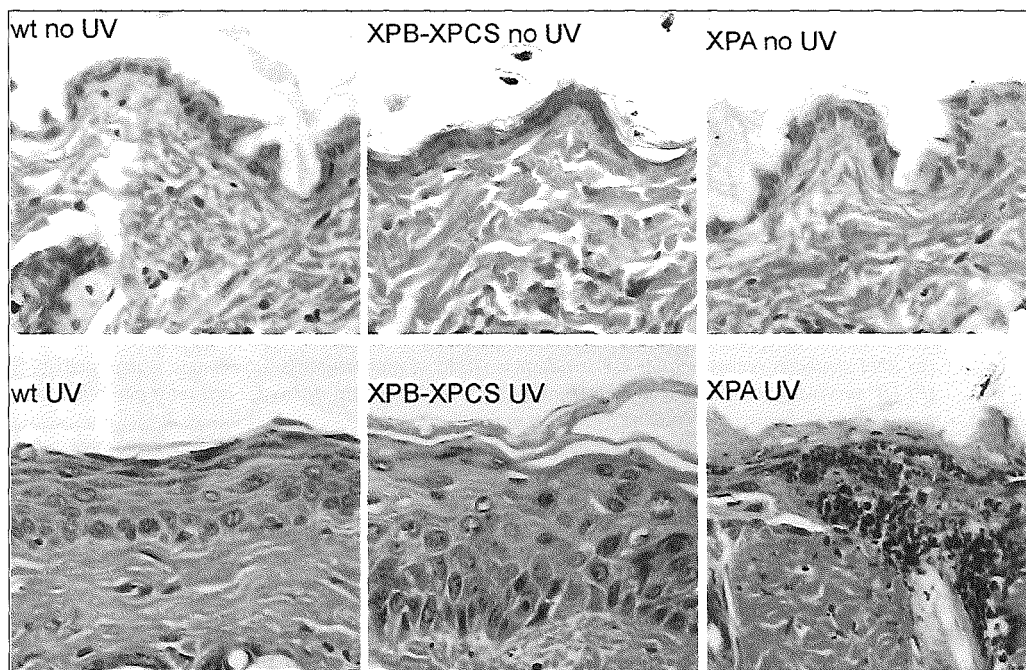
Figure 3. *Acute effects of UV-B on the skin of XPB-XPCS mice.*
HE staining of dorsal skin sections from shaven mice exposed to daily doses of 500J/m2 UV-B for 4 consecutive days and sacrificed 1 week after the start of the treatment. Note the moderate epidermal hyperplasia, consisting of an increased number of cell layers (acanthosis) in the XPB-XPCS skin and the much more severe effect in XPA mice as evident from hyperemia (dilated capillaries filled with blood) and the absence of keratinized and epidermal layers, reflecting severe "scaling of the skin". Magnification 400X

Xpb^{XPCS} mice are devoid of Cockayne features

To investigate whether Xpb^{XPCS} mice develop CS features, animals were screened for occurrence of developmental delay, neuromotor deficiencies, fecundity and cachexia. Measurements of bodyweight, starting from 12 days of age, failed to reveal any developmental delay in Xpb^{XPCS} mice (data not shown). Neuromotor function was tested by tail-suspension and accelerating Rotarod tests and appeared to be normal. Both male and female Xpb^{XPCS} mice were fertile at least up to 7 months of age, with litter sizes comparable to that of wt littermates.

Furthermore, Xpb^{XPCS} mice (n=6) monitored up to 24 years of age, appeared to age normally (data not shown). Detailed histological examination at age 1.5 years revealed no obvious pathological abnormalities in brain, sciatic nerve, eye, heart, lungs, lymph node, kidney, liver, colon, intestine, spleen, thymus, pancreas, gall bladder, urinary bladder, testis, ovaries, bones (femur/joint), skin and skeletal muscle. Compared to the littermate controls, no increase or decrease in the number of tumors was noted (n=9 Xpb^{XPCS} mice analyzed).

In conclusion, although Xpb^{XPCS} mice display UV hypersensitivity, they do not show detectable CS like developmental or accelerated ageing features.

Induction of Cockayne Syndrome features by further impairment of DNA repair

Defective transcription coupled repair of oxidative DNA lesions and concomitant cellular hypersensitivity to oxidative stress is thought to be a hallmark feature of CS and has been proposed to explain some, if not all CS features (Cooper et al. 1997; Le Page et al. 2000). The absence of CS-like features in Xpb^{XPCS} mice suggests that in this scenario, repair of oxidative DNA lesions in vivo is still proficient enough to battle chronic endogenous DNA damage at the organismal level. Since Xpb^{XPCS} mice carry a partial NER defect, we next asked whether complete inactivation of TC-NER and GG-NER by inactivation of the *Xpa* gene would trigger CS features. To this end we intercrossed double heterozygous *Xpa/Xpb*^{XPCS} animals, and homo-and heterozygous for either *Xpa* or Xpb^{XPCS} animals and noticed that double mutant *Xpa/Xpb*^{XPCS} mice were born at the expected Mendelian frequencies and developed normally. However, 10 days after birth they failed to gain weight at a comparable rate to wt, single mutant and double heterozygous littermates. In the 3th and 4th week mortality rate among *Xpa/Xpb*^{XPCS} mice was ~20%. Within this group of non-survivors the average lifespan was 23.3 days (SEM=1.1days, n=7) (see Figure 4A). Interestingly, the majority of *Xpa/Xpb*^{XPCS} animals survived weaning, which markedly contrasts the 1-3 weeks lifespan noted for ~100% of the *Xpa/Xpd*^{XPCS} or *Xpa/Xpd*^{TTD} animals (de Boer et al. 2002)(J.O.A. et al., manuscript in prep.).
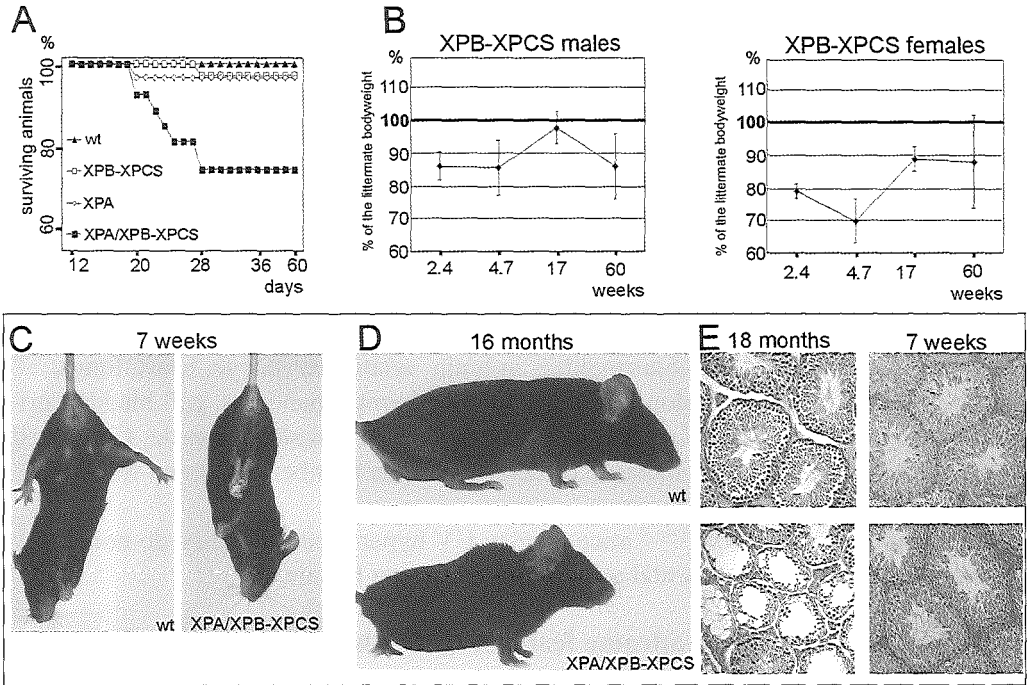
Figure 4. *Effects of additional DNA repair defect in XPB-XPCS mice*
(A) Increased juvenile mortality in XPA/XPB-XPCS mice. (Wt n=36, XPA n=34, XPB-XPCS n=41, XPA/XPB-XPCS n=30).
(B) Body weight in XPA/XPB-XPCS mice, plotted as a percentage of age and gender matched littermate controls. Note the increase in bodyweight between 33 and 122 days. Error bars indicate standard error of the mean.
(C) Tail suspension test of 7 week old male mice. The wt mouse depicted displays normal spreading of the hind limbs. XPA/XPB-XPCS mice display heterogeneous behaviour, ranging from nearly normal to severe cramp-like seizures, spastic movements and tremors of hind limbs as depicted here. Note also the smaller size of XPA/XPB-XPCS mice.
(D) Severe kyphosis in 16 month old male XPA/XPB-XPCS mice.
(E) Premature testicular tubular atrophy of XPA/XPB-XPCS mice. HE stained sections of the testis of 7 week and 18 month old wt and XPA/XPB-XPCS mice. Note the reduced thickness of the germinal epithelium, reduced occurrence of mature spermatids and the increase in interstitial cells in XPA/XPB-XPCS males at 18 months but not at 7 weeks. Magnification 100X

The relatively low mortality rate around weaning provided an excellent opportunity to study the effects of combined homozygosity of Xpa and Xpb^{XPCS} in surviving animals later in life. By ~3 months of age most Xpa/Xpb^{XPCS} mice (n=23) caught up in bodyweight with littermate controls (Figure 4B). To analyze whether Xpa/Xpb^{XPCS} mice display CS features like spasticity, tremors, hind coordination abnormalities or other neuromotoral deficits, we performed tail-suspension and rotarod tests. Tail-suspension test revealed occasional tremors and ataxia, spasticity and abnormal coordination of hind limbs up to ~ 2 months of age (Figure 4C). Interestingly, later in life

these features became less pronounced and gradually disappeared among ~50% of the double-mutant mice. No clear coordination anomalies were detected by accelerating Rotarod test (conducted at 6-8 months of age). Visual observation revealed abnormal hyperactivity, easy excitability and "nervous" behavior for in 5 out of 23 double mutant mice, yet only one sustained these features above ~2 months of age. Both male and female Xpa/Xpb^{XPCS} mice were fertile until at least 7 months of age with litter size comparable to those of wt animals. Between 6 and 12 months of age, Xpa/Xpb^{XPCS} mice displayed premature kyphosis (Figure 4 D) with heterogeneous penetrance (~50%) , unrelated to sustained neurological features. Gait abnormalities were observed during both the juvenile developmental delay period (from ~12 days of age up to ~ 1-2 months of age) among the most affected individuals as well as among the ageing mice with the most pronounced kyphosis. At 1.5 year of age Xpa/Xpb^{XPCS} and age matched single homozygous mutant, and double, -or single-heterozygous controls (hereafter referred to as controls) mice were sacrificed for a comparative histological analysis. Similarly 7-8 week old Xpa/Xpb^{XPCS} mice and controls were studied. Macroscopical examination revealed that the skulls of 1.5 years old double mutant mice with the most pronounced kyphosis (n=5; ~20% of Xpa/Xpb^{XPCS} animals studied) showed deformation and thickening mainly in the occipital region, which most likely relates to the severe kyphosis of the vertebral column. All 1.5 year old male Xpa/Xpb^{XPCS} mice investigated (n=5), revealed tubular testicular atrophy, which was not noted in control mice (Figure 4E). Testicular atrophy is associated with normal ageing in mice but occurs at a much later age and is believed to reflect the gradual loss of germinal stem cells (Tanemura et al. 1993; Syntin et al. 2001).

Except for the kyphosis, X-ray imaging of the Xpa/Xpb^{XPCS} and control skeletons (oldest individual studied at 23 months of age) did not display abnormalities and histological analysis of trabecular and cortical bone at 1.5 years of age did not reveal any overt histopathological changes (data not shown). Neither did Xpa/Xpb^{XPCS} mice show an increased or decreased tumor incidences as compared with the single mutant or double heterozygote controls.

Xpd^{TTD}/Xpb^{XPCS} double mutant mice display normal in utero development but die within 1-2 days after birth.

To gain more insight into the mechanism of TTD and XPCS, we intercrossed Xpb^{XPCS}/Xpd^{TTD} double heterozygote animals. At the age of genotyping (10-12 days after birth), double homozygous Xpb^{XPCS}/Xpd^{TTD} mice were never seen. Observation of the litters immediately after birth and genotyping at the early stages revealed, that double-mutant mice were born and showed normal movements and activity. However, animals failed to grow and died within 1-2 days. The oldest double mutant mouse observed alive was ~ 36h old. Absence of any signs of violence and as well as the presence of milk in the stomachs of dead Xpb^{XPCS}/Xpd^{TTD} mice suggested that they

were nursed normally by the mother, but died due to some internal complication. All the newborn double-mutant animals analysed (Table 1) appeared slightly smaller (Figure 5A), but their bodyweights were still within the normal newborn variance range (data not shown). Anatomical and histological examination of major organ systems and blood in 3 double mutant animals found alive after birth did not disclose any pathological or developmental anomalies (data not shown). Analysis of E13.5 and E18.5 embryos revealed no difference in size and bodyweight from littermate controls and the number of Xpb^{XPCS}/Xpd^{TTD} mice found in utero suggested Mendelian inheritance (Table 1). TUNEL staining of the liver, lung, heart and kidney isolated from E18.5 and ~12h after birth did not reveal differences in the amount of apoptotic cells, leaving the reason of death in the double mutants enigmatic.

	Pups/ embryos	Expected*		*Table 1.* Analysis of Xpb^{XPCS}/Xpd^{TTD} embryos and mice F.D.- found dead; F.A.- found alive
	analyzed	(if Mendelian)	Found	
Age				
10-12 days	155	14.25	0	
newborns, 0.5-1.5 days	61	10.375	2 F.D. 3 F.A.	
E18.5	4	1	2	
E13.5	14	1.75	2	

Normal in utero development of Xpb^{XPCS}/Xpd^{TTD} mice demonstrates that at least until birth, the transcription function of double mutated TFIIH is sufficient to support normal ontogenesis.
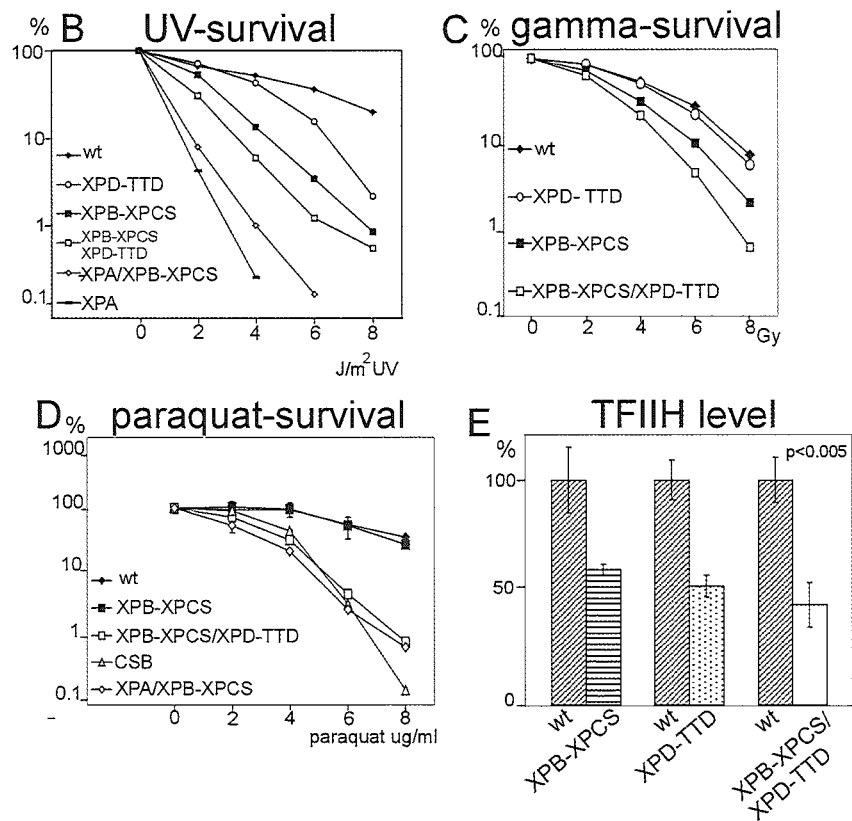
DNA repair in Xpd^{XPCS}/Xpb^{TTD} and Xpa/Xpb^{XPCS} double mutant cells

Although in human patients and mutant mouse models cellular sensitivity to UV light and UV induced DNA repair kinetics do not correlate with the severity of CS or TTD symptoms, these parameters were interesting to measure as Xpb^{XPCS}/Xpd^{TTD} double mutation in TFIIH has not been characterized before. Consistent with the crucial role of Xpa in the classical NER pathway, the ability of cells to survive increasing doses of UV (UV survival) was the most reduced in Xpa and Xpa/Xpb^{XPCS} cells. Xpb^{XPCS}/Xpd^{TTD} cells showed mildly enhanced sensitivity compared to each single mutant (Figure 5B). We then measured GG-NER and TC-NER capacity after UV irradiation by Unscheduled DNA Synthesis (UDS) and Recovery of RNA Synthesis (RRS) assays. Xpb^{XPCS}/Xpd^{TTD} cells displayed ~ 8% UDS and ~ 24% RRS residual activity which show that residual GG-NER and TC-NER is significantly higher in Xpb^{XPCS}/Xpd^{TTD} cells than in completely NER defective Xpa and Xpa/Xpb^{XPCS} cells (data no shown), explaining the enhanced UV-survival of Xpb^{XPCS}/Xpd^{TTD} cells relative to Xpa deficient cells.

A

XPB-XPCS/XPD-TTD

control
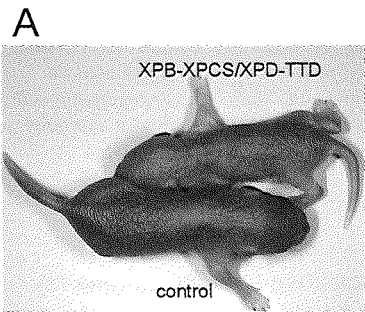
Figure 5 *Phenotype of XPB-XPCS/XPD-TTD double mutant mice and cells*
(A) Photograph of a ~24h old XPB-XPCS/XPD-TTD double mutant and a double heterozygote littermate. After normal embryogenesis, double mutant mice fail to grow and die within ~ 36 hours.
(B) Representative UV survival graph. The experiment was repeated 2 times. At least 2 cell lines per genotype were analyzed. Error bars indicate SEM within the experiment.
(C) Hypersensitivity of XPB-XPCS/XPD-TTD cells to acute oxidative damage. Gamma ray survival curves averaged from 2 independent experiments with 2 cell lines per genotype. Error bars indicate SEM between experiments.

B % UV-survival

wt
XPD-TTD
XPB-XPCS
XPB-XPCS XPD-TTD
XPA/XPB-XPCS
XPA

J/m²UV

C % gamma-survival

wt
XPD-TTD
XPB-XPCS
XPB-XPCS/XPD-TTD

Gy

D % paraquat-survival

wt
XPB-XPCS
XPB-XPCS/XPD-TTD
CSB
XPA/XPB-XPCS

paraquat ug/ml

E TFIIH level

p<0.005

wt XPB-XPCS wt XPD-TTD wt XPB-XPCS/XPD-TTD

(D) Hypersensitivity of XPB-XPCS/XPD-TTD and XPA/XPB-XPCS cells to chronic oxidative injury. MEF cells of the indicated genotype were cultured in the continuous presence of the indicated concentration of paraquat for 3 days. Two cell-lines per genotype were tested. For reasons of simplicity, on the depicted representative survival experiment results from two independent cell-lines for XPB-XPCS and XPA/XPB-XPCS cells were averaged and error bars depict SEM between two independent cell lines within the given experiment. For the other genotypes in the given experiment one cell line per genotype was used and error bars depict SEM within the experiment.
(E) Reduction of TFIIH protein levels in XPB-XPCS, XPD-TTD single, and XPB-XPCS/XPD-TTD

double mutant primary MEFs by comparative immunofluorescence. Quantification of the immuno-
fluorescence signal is based on analysis of at least 50 nuclei per genotype in 2 separate experiments
with 2 independent cell lines per genotype. Wt cells are labelled with latex beads, mixed with the
mutant cells and cultured and immunostained on the same microscopic slide. Bars representing cell
lines analysed on the same microscopic slide are depicted side by side. P value indicates minimum
significant difference between cell lines analysed on the same microscopic slide within one
experiment.

Human and mouse CS (but not TTD or XPA) cells are sensitive to acute gamma ray induced damage - a feature attributed to defective TCR of 8-oxoguanine and other types of oxidative damage (Le Page et al. 2000). Analysis of the gamma ray sensitivity of double mutant Xpb^{XPCS}/Xpd^{TTD} cells revealed an increase in sensitivity relative to Xpb^{XPCS} single mutant (Figure 5C), whereas the sensitivity of Xpa/Xpb^{XPCS} cells did not reveal any increase and (data not shown). Next, we analyzed the sensitivity to chronic low dose oxidative injury by continuous exposure of cells to paraquat for 3 days. In concordance with our previous findings Xpa and Xpd^{TTD} cells were found insensitive. Surprisingly also Xpb^{XPCS} single mutant cells where found insensitive, whereas both Xpa/Xpb^{XPCS} and Xpb^{XPCS}/Xpd^{TTD} double mutant cells were clearly more sensitive (Figure 5D), showing a survival curve similar to that of Csb deficient cells, which are known to be sensitive to oxidative DNA damage (Le Page et al. 2000; de Boer et al. 2002; de Waard et al. 2004).

The mild synergistic effect of Xpa/Xpb^{XPCS} double mutation on organismal level and in terms of cellular sensitivity to chronic but not acute exposure to oxidative damage; as well as severe synergistic effect of Xpb^{XPCS}/Xpd^{TTD} double mutation on organismal and in terms of cellular sensitivity both to chronic and acute exposure to oxidative damage provides evidence for a casual link between DNA damage, repair and the extent of accelerated ageing features.

To investigate the effects of Xpa/Xpb^{XPCS} and Xpb^{XPCS}/Xpd^{TTD} double mutations on cellular TFIIH level, we performed comparative immunofluorescence analysis. We detected no change in the TFIIH complex level in Xpa/Xpb^{XPCS} cells. Although it is difficult to quantitatively compare different experiments, indication for the mild reduction of TFIIH level in Xpb^{XPCS}/Xpd^{TTD} cells (Figure 5E and data not shown) relative to the TFIIH levels in the single mutants in comparison to the same wt control cell line was noticed. Nevertheless, the further reduction of TFIIH level in the Xpb^{XPCS}/Xpd^{TTD} double mutant cells (if present) is an unlikely cause for the observed phenotypes, as no correlation between TFIIH level and severity of ageing features has been found in TTD or XPCS patients (Botta et al. 2002) and mice (J.O.A. et al., manuscript in prep.).

Impact of NER mutations on spatio-temporal architecture of the NER reaction
Following DNA damage, cellular and subsequently organismal responses are determined by protein-DNA and protein-protein interactions where conformation and timing

of NER reaction may play an important role. Unfortunately, methods for visualization of TCR, likely the most affected repair pathway in CS and TTD symptomology, have remained unavailable. Therefore, we studied build-up and timing of GG-NER, which shares most (if not all) of its components with TCR. We compared Xpb^{XPCS}/Xpd^{TTD} cells with a panel of single and double NER mutant cells (Xpa, Xpb^{XPCS}, Xpd^{TTD}, Xpa/Xpd^{TTD}, Xpa/Xpb^{XPCS}). We applied UV induced DNA damage to small areas of the nucleus (local UV induced DNA damage)(Volker et al. 2001). Shortly after local UV-irradiation (within 15 minutes), NER factors accumulate at the site where local damage is inflicted. In wt cells the damage is removed within 1-2 hours accompanied by loss of staining. (D. Hoogstraten et al., unpublished). For positioning local UV damage, we performed immunostaining of XPC protein, the initial damage sensor in the NER reaction (Mone et al. 2001; Volker et al. 2001). We found that in Xpa cells TFIIH accumulates at the sites of local damage 15 minutes after irradiation and as such are very similar to wt cells. Yet, unlike in wt cells, TFIIH retains at the sites of damage even 3 hours after irradiation, indicating that XPA protein is not required for TFIIH retention at damaged sites, but is critical for completing the NER reaction (Figure 6). Xpb^{XPCS} and Xpd^{TTD} single mutants display strong and moderate retention of TFIIH complex 3 hours after UV irradiation at the sites of damage respectively, likely reflecting the reduced rate of damage removal by hampered TFIIH. When Xpa defect is combined with a mutation in TFIIH, such as Xpd^{TTD} or Xpb^{XPCS} (or Xpd^{XPCS} (J.O.A. et al., manuscript in prep.)) then the complex binding to the damaged sites is severely affected relative to the corresponding single TFIIH mutant. Only half of the locally damaged cells display weak staining of TFIIH with no change in signal intensity and number of positive cells even 3 hours after damage delivery. Thus, in the absence of Xpa, different helicase mutations in TFIIH seriously affect TFIIH binding and retention time at the damaged areas of the nucleus. While Xpd^{TTD} cells at the 3-hour time-point only showed a moderate accumulation of TFIIH, Xpb^{XPCS} and Xpb^{XPCS}/Xpd^{TTD} cells displayed pronounced accumulation of TFIIH both at 15 minutes and 3 hours following UV damage. Thus, in the presence of Xpa, Xpb^{XPCS} and Xpd^{TTD} helicase mutations lead to an enhanced TFIIH retention at the locally damaged sites. Although it is difficult to make a firm assumption, TFIIH withholding seemed to be the highest in Xpb^{XPCS}/Xpd^{TTD} double mutant cells. These results indicate that mutations in NER proteins significantly affect the structure and timing of GG-NER but likely also other subpathways of NER.
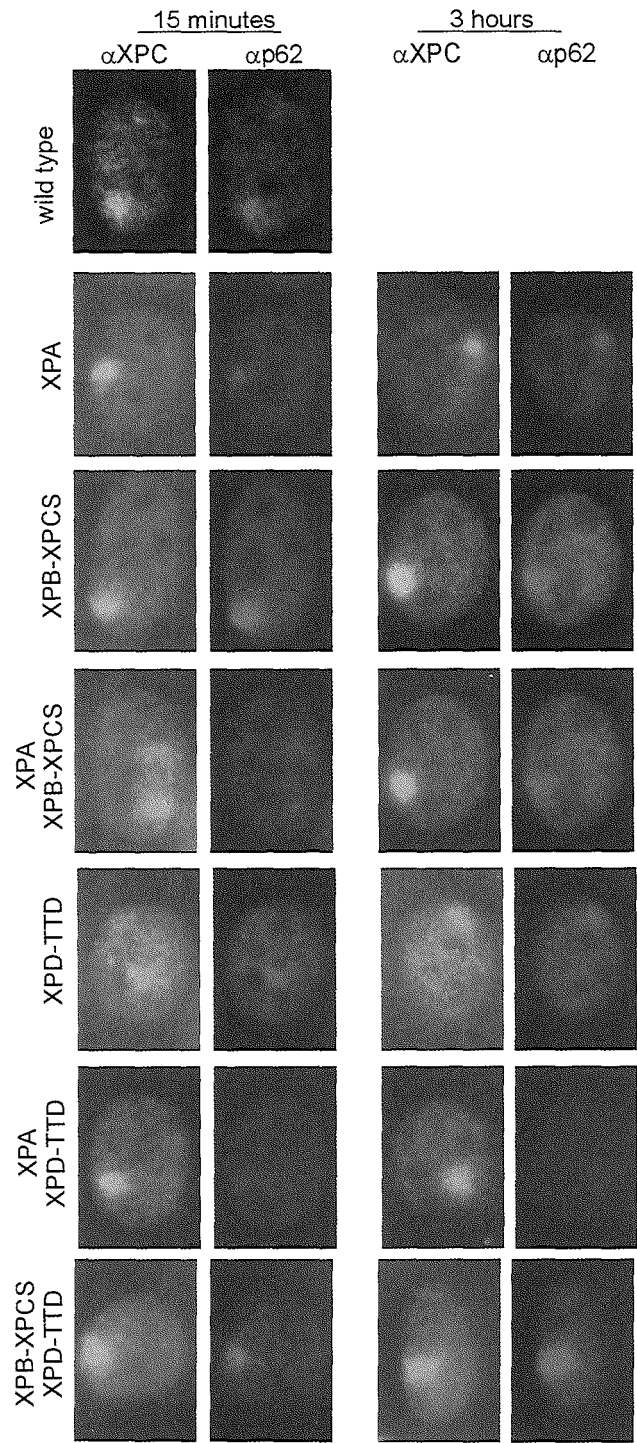
Figure 6. Mutations in XPB and XPD helicases affect GG-NER structure and timing. Localization and retention of XPC and the p62 component of TFIIH at the locally UV irradiated site is depicted. In the absence of XPA, XPC and TFIIH are preserved at the locally damaged areas. Defects in either the XPD or XPB helicase lead to a similar molecular phenotype. Concomitant XPA deficiency with either XPD or XPB helicase defect severely affects TFIIH accumulation on damaged sites. Concomitant mutations in both helicases in XPB-XPCS/XPD-TTD cells causes a profound and persistent accumulation of TFIIH at the damaged sites.

Discussion

Here, we have generated a mouse model for Xpb^{XPCS} by mimicking the causative spli-ce-site mutation from XPCS patient XP11BE in the murine Xpb locus. This mutation leads to insertion of 4bp of intronic sequence and results a frameshift into the last exon of XPB. In our initial attempt to generate Xpb^{XPCS} mice, we inserted the frames-hift-causing 4bp into the corresponding position in the murine Xpb. We found that the mRNA originating from the resulting Xpb^{fs} allele was ~10 times under represented in the heterozygous ES cells, likely due to the presence of selectable marker gene within the last intron of the targeted Xpb^{fs} allele. Similar to the phenotypic consequence of complete inactivation or underexpression of the mutated Xpd in mice, homozygosity for Xpb^{fs} appeared embryonic lethal. This is likely due to the insufficiency in the basal transcription function of TFIIH, of which XPD and XPB are helicase compo-nents. The XPB splice-site mutation in XP11BE patient "in theory" can result in both aberrant as well as wt splicing. Although no wt XPB transcripts or protein was detec-ted in the XP11BE lymphoblastoid cells, it can not be excluded that during ontogene-sis in some cells and tissues wt XPB is produced, which might explain the relatively long life-span and mild CS features of this patient. With this in mind, we mimicked the splice-site mutation in the murine Xpb.

Xpb^{XPCS} mice were viable and born at Mendelian frequency. We were able to detect wt XPB transcripts in several tissues in the homozygous Xpb^{XPCS} mice, indicating that at least in mice the XP11BE splice-mutation can yield wt XPB mRNA. Nevertheless, despite the presence of the wt mRNA, Western blotting analysis of Xpb^{XPCS} cells failed to detect wt XPB protein. Defective GG-NER, TC-NER, TCR and hypersensitivity of Xpb^{XPCS} cells to acute genome damaging agents such as UV and gamma irradiation further argued that wt XPB protein is either absent or present in minute amounts in Xpb^{XPCS} cells. Absence of CS and/or accelerated ageing in Xpb^{XPCS} mice argued that this XPB mutation has either a mild associated phenotype and/or the presence of minute amounts of wt XPB protein to alleviate the ageing phe-notype. CS features in the XP11BE patient were relatively mild (she survived until 4th decade of her life while average life-span of CS patients is 12.5 years). Since NER-associated severe progeroid conditions, such as CS, XPCS and TTD in general reconstitute in a mild form in mice (van der Horst et al. 1997; de Boer et al. 1998a; van der Horst et al. 2002)(J.O.A. et al., manuscript in prep.) absence of or very placid reconstitution of CS in Xpb^{XPCS} mice was not surprising. XP features, on the other hand, were clearly manifest in Xpb^{XPCS} mice, as concluded from deficits in GG-NER and TC-NER pathways and cellular and organismal hypersensitivity to UV irradia-tion. Recently, we found that mice carrying XPCS causative (XPD-G602D) mutation in the Xpd gene are enormously predisposed to UV induced skin and eye cancer (J.O.A. et al., manuscript in prep.). In the future, it would be of great interest to study this important aspect of XPB-XPCS in Xpb^{XPCS} mice.

DNA repair deficit can determine the pace of accelerated ageing

Sensitivity of Xpb^{XPCS} cells to gamma rays indicated a deficiency in TCR of oxidative lesions, a feature proposed as a hallmark of, and perhaps causative of CS (Le Page et al. 2000). The lack of CS and/or accelerated ageing in Xpb^{XPCS} mice suggests that while TCR in Xpb^{XPCS} cells fails to deal with an acute damage (delivered in cellular gamma survival assays), it is likely proficient enough to battle chronic low-dose endogenous damage believed to contribute to ageing and CS (Le Page et al. 2000; de Boer et al. 2002; Mitchell et al. 2003)(J.O.A. et al., manuscript in prep.). In concordance with this notion, we found that sensitivity of Xpb^{XPCS} cells to chronic low-dose oxidative injury (i.e. 3 days culturing in the presence of paraquat) is comparable to that of wt cells.

Next we asked whether further reduction of DNA repair capacity by knocking down GG-NER and TC-NER pathways via concomitant Xpa inactivation can trigger acceleration of ageing and/or CS features in Xpb^{XPCS} mice. XPA inactivation in Xpb^{XPCS} mice triggered ~20% mortality around weaning, developmental delay, juvenile neuropathies, early kyphosis, mild cachexia and testicular atrophy. This is in sharp contrast to the phenotype of Xpa/Xpd^{TTD}, Xpa/Xpd^{XPCS}, Xpa/Csa and Xpa/Csb mice which uniformly display severe enhancement of TTD or CS features but die within 1-3 weeks after birth (de Boer et al. 2002) (J.O.A. et al., manuscript in prep., I van der Pluijm et al., manuscript in prep.).

Notably, hallmark features of normal ageing in mice including loss of germinal epithelium, kyphosis and cachexia, appeared early in Xpa/Xpb^{XPCS} mice, pointing to endogenous DNA damage-induced acceleration of this process. Early germinal epithelium degeneration and cachexia has also been noted in other accelerated ageing models, including mice with a mitochondrial DNA polymerase defect (Trifunovic et al. 2004) and DNA repair defective Xpb^{XPCS} mice (J.O.A. et al., manuscript in prep.). Xpd^{TTD} and Ku80 deficient mice display progressive cachexia and kyphosis (de Boer et al. 2002) and Csb deficient animals display cachexia while they age (I. van der Pluijm et al., manuscript in prep.), pointing to the uniform causative effect of DNA damage in CS and normal ageing. Since the above mice are all in different genetic backgrounds (e.g. Xpa/Xpb^{XPCS} mice are in the C57bl6 genetic background; Xpb^{XPCS} mice are in a mixed FVB/C57Bl6/129Ola background) the overlap in phenotype suggests that CS features in mice are uniform, partially overlie with that of normal ageing and reconstitute in a process dependent , but causative gene(s) and genetic background independent manner. This resembles the human situation, in which CS features are uniform and independent of the race and causative gene (Nance and Berry 1992)(I. Rapin per. comm., R. Brumback per. comm.). At the cellular level, Xpa/Xpb^{XPCS} double mutant MEFs were found to display enhanced sensitivity to low dose chronic exposure to paraquat, thereby revealing the inability to deal with chronic oxidative damage exposure and perhaps explaining the root cause of accelerated

ageing in Xpa/Xpb^{XPCS} mice. The likely phenotype causing lesions in Xpa/Xpb^{XPCS} mice are endogenously rising DNA helix distorting NER substrates such as cyclo-purines. These lesions can be induced by endogenous ROS and are substrates for GG-NER and TC-NER pathways (Brooks et al. 2000). The more general TCR pathway on the other hand is believed to remove all kinds of transcription interfering lesions ranging from helix distorting lesions to small single base adducts (Citterio et al. 2000b; Le Page et al. 2000; van den Boom et al. 2002; Mitchell et al. 2003).

We next studied the phenotypic effect of Xpb^{XPCS} and Xpd^{TTD} double mutation. This question was of particular interest, since mutations causative of both TTD (XPD-R722W) and XPCS (XPB-frameshift of the last exon) have been shown to result in defective basal transcription initiation in vitro, a deficit often suggested as causative for TTD and CS (Coin et al. 1999; Dubaele et al. 2003). Xpb^{XPCS}/Xpd^{TTD} double mutant mice developed normally in utero, demonstrating that the basal transcription function of double mutated TFIIH in vivo is sufficient to support normal ontogenesis, thereby rendering basal transcription defect an unlikely cause of CS and/or TTD. After birth, Xpb^{XPCS}/Xpd^{TTD} double mutant mice died within ~36 hours. The almost exclusive postnatal onset of CS and TTD, both in man and mice, suggests a role for exogenous factors, such as atmospheric oxygen. Rapid failure to thrive suggests that postnatal acute increase in oxidative DNA damage load (Brooks 2002) may have a causative role. Indeed, Xpb^{XPCS}/Xpd^{TTD} cells were found hypersensitive to both acute (gamma ray) and chronic (low dose paraquat exposure) oxidative injury, suggesting that the TCR pathway is further hampered by concomitant Xpd^{TTD} and Xpb^{XPCS} muta-tions. The absence of increased apoptosis in Xpb^{XPCS}/Xpd^{TTD} mice suggests, that con-flicting signals of proliferation (developmental requirement for postnatal growth) and growth arrest (short-coming in the TCR of oxidative injury) may result in decline in cellular function leading to death.

TCR of oxidative lesions is a very poorly understood reaction, and proteins involved in probing and signalling downstream TCR and NER are largely unknown. Nevertheless, the structure and timing of the GG-NER subpathway can be visualized in cells by immunostaining methods (Mone et al. 2001)(D. Hoogstraten et al., unpu-blished). Although due to its relative abundance, it is the only NER pathway that can be monitored, beyond the initial damage recognition step, GG-NER shares many, if not all of the factors with TC-NER and TCR. Thus, mutation-induced changes in GG-NER most likely reflect changes in other NER related repair pathways. We found that relative to the single mutant cells, concomitant Xpa inactivation in Xpd^{TTD} and Xpb^{XPCS} cells resulted in poor but persistent TFIIH binding to locally UV damaged areas within the nucleus. Thus, our results support the earlier findings in human cells suggesting that the XPA protein is required for DNA lesion demarcation and NER complex stabilization (Volker et al. 2001). Notably, TFIIH retention in Xpa/Xpd^{TTD} and Xpa/Xpd^{XPCS} cells (J.O.A. et al., manuscript in prep.) is more pronounced than in Xpa/Xpd^{XPCS} cells. Whether or not the observed differences reflect a causative link

between NER structure and timing and the remarkably milder phenotype of Xpa/Xpd^{XPCS} mice (lifespan > 1.5 years, versus 1-3 weeks in Xpa/Xpd^{TTD} and Xpa/Xpd^{XPCS} mice) remains to be elucidated. The stalling of TFIIH in Xpb^{XPCS} and Xpb^{XPCS}/Xpd^{TTD} cells occurs in the presence of XPA and thus has a different mechanistic cause related to a specific TFIIH helicase deficit. Taken together, our results indicate that mutation(s) in NER genes lead to profound changes in the spatio-temporal axis of GG-NER and likely in other NER related repair pathways, such as TCR. The severity and type of NER associated disease may depend on the effect of a given mutation on the spatio-temporal axis of the NER or TCR reaction. Different 3D structures likely lead to different cellular signals and thus result in dissimilar phenotypic outcomes. Evidence supporting the above argumentation has recently emerged. For example, while mostly frameshift and truncation type of alterations in the *CSB* gene result in classical CS (Cleaver et al. 1999), recently a CSB-COFS patient was characterized, carrying only a point-mutation in the *CSB* gene. The most severe CSB truncation, on the other hand, is associated only with UV sensitivity syndrome (K. Tanaka et al., unpublished). Another example of such an effect may include XPD-R683W patients, in which the more severe truncation in the second *XPD* allele was found to be associated with the absence of neurodegenerative processes (Ueda et al. 2004). Moreover, UV and DNA interstrand cross-linking agent mitomycinC hypersensitivity of *Ercc1*- deficient Chinese hamster ovary cells can be complemented with ERCC1 lacking the first N-terminal 92 amino acids, but not with ERCC1 containing 2 amino acid change within the same N-terminal part (N. Jaspers per. comm.). These findings argue that sometimes it might be better not to have a protein, than have one with a "bad" mutation, a phenomenon which may be designated as "mutation associated toxicity" or MAT.

Recently, a diversity of explanations have been proposed to explain NER associated premature ageing. For example, deficits in RNA-PolII initiation and/or elongation, activated transcription and RNA-PolI transcription all on their own or in combinations have been suggested (Vermeulen et al. 1994b; Bradsher et al. 2002; Keriel et al. 2002; Dubaele et al. 2003). Nevertheless, based on our current and previous findings, we favor the following explanation. The nearly exclusive postnatal onset of the ageing phenotype in NER defective patients (TTD, XPCS and CS) and mice (ERCC1, XPG, XPF, XPA/CSB, XPA/CSA, XPA/XPD-TTD, XPA/XPD-XPCS, XPC/CSB - single and double mutant mice display overlapping postnatal growth failure and 1-3 week life-span (Weeda et al. 1997; Harada et al. 1999; van der Horst et al. 2002; Tian et al. 2004b) (J.O.A. et al., manuscript in prep., I. van der Pluijm et al., manuscript in prep.) strongly suggest the involvement of a common root cause. Since the only known biological process common for all the genes affected in the above mouse models is DNA repair, we suggest postnatal accumulation of ROS-induced DNA damage on one side and the repair efficiency and 3D character of the collapsed or stalled DNA repair complexes on the other to determine the rate and type of disease

in NER patients and mice. In normal ageing, these processes occur at the natural pace in which differences in the rate of ageing are potentiated by the ordinary genetic and environmental variance.

Taken together, the gradual increase in the severity of ageing phenotype following further reduction of DNA repair in Xpb^{XPCS} mice by genetic interference with GG-NER and TC-NER or TCR pathways and the correlation between severity of organismal phenotype and cellular sensitivity to ROS provide strong evidence for the causative role of DNA lesions and repair in accelerated ageing.

Materials and methods

Targeting vectors

All recombinant DNA work was performed according to standard procedures (Sambrook et al. 1989). The gene targeting construct was prepared by subcloning a – 7 kb SaII-Nsil fragment from 129/CCE EMBL4 genomic library only containing the murine *Xpb* exon 15 (including the 3' UTR) in pGEM5Zf(+) (Promega), yielding pNS*Xpb*. The SalI restriction site is derived from the EMBL4 cloning vector. The p*Xpb^{fs}* targeting construct was generated as follows: from the above described construct, a -4 kb EcoRI fragment containing exon 15 was subcloned in a pTZ18R vector (Pharmacia). The 4-bp insertion (GATC) was introduced after the first codon of exon 15, introducing a diagnostic Bglll site by site-directed mutagenesis, using primer p79 and the Mutagenesis kit (Stratagene). In addition, we introduced a unique Clal restriction site in intron 14, approximately -0.3 kb upstream exon 15, changing a BamHI restriction site in the intron in order to insert the pMC1neo resistance gene, using primer p78 (see Figure1). The Xpb^{XPCS} mutation was introduced in a similar fashion using primers p166 and p218. After mutagenesis, the introduced mutations, coding and non-coding region of exon 15, including splice-acceptor site were confirmed by ds-DNA sequence analysis (Sanger et al. 1977). The wild-type -4 kb EcoRI fragments of the original targeting vector (pNS) was replaced by EcoRI fragments containing the two different *Xpb* mutations. In the Xpb^{XPCS} targeting construct the hygromycin selectable marker, driven by the PGK-promoter was inserted in the unique Xbal restriction site downstream the *Xpb* gene in the same transcriptional orientation as the *Xpb* gene. The unique Sall and Nsil restriction sites were used for linearization before transfection to ES cells. The primers used for the gene targeting constructs are indicated below:

p73 (5' AACCTAGGACCCACGAAGGC)
p78 (5' TGTCCAGTTCCTATCGATCCAACACTC)
p79 (5' ACAGCGTCGGGAGATCTGCCTGTGGGGAG)
p108 (5' CGACGCTGTGGCACCATGAG)
p166(5' TCGGGATGCCTGTCTGGAGAGGGGGGAGC)
p218 (5' TGCCACAGCGCCTAGATGCCTGT)

Embryonic stem cells and transfection

The targeting constructs were linearized and separated from vector sequences by gel electrophoresis, purified by electroelution and introduced into 129/Ola-derived ES cells by electroporation. E14 cells were cultured and selected as described earlier (de Boer et al. 1998b). Chromosomal DNA was digested with Ncol and analyzed by Southern blot using a genomic 5' -0.6 kb Ncol/Bglll probe flanking the targeting construct (probe A, Figure 1B). Positively targeted clones were reconfirmed using a neo or hyg probe (probe C) covering the coding regions (see Figure 1) and a additional internal probe covering mouse *Xpb* exon 15 (probe B, Figure 1B and E). This latter probe was generated by PCR using mouse *Xpb* gene specific primers (p108 and p73). All homologous recombinant ES clones showed bands diagnostic for correct integration of the neo or hyg markers without the presence of additional copies of the targeting constructs due to non-homologous integration.

Reverse transcriptase PCR and dot-blot analysis

Total RNA was prepared by the LiCl/urea method (Auffray and Rougeon 1980). The RNA was used for preparing cDNA with primers p73 (exon 15) and p100 (exon 14). Amplified DNA was spotted on to nitrocellulose and hybridized under stringent conditions with a "P-labelled wild-type primer p230, mutant primers p165 containg the 4-bp insertion, p231, containing the splice-acceptor mutation and stopcodon mutation p234. The PCR fragments were subcloned in a Bluescript-TA cloning vector and individual clones were analysed. Plasmid DNA was used for dot-blot analysis and sequence analysis as described above. Primers used for RT-PCR and Dot-blot analysis are indicated below:

p73 (5'AACCTAGGACCCACGAAGGC)
p100 (5 'AGCTGGCGTTCTCCACCAAA)
p165 (5'GGCCAGGCAGATCTCCCG)
p230 (5'TCTGGCCAGGCATCCCGACGCT)
p231 (5'TGGCCAGACAGGCATCTAGGCG)
p234 (5'TCTGGCCAGGCATCTAGGCGCT)

Generation of *Xpb* mutant mice

Chimeric mice were obtained by injecting 10-15 cells of two independent targeted ES cell clones into C57/Bl6 blastocysts. Male chimeras were bred to C57/Bl6 animals. Targeted ES clones produced male chimeras whose germline transmitted the agouti coat collar marker in nearly all offspring. Approximately, half of the offspring genotyped as positive for the targeted mutation. Heterozygous F1 mice were intercrossed. Southern blot analysis using probe A was used to genotype embryos and offspring. Genotyping *Xpb^fs* mice was performed by Southern blotting using probe C (see Figure 1C). Genotyping *Xpb^XPCS* mice was performed by Southern blot analysis and/or PCR assay using p259 (mouse *Xpb* exon 15), p253 (promoter PGK) and p269

(3' of the Xbal restriction site, downstream the *Xpb* gene. Oligonucleotides used for genotyping are indicated below:
p253 (5'GCTGCTAAAGCGCATGCTCC)
 p259 (5'GACTGGCTGCCTGGATCCG)
 p269 (5' GTGAGCCTCTCCCTTGAGAAAAC)

XPB-XPCS mice were back crossed with wt C57/Bl6 for more than 8 generations. All the mice used in this study were in C57/Bl6 isogenic background.

DNA-damage sensitivity assays
UV-induced UDS, RSR as well as UV, gamma ray and paraquat survival assays were performed as described previously (Vermeulen et al. 1994a; de Boer et al. 2002; de Waard et al. 2003).

Immuno-blotting
Anti-XPB (1B3) MAb was described earlier (Schaeffer et al. 1993). MAb2G12 is a monoclonal antobody raised towards the human wildtype 42 C-terminal amino acids of XPB. Proteins from cell extracts were separated by 11% SDS-polyacrylamide gel electrophoresis (PAGE) and transferred to polyvinylidine difluoride membranes (Milipore) or nitrocellulose in 25 mM Tris-HCI glycine buffer (pH 8.3) containing 20% methanol. Antigen-bound antibodies were detected with a horseradish peroxida-se-linked Goat anti- mouse IgG and a enhanced chemiluminescence detection system.

Comparative immunofluorescence analysis of p62 subunit of TFIIH and local UV damage
Latex bead labelling and comparative immunofluorescence analysis of the p62 sub-unit of the TFIIH as well as locally applied UV damage assays were performed essentially as described earlier in the similar studies (Vermeulen et al. 2000; Mone et al. 2001; Vermeulen et al. 2001; Volker et al. 2001). For local UV damage, cells were rinsed with PBS and covered with an isopore polycarbonate filter (Millipore) contai-ning 5 micrometer pores before UV irradiation with a Philips TUV lamp (254 nm) at a dose rate of ~0.9 $J.m^2/s$. In total 48 $J.m^2/s$ were given and cells were put back into medium for 15 minutes or 3 hours. We fixed cells with 2% paraformaldehyde for 10 minutes RT, permeabilized 2 times for 10 minutes with 0.1% TritonX-100, followed by wash with PBS+ (PBS + 0.15% glycine and 0.5% BSA). Anti-p62 (3C9) antibo-dies were diluted 1:2000 and anti-XPC antibodies 1:500in PBS+ and incubated RT for 1h in the moist-chamber. After incubation, we washed coverslips 5 times 5 minu-tes with PBS+0.1% TritonX-100 followed by incubation with Cy3 conjugated goat-anti-mouse (The Jackson Laboratory) diluted in PBS+ 1:800. After 45 minutes incu-bation and the same wash procedure, we mounted coverslips in Vectashield mounting medium (Vector Laboratories) containing 1.5 µg/ml DAPI and stored at +40 C in the

dark. We produced epiflourescent and phase-contrast images on a Leitz-Aristoplan microscope, equipped with a 3-CCD camera (DXC-950P Sony) and digitally processed using Adobe Photoshop 4.0. For TFIIH level quantification, 25-50 microscopic fields in each experiment was photographed in a "blind" fashion. Background levels were measured beside each individual nucleus. The obtained values were processed further by subtracting the background red fluorescence from the nuclear red fluorescence, the obtained numbers were processed with Excel. Standard Student T-test using 2 tailed two-sample equal variance setting was used to verify the statistical significance of the data. Standard karyotyping was performed to verify that the observed differences in signal intensity are not due to altered karyotype of the primary MEF cells. In all the cell-lines used in this study ~80% of the nuclei were found to be diploid while ~20% had a tetraploid karyotype. 2 or more cell-lines per genotype were used in this study.

Reconstitution of CS-like pathology in mice: a powerful model system to define a therapy

Jaan-Olle Andressoo[1], Willeke M.C. Jong[1], James R. Mitchell[1], Chris I. de Zeeuw[2], Jan Huijmans[3], Jan H. Hoeijmakers[1] and Gijsbertus T.J.van der Horst[1]

1 Medical Genetics Center, Department of Cell Biology and Genetics,
  Center of Biomedical Genetics,
2 Department of Neuroscience,
3 Department of Clinical Genetics, PO Box 1738, Erasmus MC, 3000DR Rotterdam,
  The Netherlands

Work in progress

Reconstitution of CS like pathology in mice

One of the obstacles in defining therapy for CS and TTD is the fact that some impor-
tant features of the disease in particular the neurological aspects are poorly reconsti-
tuted in the current mouse models. In humans, the time of onset of neuropathy is pre-
dictive for life-span and severity of the disease (Nance and Berry 1992; Itoh et al.
1999). CS and TTD mice have only very mild neurological manifestations without
clear progressive character and live often 2 or more years. Mice lacking ERCC1,
XPF or XPG or e.g. XPA/TTD or XPA/XPCS double-mutants live only 1-3 weeks,
leaving a very short timeframe for intervention discovery. Moreover, the severely
arrested development, overall weakness, small body-size, and death before weaning
makes clinical applications, such as feeding of drugs, injections, anesthesiology and
surgery extremely complicated. The optimal mouse model system would enable the
above applications while displaying clearly scorable and progressive CS features
within a relatively short period of time.

In this thesis we showed interallelic complementation (IAC) at the mouse *Xpd* locus.
Next, we asked whether IAC can occur in the absence of XPA. XPA-deficient mice
compound heterozygous for the TTD (XPD-R722W) and XPCS (XPD-G602D)
mutation (designated as TTD|XPCS/XPA mice) were born at mendelian frequency
and 8 out of 10 pups survived the critical period of 3 weeks displaying pathology clo-
sely resembling that of the human CS condition. Symptoms of TTD|XPCS/XPA mice
include profound developmental delay, infertility (only 2 females tested), kyphosis
from 2 months of age, cachexia, ataxia, tremors, stooped gait, spasticity and easy
excitability. Due to progressive neurologic dysfunctioning and profound cachexia, the
oldest TTD|XPCS/XPA mouse had to be sacrificed at 5.5 months of age (Figure 1
and data not shown). The two oldest mice have displayed dysmetria (a polar neuropa-
thological condition, where one body side is affected more than the other) ((age of
onset at 5 and 3.5 months respectively), a feature also reported for XPG-XPCS
patient XP20BE (Lindenbaum et al. 2001). Other TTD|XPCS/XPA (n=7) mice are 3
months old and display similar disease features.

Age: 37 days   2 months   4 months   5.5 months
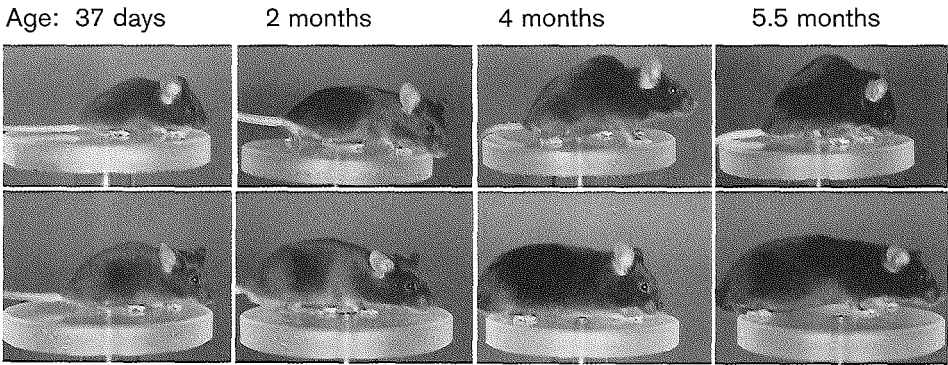
Figure 1 *Disease etiology in TTD|XPCS/XPA mouse*
upper panel: TTD|XPCS/XPA mouse; lower panel: littermate control

In concordance with profound cachexia and kyphosis necropsy revealed a very weak and soft vertebral column. Reminiscent of the human CS condition, most of TTD|XPCS/XPA mice needed assistance for feeding (i) during development from ~12 days to 6-8 weeks of age and (ii) during the late stage of the disease (for the latter time point, one mouse tested). Likely due to overall weakness, ataxia and balance problems TTD|XPCS/XPA mice were unable to eat dry food and were provided water-moistured food pellets. The condition progressed rapidly when assistance in feeding was stopped too early in development. Compared to the normal mice, who are able to feed independently after weaning (~23 days of age), TTD|XPCS/XPA mice were strong enough to feed on their own only at about 6-8 weeks of age. While normal mice feed mostly during the night, TTD|XPCS/XPA mice were found "snacking" all the time during the daytime. Total food intake per 24 hours was found to be significantly higher than that of the littermate controls when measured at the age of 37 and 38 days ($p < 0.02$) respectively. When compared to bodyweight matched control mice (measured at the age of 21 and 22 days), the food intake between TTD|XPCS/XPA and control mice did not differ (Figure 2).
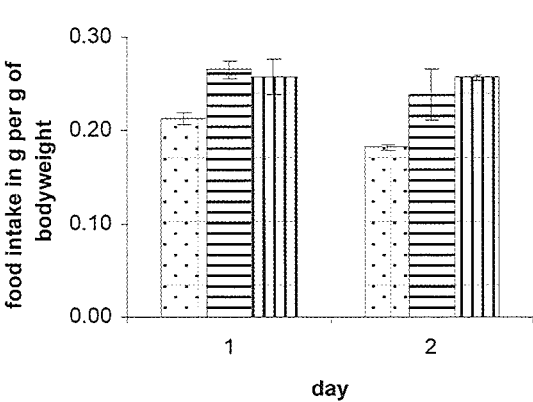
Figure 2 *Food intake of TTD|XPCS/XPA mice (horizontal bars) and littermate controls (dotted bars) at the age of 37-38 days; vertical bars-food intake of TTD|XPCS/XPA bodyweight matched control mice (measured at age 21-22 days). n=3 female mice per group per day.*

At the age of 38 days TTD|XPCS/XPA mice display segmental developmental retardation-they display disproportionally big head and weigh only~12 grams, which is a normal bodyweight of ~22 day old mouse (Figure1). Their food intake seems to correlate with bodyweight and not with age. Remarkably, TTD|XPCS/XPA mice (but not control mice) preferred fresh water softened pellets for the ones moistured a day before and re-moistured the next day, although the latter are softer and thus should be easier to eat. A possible explanation for this preference could be, that pellets from the day before have lost their vitamin and/or antioxidant content and the animals can smell it. Interestingly, a mother of a TTD patient described her son as constantly

"snacking" and with dedicated preference to fresh and healthy food (J.O.A. per. comm. with TTD parent).

Another CS parent described a case, where 2 CS siblings in a poor condition were transported from Mexico to the US where they substantially improved. Since there is no medical cure for CS, these details may refer to the potential of certain components in the diet, such as vitamins and/or antioxidants to alleviate the CS symptoms at least transiently. For example, folic acid, B6 and B12 pathway serves as a good candidate, as these vitamins are crucial for neurogenesis, are involved in ROS regulation and have implications for DNA repair activity (Kruman et al. 2002). Personal communication with CS parents from Cockayne syndrome society "Share and Care" revealed, that providing special vitamin mixes either orally or by the tube, can alleviate the disease. Although the exact numbers await to be published, personal communication with doctors and patient parents suggested that the average 12 year lifespan of CS patients has nowadays increased. What the role of vitamin supplementation is for this phenomenon is unknown. Although anecdotal the above cases could point to a real window of opportunities for improvement of the condition of CS patients. The discussed TTD|XPCS/XPA mice could serve as a valuable model for defining the "best" diet for CS patients. Detailed physiological and pathological analysis of TTD|XPCS/XPA mice is currently underway.

Therapeutic potential of bone marrow transplantation and steroid hormones

CS and TTD are very rare diseases (the number of patients reported does not exceed 300) and thus not much effort has been invested in intervention-discovery. The most devastating feature of CS and TTD (and COFS) is oligodendrocyte-associated neuropathy which results in dramatic loss of white matter in the brain and periphery (Nance and Berry 1992; Brooks 2002). Developmental delay may be secondary to the neuropathy (P.J. Brooks per. comm.). During recent years, progress has been made in alleviating fatal neuro-developmental disorders with oligodendrocyte involvement such as metachromatic leukodystrophy, adrenoleukodystrophy, globoid cell leukodystrophy, Hurler syndrome, Maroteaux-Lamy and Gaucher disease with bone marrow transplantation (BMT). These disorders involve a deficiency in lysosomal or peroxisomal enzymes (Peters and Steward 2003). After BMT stem cells for microglia from the transplanted bone marrow cross the blood-brain barrier and are thought to secrete the wt enzymes, followed by take-up by oligodendrocytes and neurons of the host. The mechanism of the latter events is still poorly understood since the proportion of microglia is only 5% in the white matter and ~12% in the grey matter in the CNS, yet the therapeutic effects can be quite profound. In mice, 1 week after BMT about 25% of microglia is of donor origin, suggesting a quick cellular turnover

(Krivit et al. 1995) and perhaps a selective advantage of the donor cells in this model. Microglial cells are important in coordinating the differentiation of oligodendrocyte precursor cells to myelinating cells both during development and adulthood (Bartzokis 2004). As the nature of the oligodendrocyte defect in NER disorders is still unknown, it is also possible, that it is, at least partially secondary to a microglia defect and thus CNS pathology could potentially be alleviated by BMT without genetic manipulation. Moreover, the potential of bone-marrow stem cells to differentiate into neurons and other cell types is most likely underestimated. Recent experiments with GFP labeled BM cells revealed, that BM cells can give rise to new Purkinje neurons (Priller et al. 2001), thus to the cells causing the ataxia in NER syndromes; as well as in AT patients. Due to the fact that osteoclast and osteoblast as well as fat-tissue stem cells lie in the bone marrow, BMT has a potential to alleviate CS and TTD skeletal anomalies as well as lipodystrophy.

It is unlikely that -without addition of special signal sequences- NER proteins will be excreted and taken-up similar to lysosomal and peroxisomal proteins. For the latter option, potent canditates would be 10-25 aminoacid membrane penetrating peptide tags, such as those derived from HIV-TAT, antennapedia or transportan proteins, which have been shown to work in vivo (Lindsay 2002). Lentiviral delivery vehicles of tagged NER genes to BM cells can be used, as this method has been proven to be successful in BMT experiments (Galimi et al. 2002).

For discovery of intervention, TTD|XPCS/XPA mice provide multiple non-invasive out-read opportunities and as such will hopefully serve as a powerful model system. The next interesting question is, what is the effect of gonadal steroids on TTD, CS and or XP-DSC neuropathy? On one hand, gonadal hormones are known to have neuroprotective effects (Ibanez et al. 2003; Schumacher et al. 2003) whereas on the other hand, NER patients with severe neurological manifestations display hypogonadism (Nance and Berry 1992). For example, the CNS of castrated rats is more susceptible to ectopic toxin-induced neurodegeneration (Schumacher et al. 2003). Also mouse models, like XPD-XPCS or XPB-XPCS/XPA mice generated in this study, display loss of germinal epithelium as a function of time. It would be important to find out whether these mice display e.g. a stronger neurological phenotype, when castrated at early age. A pilot study involving surgical removal of the testis in e.g. XPD-XPCS, CSB and XPA mice followed by behavioural and pathological analysis would be relevant. If endogenous gonadal hormones appear neuroprotective in these model systems, they would have therapeutic potential.

Mouse models in perspective

Although a panel of interesting experiments can be envisaged, two of the most intriguing ones are listed below.

(i) The paradigm of the mechanism of CS and TTD is based on the idea that profound accumulation of DNA damage is the root cause of the disease. Yet, the paradigm is not formally proven. Towards that end, chronic low-dose exposure of e.g. XPD-XPCS, CSB and XPA mice to an external damage source such as paraquat, H2O2, or gamma irradiation could be used. CS features in XPD-XPCS or CSB and XP-DSC features in XPA mice can be scored in parallel with oxidative damage quantification on genomic DNA. For the latter, specialized mass spectrometric methods are required for quantification of DNA injuries such as cyclopurines, Fapy A, Fapy G, 8-OH-dA, 5-OH cytosine and 5-OH-5-Me-hydantoin (such as available in the laboratory of P.J. Brooks).

(ii) In despite of established involvement of ROS in age associated brain pathology, the primary events are still unknown (Mandel et al. 2003). In that regard, NER mice could serve as potential models systems. For example, specific brain areas like the substantia nigra (SN) display neuronal loss in XP-DSC, as well as in normal ageing (Cruz-Sanchez et al. 1997; Itoh et al. 1999), resulting in e.g. Parkinson's disease's or dementia. Usage of NER defective mouse models for e.g. chemical induction (such as MPTP, 6-OHDA or methamphetamine;(Mandel et al. 2003)) of Parkinson disease would be of general interest.

CHAPTER 7

Lesson from mouse models- insight into the mechanism of NER associated disease

Jaan-Olle Andressoo, Jay Mitchell, Gijsbertus T.J.van der Horst and
Jan H. Hoeijmakers

Department of Cell Biology and Genetics
Erasmus MC
PO Box 1738
3000DR Rotterdam
The Netherlands

Lesson from mouse models- insight into the mechanism of NER associated disease

In this thesis, a panel of mouse models carrying single,- double, and/or compound heterozygote mutations in NER genes were generated, with phenotypes ranging from extremely severe (pre-blastocyst stage embryonic lethal) to mild. According to the severity of the phenotype, mice were divided into 6 groups, from A-F, with A representing the most severe, and F the mildest phenotype (Figure 2). In Figure 2, a representative mouse model for each phenotypic group is depicted, except for the group F which is indistinguishable from the wt by eye. Genotypes for mouse models depicted in Figure 2 are listed in shaded boxes in italics in Table 1 below. Other genotypes generated within the frame of this thesis are indicated in italics. NER mouse models generated earlier or elsewhere were grouped in Table 1 according to the phenotypic overlap with groups A-F.

Figure 2. *NER mouse models categorized according to the phenotype, A-the most severe; E, the mildest.*
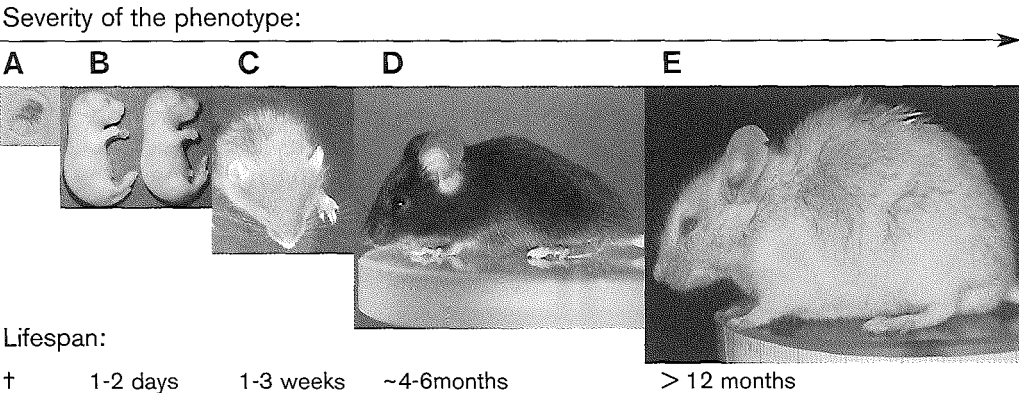
Severity of the phenotype:

| A | B | C | D | E |

Lifespan:

| † | 1-2 days | 1-3 weeks | ~4-6months | > 12 months |

Table 1. *Genotypes of NER mouse models grouped according to phenotype*

A	B	C	D	E	F
XPD-†XPCS (homozygous lethal)	*XPD-TTD/ XPB-XPCS* (double homozygote)	*XPD-XPCS/ XPA* (double homozygote)	*TTD|XPCS/XPA* (XPD-compound heterozygote)	*XPD-XPCS* (homozygous viable)	XPA
XPD-†XP6BE		*XPD-TTD/XPA*	ERCC1|ERCC1Δ7 (ERCC1Δ7 hemizygote)	XPD-TTD	*XPB-XPCS*
XPD-KO		CSA/XPA		*XPB-XPCS/XPA*	XPC
		CSA/XPC		CSA	
		CSB/XPA		CSB	
		CSB/XPC			
		XPF			
		ERCC1			
		XPG			

Group A

Homozygosity for the *Xpd*-knockout allele (de Boer et al. 1998b) as well as for ~ 5 times underexpressed XPD-†XPCS and XPD-†XP6BE alleles (this thesis) results in pre-blastocyst stage embryonic lethality. Since XPD is essential for basal transcription by RNA-PolII and I, the likely common cause for the overlapping phenotype is a complete basal transcription defect.

Group B

Combined homozygosity of XPD-TTD and XPB-XPCS results in normal embryonal development arguing, that the basal transcription function of double-mutated TFIIH is still sufficient to meet the demands of rapid in utero ontogenesis. Double mutant mice are born alive, but despite of proper nursing by the mother, die within 1-2 days after birth. Gross pathological examination did not reveal defects in any organ. TUNEL labeling did not reveal increased apoptosis in the liver, kidney and lungs (data not shown). The cause of death remains unknown. Sensitivity of double mutant cells to oxidative agents suggests that early lethality may be related to deficiency in repairing postnatal increase in oxidative DNA damage (Randerath et al. 1997a; Randerath et al. 1997b; Randerath et al. 2001), which may result in profound cell-cycle arrest or senescence, rather than apoptosis.

Group C

This group consists of mice displaying a strikingly similar pathology. Like CS and TTD patients, these mice develop normally in utero, but postnatally display progressive growth failure and cachexia resulting in death usually around weaning (van der Horst et al. 1997; Weeda et al. 1997; Harada et al. 1999; de Boer et al. 2002; van der Horst et al. 2002; Sun et al. 2003; Tian et al. 2004b). A similar rate of cachexia, balance problems, spasticity, ataxia and inactivity preceding death has been observed in our lab for XPA or XPC combined homozygotes with CSA or CSB, XPD-TTD/XPA and XPD-XPCS/XPA double mutant mice and ERCC1 mice. Immuno-histochemical examination of the cerebellum of XPD-XPCS/XPA, CSB/XPA, ERCC1 and XPG mice with calbindin-specific antibody revealed loss of Purkinje cells. (Murai et al. 2001; Sun et al. 2001; this thesis)(J.O.A. manuscript in prep.). Except for the neuronal compartment and similar to human patients, the group C genotypes did not reveal overt defects in any other organ system. Concomitant with the profound cachexia, organs were found to be smaller, yet histologically normal. Additionally, ERCC1- and XPF-deficient mice display enlarged (polyploid) nuclei in kidney and liver. The latter is a marker for liver ageing. Since cells from ERCC1 and XPF deficient mice are very sensitive to DNA cross-linking agent mitomycin C, a causative link between this type of damage and the phenotype has been put forward (Weeda et al. 1997; Tian et al. 2004b). Nevertheless, the notion, that ERCC1 mice die because of endogenous interstrand cross-link induced liver failure, as concluded from

extension of lifespan of ERCC1 mice with liver specific transgenic overexpression of ERCC1, might require more careful assessment since the transgene was also expressed at low levels in the brain and in the testis of those animals (Selfridge et al. 2001). ERCC1 expression in the brain may have had effects on the lifespan, as brain neuropathy is the main pathological feature in all severe NER conditions. Moreover, cells from CSA mice, which have close to normal life-span, are also (albeit mildly) sensitive to MMC (H. de Waard et al., unpublished). Taken together, the contribution of endogenously generated interstrand cross-links to the phenotype of ERCC1 and XPF mice remains unclear. In spite of intensive research, no common sensitivity for any DNA damaging agent has been found for NER-defective cells that correlates with genotype and phenotype. How to explain the quite uniform lifespan and pathology in group C mice? A plausible explanation is that the overlapping pathology results from similar DNA damage response signals in the same cell-types, e.g. Purkinje cells in the cerebellum. It is possible, that stalled RNA-PolII and/or hampered TCR complexes stalled for similar reasons serve as initiators of the signal, which is then processed and responded according to the genetic program of the specific cell and tissue. Keeping in mind that the most severely affected cells are post-mitotic neuronal cells, where e.g. interstrand cross-links are not as cytotoxic as in dividing cells, it would be reasonable to imagine, that common pathology and lifespan results from a similar rate of damage accumulation and response. The most likely common origin for the above phenotypes is defective general TCR of the most abundant type of endogenous lesions –the class of transcription-blocking oxidative damage. An alternative explanation is that TCR of non-NER type lesions is intact in e.g. XPF and ERCC1 mice and the overlapping phenotype of those mice with other mice in group C results from defective repair of inter-strand cross-links. Nevertheless, it is difficult to envision, that inter-strand crosslinks, which are likely orders of magnitude less abundant than e.g. oxidative lesions, affect the same cell types (e.g. Purkinje neurons) with a same rate of functional decline resulting in overlap in lifespan and overall phenotype. A further argument against the latter interpretation is derived from the studies of H. de Waard et al, who recently found that NER mutated (XPA, CSA, CSB) fibroblasts, keratinocytes and embryonic stem cells display different sensitivity patterns to oxidative, versus inter-strand cross-linking agents (de Waard et al. 2003)(H. de Waard et al., unpublished).

Is there a common involvement of basal or activated transcription defect in CS and TTD? The overlapping phenotypes of mice carrying genotypes of mutated NER proteins with no proven involvement in transcription (e.g. XPG, ERCC1, XPF, CSA/XPA, and CSA/XPC) and mice which carry defects in NER genes which are implicated in transcription initiation, (XPD-TTD/XPA, XPD-XPCS/XPA) or elongation (CSB/XPA, CSB/XPC) argues that primary transcriptional involvement in CS and TTD is absent or minimal. Transcriptional impairment is likely secondary to the TCR defect and the common phenotype in group C likely emerges from signals

resulting from elongation phase lesion-stalled and/or improperly processed RNA-PolII-complexes. The recent discovery of XPCS- and COFS-like patients with mutations in the XPF and in ERCC1 genes respectively (N. Jaspers per. comm.) extends the above conclusion beyond the murine species boundary. If the above reasoning holds true, then why is TTD exclusively associated with mutations in TFIIH? The TTD hallmark features -brittle hair and nails- most likely result from a cell-type specific primary transcriptional defect as a consequence of a TTD-specific reduction in TFIIH levels. The above hypothesis is supported by the following notions: (i) TTD type mutations in XPD, XPB and p8 lead to a severe reduction of TFIIH levels (Vermeulen et al. 2000; Botta et al. 2002; Giglia-Mari et al. 2004) (ii) a TTD patient carrying a temperature sensitive mutation displays enhanced brittleness of hair during the episodes of fever; cells isolated from this patient show a strong reduction of TFIIH upon temperature shift (Vermeulen et al. 2001) (iii) co-expression of the XPD-XPCS allele at low, or normal levels in XPD-TTD mice results in partial and full rescue respectively (J.O.A. submitted). The most likely explanation is, that in enucleating cells, like terminally differentiating keratinocytes, de novo synthesis cannot compensate for the reduced TFIIH levels and skin and hair are delivered in an unfinished state.

Group D

Mouse models in group D display progressive neurological manifestations such as ataxia, kyphosis and cachexia leading to death around 4-6 months of age (J.O.A. work in progress, A. Lalai et al., unpublished). This category of mutants encompasses XPA-deficient *Xpd* compound heterozygote mice which carry a TTD (XPD-R722W) mutation in one *Xpd* allele and a XPCS (XPD-G602D) mutation in the other. Notably both alleles, when homozygous in an XPA-deficient background, result in death within first 3 weeks of life (and thus fall into group C). The remarkably extended lifespan of TTD|XPCS/XPA mice is explained by interallelic complementation (IAC) between two defective *Xpd* alleles. What is the role for the core NER complex in IAC? XPA is required for the core NER complex formation (Volker et al. 2001). The fact that in the absence of XPA IAC between two defective *Xpd* alleles can significantly prolong the life-span is in concordance with the idea that the general TCR pathway does not require the absolute presence XPA. Since the rescue by IAC is nearly complete in the presence of XPA (this thesis and data not shown) the progressive disease in TTD|XPCS/XPA may be due to endogenously rising NER-type lesions, such as cyclopurines in which case IAC between XPD-TTD and XPD-XPCS alleles can be only partial. In support of this interpretation, neither TTD|†XPCS or TTD|†XP6BE compound heterozygote cells were complemented to the wt level in the UV survival and UDS experiments (J.O.A. submitted). Why do NER lesions not cause a profound disease in XPA mice? A possible explanation is, that in XPA mice, where CS proteins are still intact, the blocked RNA-PolII is removed from the dama-

ge, resulting in different or "milder" downstream signals. The notion that, the life-span of XPA mice is shorter than wt (H. van Steeg per. comm.) indicates the relevance of NER lesions in ageing also in the absence a general TCR defect. Thus, the impact of NER on life-span is likely determined by two parallel processes (i) the mode of repair applied: e.g. stalled versus released RNA-PolII from the site of damage (ii) the balance between damage and repair.

ERCC1|ERCC1Δ7 mice carry one ERCC1 knockout allele and a modification in the other resulting in a 7 amino acid deletion of the C terminus of the ERCC1 protein (L. Niedernhofer et al., unpublished). In addition to features listed in Table 1 ERCC1|ERCC1Δ7 mice display polyploidy in the liver, hinting to inability to repair inter-strand cross-links in mitotic cells. Detailed physiological and pathological studies of group D mice are currently underway.

Group E

Mouse models in group E display >12 months life-span and pathological features ranging from moderate to mild. Mice in this group display mild developmental delay, which sometimes (XPB-XPCS/XPA) can be associated with ~20% enhanced mortality around weaning. Mild juvenile neuropathy is also noted, which mostly disappears after sexual maturation. The tail suspension test reveals aberrant and spastic back-limb coordination in XPD-TTD, XPD-XPCS and XPB-XPCS/XPA mice (J. O. A. et al., unpublished). Placid gait impairment was also noted in CSB mice (I. van der Pluijm et al., unpublished). Symptoms evident later in life include mildly progressive cachexia, which is the most pronounced in XPD-TTD mice, where it is associated with kyphosis and early bone demineralization. In this phenotypic group, effects of genetic background and environment on the disease etiology are the most evident. For example, in the mixed 129Ola/C57bl6 genetic background the lifespan of TTD mice is considerably shorter, compared to a pure C57bl6 genetic background, in which case TTD mice live only few months less than littermate controls (H. van Steeg per. comm.). Effects of diet and housing conditions are probably important as e.g. TTD mice, which lack proper fur and fat tissue, are likely to be more susceptible to temperature shifts and quality of food. The rate of CS-specific retinal degeneration in CSA and CSB mice has also been found to be genetic background dependent (T. Gorgels., et al unpublished). Last but not the least- in despite of isogenic C57bl6 genetic background, XPB-XPCS/XPA mice displayed a remarkably variable phenotype ranging from death around weaning to nearly normal development. Thus, in case of relatively mild disease progression, environment and genetic background can have profound effects on the disease etiology. Effects of genetic background can be also strong in other groups. For example, XPA/CSB and ERCC1 mice in group C live even shorter in a pure C57bl6 background (I. van der Pluijm et al., unpublished, L. Niedernhofer per. comm.).

The phenotype of XPB-XPCS/XPA double mutant mice can be considered as very informative also from the mechanistic point of view. The XPB-XPCS mutation in mice does not trigger detectable CS features. Cell culture studies revealed sensitivity of XPB-XPCS cells to UV and gamma irradiation, pointing both to NER, and general TCR defects. When mice were further challenged with concomitant XPA inactivation, CS symptoms similar to what observed in XPD-XPCS (such as progressive tubular atrophy in the testis, mild neuropathy, cachexia and kyphosis) were noted. This result suggests, that the general TCR deficiency in XPB-XPCS mice is present, but in a milder form compared to that of XPD-XPCS, XPD-TTD, CSA or CSB mice as XPA inactivation in the latter leads to death within 3 weeks, similar to XPG, XPF and ERCC1 single KO mutants in group C. These data indicate that (i) the CS defect, independent of the causative gene(s), results in a similar pathology in mice (ii) the severity of CS is determined by the balance between DNA damage and repair.

Group F

The phenotype of the mice in group F is the mildest, yet very informative. XPA mice, which are defective in both GG-NER and TC-NER but presumably intact in the general TCR trail display a slightly reduced lifespan, without clear pathological manifestations (H. van Steeg et al., unpublished) revealing the impact of endogenously generated NER-type of lesions in mammalian lifespan.

XPB-XPCS carry a "latent" general TCR defect, which on its own is too mild to result in CS in mice. As the CS phenotype in mice in general is milder than in man, this notion is perhaps not surprising - compared to other CS patients, all XPB-XPCS patients displayed relatively mild CS features and lived until the 3rd-4th decade of life (average lifespan of CS patients is ~12 years) (Rapin et al. 2000).

A summary of symptoms displayed by each phenotypic group is reviewed in Table 2 below. Please note that the number in parenthesis indicates cases which require further explanation.

__Table 2__ A summary of organismal and cellular features of NER mutant mice.

Phenotypic group:	B	C	D	E	F
Genotype:		XPD-TTD/XPA	TTD|XPCS/XPA	XPD-XPCS	XPA
		XPD-XPCS/XPA	ERCC1|ERCC1Δ7	XPD-TTD	XPC
	XPD-TTD/XPB-XPCS	CSB/XPA CSB/XPC		XPB-XPCS/XPA	XPB-XPCS
		CSA/XPA CSA/XPC		CSA	
		XPF		CSB	
		ERCC1			
		XPG			
Symptoms					
Cellular UV sensitivity	++	+++[1]	?	+++[6]	++[14]
Cellular ROS sensitivity	++	++[2]	?	++[7]	+[15]
Cellular MMCsensitivity	-	+++[3]	?	++[8]	-
Cancer susceptibility	n.a.	n.a.	?	++++[9]	+++[16]
Developmental delay	+	+++	++	+	-
Juvenile neuropathy	n.a.	+++	++	+	-
Cachexia	n.a.	+++	++	+	-
Retinal degeneration	n.a.	n.a.	?	++[10]	-
Tremours	n.a.	++	+	+[11]	-
Spasticity	n.a.	++	+	-	-
Ataxia	n.a.	++	+	-	-
Purkinje cell loss	?	++[4]	?	-	-
Kyphosis	n.a.	+	++	+[12]	-
Bone demineralization	n.a.	?	+[5]	+[13]	-
Testicular atrophy	n.a.	n.a.	?	+[14]	-
Lifespan	1-2 days	1-3 weeks	4-6 months	>12 months	reduced[17]
Brittle hair	n.a.	-	-	++[13]	-
Hyperkeratosis	-	-	?	++[13]	-

n.a. not applicable

Comments:

Group C:

(1) Cellular UV sensitivity: CSB/XPC=CSA/XPC>CSB/XPA=CSA/XPA (I. van der Pluijm et al. unpublished).
XPG, XPF and ERCC1 cells are likely to be less sensitive than the other genotypes (Weeda et al.
1997; Harada et al. 1999; Tian et al. 2004a). Not measured for XPD-XPCS/XPA.

(2) Cellular ROS sensitivity: XPD-TTD/XPA cells are sensitive to gamma rays and paraquat.
Other genotypes in this group not tested or do not display this feature (de Boer et al. 2002)
(this thesis).

(3) Cellular MMC sensitivity: ERCC1 and XPF cells are sensitive to MMC. Other genotypes not tested or do
not display this feature (Weeda et al. 1997; Tian et al. 2004b).

(4) Loss of Purkinje cells: XPD-XPCS/XPA, ERCC1, XPG and CSB/XPA mice display Purkinje cell loss
(Murai et al. 2001; Sun et al. 2001)(L. Niedernofer et al., unpublished, J.O.A. manuscript in
prep.).Other genotypes in this group not tested, but based on the phenotype are likely to display this
feature.

Group D

(5) Bone demineralization: preliminary observation in TTD/XPCS/XPA mice (J.O.A. ongoing work).

Group E

(6) Cellular UV sensitivity: XPB-XPCS/XPA>XPD-XPCS>CSB=CSA>XPD-TTD>wt (van der Horst et al.
1997; de Boer et al. 1998a)(this thesis)

(7) Cellular ROS sensitivity: CSB and XPB-XPCS/XPA cells are sensitive to paraquat (XPD-XPCS not tested);
CSB and XPCS cells are sensitive to gamma rays (XPB-XPCS/XPA cells are not); CSA and XPD-
TTD are not sensitive to either paraquat or gamma rays (de Waard et al. 2003, de Boer et al. 2002)
(this thesis).

(8) Cellular MMC sensitivity: CSA cells are MMC sensitive; CSB, XPB-XPCS/XPA and XPD-TTD cells are
not (H. de Waard et al., unpublished)(this thesis).

(9) cancer susceptibility: XPD-XPCS>CSA=CSB>>XPD-TTD. XPB-XPCS/XPA mice not tested (van der
Horst et al. 1997; de Boer et al. 1999; van der Horst et al. 2002)(J.O.A. manuscript in prep.)..

(10) Retinal degeneration: present in CSA and CSB mice, absent in XPD-TTD and XPB-XPCS/XPA mice,
XPD-XPCS not tested (T. Gorgels et al. unpublished; J. O. A., unpublished).

(11) Tremors: evident in XPD-TTD mice; noted in some ~1.5 year old XPD-XPCS mice; absent in CSA and
CSB mice (de Boer et al. 2002).

(12) Kyphosis: onset ~3 months in XPD-TTD mice; noted in few 1 year old XPD-XPCS mice, absent in CSA
and CSB mice (van der Horst et al. 1997; de Boer et al. 1998a; van der Horst et al. 2002)
(this thesis).

(13) Bone demineralization, brittle hair and kyphosis are specific for XPD-TTD (de Boer et al. 2002).

Group F

(14) Cellular UV sensitivity: XPA>>XPC=XPB-XPCS (de Vries et al. 1995; de Waard et al. 2003)(J.O.A.
manuscript in prep.).

(15) Cellular ROS sensitivity: XPB-XPCS cells are sensitive to gamma rays, not sensitive to paraquat. XPA
and XPC cells are not sensitive to either gamma rays or paraquat (de Boer et al. 2002;
de Waard et al. 2003).

(16) Cancer susceptibility: XPA>XPC; XPB-XPCS not tested (de Vries et al. 1995; Berg et al. 1998).

(17) XPA mice live few months shorter than wt (H. van Steeg et al., unpublished) , others genotypes not tested.

Note: Cellular UV sensitivity studies have been performed with primary MEF cells, ROS and MMC sensi-
tivity studies with transformed MEF cells.

From the symptoms listed in Table 2, two main trends can be deduced: (i) like in human disease, the severity of the condition correlates with the severity of the neurological manifestations (ii) no cellular assay has been defined sofar that correlates with the genotype and phenotype. Another very interesting notion is, that cancer predisposition does not seem to interfere with the premature ageing phenotype. Despite UV sensitivity and defective repair of UV lesions, no increased cancer incidence has been noted for CS and TTD patients. But does cancer predisposition affect the rate of accelerated ageing? From 9 human XPCS patient phenotypes described sofar, conclusions were hard to draw, as both the CS and XP phenotypes appeared variable, ranging from no-, to early malignancies (Rapin et al. 2000). Furthermore, human patients differ in genetic background and carry dissimilar mutations in different XPCS causative genes. Comparison of cancer predisposition of genetically uniform XPD-TTD and XPD-XPCS mice reveals a profound difference, yet, when crossed to XPA, both double mutants display an equally harsh phenotype and die within the first 3 weeks of life. This result indicates, that at least in this model system, cancer predisposition is not influencing the rate of segmental accelerated ageing.

What is the molecular mechanism of NER-associated neurodevelopmental disease? We propose the following model: damage blocked RNA-PolII initiates CSB/CSA mediated assembly of a complex involving proteins implicated in CS, TTD and COFS. The severity of the disease may depend on the effect the given mutation delivers on the spatio-temporal action of this complex, thereby resulting in cellular signals with dissimilar phenotypic outcome. For example, while mostly frame shift and truncation type of alterations in the *CSB* gene result in classical CS, recently a severe CSB-COFS patient was characterized, carrying only a point-mutation in the C-terminus of the *CSB* gene. The most severe CSB truncation on the other hand, is associated only with the mild UV sensitivity syndrome (K. Tanaka unpublished). Another example of such an effect may include XPD-R683W patients, where the more severe truncation in the second *XPD* allele was found to be associated with the absence of neurodegenerative processes (Ueda et al. 2004). These findings argue, that sometimes it might be better not to have a protein, than having one with a "bad" mutation, a phenomenon which may be called "mutation associated toxicity" or MAT. A combination of MAT like, and interallelic effects may well explain the enormous clinical potential associated with the *XPD* locus, e.g. why the allelic combination of XPD-D681N|XPD-R616W results in COFS (Graham et al. 2001), while XPD-R685G|XPD-R616W results in TTD. Cellular signals emerging from 3D structure and timing of stalled TCR complex likely determine the severity of the phenotype. Common cerebellar ataxia as a function of Purkinje cell loss and bizarre astrocyte structures in CS (general TCR defect) and AT (DNA damage down-stream signaling defect) provides a further support to this notion (Rapin et al. 2000; Lindenbaum et al. 2001; Brooks 2002). A model for the molecular mechanism of TCR associated neurodevelopmental disease is depicted on Figure 3.
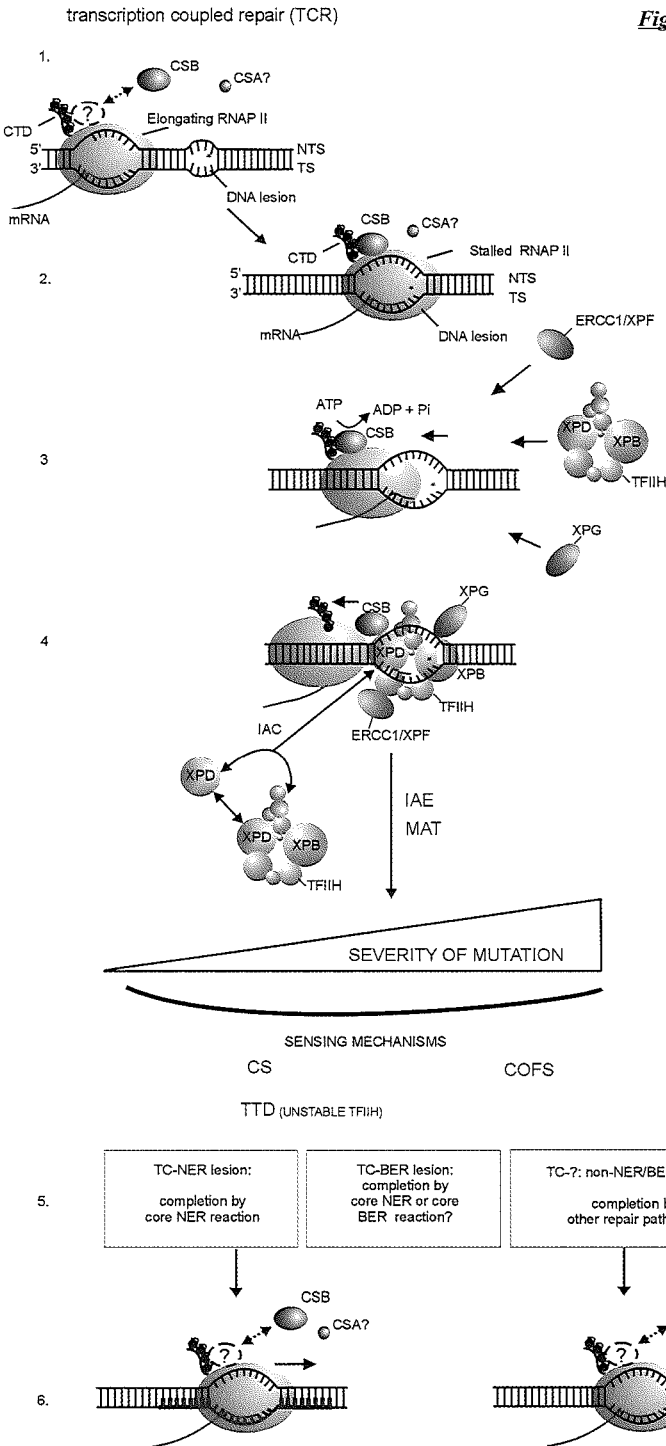
Figure 3. *Model for the molecular mechanism of general TCR-associated disease.*

1-2. Lesion stalled RNA-PolII initiates recruitment of the TCR machinery, which may involve the chromatin remodeling function of CSB (Citterio et al. 2000a). 3. TFIIH, ERCC1/XPF and XPG likely facilitate the back-tracking or release of RNA-PolII from the site of the lesion (Citterio et al. 2000b; van den Boom et al. 2002). 4. Normal polymorphisms or mutations in TCR proteins can result in interallelic effects (IAE) like IAC or mutation-associated toxicity (MAT). IAC associated with XPD may occur via exchange of XPD molecules between the free XPD-CAK complex and free/or TCR-engaged TFIIH. The hampered TCR is sensed according to the effect the given alteration delivers on the spatio-temporal axis of the TCR complex.
5-6. In the wt situation, the reaction proceeds to either the core NER reaction or handover of the damaged site to the lesion-specific repair pathway.

Experiments presented in chapter 3 demonstrate the potential of compound heterozygous *XPD* alleles to reach biological endpoints unpredictable from the genotype. These results indicate that the possible effects of the second allele should always be taken in account while considering genotype-phenotype relationship of recessive genes. Not only can phenotypic effects of proteins originating from two recessive alleles range from detrimental to complementing, similar effects can be envisaged between proteins resulting from different genes, but delivering their function in the common protein complex, a mechanism which may well explain the phenomenon of "mutation associated toxicity" or MAT. In a larger biological scale one can envisage such allelic mechanisms, based on genetic diversity resulting from meiotic recombination and SNP-s, to not only underlie a subset of normal differences between individuals but also determine the rate of ageing and lifespan.

References

Adimoolam, S. and J.M. Ford. 2003. p53 and regulation of DNA damage recognition during nucleotide excision repair. DNA Repair (Amst) 2: 947-54.

Akoulitchev, S. and D. Reinberg. 1998. The molecular mechanism of mitotic inhibition of TFIIH is mediated by phosphorylation of CDK7. Genes Dev 12: 3541-50.

Araujo, S.J., E.A. Nigg, and R.D. Wood. 2001. Strong functional interactions of TFIIH with XPC and XPG in human DNA nucleotide excision repair, without a preassembled repairosome. Mol Cell Biol 21: 2281-91.

Ariza, R.R., S.M. Keyse, J.G. Moggs, and R.D. Wood. 1996. Reversible protein phosphorylation modulates nucleotide excision repair of damaged DNA by human cell extracts. Nucleic Acids Res 24: 433-40.

Auffray, C. and F. Rougeon. 1980. Purification of mouse immunoglobulin heavy-chain messenger RNAs from total myeloma tumor RNA. Eur J Biochem 107: 303-14.

Azcoitia, I., L.L. DonCarlos, and L.M. Garcia-Segura. 2003. Are gonadal steroid hormones involved in disorders of brain aging? Aging Cell 2: 31-7.

Barja, G. and A. Herrero. 2000. Oxidative damage to mitochondrial DNA is inversely related to maximum life span in the heart and brain of mammals. Faseb J 14: 312-8.

Bartzokis, G. 2004. Age-related myelin breakdown: a developmental model of cognitive decline and Alzheimer's disease. Neurobiol Aging 25: 5-18; author reply 49-62.

Bastien, J., S. Adam-Stitah, T. Riedl, J.M. Egly, P. Chambon, and C. Rochette-Egly. 2000. TFIIH interacts with the retinoic acid receptor gamma and phosphorylates its AF-1-activating domain through cdk7. J Biol Chem 275: 21896-904.

Beckman, K.B. and B.N. Ames. 1997. Oxidative decay of DNA. J Biol Chem 272: 19633-6.

Berg, R.J., H.J. Ruven, A.T. Sands, F.R. de Gruijl, and L.H. Mullenders. 1998. Defective global genome repair in XPC mice is associated with skin cancer susceptibility but not with sensitivity to UVB induced erythema and edema. J Invest Dermatol 110: 405-9.

Bergmann, E. and J.M. Egly. 2001. Trichothiodystrophy, a transcription syndrome. Trends Genet 17: 279-86.

Berneburg, M., J.E. Lowe, T. Nardo, S. Araujo, M.I. Fousteri, M.H. Green, J. Krutmann, R.D. Wood, M. Stefanini, and A.R. Lehmann. 2000. UV damage causes uncontrolled DNA breakage in cells from patients with combined features of XP-D and Cockayne syndrome. Embo J 19: 1157-66.

Betarbet, R., T.B. Sherer, and J.T. Greenamyre. 2002. Animal models of Parkinson's disease. Bioessays 24: 308-18.

Bootsma, D. and J.H.J. Hoeijmakers. 1993. Engagement with transcription. Nature 363: 114-115.

Bootsma, D., K.H. Kraemer, J.E. Cleaver, and J.H. Hoeijmakers. 2002. Nucleotide Excision Repair Syndromes:Xeroderma Pigmentosum, Cockayne Syndrome, and Trichothiodystrophy. In The Genetic Basis of Human Cancer (ed. B. Vogelstein and K.W. Kinzler), pp. 211-237. McGraw-Hill Medical Publishing Devision.

Botta, E., T. Nardo, B.C. Broughton, S. Marinoni, A.R. Lehmann, and M. Stefanini. 1998. Analysis of mutations in the XPD gene in Italian patients with trichothiodystrophy: site of mutation correlates with repair deficiency, but gene dosage appears to determine clinical severity. Am J Hum Genet 63: 1036-1048.

Botta, E., T. Nardo, A.R. Lehmann, J.M. Egly, A.M. Pedrini, and M. Stefanini. 2002. Reduced level of the repair/transcription factor TFIIH in trichothiodystrophy. Hum Mol Genet 11: 2919-28.

Bradsher, J., J. Auriol, L. Proietti de Santis, S. Iben, J.L. Vonesch, I. Grummt, and J.M. Egly. 2002. CSB is a component of RNA pol I transcription. Mol Cell 10: 819-29.

Bremer, H.J., M. Duran, J. Kamerling, H. Przyrembel, and S.K. Wadman. 1981. Malnutrition in childeren. In Distrurbances of amino acid metabolism: clinical chemistry and diagnosis (ed. Urban and Schwarzenegger), pp. 405, Baltimore, Munich.

Brooks, P.J. 2002. DNA repair in neural cells: basic science and clinical implications. Mutat Res 509: 93-108.

Brooks, P.J., D.S. Wise, D.A. Berry, J.V. Kosmoski, M.J. Smerdon, R.L. Somers, H. Mackie, A.Y. Spoonde, E.J. Ackerman, K. Coleman, R.E. Tarone, and J.H. Robbins. 2000. The oxidative DNA lesion 8,5'-(S)-cyclo-2'-deoxyadenosine is repaired by the nucleotide excision repair pathway and blocks gene expression in mammalian cells. J Biol Chem 275: 22355-62.

Broughton, B.C., M. Berneburg, H. Fawcett, E.M. Taylor, C.F. Arlett, T. Nardo, M. Stefanini, E. Menefee, V.H. Price, S. Queille, A. Sarasin, E. Bohnert, J. Krutmann, R. Davidson, K.H. Kraemer, and

A.R. Lehmann. 2001. Two individuals with features of both xeroderma pigmentosum and trichothiodystrophy highlight the complexity of the clinical outcomes of mutations in the XPD gene. Hum Mol Genet 10: 2539-47.

Broughton, B.C., A.F. Thompson, S.A. Harcourt, W. Vermeulen, J.H.J. Hoeijmakers, E. Botta, M. Stefanini, M.D. King, C.A. Weber, J. Cole, C.F. Arlett, and A.R. Lehmann. 1995. Molecular and cellular analysis of the DNA repair defect in a patient in xeroderma pigmentosum complementation group D who has the clinical features of xeroderma pigmentosum and Cockayne syndrome. Am. J. Hum. Genet. 56: 167-174.

Brownlee, M. 2001. Biochemistry and molecular cell biology of diabetic complications. Nature 414: 813-20.

Butterfield, D.A., J. Drake, C. Pocernich, and A. Castegna. 2001. Evidence of oxidative damage in Alzheimer's disease brain: central role for amyloid beta-peptide. Trends Mol Med 7: 548-54.

Campisi, J. 2000. Cancer, aging and cellular senescence. In Vivo 14: 183-8.

Chang, S., A.S. Multani, N.G. Cabrera, M.L. Naylor, P. Laud, D. Lombard, S. Pathak, L. Guarente, and R.A. DePinho. 2004. Essential role of limiting telomeres in the pathogenesis of Werner syndrome. Nat Genet 36: 877-82.

Chen, J., S. Larochelle, X. Li, and B. Suter. 2003. Xpd/Ercc2 regulates CAK activity and mitotic progression. Nature 424: 228-32.

Chmiel, J.F., M.L. Drumm, M.W. Konstan, T.W. Ferkol, and C.M. Kercsmar. 1999. Pitfall in the use of genotype analysis as the sole diagnostic criterion for cystic fibrosis. Pediatrics 103: 823-6.

Citterio, E., V. Van Den Boom, G. Schnitzler, R. Kanaar, E. Bonte, R.E. Kingston, J.H. Hoeijmakers, and W. Vermeulen. 2000a. ATP-dependent chromatin remodeling by the Cockayne syndrome B DNA repair-transcription-coupling factor. Mol Cell Biol 20: 7643-53.

Citterio, E., W. Vermeulen, and J.H. Hoeijmakers. 2000b. Transcriptional healing. Cell 101: 447-50.

Cleaver, J.E., L.H. Thompson, A.S. Richardson, and J.C. States. 1999. A summary of mutations in the UV-sensitive disorders: xeroderma pigmentosum, Cockayne syndrome, and trichothiodystrophy. Hum Mutat 14: 9-22.

Coin, F., E. Bergmann, A. Tremeau-Bravard, and J.M. Egly. 1999. Mutations in XPB and XPD helicases found in xeroderma pigmentosum patients impair the transcription function of TFIIH. Embo J 18: 1357-66.

Conforti, G., T. Nardo, M. D'Incalci, and M. Stefanini. 2000. Proneness to UV-induced apoptosis in human fibroblasts defective in transcription coupled repair is associated with the lack of Mdm2 transactivation. Oncogene 19: 2714-20.

Cooper, P.K., T. Nouspikel, S.G. Clarkson, and S.A. Leadon. 1997. *Defective transcription-coupled repair of oxidative base damage in Cockayne syndrome patients from XP group G. Science 275: 990-993.*

Cruz-Sanchez, F.F., A. Cardozo, C. Castejon, E. Tolosa, and M.L. Rossi. 1997. *Aging and the nigro-striatal pathway. J Neural Transm Suppl 51: 9-25.*

Dahmus, M.E. 1995. *Phosphorylation of C-terminal domain of RNA polymerase II. Biochemica et Biophysica Acta 1261: 71-82.*

Day, B.J. and J.D. Crapo. 1996. *A metalloporphyrin superoxide dismutase mimetic protects against paraquat-induced lung injury in vivo. Toxicol Appl Pharmacol 140: 94-100.*

de Boer, J., J.O. Andressoo, J. de Wit, J. Huijmans, R.B. Beems, H. van Steeg, G. Weeda, G.T. van der Horst, W. van Leeuwen, A.P. Themmen, M. Meradji, and J.H. Hoeijmakers. 2002. *Premature aging in mice deficient in DNA repair and transcription. Science 296: 1276-9.*

de Boer, J., J. de Wit, H. van Steeg, R.J.W. Berg, M. Morreau, P. Visser, A.R. Lehmann, M. Duran, J.H.J. Hoeijmakers, and G. Weeda. 1998a. *A mouse model for the basal transcription/DNA repair syndrome trichothiodystrophy. Mol. Cell 1: 981-990.*

de Boer, J., I. Donker, J. de Wit, J.H.J. Hoeijmakers, and G. Weeda. 1998b. *Disruption of the mouse xeroderma pigmentosum group D DNA repair/basal transcription gene results in preimplantation lethality. Cancer Res. 58: 89-94.*

de Boer, J. and J.H.J. Hoeijmakers. 1999. *Cancer form the outside, aging from the inside: Mouse models to study the consequences of defective nucleotide excision repair. Biochimie 81: 127-137.*

de Boer, J., H. van Steeg, R.J.W. Berg, J. Garssen, J. de Wit, C.T.M. van Oostrom, R.B. Beems, G.T.J. van der Horst, C.F. van Kreijl, F.R. de Gruijl, D. Bootsma, J.H.J. Hoeijmakers, and G. Weeda. 1999. *Mouse model for the DNA repair/basal transcription disorder trichothiodystrophy reveals cancer predisposition. Cancer Res. 59: 3489-3494.*

de Laat, W.L., N.G.J. Jaspers, and J.H.J. Hoeijmakers. 1999. *Molecular mechanism of nucleotide excision repair. Genes Dev. 13: 768-785.*

de Vries, A., C.T.M. van Oostrom, F.M.A. Hofhuis, P.M. Dortant, R.J.W. Berg, F.R. de Gruijl, P.W. Wester, C.F. van Kreijl, P.J.A. Capel, H. van Steeg, and S.J. Verbeek. 1995. *Increased susceptibility to ultraviolet-B and carcinogens of mice lacking the DNA excision repair gene XPA. Nature 377: 169-173.*

de Waard, H., J. de Wit, J.O. Andressoo, D.T.M. van Oostrom, B. Riis, A. Weimann, H.E. Poulsen, H. van Steeg, J.H.J. Hoeijmakers, and G.T.J. van der Horst. 2004. *Different effect of CSA and CSB deficiency on sesnsitivityto oxidative DNA damage. Molecular and Cellular Biology, September 2004, Vol 24, Issue 18, in press.*

de Waard, H., J. de Wit, T.G. Gorgels, G. van den Aardweg, J.O. Andressoo, M. Vermeij, H. van Steeg, J.H. Hoeijmakers, and G.T. van der Horst. 2003. *Cell type-specific hypersensitivity to oxidative damage in CSB and XPA mice. DNA Repair (Amst) 2: 13-25.*

de Wind, N., M. Dekker, A. Berns, M. Radman, and H. te Riele. 1995. *Inactivation of the mouse Msh2 gene results in mismatch repair deficiency, methylation tolerance, hyperrecombination, and predisposition to cancer. Cell 82: 321-30.*

Del Bigio, M.R., C.R. Greenberg, L.B. Rorke, R. Schnur, D.M. McDonald-McGinn, and E.H. Zackai. 1997. *Neuropathological findings in eight children with cerebro-oculo-facio-skeletal (COFS) syndrome. J Neuropathol Exp Neurol 56: 1147-57.*

Dolle, M.E., H. Giese, C.L. Hopkins, H.J. Martus, J.M. Hausdorff, and J. Vijg. 1997. *Rapid accumulation of genome rearrangements in liver but not in brain of old mice. Nat Genet 17: 431-434.*

Dubaele, S., L.P. De Santis, R.J. Bienstock, A. Keriel, M. Stefanini, B. Van Houten, and J.M. Egly. 2003. *Basal transcription defect discriminates between xeroderma pigmentosum and trichothiodystrophy in*

XPD patients. Mol Cell 11: 1635-46.

Duker, N.J. 2002. Chromosome breakage syndromes and cancer. Am J Med Genet 115: 125-9.

Dupuy, J.M., D. Lafforet, and F. Rachman. 1974. Xeroderma pigmentosum with liver involvement. Helv Paediatr Acta 29: 213-9.

Egly, J.M. 2001. The 14th Datta Lecture. TFIIH: from transcription to clinic. FEBS Lett 498: 124-8.

Ellis, N.A., J. Groden, T.Z. Ye, J. Straughen, D.J. Lennon, S. Ciocci, M. Proytcheva, and J. German. 1995. The Bloom's syndrome gene product is homologous to RecQ helicases. Cell 83: 655-66.

Evans, E., J.G. Moggs, J.R. Hwang, J.-M. Egly, and R.D. Wood. 1997. Mechanism of open complex and dual incision formation by human nucleotide excision repair factors. EMBO J. 16: 6559-6573.

Falck, J., J.H. Petrini, B.R. Williams, J. Lukas, and J. Bartek. 2002. The DNA damage-dependent intra-S phase checkpoint is regulated by parallel pathways. Nat Genet 30: 290-4.

Feig, D.I., T.M. Reid, and L.A. Loeb. 1994. Reactive oxygen species in tumorigenesis. Cancer Res 54: 1890s-1894s.

Finch, C.E. and E.L. Schneider. 1985. Handbook of the biology of aging. Van Nostrand Reinhold Company, New York.

Finkel, T. and N.J. Holbrook. 2000. Oxidants, oxidative stress and the biology of ageing. Nature 408: 239-47.

Friedberg, E.C., J.P. Bond, D.K. Burns, D.L. Cheo, M.S. Greenblatt, L.B. Meira, D. Nahari, and A.M. Reis. 2000. Defective nucleotide excision repair in xpc mutant mice and its association with cancer predisposition. Mutat Res 459: 99-108.

Friedberg, E.C., G.C. Walker, and W. Siede. 1995. DNA repair and mutagenesis. ASM Press, Washington D.C.

Galimi, F., M. Noll, Y. Kanazawa, T. Lax, C. Chen, M. Grompe, and I.M. Verma. 2002. Gene therapy of Fanconi anemia: preclinical efficacy using lentiviral vectors. Blood 100: 2732-6.

Gao, Y., D.O. Ferguson, W. Xie, J.P. Manis, J. Sekiguchi, K.M. Frank, J. Chaudhuri, J. Horner, R.A. DePinho, and F.W. Alt. 2000. Interplay of p53 and DNA-repair protein XRCC4 in tumorigenesis, genomic stability and development. Nature 404: 897-900.

Giglia-Mari, G., F. Coin, J.A. Ranish, D. Hoogstraten, A. Theil, N. Wijgers, N.G. Jaspers, A. Raams, M. Argentini, P.J. Van Der Spek, E. Botta, M. Stefanini, J.M. Egly, R. Aebersold, J.H. Hoeijmakers, and W. Vermeulen. 2004. A new, tenth subunit of TFIIH is responsible for the DNA repair syndrome trichothiodystrophy group A. Nat Genet 36: 714-9.

Gosden, R.G., S.C. Laing, L.S. Felicio, J.F. Nelson, and C.E. Finch. 1983. Imminent oocyte exhaustion and reduced follicular recruitment mark the transition to acyclicity in aging C57BL/6J mice. Biol Reprod 28: 255-60.

Goyns, M.H. and W.L. Lavery. 2000. Telomerase and mammalian ageing: a critical appraisal. Mech Ageing Dev 114: 69-77.

Graham, J.M., Jr., K. Anyane-Yeboa, A. Raams, E. Appeldoorn, W.J. Kleijer, V.H. Garritsen, D. Busch, T.G. Edersheim, and N.G. Jaspers. 2001. Cerebro-oculo-facio-skeletal syndrome with a nucleotide exci-sion-repair defect and a mutated XPD gene, with prenatal diagnosis in a triplet pregnancy. Am J Hum Genet 69: 291-300.

Grube, K. and A. Burkle. 1992. Poly(ADP-ribose) polymerase activity in mononuclear leukocytes of 13 mammalian species correlates with species-specific life span. Proc Natl Acad Sci U S A 89: 11759-63.

Hanawalt, P.C. 2000. DNA repair. The bases for Cockayne syndrome [news]. Nature 405: 415-6.

Harada, Y.N., N. Shiomi, M. Koike, M. Ikawa, M. Okabe, S. Hirota, Y. Kitamura, M. Kitagawa,

T. Matsunaga, O. Nikaido, and T. Shiomi. 1999. Postnatal growth failure, short life span, and early onset of cellular senescence and subsequent immortalization in mice lacking the xeroderma pigmentosum group G gene. Mol Cell Biol 19: 2366-72.

Harman, D. 1956. Aging: a theory based on free radical and radiation chemistry. J Gerontol 11: 298-300.

Harper, J.W. and S.J. Elledge. 1998. The role of Cdk7 in CAK function, a retro-retrospective. Genes Dev 12: 285-9.

Hasty, P., J. Campisi, J. Hoeijmakers, H. van Steeg, and J. Vijg. 2003. Aging and genome maintenance: lessons from the mouse? Science 299: 1355-9.

Hayashi, M. 1999. [Apoptotic cell death in child-onset neurodegenerative disorders]. No To Hattatsu 31: 146-52.

Hekimi, S. and L. Guarente. 2003. Genetics and the specificity of the aging process. Science 299: 1351-4.

Herrero, A. and G. Barja. 1999. 8-oxo-deoxyguanosine levels in heart and brain mitochondrial and nuclear DNA of two mammals and three birds in relation to their different rates of aging. Aging (Milano) 11: 294-300.

Hoeijmakers, J.H. 2001. Genome maintenance mechanisms for preventing cancer. Nature 411: 366-74.

Holstege, F.C.P., P.C. Van der Vliet, and H.T.M. Timmers. 1996. Opening of an RNA polymerase II promoter occurs in two distinct steps and requires the basal transcription factors TFIIE and TFIIH. EMBO J. 15: 1666-1677.

Hoogstraten, D., A.L. Nigg, H. Heath, L.H. Mullenders, R. van Driel, J.H. Hoeijmakers, W. Vermeulen, and A.B. Houtsmuller. 2002. Rapid switching of TFIIH between RNA polymerase I and II transcription and DNA repair in vivo. Mol Cell 10: 1163-74.

Ibanez, C., S.A. Shields, M. El-Etr, E. Leonelli, V. Magnaghi, W.W. Li, F.J. Sim, E.E. Baulieu, R.C. Melcangi, M. Schumacher, and R.J. Franklin. 2003. Steroids and the reversal of age-associated changes in myelination and remyelination. Prog Neurobiol 71: 49-56.

Iben, S., H. Tschochner, M. Bier, D. Hoogstraten, P. Hozak, J.M. Egly, and I. Grummt. 2002. TFIIH plays an essential role in RNA polymerase I transcription. Cell 109: 297-306.

Itin, P.H. and M.R. Pittelkow. 1990. Trichothiodystrophy: review of sulfur-deficient brittle hair syndromes and association with the ectodermal dysplasias. J. Am. Acad. Dermatol. 22: 705-717.

Itin, P.H., A. Sarasin, and M.R. Pittelkow. 2001. Trichothiodystrophy: update on the sulfur-deficient brittle hair syndromes. J Am Acad Dermatol 44: 891-920; quiz 921-4.

Itoh, M., M. Hayashi, K. Shioda, M. Minagawa, F. Isa, K. Tamagawa, Y. Morimatsu, and M. Oda. 1999. Neurodegeneration in hereditary nucleotide repair disorders. Brain Dev 21: 326-33.

James, M., J. Mansbridge, and C. Kidson. 1982. Ultraviolet radiation sensitivity of proliferating and differentiated human neuroblastoma cells. Int J Radiat Biol Relat Stud Phys Chem Med 41: 547-56.

Jeggo, P.A. 1997. DNA-PK: at the cross-roads of biochemistry and genetics. Mutat Res 384: 1-14.

Johnson, F.B., D.A. Sinclair, and L. Guarente. 1999. Molecular biology of aging. Cell 96: 291-302.

Keriel, A., A. Stary, A. Sarasin, C. Rochette-Egly, and J.M. Egly. 2002. XPD mutations prevent TFIIH-dependent transactivation by nuclear receptors and phosphorylation of RARalpha. Cell 109:125-35.

Kirkwood, T.B. 1989. DNA, mutations and aging. Mutat Res 219: 1-7.

Kirkwood, T.B. and S.N. Austad. 2000. Why do we age? Nature 408: 233-8.

Kraemer, K.H., M.M. Lee, and J. Scotto. 1984. DNA repair protects against cutaneous and internal neoplasia: evidence from xeroderma pigmentosum. Carcinogenesis 5: 511-4.

Kraemer, K.H., Lee M.M., Scotto J. 1987. *Xeroderma pigmentosum. Cutaneous, ocular, and neurologic abnormalities in 830 published cases. Arch Dermatol 123: 241-50.*

Krivit, W., J.H. Sung, E.G. Shapiro, and L.A. Lockman. 1995. *Microglia: the effector cell for reconstitution of the central nervous system following bone marrow transplantation for lysosomal and peroxisomal storage diseases. Cell Transplant 4: 385-92.*

Krokan, H.E., R. Standal, and G. Slupphaug. 1997. *DNA glycosylases in the base excision repair of DNA. Biochem J 325 (Pt 1): 1-16.*

Kruman, II, T.S. Kumaravel, A. Lohani, W.A. Pedersen, R.G. Cutler, Y. Kruman, N. Haughey, J. Lee, M. Evans, and M.P. Mattson. 2002. *Folic acid deficiency and homocysteine impair DNA repair in hippocampal neurons and sensitize them to amyloid toxicity in experimental models of Alzheimer's disease. J Neurosci 22: 1752-62.*

Ku, H.H., U.T. Brunk, and R.S. Sohal. 1993. *Relationship between mitochondrial superoxide and hydrogen peroxide production and longevity of mammalian species. Free Radic Biol Med 15: 621-7.*

Kumar, P., S.P. Barton, and R. Marks. 1988. *Tissue measurements in senile sebaceous gland hyperplasia. Br J Dermatol 118: 397-402.*

Kuraoka, I., C. Bender, A. Romieu, J. Cadet, R.D. Wood, and T. Lindahl. 2000. *Removal of oxygen free-radical-induced 5',8-purine cyclodeoxynucleosides from DNA by the nucleotide excision-repair pathway in human cells. Proc Natl Acad Sci U S A 97: 3832-7.*

Lafforet, D. and J.M. Dupuy. 1978. *Photosensibilite et reparation de l'ADN. Possibilite d'une parente nostologique entre xeroderma pigmentosum et syndrome de Cockayne. Arch. franc. Pediat. (Supplt) 35: 65-74.*

Lambert, A.J. and B.J. Merry. 2004. *Effect of caloric restriction on mitochondrial reactive oxygen species production and bioenergetics: reversal by insulin. Am J Physiol Regul Integr Comp Physiol 286: R71-9.*

Larsen, P.L. 1993. *Aging and resistance to oxidative damage in Caenorhabditis elegans. Proc Natl Acad Sci U S A 90: 8905-9.*

Le Page, F., E.E. Kwoh, A. Avrutskaya, A. Gentil, S.A. Leadon, A. Sarasin, and P.K. Cooper. 2000. *Transcription-coupled repair of 8-oxoguanine: requirement for XPG, TFIIH, and CSB and implications for Cockayne syndrome. Cell 101: 159-71.*

Leadon, S.A. and P.K. Cooper. 1993. *Preferential repair of ionizing radiation-induced damage in the transcribed strand of an active human gene is defective in Cockayne syndrome. Proc Natl Acad Sci U S A 90: 10499-10503.*

Lehmann, A.R. 2001. *The xeroderma pigmentosum group D (XPD) gene: one gene, two functions, three diseases. Genes Dev 15: 15-23.*

Lehmann, A.R., C.F. Arlett, B.C. Broughton, S.A. Harcourt, H. Steingrimsdottir, M. Stefanini, A. Malcolm, R. Taylor, A.T. Natarajan, S. Green, M.D. King, R.M. MacKie, J.B.P. Stephenson, and J.L. Tolmie. 1988. *Trichothiodystrophy, a human DNA repair disorder with heterogeneity in the cellular response to ultraviolet light. Cancer Res 48: 6090-6096.*

Lindahl, T. and R.D. Wood. 1999. *Quality control by DNA repair. Science 286: 1897-905.*

Lindenbaum, Y., D. Dickson, P. Rosenbaum, K. Kraemer, I. Robbins, and I. Rapin. 2001. *Xeroderma pigmentosum/cockayne syndrome complex: first neuropathological study and review of eight other cases. Eur J Paediatr Neurol 5: 225-42.*

Lindsay, M.A. 2002. *Peptide-mediated cell delivery: application in protein target validation. Curr Opin Pharmacol 2: 587-94.*

Liu, J., S. Akoulitchev, A. Weber, H. Ge, S. Chuikov, D. Libutti, X.W. Wang, J.W. Conaway, C.C. Harris,

R.C. Conaway, D. Reinberg, and D. Levens. 2001. *Defective interplay of activators and repressors with TFIH in xeroderma pigmentosum. Cell 104: 353-63.*

Ljungman, M. and F. Zhang. 1996. *Blockage of RNA polymerase as a possible trigger for u.v. light-induced apoptosis. Oncogene 13: 823-31.*

Longo, V.D. and C.E. Finch. 2003. *Evolutionary medicine: from dwarf model systems to healthy centenarians? Science 299: 1342-6.*

Lusis, A.J. 2000. *Atherosclerosis. Nature 407: 233-41.*

Magana-Schwencke, N., J.A. Henriques, R. Chanet, and E. Moustacchi. 1982. *The fate of 8-methoxypsoralen photoinduced crosslinks in nuclear and mitochondrial yeast DNA: comparison of wild-type and repair-deficient strains. Proc Natl Acad Sci U S A 79: 1722-6.*

Mandel, S., E. Grunblatt, P. Riederer, M. Gerlach, Y. Levites, and M.B. Youdim. 2003. *Neuroprotective strategies in Parkinson's disease : an update on progress. CNS Drugs 17: 729-62.*

Martin, G.M., S.N. Austad, and T.E. Johnson. 1996. *Genetic analysis of ageing: role of oxidative damage and environmental stresses. Nat Genet 13: 25-34.*

Martin, G.M. and J. Oshima. 2000. *Lessons from human progeroid syndromes. Nature 408: 263-6.*

McCuaig, C., D. Marcoux, J.E. Rasmussen, M.M. Werner, and N.E. Genter. 1993. *Trichothiodystrophy associated with photosensitivity, gonadal failure, and striking osteosclerosis. J. Am. Acad. Dermat. 28: 820-826.*

Mitchell, J.R., J.H. Hoeijmakers, and L.J. Niedernhofer. 2003. *Divide and conquer: nucleotide excision repair battles cancer and ageing. Curr Opin Cell Biol 15: 232-40.*

Modrich, P. 1997. *Strand-specific mismatch repair in mammalian cells. J Biol Chem 272: 24727-30.*

Modrich, P. and R. Lahue. 1996. *Mismatch repair in replication fidelity, genetic recombination, and cancer biology. Annu Rev Biochem 65: 101-33.*

Mone, M.J., M. Volker, O. Nikaido, L.H. Mullenders, A.A. van Zeeland, P.J. Verschure, E.M. Manders, and R. van Driel. 2001. *Local UV-induced DNA damage in cell nuclei results in local transcription inhibition. EMBO Rep 2: 1013-7.*

Moshell, A.N., M.B. Ganges, M.A. Lutzner, H.G. Coon, S.F. Barrett, J.-M. Dupuy, and J.H. Robbins. 1983. *A new patient with both xeroderma pigmentosum and Cockayne syndrome establishes the new xeroderma pigmentosum complementation group H. In Cellular responses to DNA damage (ed. E.C. Friedberg and B.A. Bridges), pp. 209-213. Liss, New York.*

Mounkes, L.C. and C.L. Stewart. 2004. *Aging and nuclear organization: lamins and progeria. Curr Opin Cell Biol 16: 322-7.*

Murai, M., Y. Enokido, N. Inamura, M. Yoshino, Y. Nakatsu, G.T. van der Horst, J.H. Hoeijmakers, K. Tanaka, and H. Hatanaka. 2001. *Early postnatal ataxia and abnormal cerebellar development in mice lacking Xeroderma pigmentosum Group A and Cockayne syndrome Group B DNA repair genes. Proc Natl Acad Sci U S A 98: 13379-84.*

Murakami, M., K. Eguchi-Kasai, and K. Sato. 1995. *Biological effects of active oxygen on an X-ray-sensitive mutant mouse cell line (SL3-147). Mutat Res 336: 215-21.*

Nakane, H., S. Takeuchi, S. Yuba, M. Saijo, Y. Nakatsu, T. Ishikawa, S. Hirota, Y. Kitamura, Y. Kato, Y. Tsunoda, H. Miyauchi, T. Horio, T. Tokunaga, T. Matsunaga, O. Nikaido, Y. Nishimune, Y. Okada, and K. Tanaka. 1995. *High incedence of ultraviolet-B- or chemical-carcinogen-induced skin tomours in mice lacking the xeroderma pigmentosum group A gene. Nature 377: 165-168.*

Nakura, J., L. Ye, A. Morishima, K. Kohara, and T. Miki. 2000. *Helicases and aging. Cell Mol Life Sci 57: 716-30.*

Nance, M.A. and S.A. Berry. 1992. *Cockayne syndrome: Review of 140 cases. Am. J. Med. Genet. 42: 68-84.*

Nehlin, J.O., G.L. Skovgaard, and V.A. Bohr. 2000. *The Werner syndrome. A model for the study of human aging. Ann N Y Acad Sci 908: 167-79.*

Nouspikel, T. and P.C. Hanawalt. 2000. *Terminally differentiated human neurons repair transcribed genes but display attenuated global DNA repair and modulation of repair gene expression. Mol Cell Biol 20: 1562-70.*

Ohya, Y. and D. Botstein. 1994. *Diverse essential functions revealed by complementing yeast calmodulin mutants. Science 263: 963-6.*

Orr, W.C. and R.S. Sohal. 1994. *Extension of life-span by overexpression of superoxide dismutase and catalase in Drosophila melanogaster. Science 263: 1128-30.*

Oshima, J. 2000. *Comparative aspects of the Werner syndrome gene. In Vivo 14: 165-72.*

Parkes, T.L., A.J. Elia, D. Dickinson, A.J. Hilliker, J.P. Phillips, and G.L. Boulianne. 1998. *Extension of Drosophila lifespan by overexpression of human SOD1 in motorneurons. Nat Genet 19: 171-4.*

Parrinello, S., E. Samper, A. Krtolica, J. Goldstein, S. Melov, and J. Campisi. 2003. *Oxygen sensitivity severely limits the replicative lifespan of murine fibroblasts. Nat Cell Biol 5: 741-7.*

Peters, C. and C.G. Steward. 2003. *Hematopoietic cell transplantation for inherited metabolic diseases: an overview of outcomes and practice guidelines. Bone Marrow Transplant 31: 229-39.*

Priller, J., D.A. Persons, F.F. Klett, G. Kempermann, G.W. Kreutzberg, and U. Dirnagl. 2001. *Neogenesis of cerebellar Purkinje neurons from gene-marked bone marrow cells in vivo. J Cell Biol 155: 733-8.*

Randerath, E., G.D. Zhou, and K. Randerath. 1997a. *Organ-specific oxidative DNA damage associated with normal birth in rats. Carcinogenesis 18: 859-66.*

Randerath, K., G.D. Zhou, S.A. Monk, and E. Randerath. 1997b. *Enhanced levels in neonatal rat liver of 7,8-dihydro-8-oxo-2'-deoxyguanosine (8-hydroxydeoxyguanosine), a major mutagenic oxidative DNA lesion. Carcinogenesis 18: 1419-21.*

Randerath, K., G.D. Zhou, R.L. Somers, J.H. Robbins, and P.J. Brooks. 2001. *A 32P-postlabeling assay for the oxidative DNA lesion 8,5'-cyclo-2'-deoxyadenosine in mammalian tissues: evidence that four type II I-compounds are dinucleotides containing the lesion in the 3' nucleotide. J Biol Chem 276: 36051-7.*

Rapin, I., Y. Lindenbaum, D.W. Dickson, K.H. Kraemer, and J.H. Robbins. 2000. *Cockayne syndrome and xeroderma pigmentosum. Neurology 55: 1442-9.*

Rotman, G. and Y. Shiloh. 1998. *ATM: from gene to function. Hum Mol Genet 7: 1555-63.*

Rudolph, K.L., S. Chang, H.W. Lee, M. Blasco, G.J. Gottlieb, C. Greider, and R.A. DePinho. 1999. *Longevity, stress response, and cancer in aging telomerase-deficient mice. Cell 96: 701-12.*

Sakai, K. and J. Miyazaki. 1997. *A transgenic mouse line that retains Cre recombinase activity in mature oocytes irrespective of the cre transgene transmission. Biochem Biophys Res Commun 237: 318-24.*

Sambrook, J., E.F. Fritsch, and T. Maniatis. 1989. *Molecular cloning: a laboratory manual. Cold Spring Harbor Laboratory Press, Cold Spring Harbor, NY.*

Sands, A.T., A. Abuin, A. Sanchez, C.J. Conti, and A. Bradley. 1995. *High susceptibility to ultraviolet-induced carcinogenesis in mice lacking XPC. Nature 377: 162-165.*

Sanger, F., S. Nicklen, and A.R. Coulson. 1977. *DNA sequencing with chain-terminating inhibitors. Proc. Natl. Acad. Sci. USA 74: 5463-5467.*

Schaeffer, L., V. Moncollin, R. Roy, A. Staub, M. Mezzina, A. Sarasin, G. Weeda, J.H.J. Hoeijmakers, and J.M. Egly. 1994. *The ERCC2/DNA repair protein is associated with the class II BTF2/TFIIH transcription factor. EMBO J. 13: 2388-2392.*

Schaeffer, L., R. Roy, S. Humbert, V. Moncollin, W. Vermeulen, J.H.J. Hoeijmakers, P. Chambon, and J. Egly. 1993. *DNA repair helicase: a component of BTF2 (TFIIH) basic transcription factor.*

Science 260: 58-63.

Schumacher, M., S. Weill-Engerer, P. Liere, F. Robert, R.J. Franklin, L.M. Garcia-Segura, J.J. Lambert, W. Mayo, R.C. Melcangi, A. Parducz, U. Suter, C. Carelli, E.E. Baulieu, and Y. Akwa. 2003. Steroid hormones and neurosteroids in normal and pathological aging of the nervous system. Prog Neurobiol 71: 3-29.

Seip, M. and O. Trygstad. 1996. Generalized lipodystrophy, congenital and acquired (lipoatrophy). Acta Paediatr Suppl 413: 2-28.

Selfridge, J., K.T. Hsia, N.J. Redhead, and D.W. Melton. 2001. Correction of liver dysfunction in DNA repair-deficient mice with an ERCC1 transgene. Nucleic Acids Res 29: 4541-50.

Smith, J.R. and O.M. Pereira-Smith. 1996. Replicative senescence: implications for in vivo aging and tumor suppression. Science 273: 63-7.

Stewart, G.S., R.S. Maser, T. Stankovic, D.A. Bressan, M.I. Kaplan, N.G. Jaspers, A. Raams, P.J. Byrd, J.H. Petrini, and A.M. Taylor. 1999. The DNA double-strand break repair gene hMRE11 is mutated in individuals with an ataxia-telangiectasia-like disorder. Cell 99: 577-87.

Sun, X.Z., Y.N. Harada, S. Takahashi, N. Shiomi, and T. Shiomi. 2001. Purkinje cell degeneration in mice lacking the xeroderma pigmentosum group G gene. J Neurosci Res 64: 348-54.

Sun, X.Z., Y.N. Harada, R. Zhang, C. Cui, S. Takahashi, and Y. Fukui. 2003. A genetic mouse model carrying the nonfunctional xeroderma pigmentosum group G gene. Congenit Anom (Kyoto) 43: 133-9.

Syntin, P., H. Chen, B.R. Zirkin, and B. Robaire. 2001. Gene expression in Brown Norway rat Leydig cells: effects of age and of age-related germ cell loss. Endocrinology 142: 5277-85.

Takada, K. and L.E. Becker. 1986. Cockayne's syndrome: report of two autopsy cases associated with neurofibrillary tangles. Clin Neuropathol 5: 64-8.

Tanemura, K., M. Kurohmaru, K. Kuramoto, and Y. Hayashi. 1993. Age-related morphological changes in the testis of the BDF1 mouse. J Vet Med Sci 55: 703-10.

Taylor, E.M., B.C. Broughton, E. Botta, M. Stefanini, A. Sarasin, N.G. Jaspers, H. Fawcett, S.A. Harcourt, C.F. Arlett, and A.R. Lehmann. 1997. Xeroderma pigmentosum and trichothiodystrophy are associated with different mutations in the XPD (ERCC2) repair/transcription gene. Proc Natl Acad Sci U S A 94: 8658-63.

Thompson, L.H. and D. Schild. 2002. Recombinational DNA repair and human disease. Mutat Res 509: 49-78.

Tian, M., D.A. Jones, M. Smith, R. Shinkura, and F.W. Alt. 2004a. Deficiency in the nuclease activity of xeroderma pigmentosum G in mice leads to hypersensitivity to UV irradiation. Mol Cell Biol 24: 2237-42.

Tian, M., R. Shinkura, N. Shinkura, and F.W. Alt. 2004b. Growth retardation, early death, and DNA repair defects in mice deficient for the nucleotide excision repair enzyme XPF. Mol Cell Biol 24: 1200-5.

Tirode, F., D. Busso, F. Coin, and J.M. Egly. 1999. Reconstitution of the transcription factor TFIIH: assignment of functions for the three enzymatic subunits, XPB, XPD, and cdk7. Mol Cell 3: 87-95.

Toelle, S.P., E. Valsangiacomo, and E. Boltshauser. 2001. Trichothiodystrophy with severe cardiac and neurological involvement in two sisters. Eur J Pediatr 160: 728-31.

Tomasevic, G., H.L. Laurer, G. Mattiason, H. van Steeg, T. Wieloch, and K.T. McIntosh. 2004. Delayed neuromotor recovery and increased cognitive dysfunction following experimental brain trauma in mice lacking the DNA repair gene XPA. manuscript in prep.

Trifunovic, A., A. Wredenberg, M. Falkenberg, J.N. Spelbrink, A.T. Rovio, C.E. Bruder, Y.M. Bohlooly, S. Gidlof, A. Oldfors, R. Wibom, J. Tornell, H.T. Jacobs, and N.G. Larsson. 2004. Premature ageing in mice expressing defective mitochondrial DNA polymerase. Nature 429: 417-23.

Troelstra, C., R.M. Landsvater, J. Wiegant, M.v.d. Ploeg, G. Viel, C.H.C.M. Buys, and J.H.J. Hoeijmakers.

1992. Localization of the nucleotide excision repair gene ERCC6 to human chromosome 10q11-q21. *Genomics* 12: 745-749.

Tyner, S.D., S. Venkatachalam, J. Choi, S. Jones, N. Ghebranious, H. Igelmann, X. Lu, G. Soron, B. Cooper, C. Brayton, S. Hee Park, T. Thompson, G. Karsenty, A. Bradley, and L.A. Donehower. 2002. *p53 mutant mice that display early ageing-associated phenotypes. Nature* 415: 45-53.

Ueda, T., Gonzalez, V., Khan,S.G., Imoto, K., Shahlavi T., Inui H., Busch D., DiGiovanna J.J., Kraemer K.H. 2004. *The R683W common mutation occurs in xeroderma pigmentosum group D patients with and without neurological symptoms. J. Investigative Dermatol.* 122: A90.

Ullmann, A., F. Jacob, and J. Monod. 1967. *Characterization by in vitro complementation of a peptide corresponding to an operator-proximal segment of the beta-galactosidase structural gene of Escherichia coli. J Mol Biol* 24: 339-43.

Umar, A. and T.A. Kunkel. 1996. *DNA-replication fidelity, mismatch repair and genome instability in cancer cells. Eur J Biochem* 238: 297-307.

van den Boom, V., N.G. Jaspers, and W. Vermeulen. 2002. *When machines get stuck--obstructed RNA polymerase II: displacement, degradation or suicide. Bioessays* 24: 780-4.

van der Horst, G.T., L. Meira, T.G. Gorgels, J. de Wit, S. Velasco-Miguel, J.A. Richardson, Y. Kamp, M.P. Vreeswijk, B. Smit, D. Bootsma, J.H. Hoeijmakers, and E.C. Friedberg. 2002. *UVB radiation-induced cancer predisposition in Cockayne syndrome group A (Csa) mutant mice. DNA Repair (Amst)* 1: 143-57.

van der Horst, G.T.J., H. van Steeg, R.J.W. Berg, A. van Gool, J. de Wit, G. Weeda, H. Morreau, R.B. Beems, C.F. van Kreijl, F.R. de Gruijl, D. Bootsma, and J.H.J. Hoeijmakers. 1997. *Defective transcription-coupled repair in Cockayne syndrome B mice is associated with skin cancer predisposition. Cell* 89: 425-35.

van der Maazen, R.W., B.J. Kleiboer, I. Verhagen, and A.J. van der Kogel. 1993. *Repair capacity of adult rat glial progenitor cells determined by an in vitro clonogenic assay after in vitro or in vivo fractionated irradiation. Int J Radiat Biol* 63: 661-6.

van Gent, D.C., J.H. Hoeijmakers, and R. Kanaar. 2001. *Chromosomal stability and the DNA double-stranded break connection. Nat Rev Genet* 2: 196-206.

Vanfleteren, J.R. 1993. *Oxidative stress and ageing in Caenorhabditis elegans. Biochem J* 292 (Pt 2): 605-8.

Varley, J.M. 2003. *Germline TP53 mutations and Li-Fraumeni syndrome. Hum Mutat* 21: 313-20.

Venema, J., L.H.F. Mullenders, A.T. Natarajan, A.A. Van Zeeland, and L.V. Mayne. 1990. *The genetic defect in Cockayne syndrome is associated with a defect in repair of UV-induced DNA damage in transcriptionally active DNA. Proc. Natl. Acad. Sci. USA* 87: 4707-4711.

Vermeulen, W., E. Bergmann, J. Auriol, S. Rademakers, P. Frit, E. Appeldoorn, J.H. Hoeijmakers, and J.M. Egly. 2000. *Sublimiting concentration of TFIIH transcription/DNA repair factor causes TTD-A trichothiodystrophy disorder. Nat Genet* 26: 307-13.

Vermeulen, W., S. Rademakers, N.G. Jaspers, E. Appeldoorn, A. Raams, B. Klein, W.J. Kleijer, L.K. Hansen, and J.H. Hoeijmakers. 2001. *A temperature-sensitive disorder in basal transcription and DNA repair in humans. Nat Genet* 27: 299-303.

Vermeulen, W., R.J. Scott, S. Potger, H.J. Muller, J. Cole, C.F. Arlett, W.J. Kleijer, D. Bootsma, J.H.J. Hoeijmakers, and G. Weeda. 1994a. *Clinical heterogeneity within xeroderma pigmentosum associated with mutations in the DNA repair and transcription gene ERCC3. Am. J. Human Gen.* 54: 191-200.

Vermeulen, W., M. Stefanini, S. Giliani, J.H.J. Hoeijmakers, and D. Bootsma. 1991. *Xeroderma pigmentosum*

complementation group H falls into complementation group D. *Mutat Res* 255: 201-208.

Vermeulen, W., A.J. van Vuuren, M. Chipoulet, L. Schaeffer, E. Appeldoorn, G. Weeda, N.G.J. Jaspers, A. Priestley, C.F. Arlett, A.R. Lehmann, M. Stefanini, M. Mezzina, A. Sarasin, D. Bootsma, J.-M. Egly, and J.H.J. Hoeijmakers. 1994b. Three unusual repair deficiencies associated with transcription factor BTF2(TFIIH): Evidence for the existence of a transcription syndrome. *Cold Spring Harb. Symp. Quant. Biol.* 59: 317-329.

Viprakasit, V., R.J. Gibbons, B.C. Broughton, J.L. Tolmie, D. Brown, P. Lunt, R.M. Winter, S. Marinoni, M. Stefanini, L. Brueton, A.R. Lehmann, and D.R. Higgs. 2001. Mutations in the general transcription factor TFIIH result in beta-thalassaemia in individuals with trichothiodystrophy. *Hum Mol Genet* 10: 2797-802.

Vogel, H., D.S. Lim, G. Karsenty, M. Finegold, and P. Hasty. 1999. Deletion of Ku86 causes early onset of senescence in mice. *Proc Natl Acad Sci U S A* 96: 10770-5.

Volker, M., M.J. Mone, P. Karmakar, A. van Hoffen, W. Schul, W. Vermeulen, J.H. Hoeijmakers, R. van Driel, A.A. van Zeeland, and L.H. Mullenders. 2001. Sequential assembly of the nucleotide excision repair factors in vivo. *Mol Cell* 8: 213-24.

Wang, G., L. Chuang, X. Zhang, S. Colton, A. Dombkowski, J. Reiners, A. Diakiw, and X.S. Xu. 2004. The initiative role of XPC protein in cisplatin DNA damaging treatment-mediated cell cycle regulation. *Nucleic Acids Res* 32: 2231-40.

Wang, X.W., W. Vermeulen, J.D. Coursen, M. Gibson, S.E. Lupold, K. Forrester, G. Xu, L. Elmore, H. Yeh, J.H. Hoeijmakers, and C.C. Harris. 1996. The XPB and XPD DNA helicases are components of the p53-mediated apoptosis pathway. *Genes Dev* 10: 1219-32.

Weeda, G., I. Donker, J. de Wit, H. Morreau, R. Janssens, C.J. Vissers, A. Nigg, H. van Steeg, D. Bootsma, and J.H.J. Hoeijmakers. 1997. Disruption of mouse ERCC1 results in a novel repair syndrome with growth failure, nuclear abnormalities and senescence. *Curr Biol* 7: 427-39.

Weeda, G., R.C.A. Van Ham, W. Vermeulen, D. Bootsma, A.J. Van der Eb, and J.H.J. Hoeijmakers. 1990. A presumed DNA helicase encoded by ERCC-3 is involved in the human repair disorders xeroderma pigmentosum and Cockayne's syndrome. *Cell* 62: 777-791.

White, S.M., A. Lucassen, and G. Norbury. 2001. Cystic fibrosis: a further case of an asymptomatic compound heterozygote. *Am J Med Genet* 103: 342-3.

Wilson, D.M., 3rd and L.H. Thompson. 1997. Life without DNA repair. *Proc Natl Acad Sci U S A* 94: 12754-7.

Winkler, G.S., S.J. Araujo, U. Fiedler, W. Vermeulen, F. Coin, J.M. Egly, J.H. Hoeijmakers, R.D. Wood, H.T. Timmers, and G. Weeda. 2000. TFIIH with inactive XPD helicase functions in transcription initiation but is defective in DNA repair. *J Biol Chem* 275: 4258-66.

Winkler, G.S., W. Vermeulen, F. Coin, J.M. Egly, J.H. Hoeijmakers, and G. Weeda. 1998. Affinity purification of human DNA repair/transcription factor TFIIH using epitope-tagged xeroderma pigmentosum B protein. *J Biol Chem* 273: 1092-8.

www.xpdmutations.org.

Yamaizumi, M. and T. Sugano. 1994. U.v.-induced nuclear accumulation of p53 is evoked through DNA damage of actively transcribed genes independent of the cell cycle. *Oncogene* 9: 2775-84.

Yu, C.E., J. Oshima, Y.H. Fu, E.M. Wijsman, F. Hisama, R. Alisch, S. Matthews, J. Nakura, T. Miki, S. Ouais, G.M. Martin, J. Mulligan, and G.D. Schellenberg. 1996. Positional cloning of the Werner's syndrome gene. *Science* 272: 258-262.

Summary for a non-biologist

DNA, located in the nucleus of virtually every cell, encodes the genetic information according to which cells and tissues in our body multiply, carry out their specific function, and die. Inevitably, intact DNA is vital for normal functioning of an organism. Yet, DNA is constantly exposed to damaging agents, such as the UV component of sunlight, various chemicals such as those derived from cigarette smoke or reactive agents produced as a side product of normal oxidation in cells. Damaged DNA must be continuously repaired because lesions in the DNA can lead to permanent changes in the genetic code (mutations) that can ultimately cause cancer. In addition, DNA damage can cause cell death and when many cells in the given organ, for example in the brain die, diseases like dementia or Parkinson's are triggered. To avoid the deleterious consequences of DNA damage, evolution has equipped most organisms with multiple DNA repair systems. An example from everyday life of DNA damage and its consequences is sunburn: UV radiation, as present in sunlight, damages the DNA of skin cells, leading to inflammatory responses and subsequent redness and peeling of the skin. Moreover, xeroderma pigmentosum (XP) patients, carrying inborn defects in the DNA repair pathway responsible for the removal of UV-induced DNA damage, display a more than 1000 fold elevated skin cancer predisposition.

It is well known that damage in DNA can cause mutations (as a consequence of erroneous or absent repair) and thereby lead to cancer, and that the cancer frequency rises while we age. But conversely, does DNA damage also affect ageing itself? Clinical observations suggest that this indeed might be the case. Several human inborn syndromes, such as Werner syndrome, Cockayne syndrome (CS) and trichothiodystrophy (TTD) show symptoms resembling partially accelerated ageing. As the genes mutated in these syndromes are associated with DNA repair, it was proposed that defective DNA repair, and as an immediate consequence accumulation of DNA damage, may at least partially explain ageing. The question whether or not this indeed is the case has largely remained unanswered, mostly due to complexity of the process of ageing (involving the interaction of cells and organ systems in the whole organism) and for the obvious reason that experiments with humans are impossible. Moreover, it is generally impossible to predict how test tube observations correlate with ageing in an organism as a whole. Therefore, ageing research requires the use of model organisms in which disease causative gene mutations can be mimicked. To date, gene-technology methods are the most advanced for the mouse, making it the preferred model of choice. In this thesis, we investigated the role of DNA damage and the consequence of defective DNA repair in accelerated ageing/cancer syndromes trichothiodystrophy (TTD) and combined xeroderma pigmentosum Cockayne syndrome (XPCS). Interestingly, both syndromes can be triggered by mutations in the very same gene, called XPD. We established mouse models mimicking the gene mutations found in human TTD and XPCS patients. We found that specific XPD mutations cause disease symptoms in mice clearly resembling those found in human patients, demonstrating that the mouse is a valid model system for these disorders. For instance, TTD mice, like human TTD patients, display accelerated ageing, brittle hair and scaling skin (the TTD hallmark features), whereas XPCS mice display enormous cancer predisposition and mildly accelerated ageing. Since the XPD protein, apart from acting as a DNA repair protein, is also involved in several other important

cellular processes it has remained unknown whether ageing seen in TTD and XPCS patients is caused by the same or by a different mechanism. We found that further reduction of the DNA repair capacity in TTD and XPCS mice results in a dramatically accelerated and remarkably overlapping ageing phenotype. This implies that ageing in TTD and XPCS shares a common root cause in DNA repair. In general terms, our findings suggest that if an access to the information encoded in the DNA is hampered by the presence of unrepaired DNA damage, cells can no longer function properly and at least some ageing features appear at an accelerated rate. Extension of this concept implies that a similar mechanism may underlie the normal ageing process.

We also found that the enormous cancer predisposition in XPCS mice does not considerably affect accelerated ageing. Since accelerated ageing and cancer features in nucleotide excision repair disorders were previously believed to be mechanistically mutually exclusive processes, this finding may open a new way of thinking and calls for additional studies.

Another important finding made here, involves the genetics of recessive disorders. In virtually every cell of our body each gene has two copies (called alleles). One is inherited from the father and one from the mother. When an allele is not contributing to the phenotype, it is called recessive, while the phenotype determining allele is called dominant. A well-known example of dominant and recessive phenotypic feature is eye color: brown eye color is dominant blue, a recessive phenotypic feature. There are about ~3000 inborn recessive diseases known in man. In order to develop a recessive disease, both alleles of the gene involved must carry a mutation. In some cases, both alleles will carry the same mutation, a condition known as homozygosity. But in most cases patients carry different recessive mutation in each allele, a situation called compound heterozygosity. The interesting question emerging is whether in this situation one of the recessive alleles may behave "dominantly" over the other recessive allele or alternatively, whether two recessive alleles act together in determining disease progression. In the latter case, is the contribution to the disease phenotype uniformly or unequally shared between the two alleles? In other words, can there be a gradient of interallelic interactions? Last but not least, could two recessive alleles complement each other, e.g. together achieve something they would not be able to individually? While considering the phenotype of human recessive diseases, the above-mentioned options have currently remained largely ignored and unexplored for the reason that it is virtually impossible to discriminate between effects arising from normal variance in environment and genetic background on the one hand and that of each of the two affected alleles on the other hand. Such allelic effects can only be analyzed in an environmentally controlled and genetically homogeneous mammalian laboratory model system, such as the mouse. In this thesis we used the XPD-TTD and -XPCS mouse models to further investigate allelic effects and found that combined recessive alleles can have an enormous phenotypic potential. We show that even embryonic lethal alleles (causing embryonic death when present in homozygous form), can rescue a severe premature ageing condition. Extension of this principle would help to explain the huge variance of disease phenotype among the ~3000 human recessive disorders known. The medical implication of our findings is that both disease-causing alleles of a patient should always be simultaneously analyzed. Such an analysis may more accurately predict the disease progression and in turn may improve therapy and the quality of life of the patient and their families.

Samenvatting

Het DNA, gelocaliseerd in de kern van bijna iedere cel, codeert voor de informatie die bepaalt wanneer en hoe cellen, de bouwstenen van weefsels en organen, groeien, leven en sterven. De informatie die het codeert wordt continu gebruikt door cellen en organen en intact DNA is dus essentieel voor een normaal functioneren van een organisme. Het DNA staat echter continu bloot aan schadelijke factoren, zoals de UV component van het zonlicht maar ook door reactive (zij)producten die ontstaan door natuurlijke (oxidatie) processen in de cel. Aangezien fouten in het DNA kunnen leiden tot ernstige ziektes, zoals kanker, is het belangrijk dat het DNA continu gerepareerd wordt. Een alledaags voorbeeld van de consequentie van DNA schade is verbranding door zonlicht. De UV component van het zonlicht beschadigt het DNA in de huidcellen wat leidt tot een ontstekingsreactie en vervolgens het rood worden en vervellen van de huid veroorzaakt. Individuen met een aangeboren afwijking in het repareren van UV geïnduceerde DNA schade, een afwijking die bekend staat als xeroderma pigmentosum (XP), vertonen een 1000 maal verhoogde kans op huidkanker.

Het is bekend dat mutaties in het DNA, door afwezigheid van DNA reparatie of een foutieve reparatie, leiden tot kanker en dat de kans op kanker toe neemt naarmate we ouder worden. Is er echter ook een direct effect van DNA schade op het ouderdoms proces zelf? Er zijn klinische aanwijzingen dat dit inderdaad het geval is. Er zijn verschillende aangeboren menselijke afwijkingen bekend zoals Werner syndroom, Cockayne syndroom (CS) en Trichothidystrophy (TTD) waarvan de patienten symptomen vertonen die lijken op gedeeltelijke versnelde veroudering. Omdat de genen die gemuteerd zijn in deze syndromen zijn geassocieerd met DNA reparatie mechanismen is voorgesteld dat de accumulatie van DNA schade, in ieder geval gedeeltelijk, veroudering zou kunnen veroorzaken. Of dit ook daadwerkelijk het geval is blijft grotendeels onduidelijk door de complexiteit van het ouderdoms proces en voor duidelijke redenen zijn experimenten met mensen uitgesloten. Het is vrijwel onmogelijk te voorspellen hoe resultaten verkregen uit experimenten die plaatsgevonden hebben buiten het lichaam, correleren met veroudering in het levende organisme zelf. Om deze reden is een model organisme waarin de genmutaties nagebootst kunnen worden essentieel. Het meest voor de hand liggende organisme dat ook genetisch gemodificeerd kan worden is op dit moment de muis. In dit proefschrift hebben we de rol van DNA schade in de versnelde ouderdom/kanker syndromen trichothiodystrophy (TTD) en xeroderma pigmentosum (XP) gecombineerd met Cockayne syndroom (XPCS) onderzocht. Hiervoor hebben we muismodellen gegenereerd die vergelijkbare mutaties in hun DNA bevatten als TTD en XPCS patiënten. Beide syndromen worden veroorzaakt door (verschillende) mutaties in hetzelfde gen, genaamd XPD. We ontdekten dat deze mutaties in de muis leidden tot dezelfde symptomen als in de patiënt, wat laat zien dat de muis een gedegen model is voor dit onderzoek. Een van deze overeenkomsten tussen muis en mens is de, voor TTD typerende, versnelde veroudering, broze haren en schilferende huid, terwijl de XPCS muis een sterk verhoogde kans op kanker en een mild versnelde veroudering vertoont. Aangezien het XPD eiwit naast het DNA reparatie proces ook in verschillende andere processen is betrokken, is het onbekend of veroudering in TTD en XPCS patiënten door hetzelfde of door verschillende mechanismen wordt veroorzaakt. Door het verder verminderen van de DNA

reparatie capaciteit in TTD en XPCS muizen vonden wij, overlappende, extreem versnelde veroudering. Dit resultaat suggereert dat veroudering in TTD en XPCS dezelfde oorsprong in het DNA reparatie mechanisme hebben. Meer algemeen suggereert ons onderzoek dat wanneer een overvloed van de informatie, gecodeerd door het DNA, geblokkeerd is door ongerepareerde DNA schade, cellen niet meer normaal kunnen functioneren, resulterend in tenminste enkele versnelde verouderings kenmerken. In het verlengde hiervan kan er gesuggereerd worden dat een zelfde mechanisme de oorzaak is van "normale" veroudering. Daarnaast hebben wij gevonden dat de enorme gevoeligheid voor kanker van de XPCS muis geen ernstig effect heeft op de eventuele versnelde veroudering van deze muizen, terwijl voorheen in het algemeen werd verondersteld dat versnelde veroudering en kanker hand in hand gingen. De bevinding dat veroudering en kanker parallelle, maar mechanistisch, andere processen kunnen zijn opent een nieuwe manier van denken en vraagt om verder onderzoek.

Een andere belangrijke bevinding betreft recessieve genetica. In iedere cel van ons lichaam bevinden zich van ieder gen twee kopieën, waarvan er een van de moeder en een van de vader afkomstig is. Deze twee kopieën van hetzelfde gen heten allelen. Wanneer een allel niet bijdraagt aan het fenotype wordt het recessief genoemd en de ander, dat het fenotype veroorzaakt, wordt dominant genoemd. Een bekend voorbeeld hiervan is de kleur van het oog; bruin is dominant over blauw. Er zijn op dit moment ongeveer 3000 aangeboren recessieve syndromen in de mens bekend en om een recessieve ziekte te krijgen moeten beide allelen gemuteerd zijn. Maar wat gebeurt er echter wanneer beide alllelen een verschillende mutatie bevatten? Zal er een dominant worden, treedt er co-dominantie op? Of zullen de beide recessieve allelen samen bereiken wat ze alleen niet kunnen, met andere woorden, elkaar complementeren? Met deze opties wordt op dit moment weinig rekening gehouden bij het vaststellen van het fenotype van recessieve syndromen. De reden hiervoor is de moeilijkheid om de effecten te kunnen onderscheiden van normale variatie in de omgeving en genetische achtergrond en de beide allelen. Deze effecten kunnen alleen onderzocht worden in de gecontroleerde omgeving van een laboratorium met behulp van een model organisme zoals de muis. In dit onderzoek hebben we gebruik gemaakt van diverse muismodellen om de effecten van beide allelen te kunnen onderzoeken en we hebben gevonden dat gecombineerde recessieve allelen een enorme fenotypische potentie hebben. Ook laten we zien dat allelen die op zichzelf lethaal zijn, een ernstige versnelde veroudering kunnen redden. Verdere uitwerking van dit verschijnsel kan een verklaring geven voor de enorme verscheidenheid in fenotypische verschillen in de ongeveer 3000 humane recessieve syndromen. Een practische implicatie van deze studie is dat altijd beide ziekte veroorzakende allelen onderzocht zouden moeten worden. Deze analyse kan de voortgang van de betreffende ziekte beter en nauwkeuriger voorspellen wat gevolg kan hebben op de therapie en de kwaliteit van het leven van de patiënt en hun familie.

Lihtsustatud lühikokkuvõte

Keha organite, kudede ja rakkude igapäevaseks elutegevuseks vajalik informatsioon on kodeeritud DNA-sse. DNA asub peaaegu kõikide rakkude tuumades. Organid, nn aju, maks, jne täidavad oma spetsiaalseid funktsioone sellest informatsioonist lähtuvalt ning seega on ilmne, et DNA korrashoid on organismi tervise seisukohalt ülimalt oluline. Päikese valguses sisalduv ultrviolett kiirgus (UV), mitmesugused kemikaalid nagu näiteks sigarettide suitsus leiduvad ained ja rakkude normaalse elutegevuse käigus tekkivad reaktiivsed ühendid kahjustavad DNA-d. Kui DNA parandamine ei toimi või kahjustuste hulk on liiga suur, tekivad mutatsioonid ehk püsivad muutused DNA-s. Mutatsioonide kogunemise üheks tulemuseks on vähkkasvajate teke. DNA kahjustused takistavad ka seal sisalduva informatsiooni kättesaadavust, mis omakorda võib viia raku surmani. Kui mingis koes, näiteks teatavates aju osades rakud massiliselt surevad, tekivad haigused nagu näiteks dementia või Parkinsoni tõbi. Selliste ebameeldivuste vältimiseks on peaaegu kõikidel elusorganismidel evolutsiooni käigus välja arenenud tõhusad DNA parandamise mehanismid. Näiteks on tavalise päikese põletuse-naha punetuse ja kipitamise algpõhjuseks UV kiirguse poolt tekitatud DNA kahjustused naha rakkudes. Kui DNA naharakkudes jääb parandamata, nagu näiteks kaasasündinud DNA parandamise defektiga patsientides, tuleneb sellest 1000 korda kõrgendatud nahavähi oht. Sellise kaasasündinud haiguse kliiniliseks nimeks on Xeroderma pigmentosum.

On üldiselt teada, et mutatsioonid põhjustavad vähi teket ning, et vanuse kasvades tõenäosus vähi tekkeks suureneb. Kuid kas kahjustused DNA-l võivad otseselt mõjutada ka vananemisprotsessi ennast? Teatavate üliharva esinevate kaasasündinud DNA parandamise defektiga haigusjuhtumite põhjal tekkis oletus, et see tõepoolest võib nii olla. Näiteks Cockayne sündroomi (CS) ja trihhotiodüstroofia (TTD) sümptomite hulgas esineb hulk tunnuseid, mis sarnanevad enneaegse vananemisega. Vananemise uurimine on raske juba sellepärast, et see on ülimalt pikaajaline protsess mis hõlmab rakkude, kudede ja organite vahelisi keerulisi interaktsioone ajas ning katsed inimestega pole loomulikult mõeldavad. Katseklaasis sooritatud eksperimentide suureks puuduseks aga on asjaolu, et on üldiselt võimatu ennustada kas saadud tulemustel on vananemisega organismi tasemel põhjuslik seos või ei. Seega tuleb vananemise uurimiseks kasutada mudel organisme. Eelistatud mudeliks on selline loom, milles on võimalik enneaegset vananemist põhjustavaid geeni mutatsioone kunstlikult tekitada. Geenitehnoloogiliste meetoditega kõige lihtsamini geneetiliselt modifitseeritav ja inimesele kõige sarnasem mudel-organism on hiir.

Käesoleva doktoritöö üheks eesmärgiks oli selgitada kuidas DNA kahjustused ja defektne DNA parandamine mõjutab trihhotiodüstroofias (TTD) ja Xeroderma pigmentosum'i ja Cockayne sündroomi kombineeritud vormis (XPCS) enneaegse vananemise ja vähi teket. Mõlemad nimetatud haigused tulenevad mutatsioonidest geenis nimega XPD. Esimese sammuna kopeeriti TTD ja XPCS patsientides leitud XPD geeni mutatsioonid hiire XPD geenis. Ilmnes, et TTD ja XPCS haiguspilt hiirtes ja inimestes on sarnane ning seega võib väita, et hiir on vastavate haiguste uurimiseks sobiv mudel süsteem. Näiteks ilmnevad TTD sümptomid nagu enneaegne vananemine ja soomusjalt kooruv nahk sarnaselt nii TTD hiires kui ka inimeses. Samuti on kõrgendatud vähirisk ja enneaegne vananemine XPCS hiires võrreldav inimese vastava haigusega. XPD osaleb peale DNA parandamise veel väga mimesugustes olulistes rakuprotsessides nn. transkriptsioon (informatsiooni mahalugemine DNA-lt), raku pooldumise kontroll,

jne. Kuni käesoleva tööni polnud teada, kas TTD ja XPCS tüüpi mutatsioonid mõjutavad XPD sama või erinevat funktsiooni, ehk teiste sõnadega, kas enneaegne vananemine mõlemal juhul tuleneb samast või erinevast mehanismist. Sellele küsimusele vastamiseks ristati TTD ja XPCS hiired hiirtega, kes kannavad kaasasündinud mutatsiooni teises DNA parandamises osalevas geenis nimega XPA. Ristamisel saadi hiired, kes kannavad kas XPCS või TTD defekti kombinatsioonis mutatsiooniga geenis XPA mille tulemusena DNA parandamise võime langeb oluliselt. Sellistes hiirtes ilmnesid vananemisele sarnanevad sümptomid väga kiiresti, 2-3 nädala jooksul ning TTD ja XPCS haiguspilt kattus. Seega võib väita, et enneaegne vananemine mõlemas sündroomis tuleneb DNA kahjustuste kogunemisest. Laiemas mõttes võimaldavad need tulemused väita, et kui DNA kahjustuste tõttu seal sisalduva informatsiooni kättesaadavus langeb, kahaneb selle tulemusena ka rakkude funktsionaalsus ja eluvõime mille tagajärjeks on (enneaegne) vananemine. Lisaks ülaltoodule ilmnes, et vastuvõtlikus UV poolt tekitatud vähile ja enneaegne vananemine TTD-s ja XPCS-s on reguleeritud erinevate üksteisest sõltumatute mehanismide poolt. Kuna varem arvati, et vananemine ja vähk neis haigustes on omavahel põhjuslikult seotud võivad need tulemused tähendada nn. uue mõtlemise sündi ja baasi järgnevateks uuringuteks.

Allpool kirjeldatav selles doktoritöös tehtud leid on oluline kõikide retsessiivsete haiguste mõistmisel. Kõigepealt, mida tähendab retsessiivne? Igal geenil on peaaegu igas rakus kaks koopiat ehk alleeli- üks alleel on päritud emalt, teine isalt. Sageli määrab üks geen mingi konkreetse tunnuse ehk fenotüübi, näiteks silmade värvi. Kui üks kahest alleelist ei osale tunnuse kujunemisel, nimetatakse seda alleeli retsessiivseks, tunnust kujundavat alleeli aga dominantseks. Näiteks on pruun silmavärv dominante ja sinine silmavärv retsessiivne tunnus. On teada umbes ~3000 erinevat retsessiivset haigust. Selleks, et tekiks retsessiivne haigus peavad mõlemad geeni alleelid kandma mutatsiooni. Isendit, milles vastava geeni mõlemad alleelid kannavad identset mutatsiooni nimetatakse homosügoodiks. Palju sagedamini aga esineb juhtumeid, mil geeni alleelid kannavad erinevaid mutatsioone. Sellisel juhul on meil tegemist nn. kombineeritud heterosügoodiga (ingl. k.compound heterozygote), mis tekitab aga terve hulga huvitavaid küsimusi. Näitkes, kas kombineeritud heterosügoodis üks retsessiivne alleel muutub dominantseks teise retsessiivse alleeli üle või määrvad nad tunnuse või haiguspildi tekke koos? Viimasel juhul on oluline teada kas mõlemad alleelid määravad tunnuse või haiguse tekke võrdsel või erineval määral? Samuti on võimalik, et kaks retsessiivset alleeli täiendavad teineteist ja koos määravad tunnuse milleks kumbki homosügoodina poleks võimeline. Ülalmainitud võimaluste osakaalu uuritava tunnuse või haiguspildi tekkel on peaaegu võimatu eristada mõjust, mida keskkond ja teised, vastava tunnusega või haigusega otseselt mitteseotud geenid uuritavale tunnusele või haigusele avaldavad. Ning seega kombineeritud retsessiivsete alleelide potensiaal mingi tunnuse või haiguspildi määramisel on üldiselt teadmata. Antud küsimust on võimalik uurida vaid geneetiliselt defineeritud süsteemis, nagu seda on laborihiired. Kombineerides erinevaid XPD alleele hiires selgus, et kombineeritud retsessiivsetel alleelidel võib olla tunnuse või haiguse kujunemisel oluliselt suurem roll kui varem arvatud. Nimelt selgus, et kui kombineerida homosügoodina loote surma põhjustavad XPD alleelid TTD alleeliga, on enneaegne vananemine TTD hiires peatatud. Teiste sõnadega, kombineerides homosügoodina surmava alleeli enneaegset vananemist põhjustava alleeliga, saame peaaegu terved loomad. Sellest järeldub näiteks, et retsessiivsete haiguste prognoosimisel tuleb alati arvestada mõlemat alleeli ja võimalusel tuleb neid funkstionaalselt analüüsida koos. Selline lähenemine võib aidata täpsemalt ennustada retsessiivsete haiguste kulgu ja paremini määrata ravi.

Acknowledgements

ters herein never would have reached the state of smoothness as you find them now. Jay has also ideas for future experiments and he will hopefully be coordinating the follow-up for my research. Thank you Jay, and success. A special person to thank for endless discussions and strong contribution in manuscript editing and powerpoint presentation preparation is Koos Jaspers. His logic has substantially helped to groove many chapters in this thesis.

I also specially own to Marko Piirsoo, another Estonian PhD student, whose company and friendship helped me a lot both to settle in Holland and to overcome the initial homesickness.

Now I'd like to swap from my current lab to the previous one. It was about 6 years ago at Tartu University, Estonia where my friend and lab-mate Saul Kivimäe urged me to take a 3-month practicum in Holland, where I applied to and was happy to land in Jan Hoeijmakers's lab. So thanks to his pushing I actually ended up here. I'd also like to thank all my former Estonian colleagues, starting from my former boss prof. Toivo Maimets for taking and patiently keeping me in the lab and Arnold Kristjuhan, Arvi Jõers, Viljar Jaks and Sirje Kivi for excellent and educative discussions. From my earlier years I would like to express gratitude to my excellent English teacher Tiina Metsma (whom, if she ever happens to read this, I'm unfortunately again forced to disappoint with my never-improving grammar and spelling mistakes) and Kaidor Damberg, director of my high school, without who's support a lot of creative mind might have never found a proper cultivation.

And last but not the least I'd like to thank my parents and brothers. Lühidalt ja selgelt-ma teid ikka armastan ja teile südamest tänulik olen abi eest mis te mulle pikkade õppimisaastate jooksul olete osutanud. Ja Tiinale ja Erikule- Uhu!

Jaan-Olle

Curriculum Vitae

Name:	**Jaan-Olle Andressoo**
Birth date:	6th of June1972
Birth place:	Tallinn, Estonia
Nationality:	Estonian

Education:

January 1999-October 2004	prof. Jan Hoeijmakers Lab
	Department of Cell Biology and Genetics
	Erasmus University Rotterdam, phD-student
1997-1999	Department of Molecular and Cell Biology
	Tartu University, Estonia, post-graduate studies
1991 – 1997	Department of Molecular and Cell Biology
	Tartu University, Estonia, undergraduate studies
1995 February-April	Viiki Biocenter
	Helsinki University, Finland, visiting student
1999 June-September	Department of Cell Biology and Genetics
	Erasmus MC, Rotterdam, Holland, visiting student

Secondary Education:

1986-1990	English-biased Mustamäe Gymnasium
	(Former Secondary School nr 44) Tallinn, Estonia

List of publications

– **Premature Aging in Mice Deficient in DNA Repair and Transcription**
Jan de Boer, Jaan Olle Andressoo, Jan de Wit , Jan Huijmans, Rudolph B. Beems, Harry van Steeg,
Geert Weeda, Gijsbertus T.J. van der Horst, Wibeke van Leeuwen, Axel P.N. Themmen,
Morteza Meradji, and Jan H.J. Hoeijmakers
Science, Vol 296, No 5571, 17 May 2002

– **Cell type-specific hypersensitivity to oxidative damage in CSB and XPA mice**
H. de Waard, J. de Wit, T.G. Gorgels, G. van den Aardweg, J.O. Andressoo, M. Vermeij,
H. van Steeg, J.H.J. Hoeijmaekrs, G.T.J. van der Horst
DNA Repair, Vol. 2, No 1, 2Jan. 2003

– **Different effect of CSA and CSB deficiency on sesnsitivity to oxidative DNA damage**
de Waard H., de Wit J., Andressoo J.O., van Oostrom D. Th. M., Riis B.,Weimann A., Poulsen H.E.,
van Steeg H., Hoeijmakers J.H.J., van der Horst G.T.J.
Molecular and Cellular Biology, September 2004, Vol. 24, Issue 18

– **Life-saving potential of lethal recessive alleles in mammals**
J.O. Andressoo, Jay Mitchell, Judith Jans, Jan de Wit, Rudolph B. Beems, Harry van Steeg,
Jan Hoeijmakers, Gijsbertus van der Horst.
submitted

– **Cockayne syndrome and trichothiodystrophy share a common root cause in DNA repair**
J.O. Andressoo, Jay Mitchell, Deborah Hoogstraten, Jan de Wit, Rudolph B. Beems,
Harry van Steeg, Jan H.J. Hoeijmakers, Gijsbertus van der Horst.
Manuscript in preparation

– **Pace of ageing in mice carrying a latent mutation in Xpb helicase is determined
by DNA repair efficiency**
J.O. Andressoo , Jay Mitchell, Geert Weeda, Rudolph B. Beems, Jan de Wit, Harm de Waard,
Jan H.J. Hoeijmakers, Gijsbertus van der Horst.
Manuscript in preparation.

Courses and conferences

- Oncogenesis and Tumor Biology May 17 - 21, 1999, Rotterdam
- Laboratory Animal Science, June 7-18, 1999, Utrecht
- ZonMw Genetica retraite 9-10 March 1999, Rolduc, Holland
- Promovendi Workshop 19-21 april 1999, (Gent Belgium)
- Molecular Genetics Center (MGC) - ICRF Graduate Sudent Workshop, April 27-30 2000, Oxford (England),
- Towards comprehending scanned arrays; expression profiling Leiden, November 22 - 23, 2000
- The 8 th MGC Ph.D.-student workshop, Bruges, 16-19 May, 2001 (Belgium)
- The 3rd Joint ICRF-MGC Graduate student Workshop, 2002, Chaam (NL)
- MGC Annual Meetings, September 1999-2003, oral presentation in Sept. 2003
- ZonMw Genetica retraite 11-12 March 2004, Rolduc, Holland
- DNA Repair Meeting, September the 9th 2001, Noordwijkerhout, Holland. Poster presentation and selected speaker
- DNA Helicases, Cancer and Ageing, March 12-17, 2002, Gralinbanken Resort, Tahoe City, California, USA. Poster presentation
- Functional Genomics of Ageing, April 28-May 1, 2004, Maris Hotel, Crete, Greece. Poster presentation
- Cockayne Syndrome and related disorders of DNA repair and transcription:from bench to bedside and back, May 23-26, 2004, National Conference Center, Lansdowne, VA, USA. Invited speaker
- 2004 Workshop on Innovative Mouse Models, June 17, 2004, Leiden University Medical Center, NL. Selected speaker

Scholarships and awards

- Tempus Phare Project Grant Fellow 01.06-01.09 1998; S_JEP-11212-96
- Estonian Students Fund in USA Reward, Januray 1999
- "Best Abstract" Reward, at DNA Helicases, Cancer and Ageing Meeting March 12-17, 2002, Gralinbanken Resort, Tahoe City, California, USA.